REGULATION OF UROPATHOGENIC *ESCHERICHIA COLI* STRESS RESPONSE AND PERSISTENCE IN THE URINARY TRACT

by

Matthew George Blango

A dissertation submitted to the faculty of
The University of Utah
in partial fulfillment of the requirements for the degree of

Doctor of Philosophy

in

Microbiology and Immunology

Department of Pathology

The University of Utah

August 2012

The University of Utah Graduate School

STATEMENT OF DISSERTATION APPROVAL

The dissertation of **Matthew G. Blango**

has been approved by the following supervisory committee members:

Matthew A. Mulvey	, Chair	**May 9, 2012** Date Approved
Brenda L. Bass	, Member	**May 9, 2012** Date Approved
Sherwood R. Casjens	, Member	**May 9, 2012** Date Approved
David J. Stillman	, Member	**May 9, 2012** Date Approved
John H. Weis	, Member	**May 9, 2012** Date Approved

and by **Peter E. Jensen**, Chair of the Department of **Pathology**

and by Charles A. Wight, Dean of The Graduate School.

ABSTRACT

Urinary tract infections (UTIs) afflict millions of individuals yearly, constituting a tremendous global health-care burden. The primary causative agents of UTIs are the gram-negative, rod-shaped bacteria, uropathogenic *Escherichia coli* (UPEC). These pathogens are motile and adhesive, with a proclivity to colonize diverse niches within the urinary tract; including the kidneys, bladder, and ureters. In the bladder, UPEC grow to high levels and often associate with the superficial epithelial cells lining the lumen. UPEC can invade these superficial epithelial cells to form intracellular reservoir populations, which are thought to be a source of recurrent, or relapsing, infections. The susceptibility of these intracellular UPEC populations was tested using a panel of commonly prescribed antibiotics in a murine model of UTI. Intracellular UPEC were found to persist despite treatment with host cell-permeable antibiotics such as sparfloxacin and ciprofloxacin that effectively sterilize the urine. In a follow-up study, UPEC reservoir populations were more effectively targeted by treating infected bladders with chitosan, a chitin-based bladder exfoliant, prior to sparfloxacin treatment. Although chitosan administration prior to antibiotic treatment significantly decreased UPEC titers, mice still exhibited some relapsing UTIs, suggesting that reservoirs still persist either within the bladder or in other host tissue. To further elucidate mechanisms of bacterial persistence within the urinary tract, several underappreciated bacterial factors were examined that were hypothesized to affect UPEC virulence, stress resistance, and persistence.

Bacterial, small, non-coding RNAs (sRNAs) are posttranscriptional regulators of gene expression in most prokaryotes and were shown to contribute to a wide variety of UPEC stress response and virulence cascades. In a follow-up study, the putative UPEC sRNA repertoire was defined using RNA-Seq technologies and bioinformatic analyses. Several novel, candidate sRNA molecules were identified and characterized, one of which seemingly repressed UPEC virulence in the murine UTI model. In a second approach to define regulators of UPEC pathogenic behaviors, the tRNA modifying enzyme MiaA was identified as a global regulator of UPEC stress response and virulence. MiaA adds a prenyl group to A-37, adjacent to the anticodon, in a subset of tRNAs to modulate ribosome fidelity and frameshifting. MiaA expression in UPEC was responsive to several environmental stresses and deletion or overexpression of MiaA interferes with the stress resistance and virulence properties of UPEC. Taken together, this thesis defines the robust nature and resilience of intracellular UPEC reservoir populations and delineates sRNAs and MiaA as important regulators of stress resistance and persistence within the host.

In loving memory of Claire M. Bartsch and Marie G. Blango

CONTENTS

ABSTRACT iii

LIST OF TABLES ix

LIST OF FIGURES x

LIST OF ABBREVIATIONS AND ACRONYMS xiii

ACKNOWLEDGEMENTS xiv

Chapter

1. INTRODUCTION 1

    Thesis Summary 8
    References 8

2. PERSISTENCE OF UROPATHOGENIC *ESCHERICHIA COLI* IN THE FACE OF MULTIPLE ANTIBIOTICS 12

    Abstract 13
    Introduction 13
    Materials and Methods 14
    Results 15
    Discussion 18
    Acknowledgements 20
    References 20

3. FORCED RESURGENCE AND TARGETING OF INTRACELLULAR UROPATHOGENIC *ESCHERICHIA COLI* RESERVOIRS 22

    Abstract 23
    Introduction 24
    Results 28
    Discussion 41
    Materials and Methods 46
    Acknowledgements 51
    References 52

4. SMALL NONCODING RNAS REGULATE THE STRESS RESISTANCE AND VIRULENCE PROPERTIES OF UROPATHOGENIC *ESCHERICHIA COLI* 56

Abstract 57
Introduction 58
Materials and Methods 60
Results and Discussion 70
Concluding Remarks 86
Acknowledgements 88
References 88
Supplemental Material 97

5. IDENTIFICATION OF SMALL NONCODING RNAS IN UROPATHOGENIC ESCHERICHIA COLI 99

Abstract 100
Introduction 101
Results 108
Discussion 141
Materials and Methods 145
Acknowledgements 151
References 152

6. BALANCED INPUT FROM THE TRNAPRENYLTRANSFERASE MIAA CONTROLS THE STRESS RESISTANCE AND VIRULENCE POTENTIAL OF UROPATHOGENIC *ESCHERICHIA COLI* 159

Abstract 160
Author Summary 161
Introduction 161
Results 171
Discussion 191
Materials and Methods 194
Acknowledgements 203
References 203
Supplemental Material 209

7. DISCUSSION 210

References 224

Appendix

A. BACTERIAL LANDLINES: CONTACT-DEPENDENT SIGNALING IN BACTERIAL POPULATIONS 228

B. UROPATHOGENIC *ESCHERICHIA COLI* INDUCES SERUM AMYLOID A IN MICE FOLLOWING URINARY TRACT AND SYSTEMIC INOCULATION 234

LIST OF TABLES

Table PAGE

2.1 Antibiotics utilized in this study 15

2.2 Recurrence after antibiotic treatments in human studies 19

4.1 Bacterial strains and plasmids 61

4.2 Oligonucleotides employed during the study 62

4.3 Tested sRNA molecules 71

5.1 Broad scale sRNA identification studies 102

5.2 Deep sequencing statistics 111

5.3 Known sRNA in UTI89 113

5.4 Candidate sRNA 119

5.5 Target RNA predictions 128

5.6 Strains and plasmids used in this study 136

5.7 Oligonucleotides employed during the study 137

6.1 Bacterial strains and plasmids 177

6.2 Oligonucleotides employed during the study 195

LIST OF FIGURES

FIGURE PAGE

1.1 UPEC pathogenesis 4

2.1 Antibiotic effects on intracellular UPEC and host cell cytotoxicity 16

2.2 Antibiotic effects on UPEC biofilms grown *in vitro* at 37°C in M9 medium 17

2.3 Antibiotic susceptibility of UPEC within mouse bladders 17

2.4 Antibiotic susceptibility of IBCs 18

3.1 Chitosan affects *in vitro* growth of UPEC 29

3.2 Chitosan treatment results in increased biofilm formation and filamentous UPEC 31

3.3 Chitosan treatment decreases BEC invasion despite increased association 32

3.4 UPEC invades basal and intermediate bladder epithelial cells 35

3.5 Chitosan treatment causes resurgence of UPEC reservoir into the bladder lumen 36

3.6 Chitosan treatment coupled with antibiotic treatment reduces bacterial titers 38

3.7 Chitosan and antibiotic treatment fails to prevent recurrence 40

3.8 Model of UPEC action 44

4.1 sRNAs modulate biofilm formation, swim motility, and stress resistance of UTI89 73

4.2 Spot 42 and MicC modulate oxidative stress resistance in UTI89 77

4.3 Deletion of *spf* alters key metabolic processes in UTI89 82

4.4 Spot 42 modulates interactions between UTI89 and host bladder cells ... 83

4.5 Spot 42 promotes the intracellular persistence of UTI89 in a murine model of UTI ... 84

4.S1 Metabolic profile of UTI89 and UTI89Δ*spf* ... 97

5.1 Experimental approach ... 109

5.2 Identification of UPEC sRNAs ... 117

5.3 Genomic loci for each candidate sRNA ... 120

5.4 Growth and biofilm formation of candidate knockouts ... 138

5.5 UsrB represses bladder colonization ... 142

6.1 UTI89Δ*miaA* exhibits wild type growth despite severely altered metabolism ... 164

6.2 UTI89Δ*miaA* grows poorly under stress conditions in a dose-dependent manner ... 173

6.3 MiaA protein level responds to stressors ... 179

6.4 MiaA/B differentially regulate UPEC motility and biofilm formation ... 180

6.5 MiaA promotes UPEC infection of a murine host ... 184

6.6 MiaA contributes to α-hemolysin formation, possibly through manipulation of host chaperone production ... 188

6.S1 *miaA*/*B* mutants exhibit no effects on host cell invasion, association, or intracellular replication ... 209

7.1 Model of UPEC Pathogenesis ... 215

A.1 Model of the contact-dependent inhibition system ... 231

B.1 Induction and localization of SAA1/2 following inoculation of the bladder with UPEC ... 236

B.2 Quantification of SAA mRNA expression in response to UPEC ... 237

B.3 ELISA of mouse sera at different time points after infection..... 238

B.4 Growth of UTI89, F11, and MG1655 ± SAA 239

B.5 Biofilm formation by the UPEC isolates UTI89 and F11 ± SAA..... 239

LIST OF ABBREVIATIONS AND ACRONYMS

A-37 ..... Adenosine-37
ASN ..... Acidified sodium nitrite
BEC ..... Bladder epithelial cell
cAMP ..... Cyclic adenosine monophosphate
CDI ..... Contact-dependent inhibition
CFU ..... Colony forming unit
CIP ..... Ciprofloxacin
CoA ..... Coenzyme A
CRP ..... cAMP receptor protein
DMSO ..... Dimethyl sulfoxide
EDTA ..... Ethylenediaminetetraacetic acid
FOF ..... Fosfomycin
GC\MS ..... Gas Chromatography \ Mass Spectroscopy
GFP ..... Green fluorescent protein
GrxB. ..... Glutaredoxin 2
GSNO ..... S-nitrosoglutathione
HlyA ..... α-hemolysin
IBC ..... Intracellular bacterial community
IPTG ..... Isopropyl β-D-1-thiogalactopyranoside
LB ..... Luria-Bertani broth
LPS ..... Lipopolysaccharide
MES ..... 2-(N-morpholino)ethanesulfonic acid
mRNA ..... Messenger RNA
MV ..... Methyl viologen
ORF ..... Open reading frame
PanC ..... Pantothenate synthetase
PBS ..... Phosphate Buffered Saline
PCR ..... Polymerase chain reaction
PFA ..... Paraformaldehyde
RNA-Seq ..... RNA deep sequencing
RNA ..... Ribosomal RNA
tRNA ..... Transfer RNA
SAA ..... Serum amyloid A
SEM ..... Scanning electron microscopy
SPX ..... Sparfloxacin
sRNA ..... Small, non-coding RNA
UPEC ..... Uropathogenic *Escherichia coli*
UTI ..... Urinary tract infection

ACKNOWLEDGEMENTS

I am greatly indebted to my mentor, Matt Mulvey, for his devotion and guidance during the course of my thesis research. His continual support, upbeat attitude, and reckless optimism were key to my success as both a researcher and as a human being. I would also like to thank all members of the lab, past and present, for their constructive criticism and motivation over the years. I am extremely grateful to my thesis committee, John, Brenda, Sherwood, and David, for their continual guidance and assurances along the way. It is also absolutely essential to thank Janis Weis and the Microbial Pathogenesis Training Grant for both funding and personal support. Janis is a wonderful ally and has always ben there to help when needed. I would like to thank our collaborators in Slovenia for their constant optimism and support. I would also like to extend my greatest gratitude to Kael Fischer for his continuous support and bioinformatics prowess. Without Kael, I would still be trying to get python to print my name.

I would like to thank my mom for being continually supportive, loving, and critical—all wonderful traits which I would not trade for the world. I would also like to thank the rest of my family for everything they have done for me. My girlfriend Amelia also deserves great thanks for the many sacrifices she has made towards my research career. She has been great throughout this entire process. Finally, I

would like to remember and thank those who are no longer with us who have helped me along the way.

CHAPTER 1

INTRODUCTION

Escherichia coli is a Gram-negative, rod-shaped bacterium commonly found in the lower intestine of warm-blooded animals. In the intestine, commensal *E. coli* strains provide the host with essential vitamins and advantageous enzymes for digestion of metabolites. However, outside of the intestine, some *E. coli* strains can colonize diverse host niches to cause diseases ranging from neonatal meningitis to urinary tract infection (UTI) (31). Uropathogenic *E. coli* (UPEC) are the primary etiologic agent of UTI and rank among the most common bacterial infections (11, 12, 16). UTIs thus constitute a significant burden on the global health-care system, responsible for over 7.4 million physicians visits yearly, costing ~1.6 billion dollars in the U.S. alone (11, 12).

UTIs can be divided into two major classes: acute uncomplicated UTIs are self-limiting infections, whereas chronic infections are highlighted by their persistent nature and frequent association with underlying anatomical and/or immunological problems. Acute cystitis commonly presents with symptoms such as dysuria (burning during urination), frequent urination, urgency, and pyuria (cloudy urine). Chronic UTIs display symptoms similar to acute infection, but are generally more resistant to antibiotic treatments, persist over longer periods of time, and are coincident with higher levels of recurrence. In general, 25-45% of women will have an additional UTI within six months of an initial infection (7). This high rate of recurrence occurs despite treatment with antibiotics; however, increased treatment duration has shown some promise in preventing recurrence (22, 30). Additionally, the causative strain for both the index and recurrent

infection are often genetically identical, suggestive of a UPEC reservoir population present within the urinary tract or elsewhere within the host (25). Persistent UPEC reservoirs that are protected from antibiotics and most host defenses are proposed to be an important cause of both chronic and recurrent, or relapsing, UTIs.

In order to establish an infection, UPEC ascends into the bladder via the urethra and can replicate rapidly within the bladder lumen. A subpopulation of UPEC is able to adhere to and invade the large superficial epithelial cells that line the bladder lumen and take up residence (Figure 1.1) (10, 19, 20). Invasion of these superficial bladder cells occurs via a zipper-like endocytic mechanism, resulting in the uptake of UPEC within a membrane-bound vacuole. At this stage endocytosed UPEC may be trafficked back out of the epithelial cell into the bladder lumen, or enter into a late endosomal, lysosome-like compartment. These bacteria can form a long-lived-quiescent intracellular reservoir population that remains dormant and therefore less immunogenic. Alternatively, UPEC can replicate within the vacuole before breaking out into the cytoplasm, where they grow quite rapidly in conjunction with host cytokeratin intermediate filaments to form large intracellular bacterial communities (IBCs) (10, 15, 19). IBCs act as a dispersal system to propagate the infection throughout the bladder lumen, with bacteria replicating to upwards of ~5000 clones per IBC before causing disintegration of the host epithelial cell (2, 15). Dispersal from IBCs leads to reinoculation of the bladder lumen, seeding bacteria within neighboring and underlying epithelial cells. Exfoliation of bladder cells that contain IBCs may also

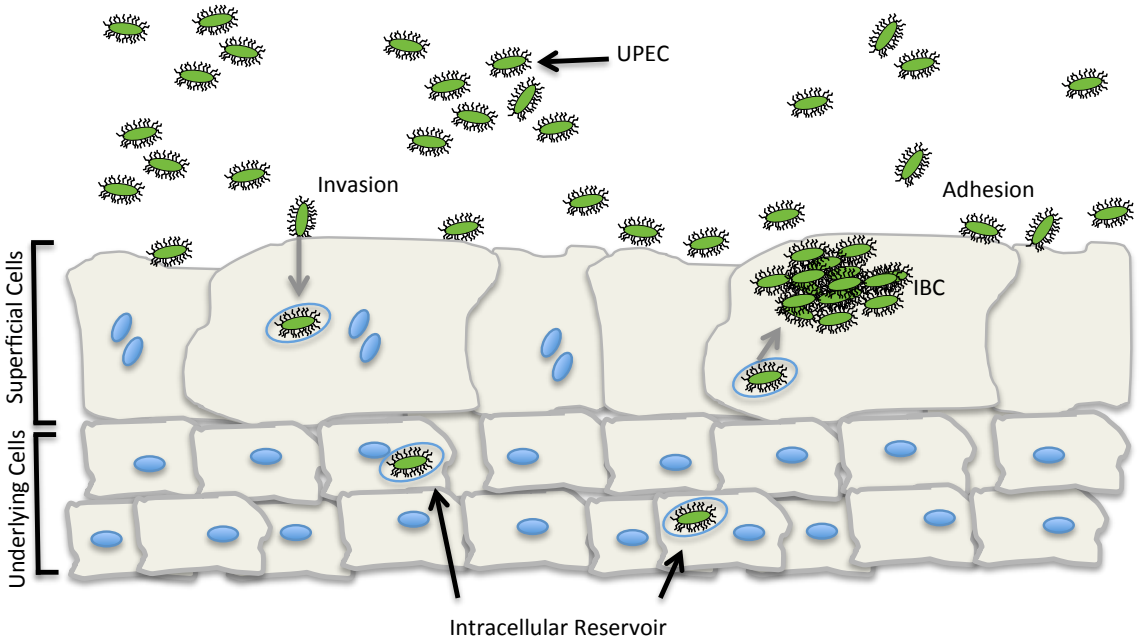

Figure. 1.1 UPEC pathogenesis

UPEC are able to enter the bladder and replicate within the urine. A subpopulation of bacteria adheres to, and infrequently invades the host epithelium to form intracellular populations of UPEC within endocytic vesicles. UPEC may then remain quiescent or begin to replicate within the vacuole, and ultimately in the cytosol in conjunction with host factors to form an IBC, which is involved in further dissemination of the infection.

promote the dispersion of UPEC outside of the host (24). Disruption of the host epithelium through IBC formation also facilitates bacterial penetration of the underlying intermediate and basal epithelial bladder cells, a process that is perpetuated by host immune mechanisms such as exfoliation of the bladder epithelium and the influx of neutrophils (10, 19). UPEC invasion of underlying tissues provides the bacteria with a stable niche due to the long half-life—roughly 52 weeks—of the urothelium (14). These entrenched, quiescent bacteria within the immature cells of the bladder are thought to form a reservoir capable of

reseeding the bladder lumen during chronic, recurrent, or relapsing infection. Once the reservoir population is established, subsequent rounds of infection occur as individual IBCs form, burst, and reinoculate the urinary tract.

Establishment and maintenance of a persistent infection is achieved through the coordinated efforts of innumerable virulence factors and other systems, including those that affect bacterial motility, adhesion to and invasion of epithelial cells, environmental sensing, immune evasion, and stress responses. UPEC have a variety of virulence factors, including multiple iron scavenging systems, adhesive organelles, and toxins such as α-hemolysin and cytotoxic necrotizing factor to disrupt host membranes, release nutrients, and manipulate host-signaling cascades (9, 29). UPEC also possess distinct polysaccharide capsules and sugar moieties on their outer membrane to reduce immunogenicity and limit exposure to environmental assaults. Relative to non-pathogenic isolates, pathogenic strains commonly exhibit increased resistance to nutrient limitation and environmental stressors (29). As an example, bacterial pathogens may acquire multiple catalase genes to enhance resistance to oxidative stress or may encode numerous iron scavenging systems to obtain necessary iron from the environment or host (28).

In addition to virulence factors, all bacteria must have mechanisms for obtaining energy from the environment. An elegant study by Alteri et. al. recently identified several metabolic systems—protein import, gluconeogenesis, and the tricarboxylic acid cycle—as indispensible for UPEC virulence in the urinary tract (1). Glycolysis, the pentose-phosphate pathway, and the Entner-Doudoroff

pathway, all of which provide the cell with energy through the generation of pyruvate, were dispensable for virulence during UTI in this study (1). The superfluous nature of these metabolic systems in the urinary tract is in contrast to their requirement in the intestinal tract, suggesting that the ability to utilize alternate energy sources and metabolic pathways significantly impacts the fitness of UPEC during a UTI. Metabolic intermediates also play a direct role in bacteria-to-bacteria signaling through processes like quorum sensing, where concentrations of metabolic breakdown products signal the bacterial population to undergo a specific behavior, such as biofilm formation (17). Similar to the mechanisms of quorum sensing, UPEC recognize host-produced metabolic compounds using them as a sort of molecular roadmap. Recognition of the amino acid D-serine, which is produced in abundance in the host urinary tract, signals UPEC to up-regulate pathways that optimize its growth, motility, and virulence within the bladder lumen (3, 23). Combined, these observations indicate complex interplay between bacterial metabolic processes, virulence, and niche recognition during the course of a UTI.

In bacteria, a multitude of regulatory mechanisms are in place to control the expression of virulence factors, metabolic enzymes, and stress response proteins. These mechanisms range from altering promoter binding efficiency and transcription factor abundance to regulation by posttranslational modifications. One of the most common forms of bacterial regulation is the two-component system, where a membrane-bound histidine kinase senses environmental stimuli and transfers a signal to a response regulator, which in turn alters gene

expression. Posttranscriptional control of gene expression by small, non-coding RNAs (sRNAs) comprises another important regulatory mechanism. sRNAs, ranging in size from 50-500 nucleotides (nt), base-pair with cognate, target mRNA sequences, often in the presence of the RNA chaperone Hfq, and thereby influence mRNA translation and stability. sRNA molecules regulate diverse cellular activities, from outer membrane porin expression and basal metabolic function to stress response and virulence (4, 5, 8, 18). Most sRNA molecules appear to function primarily in fine-tuning gene expression (26).

Contrasting with gene specific regulation by sRNA molecules are more global regulatory mechanisms such as translational control through tRNA modification. tRNAs can be modified with upwards of 100 different modifications, ranging from methylation marks to isoprenyl groups (21). Each of these modifications affects the process of translation differently, but most appear to affect translational rates and fidelity. Several tRNA modifying enzymes regulate large subsets of tRNA molecules and can have a substantial impact on protein expression (6, 13, 27). These modifying enzymes, such as MiaA and Tgt, are postulated to serve as global regulators of stress response (6, 13, 27). Regulation of these enzymes is hypothesized to enable rapid, broad-scale changes in response to environmental stresses directly altering protein abundance and, perhaps, functionality. Combined, sRNAs and tRNA modifying enzymes may provide bacteria with the ability to fine-tune gene expression to more precisely respond to environmental stimuli, optimizing metabolic activities, stress response pathways, and virulence.

Thesis Research Summary

The thesis research compiled here aims to define molecular aspects of the UPEC reservoir population during infection of the urinary tract through the use of *in vitro* assays and a murine model of infection. Chapters 2 and 3 will relate research towards understanding the confounding issues of UTI recurrence, namely the inability to clear the UPEC reservoir population from the bladder. Chapters 4 and 5 will transition to the identification and characterization of sRNA regulatory networks in UPEC, highlighting contributions of specific sRNA molecules to stress response and persistence. Chapter 6 will then describe the interplay between translational regulation by the tRNA modifying enzyme MiaA, metabolic flexibility, and stress response during a UTI. Chapters 4 through 6 begin to elucidate the molecular mechanisms that enable UPEC to persist within the urinary tract, despite attacks from the host immune system and other harsh environmental stressors. Chapter 7 will synthesize the content of this thesis and provide extrapolations on what is to come in the field of UPEC pathogenesis. Finally, several appendices will delineate bacterial communication through direct interactions with their neighbors, as well as mechanisms used by the host to influence the outcome of infection.

References

1. **Alteri, C. J., S. N. Smith, and H. L. Mobley.** 2009. Fitness of *Escherichia coli* during urinary tract infection requires gluconeogenesis and the TCA cycle. PLoS Pathog. **5:**e1000448.

2. **Anderson, G. G., K. W. Dodson, T. M. Hooton, and S. J. Hultgren.** 2004. Intracellular bacterial communities of uropathogenic *Escherichia coli* in urinary tract pathogenesis. Trends Microbiol. **12:**424-430.

3. **Anfora, A. T., and R. A. Welch.** 2006. DsdX is the second D-serine transporter in uropathogenic *Escherichia coli* clinical isolate CFT073. J. Bacteriol. **188:**6622-6628.

4. **Beisel, C. L., and G. Storz.** 2011. The base-pairing RNA spot 42 participates in a multioutput feedforward loop to help enact catabolite repression in *Escherichia coli*. Molecular Cell **41:**286-297.

5. **Beisel, C. L., T. B. Updegrove, B. J. Janson, and G. Storz.** 2012. Multiple factors dictate target selection by Hfq-binding small RNAs. EMBO J. 31(8):1961-74.

6. **Bjork, G. R., J. U. Ericson, C. E. Gustafsson, T. G. Hagervall, Y. H. Jonsson, and P. M. Wikstrom.** 1987. Transfer RNA modification. Annual Review of Biochemistry **56:**263-287.

7. **Blango, M. G., and M. A. Mulvey.** 2010. Persistence of uropathogenic *Escherichia coli* in the face of multiple antibiotics. Antimicrob. Agents Chemother. **54:**1855-1863.

8. **Chen, S., A. Zhang, L. B. Blyn, and G. Storz.** 2004. MicC, a second small-RNA regulator of Omp protein expression in *Escherichia coli*. J. Bacteriol. **186:**6689-6697.

9. **Dhakal, B. K., and M. A. Mulvey.** 2012. The UPEC pore-forming toxin alpha-hemolysin triggers proteolysis of host proteins to disrupt cell adhesion, inflammatory, and survival pathways. Cell Host Microbe **11:**58-69.

10. **Eto, D. S., J. L. Sundsbak, and M. A. Mulvey.** 2006. Actin-gated intracellular growth and resurgence of uropathogenic *Escherichia coli*. Cellular Microbiology **8:**704-717.

11. **Foxman, B.** 2003. Epidemiology of urinary tract infections: incidence, morbidity, and economic costs. Dis. Mon. **49:**53-70.

12. **Foxman, B.** 1990. Recurring urinary tract infection: incidence and risk factors. Am. J. Public Health **80:**331-333.

13. **Hagervall, T. G., J. U. Ericson, K. B. Esberg, J. N. Li, and G. R. Bjork.** 1990. Role of tRNA modification in translational fidelity. Biochimica et Biophysica acta **1050:**263-266.

14. **Hicks, R. M.** 1975. The mammalian urinary bladder: an accommodating organ. Biol. Rev. Camb. Philos. Soc. **50:**215-246.

15. **Justice, S. S., C. Hung, J. A. Theriot, D. A. Fletcher, G. G. Anderson, M. J. Footer, and S. J. Hultgren.** 2004. Differentiation and developmental pathways of uropathogenic *Escherichia coli* in urinary tract pathogenesis. Proc. Natl. Acad. Sci. U. S. A. **101:**1333-1338.

16. **Kaper, J. B., J. P. Nataro, and H. L. Mobley.** 2004. Pathogenic *Escherichia coli*. Nat. Rev. Microbiol. **2:**123-140.

17. **Kostakioti, M., M. Hadjifrangiskou, J. S. Pinkner, and S. J. Hultgren.** 2009. QseC-mediated dephosphorylation of QseB is required for expression of genes associated with virulence in uropathogenic *Escherichia coli*. Mol. Microbiol. **73:**1020-1031.

18. **Moller, T., T. Franch, C. Udesen, K. Gerdes, and P. Valentin-Hansen.** 2002. Spot 42 RNA mediates discoordinate expression of the *E. coli* galactose operon. Genes Dev. **16:**1696-1706.

19. **Mulvey, M. A., J. D. Schilling, and S. J. Hultgren.** 2001. Establishment of a persistent *Escherichia coli* reservoir during the acute phase of a bladder infection. Infect. Immun. **69:**4572-4579.

20. **Mysorekar, I. U., and S. J. Hultgren.** 2006. Mechanisms of uropathogenic *Escherichia coli* persistence and eradication from the urinary tract. Proc. Natl. Acad. Sci. U. S. A. **103:**14170-14175.

21. **Persson, B. C.** 1993. Modification of tRNA as a regulatory device. Mol. Microbiol. **8:**1011-1016.

22. **Raz, R., and S. Boger.** 1991. Long-term prophylaxis with norfloxacin versus nitrofurantoin in women with recurrent urinary tract infection. Antimicrob. Agents Chemother. **35:**1241-1242.

23. **Roesch, P. L., P. Redford, S. Batchelet, R. L. Moritz, S. Pellett, B. J. Haugen, F. R. Blattner, and R. A. Welch.** 2003. Uropathogenic *Escherichia coli* use d-serine deaminase to modulate infection of the murine urinary tract. Mol. Microbiol. **49:**55-67.

24. **Rosen, D. A., T. M. Hooton, W. E. Stamm, P. A. Humphrey, and S. J. Hultgren.** 2007. Detection of intracellular bacterial communities in human urinary tract infection. PLoS Med. **4:**e329.

25. **Russo, T. A., A. Stapleton, S. Wenderoth, T. M. Hooton, and W. E. Stamm.** 1995. Chromosomal restriction fragment length polymorphism

26. **Shimoni, Y., G. Friedlander, G. Hetzroni, G. Niv, S. Altuvia, O. Biham, and H. Margalit.** 2007. Regulation of gene expression by small non-coding RNAs: a quantitative view. Mol. Syst. Biol. **3:**138.

27. **Urbonavicius, J., Q. Qian, J. M. Durand, T. G. Hagervall, and G. R. Bjork.** 2001. Improvement of reading frame maintenance is a common function for several tRNA modifications. EMBO J. **20:**4863-4873.

28. **Vagrali, M. A.** 2009. Siderophore production by uropathogenic *Escherichia coli*. Indian J. Pathol. Microbiol. **52:**126-127.

29. **Wiles, T. J., R. R. Kulesus, and M. A. Mulvey.** 2008. Origins and virulence mechanisms of uropathogenic *Escherichia coli*. Exp. Mol. Pathol. **85:**11-19.

30. **Williams, G., and J. C. Craig.** 2011. Long-term antibiotics for preventing recurrent urinary tract infection in children. Cochrane Database Syst. Rev**:**CD001534.

31. **Yan, F., and D. B. Polk.** 2004. Commensal bacteria in the gut: learning who our friends are. Curr. Opin. Gastroenterol. **20:**565-571.

CHAPTER 2

PERSISTENCE OF UROPATHOGENIC *ESCHERICHIA COLI* IN THE FACE OF MULTIPLE ANTIBIOTICS

Reprint of: Blango, M.G. and Mulvey, M.A. (2010). Persistence of Uropathogenic *Escherichia coli* in the Face of Multiple Antibiotics. Antimicrobial Agents and Chemotherapy 54(5), 1855-1863. Reprint with permission of Antimicrobial Agents and Chemotherapy.

ANTIMICROBIAL AGENTS AND CHEMOTHERAPY, May 2010, p. 1855–1863 Vol. 54, No. 5
0066-4804/10/$12.00 doi:10.1128/AAC.00014-10

Persistence of Uropathogenic *Escherichia coli* in the Face of Multiple Antibiotics[▽]

Matthew G. Blango and Matthew A. Mulvey*

Division of Cell Biology and Immunology, Department of Pathology, University of Utah, Salt Lake City, Utah 84112

Received 5 January 2010/Returned for modification 4 February 2010/Accepted 5 March 2010

Numerous antibiotics have proven to be effective at ameliorating the clinical symptoms of urinary tract infections (UTIs), but recurrent and chronic infections continue to plague many individuals. Most UTIs are caused by strains of uropathogenic *Escherichia coli* (UPEC), which can form both extra- and intracellular biofilm-like communities within the bladder. UPEC also persist inside host urothelial cells in a more quiescent state, sequestered within late endosomal compartments. Here, we tested a panel of 17 different antibiotics, representing seven distinct functional classes, for their effects on the survival of the reference UPEC isolate UTI89 within both biofilms and host bladder urothelial cells. All but one of the tested antibiotics prevented UTI89 growth in broth culture, and most were at least modestly effective against bacteria present within *in vitro*-grown biofilms. In contrast, only a few of the antibiotics, including nitrofurantoin and the fluoroquinolones ciprofloxacin and sparfloxacin, were able to eliminate intracellular bacteria in bladder cell culture-based assays. However, in a mouse UTI model system in which these antibiotics reached concentrations in the urine specimens that far exceeded minimal inhibitory doses, UPEC reservoirs in bladder tissues were not effectively eradicated. We conclude that the persistence of UPEC within the bladder, regardless of antibiotic treatments, is likely facilitated by a combination of biofilm formation, entry of UPEC into a quiescent or semiquiescent state within host cells, and the stalwart permeability barrier function associated with the bladder urothelium.

Urinary tract infections (UTIs) currently rank among the most prevalent of infectious diseases worldwide, with chronic and recurrent infections being especially problematic (20). The primary etiologic agents associated with UTIs are strains of uropathogenic *Escherichia coli* (UPEC) (19). Although often categorized as extracellular pathogens, UPEC can in fact invade a number of host cell types, including the terminally differentiated superficial facet cells and less mature intermediate and basal epithelial cells that comprise the stratified layers of the bladder urothelium (9, 45). Host cell invasion is proposed to facilitate both the establishment and persistence of UPEC within the urinary tract.

UPEC entry into bladder epithelial cells occurs via an actin- and microtubule-dependent process that is mediated by type 1 pili, which are filamentous adhesive organelles that are encoded by virtually all UPEC isolates (10, 38, 60). The FimH adhesin associated with the distal tips of type 1 pili binds mannose-containing glycoprotein host receptors, which include uroplakin (specifically UP1a) and α3β1 integrin complexes (16, 63). Uroplakin plaques coat nearly the entire lumenal surface of the bladder, and their internalization likely facilitates UPEC entry into terminally differentiated superficial bladder cells (5, 41, 43, 45, 60, 63). Alternately, α3β1 integrin receptor complexes, which are more widely expressed within the urothelium and elsewhere, can mediate UPEC invasion of less mature bladder cells via a clathrin-dependent pathway (15, 16). Once internalized, UPEC can be either translocated back out of the host cells or trafficked into late endosomal compartments where they can persist for the long term in a seemingly quiescent state, often bound by a meshwork of actin filaments (5, 17, 44, 46, 56). Alternatively, within the superficial facet cells of the bladder where actin filaments are typically sparse, UPEC can break into the host cytosol and rapidly multiply, forming large biofilm-like inclusions in close association with host intermediate filaments (1, 17, 30, 44). These inclusions, known as intracellular bacterial communities (IBCs), have been equated in military parlance to temporary beachheads, foci in which UPEC numbers are amplified before spreading out to infect surrounding superficial cells and the underlying immature cells of the bladder urothelium (53).

As a whole, the urothelium functions as a permeability barrier on par in strength with the blood-brain barrier (2, 4). Disruption of this barrier during the course of a UTI can occur as a consequence of UPEC-induced exfoliation of infected bladder cells and the influx of neutrophils and other inflammatory responses (43, 45). While these events can be viewed as useful host defense mechanisms, they also provide UPEC with greater access to host tissues. The capacity of UPEC to invade all layers of the urothelium, as well as the development of IBCs and extracellular biofilms, is correlated with enhanced levels of UPEC persistence within the host (23, 30, 32, 43, 44, 46, 57, 62). The establishment of quiescent intracellular bacterial reservoirs within either immature or superficial bladder epithelial cells may conceal UPEC from many host immunosurveillance mechanisms, while the development of IBCs and extracellular biofilms may enable UPEC to better resist the antimicrobial activities of neutrophils and other host defenses.

Biofilm formation and host cell invasion may also provide UPEC with enhanced protection against antibiotic treatments. Relative to planktonic bacteria, biofilm-associated microbes are by and large better equipped to survive treatments with

* Corresponding author. Mailing address: Pathology Department, Division of Cell Biology and Immunology, University of Utah, 15 North Medical Drive East, Salt Lake City, UT 84112-0565. Phone: (801) 581-5967. Fax: (801) 581-4517. E-mail: mulvey@path.utah.edu.
▽ Published ahead of print on 15 March 2010.

antibiotics (21, 58). The inability of many antibiotics to readily cross host membranes may further limit their effectiveness against intracellular bacteria. This problem is likely exacerbated by UPEC infiltration of host cells within the deeper layers of the urothelial barrier. In addition, the quiescent nature of some intracellular UPEC populations could render them resistant to antibiotics that primarily target replicating microbes. The challenge associated with ridding the bladder of UPEC has been illustrated in mouse UTI model systems in which the antibiotics gentamicin, cefuroxime, trimethoprim-sulfamethoxazole (SXT), and the extended-spectrum penicillin drug amdinocillin had little effect on bacterial titers within bladder tissue, even though urine titers were drastically reduced (26, 32, 43, 45, 52). These and related observations indicated that recurrent UTIs in many individuals, including those who receive antibiotic treatments, may in actuality be relapses caused by the resurgence of UPEC from intracellular bacterial reservoirs. Epidemiological studies lend credence to this possibility, demonstrating that the bacteria responsible for recurrent UTIs are identical to the microbes that caused the initial acute infections in up to 68% of patients (6, 8, 27, 28, 31, 42, 51). In light of these findings, it has been suggested that more penetrant antibiotics might better eliminate UPEC reservoirs from the bladder and consequently reduce the incidence of chronic and recurrent UTIs (9, 32). Here, we address this possibility by testing the effects of a range of functionally distinct antibiotics on intracellular and biofilm-associated UPEC using both *in vitro* and *in vivo* assays.

MATERIALS AND METHODS

Bacteria and bladder cell culture. The UPEC cystitis isolate UTI89 and the recombinant strain UTI89/pGEN-GFP(LVA) have been described previously (7, 44, 61). Bacteria were grown from frozen stocks in either Luria-Bertani (LB) broth or M9 minimal medium (6 g/liter Na_2HPO_4, 3 g/liter KH_2PO_4, 1 g/liter NH_4Cl, 0.5 g/liter NaCl, 1 mM $MgSO_4$, 0.1 mM $CaCl_2$, 0.1% glucose, 0.0025% nicotinic acid, 0.2% casein amino acids, and 16.5 μg/ml thiamine in H_2O) at 37°C. The human bladder epithelial cell line 5637 (ATCC HTB-9) was maintained at 37°C and 5% CO_2 in RPMI 1640 medium supplemented with 10% heat-inactivated fetal bovine serum (HyClone).

Antibiotics. All antibiotics were purchased from Sigma-Aldrich and used at the final concentrations indicated. Stocks were prepared as follows: penicillin (100 mg/ml in H_2O), nafcillin (120 mg/ml in H_2O), cefadroxil (30 mg/ml in phosphate-buffered saline [PBS] diluted 1:1 with H_2O), trimethoprim-sulfamethoxazole (30 and 20 mg/ml, respectively, in H_2O), ofloxacin (100 mg/ml in H_2O), ciprofloxacin (100 μg/ml in H_2O for *in vitro* assays and 40 mg/ml for *in vivo* use), norfloxacin (100 mg/ml in H_2O), levofloxacin (30 mg/ml in H_2O), sparfloxacin (100 μg/ml in H_2O for *in vitro* assays and 14 mg/ml for *in vivo* use), nalidixic acid (100 mg/ml in H_2O), nitrofurantoin (100 mg/ml in dimethyl sulfoxide [DMSO]), fosfomycin (100 mg/ml in 50% methanol for *in vitro* assays and 20 mg/ml for *in vivo* use), tetracycline (5 mg/ml in H_2O), gentamicin (80 mg/ml in H_2O for *in vitro* assays or 4 mg/ml for *in vivo* use), kanamycin (50 mg/ml in H_2O), and amikacin (200 mg/ml in H_2O). NaOH (1 N) was added dropwise to solubilize stocks of trimethoprim-sulfamethoxazole, ofloxacin, ciprofloxacin, norfloxacin, levofloxacin, and sparfloxacin. Diluents alone were used as negative controls in all assays.

Intracellular bacterial survival assays. UTI89 was grown at 37°C for 24 h in static LB broth to induce type 1 pilus expression. Triplicate sets of confluent 5637 bladder epithelial cell monolayers grown in 24-well tissue culture plates were infected with UTI89 using a multiplicity of infection of ~15 bacteria per host cell. To facilitate and synchronize bacterial contact with the host cells, plates were centrifuged at 600 × *g* for 5 min at the start of infection. After a 2-h incubation at 37°C, samples were washed three times with PBS containing Ca^{2+} and Mg^{2+} (PBS^{2+}) to remove any nonadherent bacteria. Monolayers were then incubated for another 2 h with complete RPMI medium plus 100 μg/ml of gentamicin to kill extracellular bacteria. Following additional washes with PBS^{2+}, fresh medium containing a lower concentration of gentamicin (10 μg/ml) was added, and incubations were continued for another 14 h. This submaximal concentration of gentamicin was used to prevent extracellular growth of UPEC while limiting possible leaching of the antibiotic into the host cells during longer incubations (13). Monolayers were then washed with PBS^{2+} and incubated for another 12 h in fresh medium ± the indicated antibiotics. After final washes in PBS^{2+}, host cells were lysed in PBS plus 0.4% Triton X-100, and bacteria present within the lysates were enumerated by plating serial dilutions on LB agar plates.

Cytotoxicity assays. Luciferase-based lactate dehydrogenase (LDH) cytotoxicity assays were performed using the CytoTox-Glo cytotoxicity assay (Promega), according to the instructions from the manufacturer. Host cell integrity was also assessed using trypan blue (0.4%) exclusion assays, according to standard protocols (Sigma-Aldrich).

Biofilm assays. *In vitro* microtiter plate-based biofilm assays were performed as previously described (39). Briefly, UTI89 was diluted 1:100 from overnight shaking cultures into M9 medium, and triplicate 100-μl samples in 96-well pinchbar flat-bottomed polystyrene microtiter plates with lids (Nunc) were incubated for 48 h without shaking at 37°C. Nonadherent bacteria were then removed, and fresh M9 medium was added to each well ± antibiotics, as indicated. After an additional 24 h of incubation, the wells were washed twice with H_2O prior to addition of crystal violet (150 μl of a 0.1% solution in water; Sigma-Aldrich). After a 10-min incubation at room temperature, the wells were rinsed twice with H_2O and air dried. Dimethyl sulfoxide (200 μl; Sigma-Aldrich) was then added to each well, and the plates were shaken vigorously for 15 min on an orbital shaker to solubilize the dye. A 150-μl aliquot from each well was transferred to a fresh microtiter plate, and A_{562} was measured using a Synergy HT multidetection microplate reader (BioTek Instruments, Inc.). In separate experiments, viable bacteria within biofilms treated with or without antibiotics were visualized using the Live/Dead BacLight bacterial viability kit (Molecular Probes), according to manufacturer's instructions.

***In vivo* antibiotic protection assays.** Seven- to eight-week-old female CBA/J mice (Jackson Laboratory) were anesthetized via isoflurane inhalation and slowly inoculated via transurethral catheterization with 50 μl of a bacterial suspension (~10^7 CFU from 24-h static LB broth cultures of UTI89) in PBS as previously described (43). Bacterial reflux into the kidneys using this procedure is rare, occurring in less than 1% of the test animals. At 3 days postinoculation, antibiotic treatments were initiated by administering one dose of antibiotic daily for 3 consecutive days. Gentamicin (200 μg) was given subcutaneously, while ciprofloxacin (2 mg), sparfloxacin (700 μg), and fosfomycin (1 mg) were given orally by gavaging. Control animals were given water alone by gavaging. All antibiotics were delivered in 50-μl volumes. Mice were sacrificed 3 days after the final antibiotic treatment (day 9 postinoculation). At this time point, bladders were harvested aseptically, weighed, and homogenized in 1 ml PBS containing 0.025% Triton X-100. Bacterial titers within the homogenates were determined by plating serial dilutions on LB agar plates. Eleven mice total, from two independent experiments, were used for each condition tested. Mock-infected mice were housed in cages with the infected animals.

Disc diffusion assays. Antibiotic concentrations in mouse urine specimens were determined using disc diffusion assays modified from the Kirby-Bauer method (3). Two hours after administration of antibiotics, urine specimens were collected from mice by gently pressing their bladders over clean plastic wrap. Ten-microliter aliquots of urine obtained from individual mice were spotted onto 7-mm-diameter circular pieces of sterile filter paper, which were then placed on freshly plated lawns of UTI89 spread on LB agar plates. The diameter of clearance around each disc was measured after a 24-h incubation at 37°C. Filter discs containing known antibiotic concentrations were used to generate standard curves from which antibiotic levels in the urine specimens were calculated.

Antibiotic treatment of bladder homogenates. Three days postinoculation with UTI89, bladders from CBA/J mice were removed and homogenized in 1 ml PBS containing 0.025% Triton X-100. One hundred-microliter aliquots of the homogenates were then incubated for 4 h at 37°C ± gentamicin (400 μg/ml), ciprofloxacin (2 μg/ml), sparfloxacin (12 μg/ml), fosfomycin (700 μg/ml), or a combination of sparfloxacin and fosfomycin. Surviving bacteria present in the homogenates were then pelleted (5 min at 10,000 × *g*), washed in sterile PBS, and plated.

IBC quantification. CBA/J mice were infected with UTI89/pGEN-GFP(LVA) via transurethral catheterization. At 6 h postinoculation, mice were sacrificed, and bladders were removed, halved, splayed, and pinned down lumenal side up on silicon disks (Sylgard 184 silicone elastomer; Dow Corning Corp.) under Ringer solution (155 mM NaCl, 3 mM HCl, 2 mM $CaCl_2$, 1 mM $MgCl_2$, 3 mM NaH_2PO_4, 10 mM glucose, and 5 mM HEPES [pH 7.4]). Sparfloxacin (12 μg/ml)-fosfomycin (700 μg/ml) was then added as indicated. Green fluorescent protein (GFP)-positive IBCs were visualized and enumerated using a SZX10 stereomicroscope (Olympus) equipped with a Canon PowerShot A640 10.1 megapixel camera mounted via a CamAdapter kit.

TABLE 1. Antibiotics utilized in this study

Family/antibiotic	Primary function in *E. coli*	Effect on bacteria	Urine level (μg/ml)[a]	Amts tested (μg/ml)
β-Lactams	Cell wall synthesis inhibitor	Bactericidal		
Penicillin			597	200, 600, 1,000
Nafcillin		UPEC is resistant	285–1,188	120, 1,200, 1,800
Cefadroxil			1,200	800, 1,200, 1,600
Dihydrofolate reductase inhibitor	Folic acid synthesis inhibitor	Bacteriostatic		
Trimethoprim[b]			31–165	30, 100, 300
Sulfonamide	Folic acid synthesis inhibitor	Bacteriostatic		
Sulfamethoxazole[b]			10–133	20, 66, 200
Quinolones	Topoisomerase IV and DNA gyrase inhibitor	Bactericidal		
Ofloxacin			126–438	100, 400, 700
Ciprofloxacin			2	1, 2, 3
Norfloxacin			168–417	100, 300, 500
Levofloxacin			286	100, 200, 300
Sparfloxacin			12	12, 100, 400
Nalidixic acid			63–1,000	50, 800, 1,200
Tetracyclines	Protein synthesis inhibitor	Bacteriostatic/bactericidal		
Tetracycline			273	100, 250, 300
Aminoglycosides	Protein synthesis inhibitor	Bacteriostatic/bactericidal		
Gentamicin			400–500	100, 400, 800
Kanamycin			250–3,100	200, 1,000, 3,000
Amikacin			170–1,720	150, 1,000, 2,000
Miscellaneous				
Nitrofurantoin	DNA damage	Bactericidal	25–300	15, 300, 500
Fosfomycin	Cell wall synthesis inhibitor	Bactericidal	706	400, 700, 1,000

[a] See reference 36.
[b] Used in combination.

Statistics. *P* values were determined by Mann-Whitney U tests performed using Prism 5.01 software (GraphPad Software). Values of less than 0.05 were defined as significant.

RESULTS

Susceptibility of intracellular UPEC to antibiotics. The effectiveness of a panel of commonly prescribed antibiotics against intracellular UPEC was assessed using cell culture-based assays. The cystitis isolate UTI89 was allowed to invade monolayers of the bladder epithelial cell line 5637 for 2 h, after which extracellular bacteria were killed by addition of the host cell-impermeable antibiotic gentamicin. Following a 14-h incubation in the continued presence of gentamicin, infected monolayers were washed and treated for another 12 h with fresh gentamicin or 1 of 16 other antibiotics. These antibiotics represent several distinct functional classes, including inhibitors of cell wall synthesis, folic acid production, translation, DNA gyrase, and topoisomerase IV (Table 1). Infected monolayers were treated with antibiotic concentrations that were equal to or above the levels that normally accumulate in the urine of human patients during the course of treatment (36). Of note, in LB broth, UTI89 was sensitive to all of the tested antibiotics, with the exception of nafcillin, which served as a negative control.

Bacterial titers recovered at the end of the intracellular survival assays were normalized relative to samples treated with 800 μg/ml gentamicin (Fig. 1A). Nitrofurantoin and the quinolones ofloxacin, ciprofloxacin, norfloxacin, levofloxacin, and sparfloxacin were the most effective at eradicating intracellular UPEC. Quinolones are known to accumulate within host cells (48), and this likely contributes to their potency against internalized UPEC in these assays. Penicillin G, fosfomycin, and the drug combination trimethoprim-sulfamethoxazole (SXT) were no more effective than the control membrane-impermeable antibiotic gentamicin or other aminoglycosides. All of the tested antibiotics caused at least a small amount of cytotoxicity to the host cells relative to untreated controls, as determined using trypan blue exclusion assays (data not shown) and quantitation of host LDH release (Fig. 1B). However, the ability of an antibiotic to kill intracellular UPEC did not appear to correlate with cytotoxic effects on the host bladder cells. These results indicate that host cell invasion can provide UPEC with quantifiable survival advantages when confronted with a variety of different antibiotics, except for nitrofurantoin and most of the tested quinolones.

Antibiotic sensitivity of biofilm-associated UPEC. Antibiotic effects on biofilms formed by UTI89 were examined *in vitro* using standard microtiter plate-based assays (Fig. 2). Notably, biofilm formation in these types of *in vitro* assays often correlates with the ability of UPEC strains to cause relapsing infections in human patients (57). In our assays, all of the antibiotics, with the exception of nafcillin, appreciably reduced biofilm levels relative to untreated controls. Of the 17 antibiotics tested, the cell wall synthesis inhibitors penicillin G, cefadroxil, and fosfomycin had the most striking inhibitory effects on bio-

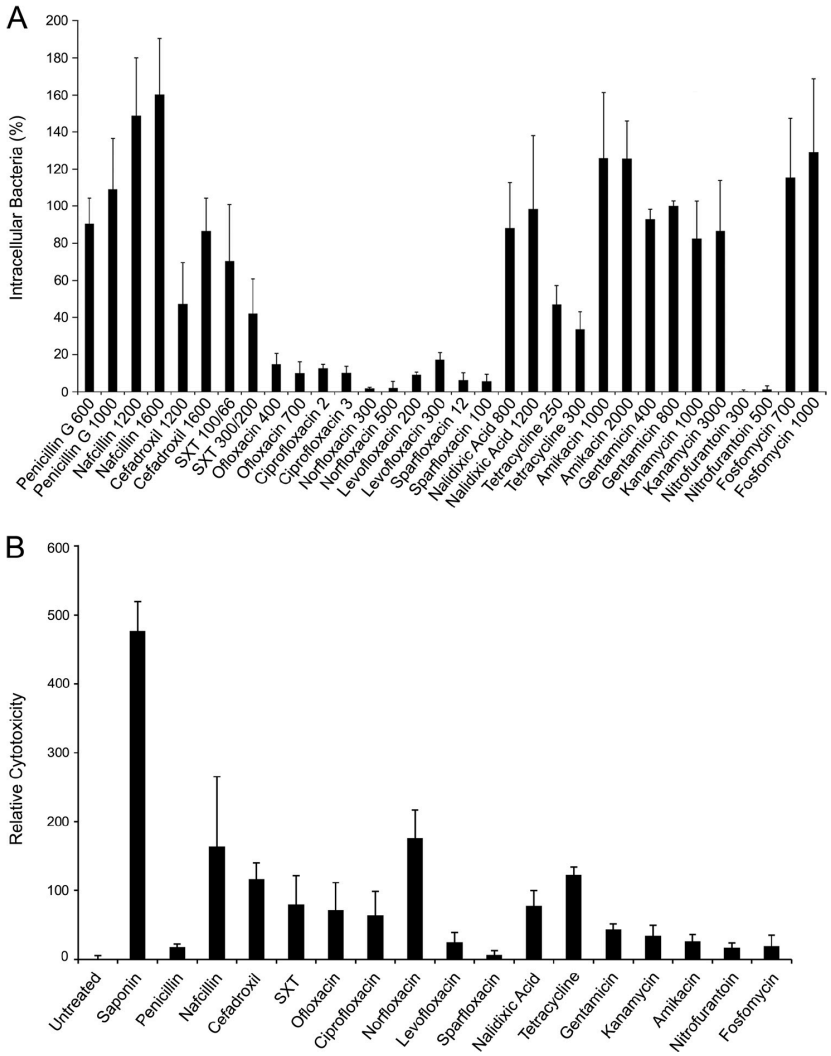

FIG. 1. Antibiotic effects on intracellular UPEC and host cell cytotoxicity. (A) 5637 bladder epithelial cell monolayers infected with UTI89 were incubated for 14 h in media containing 10 μg/ml gentamicin to prevent extracellular bacterial growth and to allow time for the establishment of UPEC within the host bladder cells. Following washes with PBS^{2+}, infected monolayers were incubated for an additional 12 h with two concentrations (μg/ml) of each of the different antibiotics being tested, as indicated. Surviving bacterial titers are presented relative to reference samples that were treated with 800 μg/ml gentamicin. Data represent the mean results ± SEM from three or more independent assays performed in triplicate. (B) Cytotoxic effects of each antibiotic (used at the higher of the two concentrations indicated in panel A) on 5637 bladder cells were determined after 12 h treatments by measuring LDH release. Cells treated with the pore-forming glycoside saponin were used as positive controls. Results indicate the means ± SEM from three independent experiments performed in duplicate or triplicate.

film persistence, followed closely by the quinolone sparfloxacin (Fig. 2). These antibiotics not only inhibited biofilm growth but also promoted the degeneration of preexisting biofilm communities. Microscopy coupled with Live/Dead staining validated these results and, in addition, confirmed the presence of viable UTI89 within the biofilms that withstood antibiotic treatments (data not shown).

Susceptibility of UPEC to antibiotics *in vivo* within the bladder. A subset of the antibiotics used above was tested for effectiveness against UPEC reservoirs in a mouse UTI model system. Adult female CBA/J mice were infected with UTI89 via transurethral inoculation, and antibiotic treatments were initiated 3 days later, allowing time for UTI89 to first establish reservoir populations within the bladder. Fosfomycin was chosen for its superior ability to clear biofilm growth *in vitro* (Fig. 2). Ciprofloxacin and sparfloxacin were tested as two separate types of quinolones shown to be effective against intracellular UTI89 in our *in vitro* assays (Fig. 1A). The antibiotic nitro-

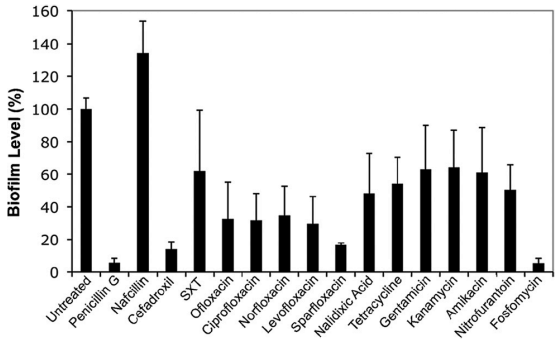

FIG. 2. Antibiotic effects on UPEC biofilms grown *in vitro* at 37°C in M9 medium. Biofilm levels were quantified relative to untreated controls following 24-h treatments with the indicated antibiotics, which were used at the higher of the two concentrations specified in Fig. 1A. Data represent the mean results ± SEM from three independent experiments performed in triplicate.

furantoin, although also very effective at clearing intracellular UPEC, was not used since it has notable toxic side effects in human subjects (55, 59). A combination treatment of sparfloxacin-fosfomycin was also included, with the idea that together these antibiotics might have enhanced activity against UPEC reservoirs within the bladder. Support for this possibility comes from previous work in which fosfomycin used in combination with another quinolone, ulifloxacin, significantly enhanced the clearance of *Pseudomonas aeruginosa* within biofilms better than either antibiotic on its own (40).

In our assays, antibiotics were administered to infected mice daily for 3 days, with control groups given either water alone or gentamicin. After an additional 3 days without antibiotic treatments (9 days total postinoculation), mice were sacrificed, and bacterial titers present within the bladders were enumerated. By waiting 3 days after cessation of the antibiotic treatments, we minimized the risk that residual levels of antibiotics in the host might kill off any surviving UPEC reservoirs during the bladder tissue homogenization process. Furthermore, this experimental setup represents a convenient model of how relapsing or persistent UTIs may proceed in human populations, with UPEC possibly maintaining a presence in the bladder in the days to weeks after antibiotic treatments have ended. Antibiotic concentrations employed in our *in vivo* assays were based on standard doses given to human patients, scaled down for use in mice (36). Disc diffusion assays with urine specimens collected from treated mice confirmed that each antibiotic reached concentrations in the urine that were sufficient to kill free-living UTI89. Specifically, within 2 h postadministration, effective antibiotic concentrations in the urine reached 2.0 mg/ml for gentamicin, 1.0 mg/ml for ciprofloxacin, 0.3 mg/ml for sparfloxacin, and 4.0 mg/ml for fosfomycin. These values are all at least 20-fold higher than the levels found in human urine following treatment (36).

As shown in Fig. 3A, UTI89 was able to persist within the bladder regardless of any of the antibiotic treatments used. While administration of ciprofloxacin, sparfloxacin, or the combination sparfloxacin-fosfomycin significantly reduced bacterial titers relative to controls treated with water alone, these antibiotics were at best only marginally better than gentamicin or fosfomycin. High bacterial titers of greater than 10^6 CFU/g of bladder tissue, as observed in mice treated with only water, were not recovered in any of the antibiotic-treated mice. Importantly, no bacteria were detected in the bladders of mock-infected mice that were housed in cages with infected animals during the duration of these experiments. These results indicate that reinoculation of UPEC and the dissemination of UTIs between animals are, at best, rare events in these types of studies, as has been reported previously (52).

Microscopic imaging of untreated and antibiotic-treated mouse bladders alike shows that UTI89 can invade all layers of the urothelium by 9 days postinoculation, in line with previous observations (17, 44, 46; data not shown). Bacterial penetration of the urothelial permeability barrier likely renders UPEC less susceptible to antibiotic treatments *in vivo*. To better address this possibility, bladders from UTI89-infected mice were homogenized in the presence of 0.025% Triton X-100 detergent to disrupt the urothelial barrier function, as well as indi-

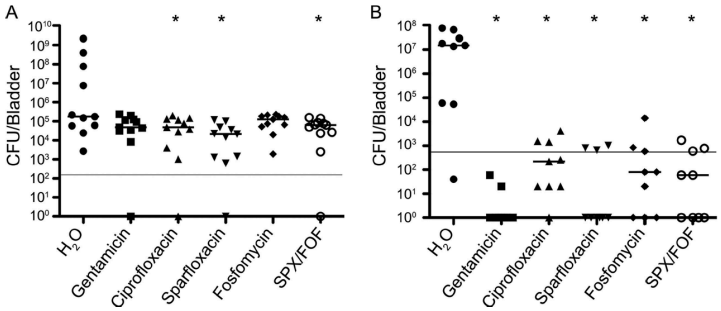

FIG. 3. Antibiotic susceptibility of UPEC within mouse bladders. (A) Starting at day 3 postinoculation with UTI89, infected CBA/J mice were treated for 3 consecutive days with the indicated antibiotics. Following an additional 3-day period, surviving bacterial titers present within the bladders were determined. The graph depicts the cumulative results from two independent assays ($n = 11$). (B) The graph shows bacterial titers in aliquots of tissue homogenates from mouse bladders ($n = 9$) recovered at 3 days postinoculation and subsequently treated for 4 h with the indicated antibiotics. Bars indicate median values for each group, while the solid lines denote the LOQ. *P* values of <0.05 (A) or <0.001 (B), relative to the water-treated controls, were determined using Mann-Whitney U tests and are labeled with asterisks. Sparfloxacin-fosfomycin, SPX/FOF.

vidual host cells, prior to antibiotic treatments. In this situation, all of the antibiotics tested significantly reduced bacterial numbers to levels near or below the limit of quantitation (LOQ) (Fig. 3B). Lack of accessibility to UPEC within urothelial barriers thus appears to reduce the effectiveness of antibiotics, including quinolones that can readily penetrate host cell monolayers in cell culture-based assays. Of note, antibiotic treatments of homogenates from infected bladders did not completely eradicate UPEC in all cases, reaffirming the possible development during UTIs of metabolically quiescent reservoirs, or persister cells, that may be innately less susceptible to antibiotics regardless of antibiotic accessibility issues (11, 37, 44, 46).

Antibiotic effects on IBCs. The persistence of UPEC reservoir populations in the bladder following antibiotic treatments, as seen in Fig. 3A, may also be in part attributable to the presence of IBCs. If so, IBCs should be resistant to the antibiotics used in our *in vivo* assays. To address this possibility, CBA/J mice were inoculated with UTI89 carrying pGEN-GFP (LVA), a high-retention, low-copy-number plasmid that constitutively expresses a destabilized variant of GFP (61). Use of this strain allows for direct observation by fluorescent microscopy of viable, or recently viable, bacteria. Within 6 h postinoculation into the bladder, UTI89/pGEN-GFP(LVA) is able to invade the superficial cells of the bladder urothelium and form IBCs that can be enumerated by imaging bladder explants. Incubation of these explants in the absence of antibiotics for 18 h does not appreciably affect the numbers of IBCs (Fig. 4A), although the overall sizes and intensities of the IBCs do increase (Fig. 4B). In contrast, incubation in the presence of the drug combination sparfloxacin-fosfomycin leads to significantly reduced IBC numbers (Fig. 4A and B). Similar results were obtained in experiments using only sparfloxacin (data not shown). These data indicate that IBCs can be fairly sensitive to antibiotic treatments. Microscopic analysis of bladders recovered from antibiotic-treated mice at 9 days postinoculation support this conclusion, revealing a scarcity of IBCs at this late time point (data not shown). Even in the absence of antibiotic treatments, IBCs do not appear to be particularly long-lived, being key targets of infiltrating neutrophils and subject to attrition as the host cells that they occupy fall apart and/or exfoliate (30, 44, 45; our unpublished observations). Together, these observations suggest that IBCs do not act as primary reservoirs for the long-term persistence of UPEC within the bladder, although they likely function in the establishment of reservoir populations.

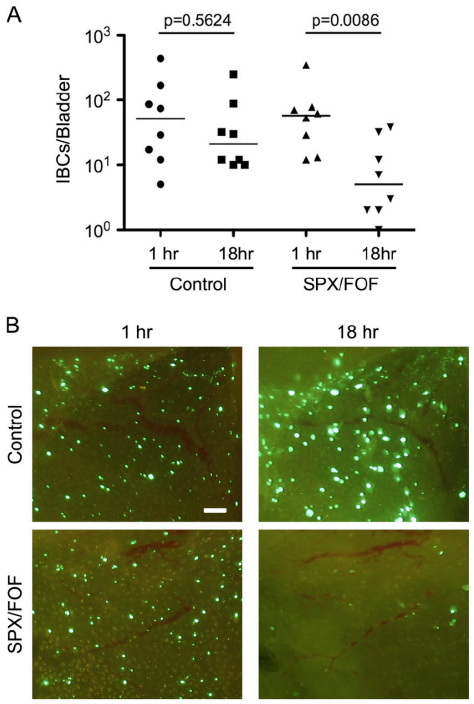

FIG. 4. Antibiotic susceptibility of IBCs. At 6 h postinoculation with UTI89/pGEN-GFP(LVA), bladders obtained from CBA/J mice were collected, splayed, and incubated in the presence or absence of the antibiotic combination sparfloxacin-fosfomycin. (A) Using fluorescence microscopy, IBCs were enumerated at the indicated times after addition of the antibiotics. Bars denote median values. *P* values were calculated using the Mann-Whitney U test ($n = 8$ mice per group). (B) Representative images showing IBCs in control and sparfloxacin-fosfomycin-treated bladder explants at the 1- and 18-h time points. Scale bar = 100 μm.

DISCUSSION

In human studies, recurrent UTI rates in untreated individuals have been reported to range from about 25% to greater than 40% (Table 2). Administration of commonly used antibiotics, including several of the ones used here, can reportedly reduce UTI recurrence rates. Some alternative therapeutic approaches may also be of benefit, as suggested by recent meta-analyses showing that the long-term intake of cranberry juice or cranberry juice extracts can reduce recurrent UTI rates in young to middle-aged women by about 35% (22). Variations in study design and execution make direct comparison of results from different treatment approaches difficult. However, it is clear from the literature that recurrent UTIs remain problematic for many individuals, regardless of therapeutic intervention (Table 2).

A growing number of studies indicate that many recurrent UTIs may in effect be relapses caused by the resurgence of intracellular bacterial reservoirs that can persist for many weeks to months within the urothelium (26, 32, 43–45, 52). Here, using bladder cell culture-based assays, we found that intracellular UPEC strains are protected against several different classes of antibiotics, with the exceptions of nitrofurantoin and several fluoroquinolones (Fig. 1A). These antibiotics are known to penetrate host cell membranes and accumulate to high concentrations intracellularly (48). Interestingly, in human studies, patients who received fluoroquinolones often appeared to have fewer recurrent UTIs overall, in comparison with patients who were given other antibiotic treatments (Table 2). However, with respect to bacterial clearance from bladder tissues in our mouse UTI model system, the fluoroquinolones ciprofloxacin and sparfloxacin were statistically no better than the membrane-impermeable antibiotic gentamicin, al-

TABLE 2. Recurrence after antibiotic treatments in human studies[a]

Treatment	Abbreviation	Treatment duration	Recurrence rate	Time of recurrence	Reference
Untreated			27.8	<3 mo	8
			44	>1 mo	27
			27	<6 mo	20
			36	12 mo	33
Cranberry juice		6 mo	16	12 mo	33
Trimethoprim-sulfamethoxazole	SXT	7 d	2	5 wk	25
		NR	43	<5 mo	35
		NR	7.1	NR	54
Ofloxacin	OFX	1 d	19	5 wk	25
		3 d	11	5 wk	25
Ciprofloxacin	CIP	7 d	7.7	4–6 wk	24
		NR	4.7	NR	54
Norfloxacin	NOR	NR	14.8	NR	54
		NR	11	4–6 wk	50
Levofloxacin	LVX	1 d	17.4	<3 mo	34
		3 d	5.6	<3 mo	34
Sparfloxacin	SPX	1 d	12	4–6 wk	24
		3 d	8.1	4–6 wk	24
Nalidixic acid/citrate	NAL	5 d	17	1 mo	18
		NR	33	4–6 wk	50
Nitrofurantoin	NIT	NR	35.3	NR	54
Fosfomycin	FOF	NR	0.2	NR	54
Fosfomycin trometamol	FT	1 d	14	1 mo	12
Gentamicin	GEN	10 d	42	30 d	49

[a] NR = not reported.

though all three of these antibiotics were significantly better than no treatment at all (Fig. 3A).

Surprisingly, none of the antibiotics tested in mice, regardless of their effectiveness against internalized UPEC in cell culture work, were able to completely eradicate UPEC reservoir populations in the mouse bladder. The redoubtable permeability barrier function of the bladder urothelium likely limits the effectiveness of these antibiotics *in vivo*. The increased susceptibility of UPEC to ex vivo antibiotic treatments following disruption of bladder tissue and cells supports this conclusion (Fig. 2). These observations also raise the intriguing possibility that host cell cytotoxic effects associated with some antibiotics could enhance their efficacy against internalized UPEC by disrupting cell and tissue barriers, although increased host cytotoxicity did not necessarily correlate with improved bacterial killing by antibiotics in our cell culture-based assays (Fig. 1B).

In addition to host cell invasion, IBC formation within superficial bladder cells and the development of biofilms in association with catheter and urothelial surfaces may also render UPEC resistant to antibiotic treatments. Our *in vitro* biofilm assays indicated that only a limited subset of the tested antibiotics were able to effectively eradicate UPEC growing in biofilms. The most potent antibiotics in these assays were the cell wall synthesis inhibitor fosfomycin, the fluoroquinolone sparfloxacin, and the β-lactam antibiotics penicillin G and cefadroxil. These antibiotics prevented growth of new biofilms and disrupted preexisting biofilm communities. In contrast, the β-lactam antibiotic nafcillin appeared to significantly enhance biofilm formation relative to untreated controls (Fig. 2). However, if nafcillin was added at the start of our biofilm assays, UTI89 was not able to initiate biofilm formation. This antibiotic has only a slight effect on UTI89 growth rates, but it does alter the morphology of the bacteria substantially, causing them to become more elongated and crescent shaped (data not shown). This observation suggests that nafcillin causes significant stress to UTI89, even though UTI89 and most other *E. coli* isolates are inherently resistant to this antibiotic (47). The apparent stimulation of biofilm formation by nafcillin may be a consequence of this stress, morphological alterations of the bacteria, and/or other as yet undefined factors.

Ineffective antibiotic diffusion within biofilms, as well as alterations in the metabolic state of biofilm-associated microbes (21, 58), likely decreases the sensitivity of UTI89 to many of the antibiotics used in our assays. Consequently, the development of biofilm-like communities, including IBCs, may promote UPEC persistence within the urinary tract, despite the administration of antibiotics. However, while it is probable that IBCs contribute to the establishment of long-term bacterial reservoirs within the bladder, we propose that IBCs are likely not the major embodiment of the reservoir populations. This conclusion is based on results showing that IBCs are rather sensitive in ex vivo assays to antibiotics like sparfloxacin, which nonetheless fail to eradicate UPEC reservoirs *in vivo*. Furthermore, previous work from our lab and others indicates that IBCs do not persist in the bladder for long durations even in the absence of antibiotic treatments (30, 44, 45).

In total, our data indicate that bacterial reservoir populations within the bladder are protected from even highly membrane-permeable antibiotics such as quinolones, as well as drugs like fosfomycin that have the ability to disrupt UPEC biofilms and IBCs. The results presented here are in agreement with previous findings suggesting that long-lived UPEC reservoirs within the bladder consist primarily of small bacterial clusters or single microbes that are bound by actin and compartmentalized within the urothelium barrier (17, 30, 46). In addition to their localization within the urothelial barrier, the quiescent nature of the UPEC reservoirs and, perhaps, the generation of so-called persister bacterial cells may provide further protection against antibiotics (11, 17, 29, 37). Interestingly, it has been reported that fluoroquinolones like sparfloxacin have some bactericidal activity against nonreplicating and slowly growing *E. coli* (14), characteristics that may contribute to the effectiveness of sparfloxacin and related antibiotics against intracellular and biofilm-associated UPEC.

It is possible that longer-term antibiotic treatments, beyond the 3-day regimen common in the clinic and used here with infected mice, may better eliminate UPEC reservoir populations and potentially reduce recurrent UTI rates. However, longer-term antibiotic treatments may be associated with increased financial costs, decreased patient compliance, and increased risks for selection of antibiotic-resistant pathogens. The effectiveness of longer-term treatments will also likely be critically dependent upon the permeability and bactericidal properties of the antibiotics used. Of note, with respect to the long-term persistence of UPEC within the urinary tract, previous work indicated that mice treated for 3 days with the host membrane-impermeable antibiotic combination trimethoprim-sulfamethoxazole were not significantly better off than mice treated for 10 days (52). Likewise, in human studies, children treated with gentamicin for 10 days still had high rates of recurrence (Table 2) (49). Ultimately, the development of antimicrobials that can both readily penetrate tissue barriers like the urothelium and target nonreplicating microbes, coupled

with optimized treatment regimes, may provide substantially improved protection against chronic and recurrent UTIs.

ACKNOWLEDGMENT

This work was supported by Public Health Service grant DK068585 from the National Institute of Diabetes and Digestive and Kidney Diseases.

REFERENCES

1. **Anderson, G. G., J. J. Palermo, J. D. Schilling, R. Roth, J. Heuser, and S. J. Hultgren.** 2003. Intracellular bacterial biofilm-like pods in urinary tract infections. Science **301:**105–107.
2. **Apodaca, G.** 2004. The uroepithelium: not just a passive barrier. Traffic **5:**117–128.
3. **Bauer, A. W., W. M. Kirby, J. C. Sherris, and M. Turck.** 1966. Antibiotic susceptibility testing by a standardized single disk method. Am. J. Clin. Pathol. **45:**493–496.
4. **Beckel, J. M., A. Kanai, S. J. Lee, W. C. de Groat, and L. A. Birder.** 2006. Expression of functional nicotinic acetylcholine receptors in rat urinary bladder epithelial cells. Am. J. Physiol. Renal Physiol. **290:**F103–F110.
5. **Bishop, B. L., M. J. Duncan, J. Song, G. Li, D. Zaas, and S. N. Abraham.** 2007. Cyclic AMP-regulated exocytosis of Escherichia coli from infected bladder epithelial cells. Nat. Med. **13:**625–630.
6. **Brauner, A., S. H. Jacobson, and I. Kuhn.** 1992. Urinary Escherichia coli causing recurrent infections—a prospective follow-up of biochemical phenotypes. Clin. Nephrol. **38:**318–323.
7. **Chen, S. L., C. S. Hung, J. Xu, C. S. Reigstad, V. Magrini, A. Sabo, D. Blasiar, T. Bieri, R. R. Meyer, P. Ozersky, J. R. Armstrong, R. S. Fulton, J. P. Latreille, J. Spieth, T. M. Hooton, E. R. Mardis, S. J. Hultgren, and J. I. Gordon.** 2006. Identification of genes subject to positive selection in uropathogenic strains of Escherichia coli: a comparative genomics approach. Proc. Natl. Acad. Sci. U. S. A. **103:**5977–5982.
8. **Czaja, C. A., W. E. Stamm, A. E. Stapleton, P. L. Roberts, T. R. Hawn, D. Scholes, M. Samadpour, S. J. Hultgren, and T. M. Hooton.** 2009. Prospective cohort study of microbial and inflammatory events immediately preceding Escherichia coli recurrent urinary tract infection in women. J. Infect. Dis. **200:**528–536.
9. **Dhakal, B. K., R. R. Kulesus, and M. A. Mulvey.** 2008. Mechanisms and consequences of bladder cell invasion by uropathogenic Escherichia coli. Eur. J. Clin. Invest. **38**(Suppl. 2)**:**2–11.
10. **Dhakal, B. K., and M. A. Mulvey.** 2009. Uropathogenic Escherichia coli invades host cells via an HDAC6-modulated microtubule-dependent pathway. J. Biol. Chem. **284:**446–454.
11. **Dorr, T., K. Lewis, and M. Vulic.** 2009. SOS response induces persistence to fluoroquinolones in Escherichia coli. PLoS Genet. **5:**e1000760.
12. **Elhanan, G., H. Tabenkin, R. Yahalom, and R. Raz.** 1994. Single-dose fosfomycin trometamol versus 5-day cephalexin regimen for treatment of uncomplicated lower urinary tract infections in women. Antimicrob. Agents Chemother. **38:**2612–2614.
13. **Elsinghorst, E. A.** 1994. Measurement of invasion by gentamicin resistance. Methods Enzymol. **236:**405–420.
14. **Eng, R. H., F. T. Padberg, S. M. Smith, E. N. Tan, and C. E. Cherubin.** 1991. Bactericidal effects of antibiotics on slowly growing and nongrowing bacteria. Antimicrob. Agents Chemother. **35:**1824–1828.
15. **Eto, D. S., H. B. Gordon, B. K. Dhakal, T. A. Jones, and M. A. Mulvey.** 2008. Clathrin, AP-2, and the NPXY-binding subset of alternate endocytic adaptors facilitate FimH-mediated bacterial invasion of host cells. Cell. Microbiol. **10:**2553–2567.
16. **Eto, D. S., T. A. Jones, J. L. Sundsbak, and M. A. Mulvey.** 2007. Integrin-mediated host cell invasion by type 1-piliated uropathogenic Escherichia coli. PLoS Pathog. **3:**e100.
17. **Eto, D. S., J. L. Sundsbak, and M. A. Mulvey.** 2006. Actin-gated intracellular growth and resurgence of uropathogenic Escherichia coli. Cell. Microbiol. **8:**704–717.
18. **Ferry, S., L. G. Burman, B. Widberg, and C. Calmenius.** 1987. Short-term nalidixic acid plus sodium citrate in acute lower urinary tract infection. Scand. J. Infect. Dis. **19:**469–477.
19. **Foxman, B.** 2003. Epidemiology of urinary tract infections: incidence, morbidity, and economic costs. Dis. Mon. **49:**53–70.
20. **Foxman, B.** 1990. Recurring urinary tract infection: incidence and risk factors. Am. J. Public Health **80:**331–333.
21. **Fux, C. A., J. W. Costerton, P. S. Stewart, and P. Stoodley.** 2005. Survival strategies of infectious biofilms. Trends Microbiol. **13:**34–40.
22. **Guay, D. R.** 2009. Cranberry and urinary tract infections. Drugs **69:**775–807.
23. **Hatt, J. K., and P. N. Rather.** 2008. Role of bacterial biofilms in urinary tract infections. Curr. Top. Microbiol. Immunol. **322:**163–192.
24. **Henry, D. C., R. C. Nenad, A. Iravani, A. D. Tice, D. L. Mansfield, D. J. Magner, M. B. Dorr, and G. H. Talbot.** 1999. Comparison of sparfloxacin and ciprofloxacin in the treatment of community-acquired acute uncomplicated urinary tract infection in women. Clin. Ther. **21:**966–981.
25. **Hooton, T. M., C. Johnson, C. Winter, L. Kuwamura, M. E. Rogers, P. L. Roberts, and W. E. Stamm.** 1991. Single-dose and three-day regimens of ofloxacin versus trimethoprim-sulfamethoxazole for acute cystitis in women. Antimicrob. Agents Chemother. **35:**1479–1483.
26. **Hvidberg, H., C. Struve, K. A. Krogfelt, N. Christensen, S. N. Rasmussen, and N. Frimodt-Moller.** 2000. Development of a long-term ascending urinary tract infection mouse model for antibiotic treatment studies. Antimicrob. Agents Chemother. **44:**156–163.
27. **Ikäheimo, R., A. Siitonen, T. Heiskanen, U. Kärkkäinen, P. Kuosmanen, P. Lipponen, and P. H. Mäkelä.** 1996. Recurrence of urinary tract infection in a primary care setting: analysis of a 1-year follow-up of 179 women. Clin. Infect. Dis. **22:**91–99.
28. **Jacobson, S. H., I. Kuhn, and A. Brauner.** 1992. Biochemical fingerprinting of urinary Escherichia coli causing recurrent infections in women with pyelonephritic renal scarring. Scand. J. Urol. Nephrol. **26:**373–377.
29. **Jayaraman, R.** 2008. Bacterial persistence: some new insights into an old phenomenon. J. Biosci. **33:**795–805.
30. **Justice, S. S., C. Hung, J. A. Theriot, D. A. Fletcher, G. G. Anderson, M. J. Footer, and S. J. Hultgren.** 2004. Differentiation and developmental pathways of uropathogenic Escherichia coli in urinary tract pathogenesis. Proc. Natl. Acad. Sci. U. S. A. **101:**1333–1338.
31. **Karkkainen, U. M., R. Ikaheimo, M. L. Katila, and A. Siitonen.** 2000. Recurrence of urinary tract infections in adult patients with community-acquired pyelonephritis caused by E. coli: a 1-year follow-up. Scand. J. Infect. Dis. **32:**495–499.
32. **Kerrn, M. B., C. Struve, J. Blom, N. Frimodt-Møller, and K. A. Krogfelt.** 2005. Intracellular persistence of Escherichia coli in urinary bladders from mecillinam-treated mice. J. Antimicrob. Chemother. **55:**383–386.
33. **Kontiokari, T., K. Sundqvist, M. Nuutinen, T. Pokka, M. Koskela, and M. Uhari.** 2001. Randomised trial of cranberry-lingonberry juice and Lactobacillus GG drink for the prevention of urinary tract infections in women. BMJ **322:**1571.
34. **Koyama, Y., O. Mikami, T. Matsuda, T. Murota, T. Ohara, H. Kawamura, K. Amazutsumi, J. Uchida, and T. Harada.** 2000. Efficacy of single-dose therapy with levofloxacin for acute cystitis: comparison to three-day therapy. Hinyokika Kiyo **46:**49–52. (In Japanese.)
35. **Lemieux, G.** 1974. Trimethoprim-sulfamethoxazole compared with sulfamethoxazole in urinary tract infection. Can. Med. Assoc. J. **110:**910–912.
36. **Lorian, V.** 2005. Antibiotics in laboratory medicine, 5th ed. Lippincott Williams & Wilkins, Philadelphia, PA.
37. **Ma, C., S. Sim, W. Shi, L. Du, D. Xing, and Y. Zhang.** 17 November 2009, posting date. Energy production genes sucB and ubiF are involved in persister survival and tolerance to multiple antibiotics and stresses in Escherichia coli. FEMS Microbiol. Lett. doi:10.1111/j.1574–6968.2009.01857.x.
38. **Martinez, J. J., M. A. Mulvey, J. D. Schilling, J. S. Pinkner, and S. J. Hultgren.** 2000. Type 1 pilus-mediated bacterial invasion of bladder epithelial cells. EMBO J. **19:**2803–2812.
39. **Merritt, J. H., D. E. Kadouri, and G. A. O'Toole.** 2005. Growing and analyzing static biofilms. Curr. Protoc. Microbiol. **Chapter 1:**Unit 1B.1.
40. **Mikuniya, T., Y. Kato, R. Kariyama, K. Monden, M. Hikida, and H. Kumon.** 2005. Synergistic effect of fosfomycin and fluoroquinolones against Pseudomonas aeruginosa growing in a biofilm. Acta Med. Okayama **59:**209–216.
41. **Min, G., M. Stolz, G. Zhou, F. Liang, P. Sebbel, D. Stoffler, R. Glockshuber, T. T. Sun, U. Aebi, and X. P. Kong.** 2002. Localization of uroplakin Ia, the urothelial receptor for bacterial adhesin FimH, on the six inner domains of the 16 nm urothelial plaque particle. J. Mol. Biol. **317:**697–706.
42. **Mulvey, M. A.** 2002. Adhesion and entry of uropathogenic Escherichia coli. Cell. Microbiol. **4:**257–271.
43. **Mulvey, M. A., Y. S. Lopez-Boado, C. L. Wilson, R. Roth, W. C. Parks, J. Heuser, and S. J. Hultgren.** 1998. Induction and evasion of host defenses by type 1-piliated uropathogenic Escherichia coli. Science **282:**1494–1497.
44. **Mulvey, M. A., J. D. Schilling, and S. J. Hultgren.** 2001. Establishment of a persistent Escherichia coli reservoir during the acute phase of a bladder infection. Infect. Immun. **69:**4572–4579.
45. **Mulvey, M. A., J. D. Schilling, J. J. Martinez, and S. J. Hultgren.** 2000. Bad bugs and beleaguered bladders: interplay between uropathogenic Escherichia coli and innate host defenses. Proc. Natl. Acad. Sci. U. S. A. **97:**8829–8835.
46. **Mysorekar, I. U., and S. J. Hultgren.** 2006. Mechanisms of uropathogenic Escherichia coli persistence and eradication from the urinary tract. Proc. Natl. Acad. Sci. U. S. A. **103:**14170–14175.
47. **Nikaido, H.** 1998. Multiple antibiotic resistance and efflux. Curr. Opin. Microbiol. **1:**516–523.
48. **Oliphant, C. M., and G. M. Green.** 2002. Quinolones: a comprehensive review. Am. Fam. Physician **65:**455–464.
49. **Principi, N., A. Gervasoni, E. Reali, and P. Tagliabue.** 1977. Treatment of urinary tract infections in children with a single daily dose of gentamicin. Helv. Paediatr. Acta **32:**343–350.
50. **Reeves, D. S., R. W. Lacey, R. V. Mummery, M. Mahendra, A. J. Bint, and S. W. Newsom.** 1984. Treatment of acute urinary infection by norfloxacin or nalidixic acid/citrate: a multi-centre comparative study. J. Antimicrob. Chemother. **13**(Suppl. B)**:**99–105.

51. **Russo, T. A., A. Stapleton, S. Wenderoth, T. M. Hooton, and W. E. Stamm.** 1995. Chromosomal restriction fragment length polymorphism analysis of Escherichia coli strains causing recurrent urinary tract infections in young women. J. Infect. Dis. **172:**440–445.
52. **Schilling, J. D., R. G. Lorenz, and S. J. Hultgren.** 2002. Effect of trimethoprim-sulfamethoxazole on recurrent bacteriuria and bacterial persistence in mice infected with uropathogenic Escherichia coli. Infect. Immun. **70:**7042–7049.
53. **Schilling, J. D., M. A. Mulvey, and S. J. Hultgren.** 2001. Structure and function of Escherichia coli type 1 pili: new insight into the pathogenesis of urinary tract infections. J. Infect. Dis. **183**(Suppl. 1)**:**S36–S40.
54. **Schneeberger, C., R. P. Stolk, J. H. Devries, P. M. Schneeberger, R. M. Herings, and S. E. Geerlings.** 2008. Differences in the pattern of antibiotic prescription profile and recurrence rate for possible urinary tract infections in women with and without diabetes. Diabetes Care **31:**1380–1385.
55. **Sharp, J. R., K. G. Ishak, and H. J. Zimmerman.** 1980. Chronic active hepatitis and severe hepatic necrosis associated with nitrofurantoin. Ann. Intern. Med. **92:**14–19.
56. **Song, J., B. L. Bishop, G. Li, R. Grady, A. Stapleton, and S. N. Abraham.** 2009. TLR4-mediated expulsion of bacteria from infected bladder epithelial cells. Proc. Natl. Acad. Sci. U. S. A. **106:**14966–14971.
57. **Soto, S. M., A. Smithson, J. P. Horcajada, J. A. Martinez, J. P. Mensa, and J. Vila.** 2006. Implication of biofilm formation in the persistence of urinary tract infection caused by uropathogenic Escherichia coli. Clin. Microbiol. Infect. **12:**1034–1036.
58. **Stewart, P. S., and J. W. Costerton.** 2001. Antibiotic resistance of bacteria in biofilms. Lancet **358:**135–138.
59. **Suntres, Z. E., and P. N. Shek.** 1992. Nitrofurantoin-induced pulmonary toxicity. In vivo evidence for oxidative stress-mediated mechanisms. Biochem. Pharmacol. **43:**1127–1135.
60. **Wang, H., F. X. Liang, and X. P. Kong.** 2008. Characteristics of the phagocytic cup induced by uropathogenic Escherichia coli. J. Histochem. Cytochem. **56:**597–604.
61. **Wiles, T. J., J. M. Bower, M. J. Redd, and M. A. Mulvey.** 2009. Use of zebrafish to probe the divergent virulence potentials and toxin requirements of extraintestinal pathogenic Escherichia coli. PLoS Pathog. **5:**e1000697.
62. **Wright, K. J., P. C. Seed, and S. J. Hultgren.** 2007. Development of intracellular bacterial communities of uropathogenic Escherichia coli depends on type 1 pili. Cell. Microbiol. **9:**2230–2241.
63. **Zhou, G., W. J. Mo, P. Sebbel, G. Min, T. A. Neubert, R. Glockshuber, X. R. Wu, T. T. Sun, and X. P. Kong.** 2001. Uroplakin Ia is the urothelial receptor for uropathogenic Escherichia coli: evidence from in vitro FimH binding. J. Cell Sci. **114:**4095–4103.

CHAPTER 3

FORCED RESURGENCE AND TARGETING OF INTRACELLULAR UROPATHOGENIC *ESCHERICHIA COLI* RESERVOIRS

Abstract

Chitosan, a water-soluble, chitin-based derivative, selectively triggers exfoliation of superficial bladder epithelial cells. Chitosan-induced exfoliation of superficial cells was used as a tool to show that UPEC were able to invade and form reservoir populations in underlying intermediate and basal epithelial cells. Chitosan treatment of *in vitro* growing bacteria resulted in overly adhesive bacteria, which more efficiently formed biofilms and exhibited increased association to cultured 5637 bladder epithelial cells. Scanning electron micrographs of infected mouse bladders revealed high levels of often-filamentous bacteria on the bladder surface at 3 and 7 days after chitosan treatment, suggestive of increased resurgence and exit from their intracellular niche. Treatment of infected mouse bladders with chitosan and cell-permeable antibiotics, such as sparfloxacin and ciprofloxacin, resulted in enhanced removal of UPEC reservoir populations in the murine urinary tract. Despite near-complete clearance of UPEC from the bladder after treatment, these mice still displayed recurrent infections as determined by daily urine analysis over the course of two weeks following cessation of antibiotic treatment. It remains possible that nearby tissues, such as the ureters or vaginal mucosa, may harbor UPEC populations capable of re-colonizing the bladder following antibiotic treatment. Overall, chitosan treatment followed by ≥7 days of antibiotics offers a unique treatment regiment for removal of embedded reservoir populations in the bladder epithelium by forcing UPEC resurgence. Further research will refine the efficacy

of this treatment as a therapy for use in human patients with recurrent, or relapsing, urinary tract infections.

Introduction

The mammalian bladder mucosa, being comprised of a transitional epithelium (urothelium) and an underlying lamina propria, functions as a strong permeability barrier that keeps urine and other elements within the bladder lumen from entering surrounding tissues. The highly vascularized lamina propria merges with the submucosa, which in turn sits atop a layer of smooth muscle that is surrounded in part by a serosal covering and an adventitia made up of connective tissue. The urothelium itself is composed of layers of immature intermediate and basal bladder epithelial cells (BECs) underlying a single layer of much larger, terminally differentiated binucleate superficial cells that face the bladder lumen (13, 19, 22). Intermediate, and possibly basal BECs, move towards the apical surface and differentiate to fill vacancies created as superficial cells are shed (32). Normally, the urothelium has an especially slow turnover rate of 6-12 months, but upon injury and exfoliation of the superficial cells, the underlying immature cells are rapidly mobilized and differentiated (10). As they differentiate into superficial cells, intermediate cells undergo multiple changes, including marked increases in size, fusion with neighboring intermediate cells, and finally the redistribution of actin filaments to sites along basolateral surfaces (2, 19, 22, 32). The ability of urothelium to quickly regenerate itself when damaged is impressive, and likely reflects the importance of this mucosal barrier

in guarding against the uptake of unwanted metabolites and infiltrating microbial pathogens (10, 26).

The sterility of the urinary tract is routinely challenged by a diversity of bacterial pathogens, which if not eliminated can result in the establishment of a urinary tract infection (UTI). Most UTIs are caused by strains of uropathogenic *Escherichia coli* (UPEC) (35). UPEC strains, which are often motile and encode numerous adhesive organelles and other virulence factors (35), likely originate in the colon, but can be introduced into the urinary tract via contamination of the urethra meatus and urethra, facilitated by poor hygiene, sexual intercourse, or anatomical defects (9). UTIs are often acute in nature, being associated with the transient detection of bacteria in urine and accompanying symptoms that can include pelvic pain, pyuria, dysuria, and the frequent, urgent need to urinate (8). Although often self-limiting or treatable with short-course antibiotics, UTIs are prone to recur in many individuals and can develop into chronic, long-term infections that can last from a few weeks to years. Occasionally, UPEC colonization of the bladder can also serve as a staging ground for the further spread of the pathogens into the kidneys and/or bloodstream.

The capacity of many UPEC isolates to persist within the bladder and cause recurrent and chronic UTIs is facilitated by the ability of UPEC to bind and invade the urothelium (6, 23, 30, 34). UPEC utilize adhesive fibers known as type 1 pili to both attach to and invade BECs (6, 37). Internalized bacteria can be quickly shuttled back out of the host cells or trafficked into actin-bound, lysosome-like compartments where they can persist in a seemingly quiescent

state, sequestered away from the flow of urine and host immunosurveillance mechanisms (7, 23, 24). These quiescent bacteria are thought to serve as reservoirs for recurrent (or more accurately, relapsing) and chronic UTIs (7). Within terminally differentiated superficial BECs, UPEC can break into the host cytosol and rapidly grow in close association with cytokeratin intermediate filaments, forming large biofilm-like aggregates referred to as intracellular bacterial communities (IBCs) (1, 14, 24). Triggers that stimulate the development of IBCs, versus the establishment of quiescent intracellular reservoirs, are not entirely clear, but appear to be affected by the differentiation status of the host cell and the distribution of actin filaments (7). IBCs are not especially long-lived structures and are susceptible to disruption by antibiotics (3). The build-up and eventual dispersal (or shedding) of IBCs likely facilitates the spread of UPEC both within the urinary tract and to other hosts, promoting further rounds of acute and recurrent/relapsing infections (1, 24).

Acute UTIs are commonly treated with short-course antibiotic regimens such as Bactrim (sulfamethoxazole/trimethoprim), nitrofurantoin, amoxicillin, or select fluoroquinolones, with relatively high success rates (12). Chronic UTIs respond poorly to short-course antibiotic treatments, which often fail to completely eliminate UPEC reservoir populations (3, 24, 29). Long-term antibiotic treatments show more promise, but come with a greater risk of side effects and development of antibiotic resistance, driving interest in alternative treatment options. A plethora of vaccine targets have so far yielded little clinical success in eradicating UPEC from the bladder. For example, vaccination attempts using

Solco-Urovac, a mix of 10 heat-inactivated uropathogenic strains was initially promising, but proved to be too allergenic for consistent, widespread usage (28). Other attempts at vaccine development have targeted conserved pathogenic elements such as capsule, LPS core antigen components, pili, and toxins such as α-hemolysin with limited success. Despite many years of intensive research and development, these vaccines provide only short-term protective immunity, suggesting a limited role of the adaptive immune system in fighting UTIs. Recent strategies aimed at targeting panels of pathogen-associated molecules are laying the groundwork for development of more efficacious vaccines, but the broad application and optimization of this approach remains distant (33). Novel therapeutic regimens will likely be needed to support current vaccinology efforts.

Recently, using a mouse UTI model, we demonstrated that many antibiotics effectively sterilize the urine, while leaving intracellular UPEC reservoirs buried within the urothelium mostly untouched (3). The nonreplicating status of these bacteria, coupled with the barrier function of the urothelium, likely contributes to the recalcitrant nature of UPEC reservoirs. In this study, we explored the use of the linear polysaccharide chitosan as a tool to expose and better target UPEC reservoirs within the urothelium. Chitosan is a deacetylated form of chitin derived from shellfish. It is reported to have bactericidal activity, is naturally biodegradable by lysozyme, and is approved for use in human patients as a drug carrier molecule (21, 36). Chitosan is able to disrupt epithelial cell tight junctions, and its instillation into the bladder causes rapid exfoliation of the superficial cell layer of the urothelium without eliciting any overt signs of

inflammation (16, 32). Following chitosan administration via catheterization, the urothelium barrier function is restored within 7 days ((32) and personal communication P. Veranic). Here we show that chitosan can be used to remove the superficial cell layer in murine bladders, thereby stimulating the resurgence of UPEC from intracellular reservoirs within the immature layers of the urothelium. Chitosan had minimal effect on the growth of a UPEC reference isolate in broth culture, but did promote biofilm formation and the development of unusual tubules that linked individual bacteria. When used in association with antibiotics, chitosan allowed for more complete removal of the reservoir populations within the bladder, suggesting that chitosan may be valuable for the treatment of chronic and recurrent UTIs.

Results

Chitosan affects UPEC growth and biofilm formation

In previous reports, chitosan has been shown to inhibit the growth of some bacterial strains (21). To assess the effect of chitosan on UPEC, the reference UPEC cystitis isolate UTI89 was grown shaking at 37°C in modified M9 minimal media supplemented with 0.02, 0.002, or 0.0002% chitosan or with buffer (phosphate buffer, pH 4.5) alone. Growth of UTI89 in the presence of 0.02% chitosan was delayed by over 1 h, but was otherwise unimpeded (Fig 3.1A and data not shown). In microtiter plate-based assays with static cultures, chitosan greatly enhanced biofilm formation by UTI89 in a dose-dependent fashion (Fig 3.1B). Growth of bacteria on glass coverslips in the presence of 0.002% chitosan

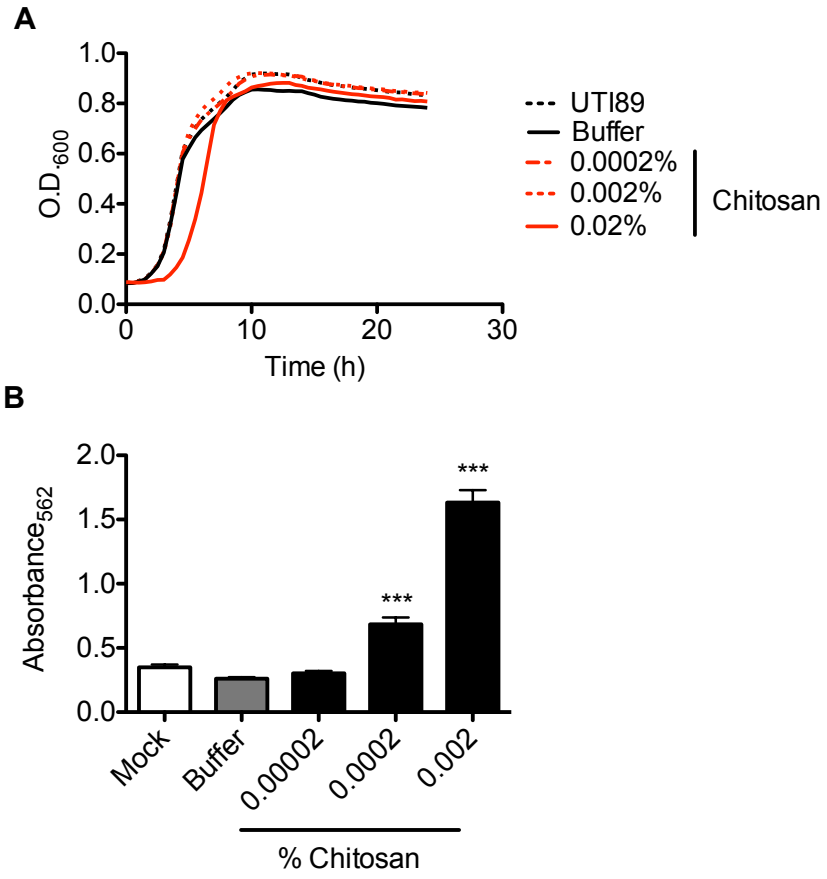

Figure 3.1 Chitosan affects *in vitro* growth of UPEC

(A) Growth of UTI89 in the presence of increasing concentrations of chitosan (0.0002, 0.002, 0.02%) or equal volumes of pH 4.5 phosphate buffer. Graph is from representative data collected from one of three experiments done in triplicate. Error bars were negligible and not shown for clarity. (B) *In vitro* biofilm formation of UTI89 incubated with increasing concentrations of chitosan or buffer as described above. Data was combined as three separate experiments performed in quadruplicate. Error bars indicate standard error of the mean with *P* = ***<0.001.

caused UTI89 to form large aggregates that were not apparent with lower concentrations of chitosan or with buffer alone (Fig. 3.2A-D). These chitosan-induced biofilm-like aggregates were associated with large amounts of undefined extracellular material (Fig. 3.2D), and also contained many filamentous bacterial cells as are often observed with bacteria under stress (Fig. 3.2C).

Chitosan increases UPEC cellular association

The effects of chitosan on interactions between UTI89 and host cells were assessed using the bladder epithelial cell line designated 5637. Chitosan (0.0002 and 0.002%) had no effect on the attachment or viability of 5637 cells, but did have a slight, though significant, inhibitory effect on growth of UTI89 in the cell culture medium (RPMI, Fig. 3.3A). Interactions between UTI89 and the BECs were drastically increased following a 2-h infection in the presence of chitosan treatment (Fig. 3.3B). In contrast, 0.002% chitosan decreased bacterial entry into the host cells (Fig. 3.3C), while having no significant effect on intracellular survival of the pathogen over a 24-h period (Fig. 3.3D).

Use of chitosan indicates that UPEC reservoirs reside within all layers of the urothelium

Previous work indicated that instillation of chitosan into the bladder lumen for 20 min will induce robust exfoliation of the superficial cells, leaving the underlying urothelium mostly intact (32). Using adult female CBA/J mice, we confirmed these findings, showing that chitosan promotes the rapid detachment of nearly all

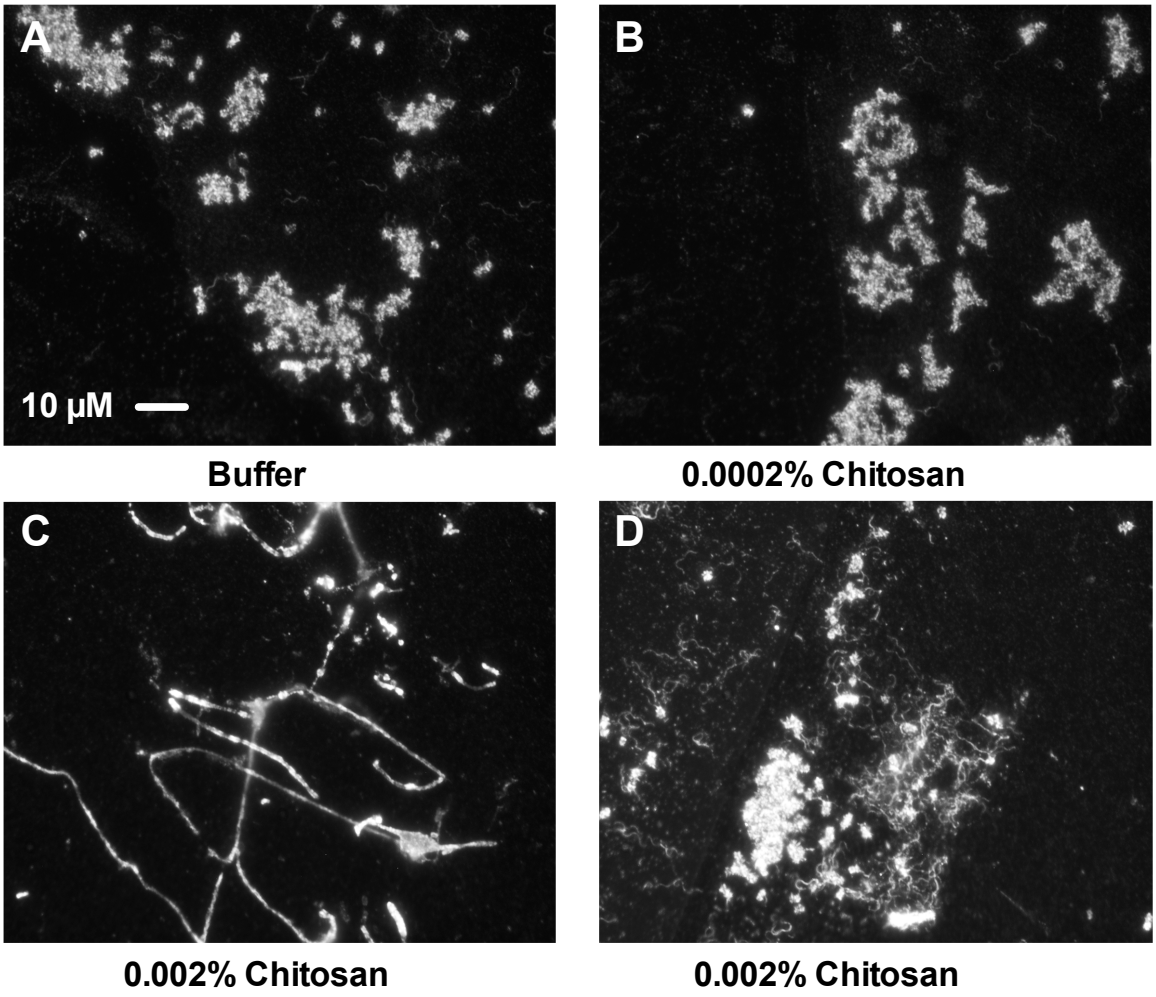

Figure 3.2 Chitosan treatment results in increased biofilm formation and filamentous UPEC

(A-D) Immunofluorescence images of UTI89 incubated with increasing concentrations of chitosan or buffer and stained with anti-*E. coli* antibody. Panel C specifically shows an example of a filamentous bacterium present after treatment with 0.02% chitosan. Experiments were repeated at least twice in triplicate with similar results.

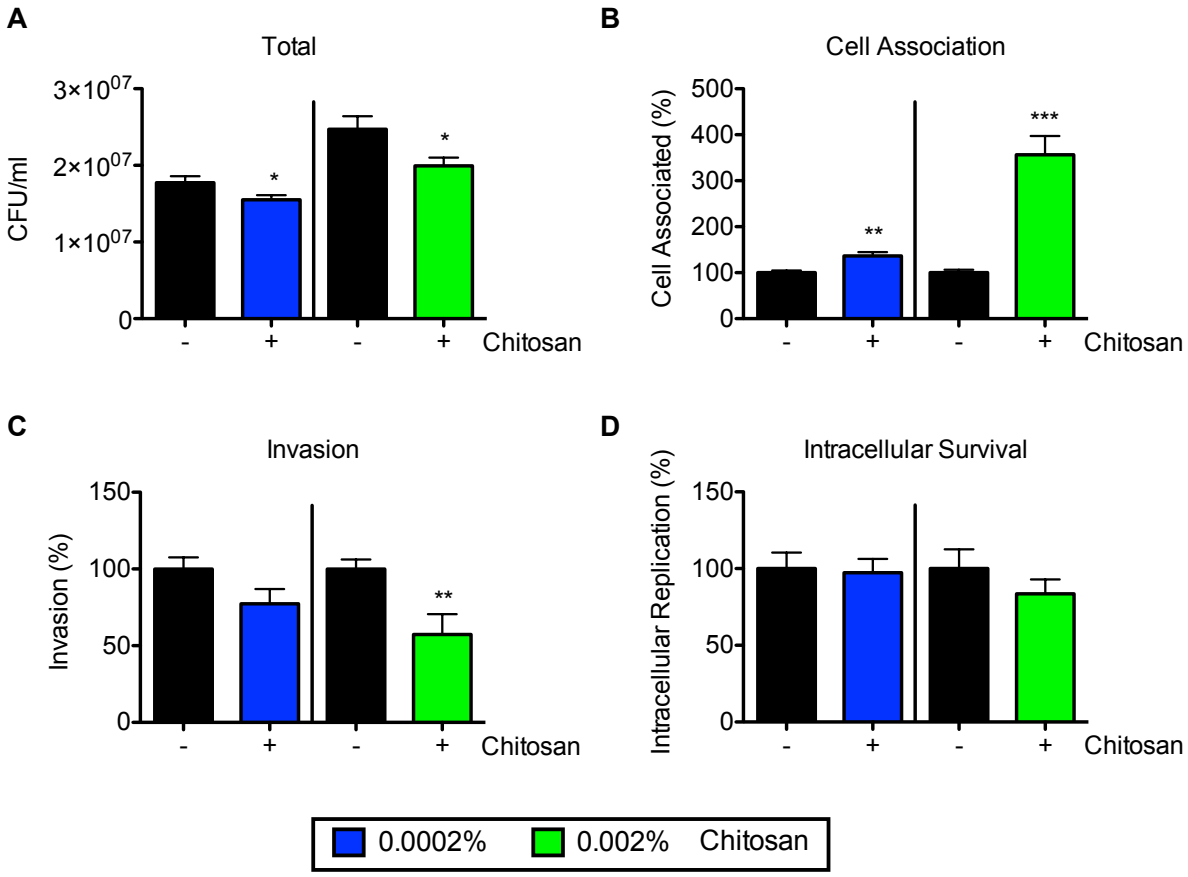

Figure 3.3 Chitosan treatment decreases BEC invasion despite increased association

(A) Chitosan treatment (0.002 or 0.02%) results in decreased growth in RPMI tissue culture media in the presence of 5637 bladder epithelial cells. (B) Chitosan treatments result in increased association of UTI89 with BECs in culture. (C) Invasion of UTI89 into BECs was measured by gentamicin-protection assays, where the cell-impermeable antibiotic gentamicin kills extracellular bacteria. Data was graphed as an index that normalizes invasion to bacteria associated with epithelial cells. (D) Intracellular replication of UTI89 was measured in the presence of chitosan or buffer after an overnight incubation in low concentrations of gentamicin. All cell culture experiments were performed at least three times in triplicate and combined. Error bars indicate standard error of the mean with *P* = *<0.05, **<0.01, ***<0.001.

of the large, binucleate superficial BECs, exposing the smaller mononucleate immature cells of the urothelium (Fig. 3.4A – B). Previous microscopy-based studies indicate that UPEC can invade all layers of the bladder urothelium (3, 7, 23, 24). Taking advantage of the ability of chitosan to strip away the topmost layer of superficial cells, we set out to quantify the ability of UPEC to invade mature versus immature BECs *in vivo*. Mice were treated with chitosan or phosphate buffer alone for 20 min followed by washes with phosphate buffered saline (PBS). Mice were then allowed to recover for 4 h prior to inoculation of UTI89 via transurethral catheterization. After 1 h, bladders were recovered, quartered, and incubated for an additional hour in the presence of gentamicin (10 μg/ml) in order to kill any extracellular bacteria. After additional washes to remove the antibiotic, bladders were homogenized and the numbers of surviving bacteria enumerated by dilution plating. Results shown in Fig. 3.4C indicate that UPEC has the capacity to invade both the superficial and immature cells of the bladder similarly.

We next asked if UPEC could penetrate and persist equally well within both mature and immature BECs. Untreated mice were inoculated with UTI89 via catheterization and the infection was allowed to proceed for 3 d. At this time point, IBCs are rare and intracellular reservoir populations have been established (1, 14). Infected mice were then treated with phosphate buffer alone or with chitosan to remove the outermost cell layer. After several washes with PBS, bladders were collected and bacteria present were quantified. In these assays, chitosan treatment decreased bacterial titers in the bladder slightly, but this

change was not statistically significant (Fig. 3.4D). These results confirm that UPEC can establish itself within all layers of the urothelium.

Resurgence of UPEC after chitosan treatment

The exfoliation of infected superficial BECs occurs normally during UTI, driving the differentiation of underlying cells that may contain UPEC reservoirs (25, 31). It has been proposed that the differentiation process, with accompanying changes in the actin cytoskeleton, can stimulate the resurgence of UPEC (7). To investigate this possibility, bladders of CBA/J mice were treated with chitosan 3 d after infection with UTI89, washed, and then collected and imaged by scanning electron microscopy (SEM) at 1, 3, and 7 d postchitosan treatment. At days 1 and 3, large numbers of bacteria were visible on the apical surface of some bladders (Fig. 3.5). Similar levels of bacteria were observed less often at day 7 and in untreated, infected bladders, and not at all in uninfected controls. These observations suggest that chitosan treatment and subsequent regeneration of the urothelium can spur the resurgent growth of UPEC from established reservoirs. Many of the bacteria present on the bladder surface following chitosan treatment were filamentous, in line with previous work showing that filamentation is not uncommon among UPEC growing within the stressful confines of BECs and the bladder lumen (11, 15). Residual levels of chitosan, as well as the presence of oxidative radicals that can activate the SOS response, may both contribute to development of the filamentous bacteria (see Fig. 3.2E and (11, 15, 20)). Of note, many of the bacteria observed in this analysis were

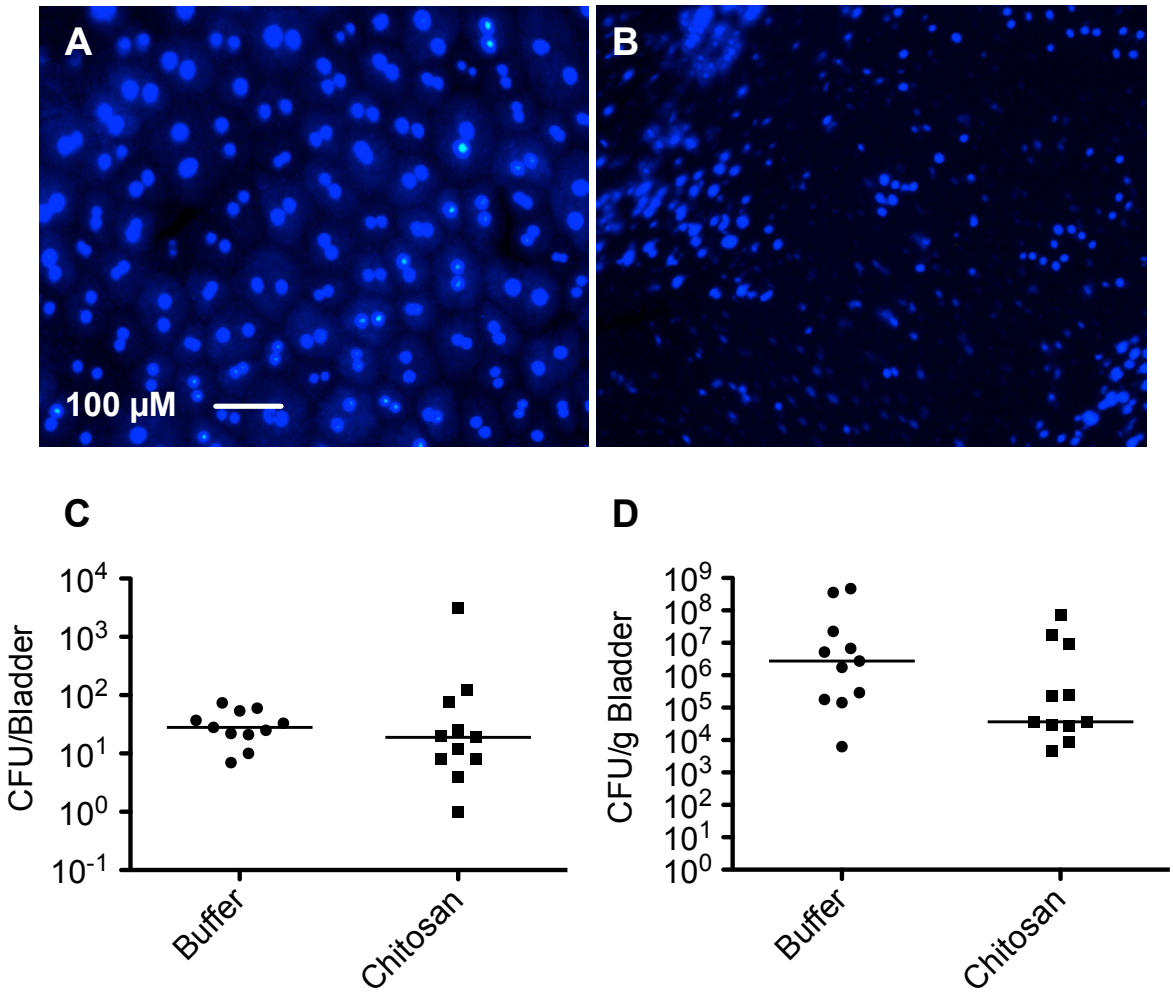

Figure 3.4 UPEC invades basal and intermediate bladder epithelial cells

7-8 wk old CBA/J mice from Jackson Laboratory were treated with (A) buffer control or (B) 50 µl of 0.02% chitosan for 20 minutes as described in the methods. Mice were sacrificed, bladders aseptically removed, splayed, and nuclei were stained with Hoeschst dye. The ability of UTI89 to invade intermediate and basal epithelial cells was tested by treating mice with control buffer or 50 µl of 0.02% chitosan for 20 minutes. 4 h after chitosan treatment, mice were infected with 10^7 UTI89 and allowed to incubate for 1 h. At this time mice were sacrificed and bladders were removed, homogenized, serially diluted, and titered for the presence of bacteria. (D) Mice were infected as described above and allowed to develop reservoir populations. At 3 d post infection, mice were treated with chitosan or buffer as previously described, washed with profusely with PBS, and immediately sacrificed. Bladders were removed, homogenized, and titered as described above. Graphs show median value with *P* values determined by the Mann Whitney U test.

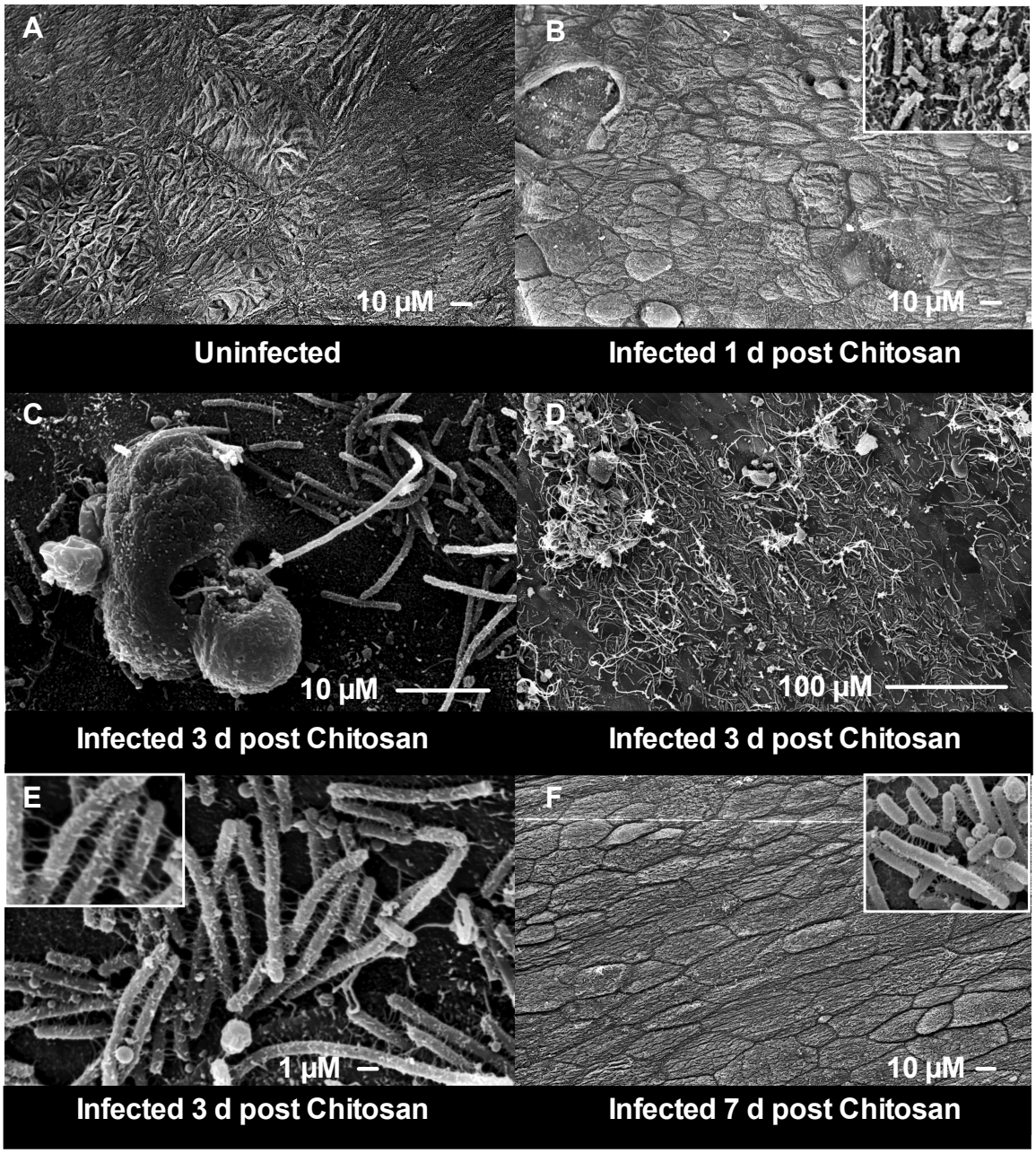

Figure 3.5 Chitosan treatment causes resurgence of UPEC reservoir into the bladder lumen

(A) SEM images of uninfected, unmanipulated bladder as a control. SEM images of (B-C) 1 d, (D-E) 3 d, and (F) 7 d time points after chitosan treatment of a 3 d infected mouse bladder. Magnifications are shown at the bottom of the images.

interconnected by tubular projections (Fig. 3.5). The nature of these projections remains unknown, but they appear too large to be pili and too numerous to be flagella as typical of this particular UPEC isolate.

Chitosan enhances the efficacy of antibiotics within the bladder

UPEC present in the bladder at 3 d postinoculation are, for the most part, localized within the urothelium barrier and are consequently protected from the effects of both host cell-impermeable and -permeable antibiotics (3). By forcing the resurgence of UPEC from reservoir populations, we reasoned that chitosan may render the bacteria more susceptible to host defenses and antibiotics. To assess this possibility, mice were treated with chitosan or phosphate buffer alone at 3 d postinoculation with UTI89. Mice were subsequently administered 3 or 7 daily doses of antibiotics, including the host cell-impermeable aminoglycoside gentamicin and two host cell-permeable fluoroquinolones, ciprofloxacin and sparfloxacin. Controls were given with water (carrier) alone by gavage. The animals were then allowed 3 additional days to clear the antibiotics from their systems before bladders were recovered, homogenized, and plated to determine bacterial titers.

In these assays, chitosan treatment without subsequent administration of antibiotics stimulated marked, though sporadic, outgrowth of UTI89 in the bladders of some, but not all of the test animals (Fig. 3.6), corroborating with results from the SEM analysis. The delivery of antibiotics for either 3 or 7 d had minimal effects on bacterial titers within the bladder tissue, in line with previous

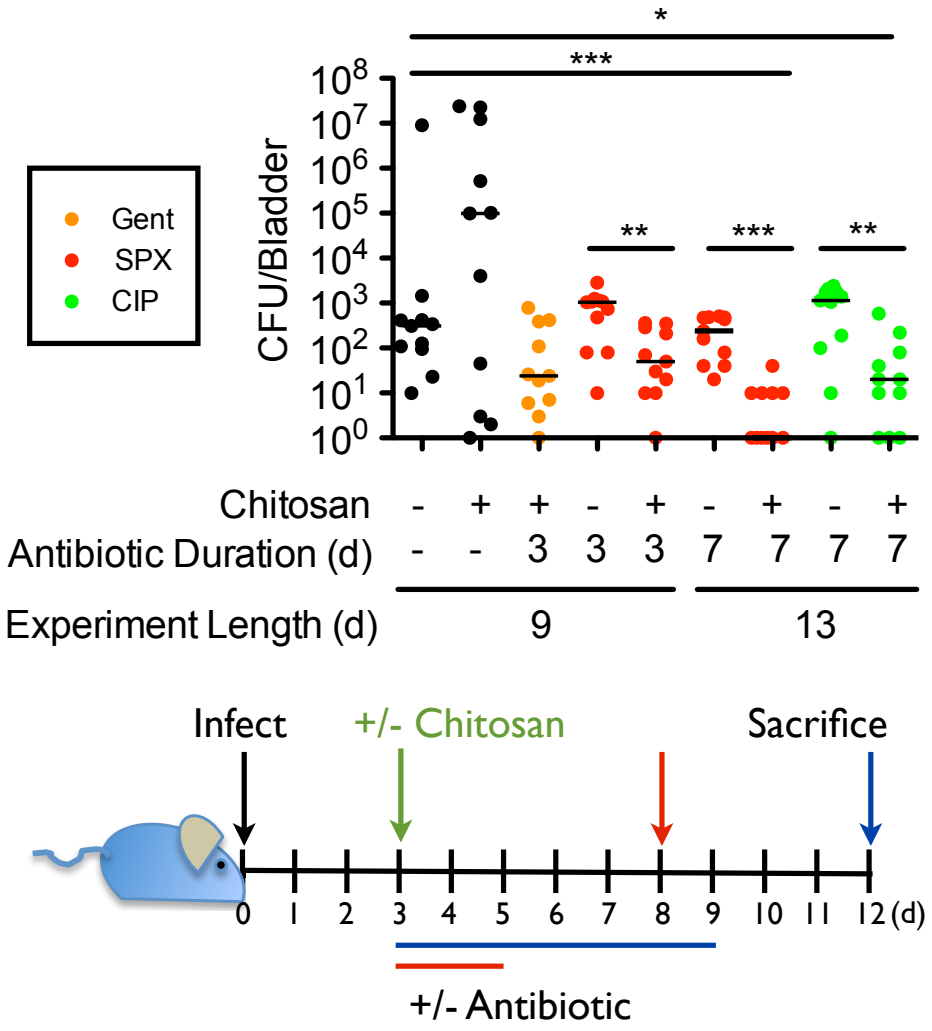

Figure 3.6 Chitosan treatment coupled with antibiotic treatment reduces bacterial titers

Mice, infected with 10^7 UTI89, were treated on day 3 with buffer or chitosan (50 µl of 0.02% chitosan). Buffer/chitosan treatment was followed by either a 3 d or 7 d control or antibiotic treatment (Gent = gentamicin, SPX = sparfloxacin, CIP = ciprofloxacin). A schematic showing the administration of chitosan and antibiotics is diagrammed below the graph. Graph is combined data from two separate experiments with greater than 11 mice per group.

observations (3). However, the treatment of bladders with chitosan prior to antibiotic administration significantly reduced bacterial titers, an effect that was much more pronounced with the 7 d antibiotic treatments (Fig. 3.6). These data indicate that chitosan can be used to enhance the efficacy of antibiotics within the bladder, likely by stimulating the efflux of UPEC reservoirs as well as decreasing the permeability barrier function of the urothelium.

Mice show recurrence despite near elimination of UPEC bladder reservoirs

By greatly reducing the level of detectable UPEC reservoirs within the bladder tissue, we hypothesized that chitosan treatment followed by the administration of sparfloxacin would result in decreased episodes of overt UTI recurrence as measured by urine titers. To test this, infected mice were treated on day 3 with chitosan or buffer, and then given sparfloxacin or water control for 7 consecutive days. Urine titers were collected once daily for >80% of the mice and plated directly on LB agar plates, noting the volume of urine collected. Samples that produced bacterial lawns when plated were assumed to contain a minimum of 4000 CFU. Urine titer data for 15 d following cessation of antibiotic treatment is shown in Fig. 3.7A. Titers of $>10^4$ colony forming units (CFU)/ml were counted as a recurrent/relapsing UTI. These were detected in all experimental groups over the course of these assays, though untreated mice receiving neither chitosan nor sparfloxacin had significantly more individual

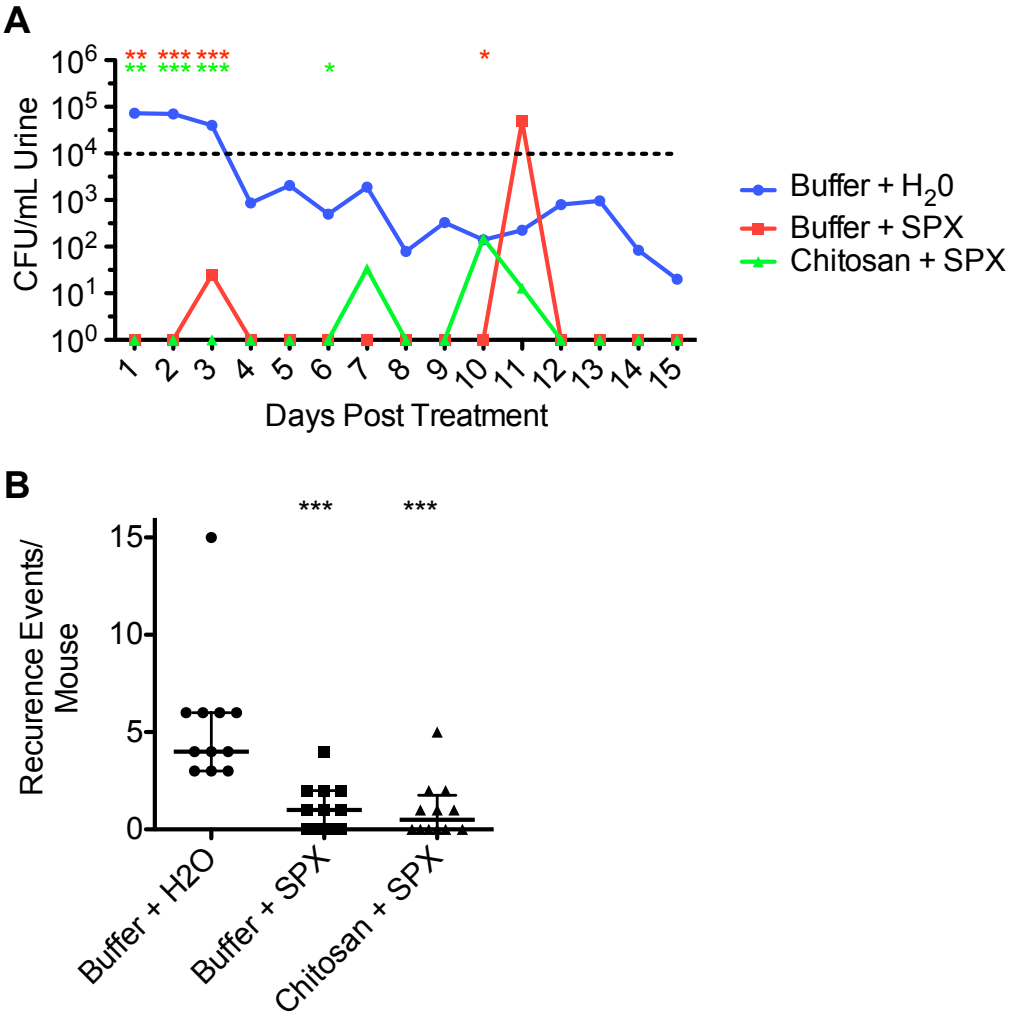

Figure 3.7 Chitosan and antibiotic treatment fails to prevent recurrence

(A) Urine titers measuring recurrence in infected mice mock treated or treated with 7 days of sparfloxacin, or sparfloxacin following chitosan treatment on day 3. Urine counts were not serially diluted, and thus a lawn, or a count over 1000 CFU/ml was considered as a recurrence event (above dotted line). (B) Total recurrence events observed for each mouse from panel A over the 15 d measurement. Each individual collection from each individual mouse was described as recurrent or below limit of recurrence. Statistics were performed as (A) Fischer's Exact Test, or (B) Mann Whitney U test with *P* = *<0.05, ***<0.001. Graphs are combined data from two separate experiments with greater than 11 mice per group.

recurrence events as determined by urine titers over the course of 15 d (Fig. 3.7B and data not shown). All 11 untreated mice exhibited a recurrence at some point during the 15 d period, whereas nearly half (5) of the mice treated with chitosan and sparfloxacin had no recurrence events (Fig. 3.7B). Mice treated with sparfloxacin alone faired only slightly worse. Both test treatments significantly delayed the onset of recurrent UTIs, with urine titers rising only after 3 or 7 days following the sparfloxacin or chitosan plus sparfloxacin treatments, respectively.

Discussion

In this manuscript, chitosan was used as a tool to trigger selective exfoliation of superficial bladder epithelial cells in a murine model of UTI. Chitosan acts to disrupt tight junctions between superficial bladder cells resulting in exfoliation of host epithelial cells, with little observable inflammation (32). Interestingly, chitosan only acts on the surface layer of the urothelium, leaving the intermediate and basal layers of epithelial cells mostly intact (32). Using chitosan, the UPEC reservoir populations were observed to be present in both the underlying layers of the urothelium and the superficial bladder epithelial cells. Additionally, UPEC was shown to invade underlying epithelial cells as efficiently as superficial cells during murine infection.

Massive efflux of UPEC into the bladder lumen was observed after chitosan treatment of mice, suggesting chitosan can force the resurgence of UPEC from the intracellular reservoirs, perhaps by triggering the differentiation of the immature host cells or otherwise altering the intracellular milieu so that

bacterial growth and release is favored. SEM imaging of infected bladders after chitosan treatment revealed numerous bacteria on lumenal surface, many of which were filamentous. These bacteria often elaborated unusual interbacterial connections that are morphologically reminiscent of recently described “nanotubes.” Bacterial nanotubes have been shown to mediate the direct transfer of proteins and, possibly, RNA between bacterial cells (5). These tubules also provide a network for exchange of molecules both within and between species and likely contribute structurally to bacterial communities. It is not yet clear if chitosan promotes the formation of these structures, although their presence at late time points following the administration of chitosan and in untreated bladders suggests that this is not the case.

Treatment of infected mouse bladders with chitosan followed by three or seven daily doses of antibiotics resulted in significant decreases in bacterial titers within the bladder tissue. In these assays, the 7 d treatments with either sparfloxacin or ciprofloxacin were notably more effective and may have substantial therapeutic potential. However, several pitfalls do exist with the proposed strategy. Chitosan can stimulate biofilm formation and increases interactions between UTI89 and BECs *in vitro*, which and could thereby promote bladder colonization under some conditions. Of even greater concern, the selective exfoliation of the superficial cell layer impairs barrier function of the urothelium and could consequently allow for broader dissemination of UPEC or enable infection by opportunistic pathogens. However, the combined use of antibiotics with chitosan ameliorates these concerns.

A model for UPEC colonization and resurgence from within the immature cells of the urothelium is presented in Fig. 3.8 UPEC may gain entry to the underlying immature cells of the bladder as the integrity of the urothelium barrier is compromised due to the exfoliation of infected superficial cells and the influx of neutrophils. Within the basal and intermediate cells of the urothelium, UPEC do not multiply and instead establishes long-lived quiescent intracellular reservoirs. These reservoirs may eventually be delivered back to the lumenal surface of the bladder as their immature host cells migrate and differentiate into superficial epithelial cells. Changes in the intracellular environment, including perhaps the redistribution of actin filaments, may enable UPEC to reinitiate growth, leading the bacteria to exit the host vacuolar compartment and multiply within the host cytosol in close association with cytokeratin intermediate filaments (7, 17). Replication and subsequent efflux into the bladder lumen promotes the further dispersal of UPEC, which in turn can stimulate host inflammatory responses and the full spectrum of symptoms associated with a recurrent UTI. By driving the resurgence of UPEC reservoirs in the presence of antibiotics, chitosan may be able to interrupt this cycle of infection that likely contributes to the widespread nature of recurrent UTIs. The fact that chitosan treatment in combination with antibiotics could not prevent recurrent/relapsing infection in all of the animals tested in our assays indicates that the use of chitosan can be further optimized to better eradicate UPEC reservoirs within the bladder that may be present at levels below our limit of detection. It is also possible that the presence of bacterial reservoirs within nearby tissues, such as the ureters or the vaginal mucosa, may

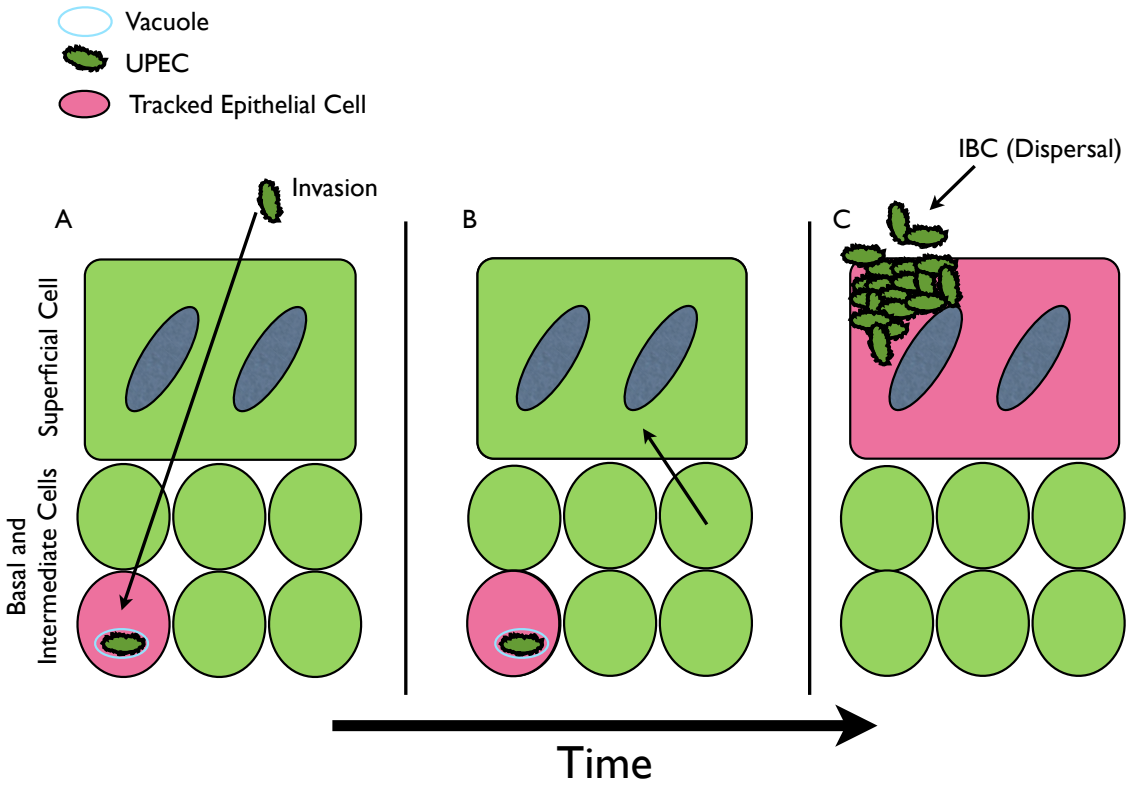

Figure 3.8 Model of UPEC action

(A) UPEC invade the transitional epithelium taking up residence in both superficial epithelial cells and underlying epithelial cells. (B) UPEC resident in underlying cells vertically move through the hierarchy of differentiating cells as a quiescent reservoir as the host cell progresses towards a terminally differentiated superficial epithelial bladder cell. (C) UPEC replicates and exits the quiescent intracellular reservoir within the host endocytic compartment (vacuole) before replicating rapidly in the cytosol to form IBCs. IBCs then act to disseminate UPEC to neighboring tissues to restart the cycle.

harbor UPEC reservoirs that can recolonize the bladder following the cessation of antibiotic treatment. Recolonization of the bladder in these assays is not likely attributable to fecal contamination of the urinary tract, as we have found that mice carrying UPEC within their intestines do not spontaneously acquire UTIs (unpublished observations). Formation of IBCs allows for dispersal of the bacteria and ultimately reinoculation of the bladder lumen, and to a low frequency, further invasion of host epithelial cells. In summary, UPEC slowly move towards the surface epithelium in differentiating epithelial cells, before undergoing resurgence to further disseminate the infection and persist within the urinary tract.

The idea of inducing bladder cell exfoliation as a therapeutic option for the treatment of chronic and recurrent UTIs is not new, and has been explored experimentally in previous work using protamine sulfate. When instilled into the bladder lumen, protamine sulfate triggers massive loss of the superficial cells as well as other BECs, often stripping away the urothelium to the basement membrane (25, 27). Chitosan offers a more restrained alternative, since it acts primarily on only the uppermost layers of cells. It also acts rapidly, induces little, if any, inflammation, and is likely less prone to elicit painful responses as does protamine sulfate (32). Finally, there are already anecdotal reports from outside of the USA of the use of chitosan to successfully treat human patients with chronic UTI (P. Veranic, unpublished), supporting our conclusion that chitosan may have tangible therapeutic value when used synergistically with antibiotics.

Materials and Methods

Reagents

Chitosan hydrochloride, low molecular weight, (FMC Corporation) was prepared as a 0.02% stock (w/v) in phosphate buffer (1.6 g NaCl, 0.095 KH_2PO_4, 0.472 $NaHPO_4$ x 12 H_2O Q.S. to 1 L H_2O; pH 4.5). All antibiotics and chemicals were purchased from Sigma-Aldrich and used at the concentrations listed in the text.

Bacterial strains and growth

The prototypic UPEC cystitis isolate UTI89 has been described previously (4, 24). Bacteria were grown from frozen stocks in either Luria-Bertani (LB) broth or modified M9 minimal medium (6 g/liter Na_2HPO_4, 3 g/liter KH_2PO_4, 1 g/liter NH_4Cl, 0.5 g/liter NaCl, 1 mM $MgSO_4$, 0.1 mM $CaCl_2$, 0.1% glucose, 0.0025% nicotinic acid, 0.2% casein amino acids, and 16.5 µg/ml thiamine in H_2O) at 37°C. Growth curve analysis was performed as previously described using a Bioscreen C machine (Growth Curves USA) with optical density measured at 600 nm every 30 m (18).

Biofilm assays

In vitro microtiter plate-based biofilm assays were performed as previously described. Briefly, UTI89 was diluted 1:100 from overnight shaking cultures into M9 medium. Quadruplicate, 100 µl samples in 96-well pinchbar flat-bottomed polystyrene microtiter plates with lids (Nunc) were incubated for 48 h without

shaking at 37°C surrounded by distilled water to limit evaporation of samples. Nonadherent bacteria were then removed by washing twice with H_2O prior to addition of crystal violet (150 µl of a 0.1% solution in water; Sigma-Aldrich). After 10 min incubation at room temperature, the wells were rinsed twice with H_2O and air-dried. Dimethyl sulfoxide (200 µl; Sigma-Aldrich) was added to each well, and the plates were shaken vigorously for 15 min on an orbital shaker to solubilize the dye, and A_{562} was measured using a Synergy HT multidetection microplate reader (BioTek Instruments, Inc.). Biofilms were also grown on glass coverslips for 48 h in 24-well tissue culture grade plates tilted at an angle to allow for a liquid-air interface to cross the coverslip. Biofilms grown on glass coverslips were visualized using a SZX10 stereomicroscope (Olympus) equipped with a QIClick Cooled Digital CCD camera (QImaging).

Association, invasion, intracellular replication assays

UTI89 was grown at 37°C for 48 h in static LB broth to induce type 1 pilus expression. Triplicate sets of confluent 5637 bladder epithelial cell monolayers grown in 24-well tissue culture plates were infected with UTI89 using a multiplicity of infection of ~15 bacteria per host cell. To facilitate and synchronize bacterial contact with the host cells, plates were centrifuged at 600 x *g* for 5 min at room temperature at the start of infection (Beckman Allegra 6 Centrifuge). Cells were infected in conjunction with chitosan (0.002% or 0.02%) for 2 h or corresponding volume of low pH phosphate buffer. After a 2 h incubation at 37°C, samples were washed three times with PBS containing Ca^{2+} and Mg^{2+} (PBS^{2+}) to

remove any nonadherent bacteria. Wells for adherence and total growth assays were collected at this time point and lysed in PBS with 0.4% Triton X-100, and bacteria present within the lysates were enumerated by plating serial dilutions on LB agar plates. Monolayers for invasion and intracellular replication assays were then incubated for another 2 h with complete RPMI medium plus 100 μg/ml of gentamicin to kill extracellular bacteria. Monolayers for invasion assays were collected at this time (4 h) and processed as described above. Invasion was graphed as normalized to associated bacteria as well as raw values for invasion CFU. For intracellular replication assays, additional washes with PBS^{2+} were performed, followed by addition of fresh medium containing a lower concentration of gentamicin (10 μg/ml). Incubations were continued for another 14 h. This submaximal concentration of gentamicin was used to prevent extracellular growth of UPEC while limiting possible leaching of the antibiotic into the host cells during longer incubations. After final washes in PBS^{2+}, host cells were again lysed as described above in PBS with 0.4% Triton X-100, with bacteria enumerated by plating serial dilutions on LB agar plates.

Mouse infection

Seven- to 8-week-old female CBA/J mice (Jackson Laboratory) were anesthetized via isoflurane inhalation and slowly inoculated via transurethral catheterization with 50 μl of a bacterial suspension (~10^7 CFU from 24 h static LB broth cultures of UTI89) in PBS as previously described. Bacterial reflux into the kidneys using this procedure is rare, occurring in less than 1% of the test animals

(unpublished data). Chitosan (0.01% in 50 µl of pH 4.5 phosphate buffer) was administered in a similar manner using transurethral catheterization of anesthetized mice for 20 min; however, mice were rotated 180° midway through the incubation to promote exfoliation of the entire bladder. At the appropriate time point, mice were sacrificed, bladders were harvested aseptically, weighed, and homogenized in 1 ml PBS containing 0.025% Triton X-100. Bacterial titers within the homogenates were determined by plating serial dilutions on LB agar plates. Eleven mice total, from two independent experiments, were used for each condition tested. Previous published results indicate no need for mock-infected mice to be housed in cages with the infected animals (3).

To determine the ability of UPEC to invade underlying tissues, mice were anesthetized and treated with chitosan. After 4 h of incubation, mice were infected as described above via transurethral catheterization. After 1 h of incubation, mice were sacrificed and bladders were aseptically removed, cut into quarters and incubated in 1 ml of gentamicin (100 µg/ml) for 1 h. Bladders were then washed and homogenized in the presence of 0.025% Triton X-100. After homogenization, bladders were serially diluted and titered as above.

To determine the contribution of mouse epithelial tissues to reservoir population, mice were infected and reservoir populations were allowed to establish for 3 d. At this time, mice were treated with chitosan or buffer. Post-treatment, mice were sacrificed and bladders were rigorously washed with PBS to remove exfoliated superficial cells and lumen localized bacteria. Bladders were

then homogenized and titered to determine the relative contribution of tissue layers towards reservoir formation.

Treatment efficacy

Mice were infected as described above. At 3 days postinoculation, treatments were initiated by transurethral catheterization of mice with buffer or chitosan. A single dose of chitosan was administered on the first day of treatment (day 3) in conjunction with antibiotic treatment. Daily antibiotic treatment continued for 3 or 7 consecutive days. Gentamicin (200 μg) was given subcutaneously, while sparfloxacin (700 μg) and ciprofloxacin (40 μg) were given orally by gavage. Control animals were given water alone by oral gavage. All antibiotics were delivered in 50 μl volumes. Mice were sacrificed 3 days after the final antibiotic treatment. At this time point, bladders were harvested aseptically, weighed, and homogenized as described above, followed by serial dilution and titering of the bacteria.

Mouse urine titers

Mice were infected as described above. After allotted treatment regimen, urine was collected daily. Mice were placed over sterile saran wrap and allowed to urinate. Urine was collected, measured for volume, and plated on LB agar plates directly after dilution in PBS to 100 μl volume if required. We were unable to create a dilution range due to limited quantity of mouse urine, and thus all

colonies were counted when possible on LB plates. A count over 10,000 CFU/ml was designated as a recurrence event.

SEM microscopy

Infected mouse bladders were excised from animals, cut longitudinally into halves and fixed for 4 h at 4°C in a mixture of 4% paraformaldehyde and 2% glutaraldehyde in 0.1 M cacodylate buffer (pH 7.4). The tissue samples were rinsed in 0.1 M cacodylate buffer and postfixed in 1% osmium tetroxide in the same buffer for 1 h at 4°C. Specimens were critical point dried, sputter-coated with gold and examined at 15 kV with a JOEL JSM 84 A scanning electron microscope.

Statistical analysis

P values were determined by Student's *t*-test and Mann-Whitney U tests performed using Prism 5.01 software (GraphPad Software). Values of less than 0.05 were defined as significant.

Acknowledgements

We are grateful to Frank Rauh (FMC Corp) for providing the chitosan. This study was funded by NIH grants AI095647, DK068585, AI090369, and AI088086. M.G.B. was supported by Award Number T32AI055434 from the National Institute of Allergy and Infectious Diseases. The content is solely the responsibility of the authors and does not necessarily represent the official views

of the National Institute Of Allergy And Infectious Diseases or the National Institutes of Health.

References

1. **Anderson, G. G., K. W. Dodson, T. M. Hooton, and S. J. Hultgren.** 2004. Intracellular bacterial communities of uropathogenic *Escherichia coli* in urinary tract pathogenesis. Trends Microbiol. **12:**424-430.

2. **Apodaca, G.** 2004. The uroepithelium: not just a passive barrier. Traffic **5:**117-128.

3. **Blango, M. G., and M. A. Mulvey.** 2010. Persistence of uropathogenic *Escherichia coli* in the face of multiple antibiotics. Antimicrob. Agents Chemother. **54:**1855-1863.

4. **Chen, S. L., C. S. Hung, J. Xu, C. S. Reigstad, V. Magrini, A. Sabo, D. Blasiar, T. Bieri, R. R. Meyer, P. Ozersky, J. R. Armstrong, R. S. Fulton, J. P. Latreille, J. Spieth, T. M. Hooton, E. R. Mardis, S. J. Hultgren, and J. I. Gordon.** 2006. Identification of genes subject to positive selection in uropathogenic strains of *Escherichia coli*: a comparative genomics approach. Proc. Natl. Acad. Sci. U. S. A. **103:**5977-5982.

5. **Dubey, G. P., and S. Ben-Yehuda.** 2011. Intercellular nanotubes mediate bacterial communication. Cell **144:**590-600.

6. **Eto, D. S., T. A. Jones, J. L. Sundsbak, and M. A. Mulvey.** 2007. Integrin-mediated host cell invasion by type 1-piliated uropathogenic *Escherichia coli*. PLoS Pathog. **3:**e100.

7. **Eto, D. S., J. L. Sundsbak, and M. A. Mulvey.** 2006. Actin-gated intracellular growth and resurgence of uropathogenic *Escherichia coli*. Cell. Microbiol. **8:**704-717.

8. **Foxman, B.** 2003. Epidemiology of urinary tract infections: incidence, morbidity, and economic costs. Dis. Mon. **49:**53-70.

9. **Foxman, B.** 1990. Recurring urinary tract infection: incidence and risk factors. Am. J. Public Health **80:**331-333.

10. **Hicks, R. M.** 1975. The mammalian urinary bladder: an accommodating organ. Biol. Rev. Camb. Philos. Soc. **50:**215-246.

11. **Horvath, D. J., Jr., B. Li, T. Casper, S. Partida-Sanchez, D. A. Hunstad, S. J. Hultgren, and S. S. Justice.** 2011. Morphological plasticity promotes resistance to phagocyte killing of uropathogenic *Escherichia coli*. Microbes Infect. **13:**426-437.

12. **Huang, E. S., and R. S. Stafford.** 2002. National patterns in the treatment of urinary tract infections in women by ambulatory care physicians. Arch. Intern. Med. **162:**41-47.

13. **Jost, S. P., J. A. Gosling, and J. S. Dixon.** 1989. The morphology of normal human bladder urothelium. J. Anat. **167:**103-115.

14. **Justice, S. S., C. Hung, J. A. Theriot, D. A. Fletcher, G. G. Anderson, M. J. Footer, and S. J. Hultgren.** 2004. Differentiation and developmental pathways of uropathogenic *Escherichia coli* in urinary tract pathogenesis. Proc. Natl. Acad. Sci. U. S. A. **101:**1333-1338.

15. **Justice, S. S., D. A. Hunstad, P. C. Seed, and S. J. Hultgren.** 2006. Filamentation by *Escherichia coli* subverts innate defenses during urinary tract infection. Proc. Natl. Acad. Sci. U. S. A. **103:**19884-19889.

16. **Kerec, M., M. Bogataj, P. Veranic, and A. Mrhar.** 2005. Permeability of pig urinary bladder wall: the effect of chitosan and the role of calcium. Eur. J. Pharm. Sci. **25:**113-121.

17. **Khandelwal, P., S. N. Abraham, and G. Apodaca.** 2009. Cell biology and physiology of the uroepithelium. Am. J. Physiol. Renal Physiol. **297:**F1477-1501.

18. **Kulesus, R. R., K. Diaz-Perez, E. S. Slechta, D. S. Eto, and M. A. Mulvey.** 2008. Impact of the RNA chaperone Hfq on the fitness and virulence potential of uropathogenic *Escherichia coli*. Infect Immun. **76:**3019-3026.

19. **Lewis, S. A.** 2000. Everything you wanted to know about the bladder epithelium but were afraid to ask. Am. J. Physiol. Renal Physiol. **278:**F867-874.

20. **Li, B., P. Smith, D. J. Horvath, Jr., F. E. Romesberg, and S. S. Justice.** 2010. SOS regulatory elements are essential for UPEC pathogenesis. Microbes Infect. **12:**662-668.

21. **Liu, H., Y. Du, X. Wang, and L. Sun.** 2004. Chitosan kills bacteria through cell membrane damage. Int. J. Food Microbiol. **95:**147-155.

22. **Martin, B. F., and Y. C. Wong.** 1981. Development and maturation of the bladder epithelium of the guinea pig. Acta Anat. (Basel) **110:**359-375.

23. **Mulvey, M. A., Y. S. Lopez-Boado, C. L. Wilson, R. Roth, W. C. Parks, J. Heuser, and S. J. Hultgren.** 1998. Induction and evasion of host defenses by type 1-piliated uropathogenic *Escherichia coli*. Science **282:**1494-1497.

24. **Mulvey, M. A., J. D. Schilling, and S. J. Hultgren.** 2001. Establishment of a persistent *Escherichia coli* reservoir during the acute phase of a bladder infection. Infect. Immun. **69:**4572-4579.

25. **Mysorekar, I. U., and S. J. Hultgren.** 2006. Mechanisms of uropathogenic *Escherichia coli* persistence and eradication from the urinary tract. Proc. Natl. Acad. Sci. U. S. A. **103:**14170-14175.

26. **Mysorekar, I. U., M. A. Mulvey, S. J. Hultgren, and J. I. Gordon.** 2002. Molecular regulation of urothelial renewal and host defenses during infection with uropathogenic *Escherichia coli*. J. Biol. Chem. **277:**7412-7419.

27. **Parsons, C. L., C. W. Stauffer, and J. D. Schmidt.** 1988. Reversible inactivation of bladder surface glycosaminoglycan antibacterial activity by protamine sulfate. Infect. Immun. **56:**1341-1343.

28. **Prat, V., K. Matousovic, M. Horcickova, M. Hatala, and Z. Milotova.** 1989. [Prevention of recurrent urinary infections using Solco Urovac, a polymicrobial vaccine]. Cas. Lek. Cesk. **128:**1106-1109.

29. **Schilling, J. D., R. G. Lorenz, and S. J. Hultgren.** 2002. Effect of trimethoprim-sulfamethoxazole on recurrent bacteriuria and bacterial persistence in mice infected with uropathogenic *Escherichia coli*. Infect. Immun. **70:**7042-7049.

30. **Schilling, J. D., M. A. Mulvey, C. D. Vincent, R. G. Lorenz, and S. J. Hultgren.** 2001. Bacterial invasion augments epithelial cytokine responses to *Escherichia coli* through a lipopolysaccharide-dependent mechanism. J. Immunol. **166:**1148-1155.

31. **Thumbikat, P., R. E. Berry, A. J. Schaeffer, and D. J. Klumpp.** 2009. Differentiation-induced uroplakin III expression promotes urothelial cell death in response to uropathogenic *E. coli*. Microbes Infect. **11:**57-65.

32. **Veranic, P., A. Erman, M. Kerec-Kos, M. Bogataj, A. Mrhar, and K. Jezernik.** 2009. Rapid differentiation of superficial urothelial cells after chitosan-induced desquamation. Histochem. Cell Biol. **131:**129-139.

33. **Vigil, P. D., C. J. Alteri, and H. L. Mobley.** 2011. Identification of in vivo-induced antigens including an RTX family exoprotein required for uropathogenic *Escherichia coli* virulence. Infect. Immun. **79:**2335-2344.

34. **Wang, H., G. Min, R. Glockshuber, T. T. Sun, and X. P. Kong.** 2009. Uropathogenic *E. coli* adhesin-induced host cell receptor conformational changes: implications in transmembrane signaling transduction. J. Mol. Biol. **392:**352-361.

35. **Wiles, T. J., R. R. Kulesus, and M. A. Mulvey.** 2008. Origins and virulence mechanisms of uropathogenic *Escherichia coli*. Exp. Mol. Pathol. **85:**11-19.

36. **Yomota, C., T. Komuro, and T. Kimura.** 1990. [Studies on the degradation of chitosan films by lysozyme and release of loaded chemicals]. Yakugaku Zasshi **110:**442-448.

37. **Zhou, G., W. J. Mo, P. Sebbel, G. Min, T. A. Neubert, R. Glockshuber, X. R. Wu, T. T. Sun, and X. P. Kong.** 2001. Uroplakin Ia is the urothelial receptor for uropathogenic *Escherichia coli*: evidence from *in vitro* FimH binding. J. Cell. Sci. **114:**4095-4103.

CHAPTER 4

SMALL NONCODING RNAS REGULATE THE STRESS RESISTANCE AND VIRULENCE PROPERTIES OF UROPATHOGENIC *ESCHERICHIA COLI*

Abstract

Small noncoding RNA (sRNA) molecules can modulate diverse bacterial functions ranging from carbon metabolism to virulence gene expression. Here, we used a series of deletion mutants, each lacking one of seven conserved sRNAs (DsrA, RprA, OxyS, RyhB, MicF, MicC, and Spot 42) for effects on the fitness and virulence potential of the reference uropathogenic *Escherichia coli* (UPEC) isolate UTI89. UPEC strains are the primary etiologic agents of urinary tract infections, which consistently rank among the most common of infectious diseases. In broth culture, each sRNA deletion mutant grew like the wild type strain, whereas in biofilm assays all but the *micC* mutant exhibited modest, though significant defects. None of the mutants displayed increased sensitivity to nitrosative stress, but the Spot 42 (*spf*) and *micC* mutants were both markedly impaired in their ability to deal with oxidative stress generated by methyl viologen. The *spf* mutant, but not the others, also had diminished swim motility. Focusing further on Spot 42, we found that deletion of this sRNA significantly altered the levels of key metabolites in UTI89, including the coenzyme A precursor pantothenate. The *spf* mutant was also defective in its ability to multiply and persist within host bladder epithelial cells in both cell culture-based assays and in a murine infection model. Cumulatively, these results demonstrate that specific sRNA molecules can impact multiple bacterial processes that control the stress resistance and virulence capacity of UPEC both *in vitro* and within the host environment.

Introduction

Small noncoding RNA (sRNA) molecules help control the translation and activity of numerous proteins in both nonpathogenic and pathogenic bacteria (7, 55, 61, 81). Base pairing between an sRNA and cognate mRNA targets can either promote or, more often, inhibit translation. Oftentimes, sRNA-mRNA interactions are facilitated by the homohexameric RNA chaperone Hfq (12). sRNAs can modulate diverse bacterial functions, including metabolism, iron utilization, the expression of outer membrane proteins (OMPs), stress resistance, and virulence (15, 25, 61, 75). Much of what we currently know about sRNAs is based on work carried out with nonpathogenic K-12 *Escherichia coli* isolates. In these bacteria the expression of about 90 different sRNA species has been confirmed, with more than 200 additional sRNAs predicted by *in silico* analyses (59, 66, 67). Many of these sRNA molecules are also encoded by pathogenic *E. coli* strains, including diarrheagenic isolates and strains of uropathogenic *E. coli* (UPEC). Previously, we reported that deletion of *hfq* in the UPEC reference isolate UTI89 rendered this pathogen severely attenuated in its ability to colonize both the bladder and kidneys in a mouse urinary tract infection (UTI) model system (34). The *hfq* mutant was also hypersensitive to oxidative and nitrosative stresses and was defective in its ability to swim and form biofilms. These results indicate that sRNAs in association with Hfq contribute significantly to the fitness and virulence potential of UPEC.

UTIs caused by UPEC are among the most common of infectious diseases worldwide, representing a daunting medical and financial burden that is

likely to worsen as antibiotic resistance among UPEC strains increases (23). Successful colonization of the urinary tract requires that UPEC deal with a panoply of stresses and host defenses, including the bulk flow of urine, nutrient limitations, the production of reactive nitrogen and oxygen radicals, the secretion of antimicrobial compounds, and the influx of phagocytes like neutrophils (26, 50). Upon entering the lumen of the bladder, UPEC expressing filamentous adhesive organelles known as type 1 pili are able to bind and subsequently invade bladder epithelial cells, gaining at least temporary reprieve from extracellular antimicrobial factors and shear forces that work to eliminate microbes. Within bladder cells, UPEC enter into actin-bound, low pH endosomal compartments where they can persist quiescently for days to many weeks (21, 49, 52). Alternatively, UPEC may break into the host cell cytosol where they can multiply, forming large intracellular biofilm-like communities (IBCs) in close association with cytokeratin intermediate filaments (31, 49). The persistence and dissemination of UPEC within the urinary tract is facilitated by multiple factors, including the formation and eventual dispersion of IBCs as well as flagella-driven motility and the optimized use of central metabolic pathways like gluconeogenesis and the TCA cycle (1, 26). The ability of UPEC to cope with changing environmental stresses within the host likely requires rapid alteration of metabolic and stress response pathways, tasks that can potentially be facilitated with the aid of sRNA molecules.

Here, taking a candidate approach using isogenic deletion mutants, we assess the effects of a panel of seven Hfq-dependent sRNA molecules on the

fitness and virulence potential of UPEC, before focusing in greater detail on a single sRNA, Spot 42.

Materials and Methods

Bacterial strains and plasmids

Strains used in this study are listed in Table 4.1. Mutant strains were constructed in the human cystitis isolate *E. coli* strain UTI89 using the primers listed in Table 4.2 and the lambda Red recombination system, as previously described (19, 51). Chloramphenicol and kanamycin resistance cassettes, each containing their own promoter and terminator, were amplified from *Salmonella* strain TT23216 or plasmid pKD4, respectively (19, 34). The primers for amplification of the cassettes were designed with overhanging ends containing ~40 bp of homology to the 5' and 3' ends of target knockout sites. PCR products were then introduced by electroporation into UTI89 carrying pKM208, which encodes IPTG (isopropyl-b-D-thiogalactopyranoside)-inducible lambda Red recombinase (19). The *spf* and *micC* double knockout strain was constructed by deleting *micC* from UTI89Δ*spf* using the kanamycin resistance cassette amplified from the plasmid pKD4. Knockout strains were verified by PCR amplification using primers specific to sequences flanking each target gene.

The plasmids used in this study are listed in Table 4.1. Plasmids pMB1_GrxB, pMB2_Gsp, pMB3_PanC, and pMB4_YggE were constructed by PCR amplifying from UTI89 genomic DNA each gene of interest with flanking KpnI and PstI restriction digestion sites. PCR products were cut using KpnI and

Table 4.1 Bacterial strains and plasmids

Strain or Plasmid	Description	Source or Reference
Strains		
E. coli		
UTI89	UPEC reference strain and cystitis isolate	(14, 49)
MG1655	K-12 laboratory *E. coli* strain	(10)
Recombinant Strains		
UTI89Δ*dsrA*	UTI89 *dsrA::cat*	This work
UTI89Δ*micC*	UTI89 *micC::cat*	This work
UTI89Δ*micF*	UTI89 *micF::cat*	This work
UTI89Δ*oxyS*	UTI89 *oxyS::cat*	This work
UTI89Δ*rhyB*	UTI89 *rhyB::cat*	This work
UTI89Δ*rprA*	UTI89 *rprA::cat*	This work
UTI89Δ*spf*	UTI89 *spf::cat*	This work
UTI89Δ*spf*Δ*micC*	UTI89 *spf::cat, micC::kan*	This work
UTI89Δ*fimH*	UTI89 *fimH::cat*	T. Wiles
TT23216	Template strain with *Cat* cassette flanked by universal primer sequences	(34)
Plasmids		
pGEN-GFP(LVA)	Encodes destabilized GFP (half-life ~40 min) under control of *em7* promoter, Ap^r	(81)
pKD4	Template plasmid for use in lambda Red Recombination, Kan^r	(18)
pKM208	IPTG-inducible lambda Red recombinase expression plasmid, Ap^r	(52)
pRR48	$lacI^q/p_{tac}$ cloning vector, Ap^r	(74)
pMB1_GrxB	*grxB* cloned into pRR48, Ap^r	This work
pMB2_Gsp	*gsp* cloned into pRR48, Ap^r	This work
pMB3_PanC	*panC* cloned into pRR48, Ap^r	This work
pMB4_YggE	*yggE* cloned into pRR48, Ap^r	This work
pACYC184	Low copy cloning plasmid, Clm^r Tet^r	NEB
pMB5_MiaA-Flag	C-terminal Flag-tagged *miaA* cloned into pACYC184, Tet^r	This work
pRRK1	Modified pRR48 lacking Shine-Delgarno sequence, Ap^r	This work
pSpot42a	*spf* cloned into pRRK1, Ap^r	This work
pMicC1	*micC* cloned into pRRK1, Ap^r	This work

Table 4.2 Oligonucleotides employed during the study

Primer[a]	**Sequence (5'-3')**[b, c, d]
DsrA-KO-F	TTCAGCGTCTCTGAAGTGAATCGTTGAATGCACAA TAAAACACCAAACACCCCCCAAAACC
DsrA-KO-R	TATTTTCTTGTCAGCGAAAAAAATTGCGGATAAGG TGATGCACACAACCACACCACACCAC
DsrA-Conf-F	GAAAGCGAAGTTCATCGCA
DsrA-Conf-R	ATTATCAAAGATGATTTTTTCGGG
MicC-KO-F	AAAATTATACTTTTAATTTTCTATACGTTATTCTGC GCGGCACCAAACACCCCCCAAAACC
MicC-KO-R	TTAAATGCTCTGGATAAGGATTATCCAATTCTA AAAAAAACACACAACCACACCACACCAC
MicC-Conf-F	GCCTTTCATCCCCATTTTG
MicC-Conf-R	ACTGGAAGAAACGTTACTTCACG
MicF-KO-F	TGTCAAAACAAAACCTTCACTCGCAACTAGAATAT CTTCCCACCAAACACCCCCCAAAACC
MicF-KO-R	CACAGAATAATGAAAAGTGTGTAAAGAAGGGTAAA AAAAACACACAACCACACCACACCAC
MicF-Conf-F	TGTTTCAGAATGTAAATGAAAGGG
MicF-Conf-R	AGATGTACAAGCGCCATTTTG
OxyS-KO-F	CTATCAGGCTCTCTTGCTGTGGGCCTGTAGAATAA AAAAACACCAAACACCCCCCAAAACC
OxyS-KO-R	GATTATCCCTATCAAGCATTCTGACTGATAATTGC TCACACACACAACCACACCACACCAC
OxyS-Conf-F	TCCTTTGCTCCGATCGTAAC
OxyS-Conf-R	GGCTAACGTGGCAGGAATC
RhyB-KO-F	CTTCCCGAGGATAAATTGAGAACGAAAGGTCAAA AAAAAACACCAAACACCCCCCAAAACC
RhyB-KO-R	GTGTTGGACAAGTGCGAATGAGAATGATTATTATT GTCTCCACACAACCACACCACACCAC
RhyB-Conf-F	AGTACATACGGCAGATGGTAACG
RhyB-Conf-R	GTGAATCTGCCTGATGGCTT
RprA-KO-F	TCTGATCGACGCAAAAAGTCCGTATGCCTACTATT AGCTCCACCAAACACCCCCCAAAACC
RprA-KO-R	TGAGGGGCGAGGTAGCGAAGCGGAAAAATGTTAA AAAAAACACACAACCACACCACACCAC
RprA-Conf-F	AAACCGAATAAGTAATTTCTCATCAG
RprA-Conf-R	CATCAATAGTCATGGCAAAAATAT
Spot42-KO-F	ATGCTTTCTGAACTGAACAAAAAAGAGTAAAGTTA GTCGCCACCAAACACCCCC CAAAACC
Spot42-KO-R	CATGGCGTATCAGGCATTACGGATCTTTTCTTTCG CCCAACACACAACCACACCACACCAC
Spot42-Conf-F	GAAAACTGGGATCAGGCG

Table 4.2 Continued

Primer[a]	**Sequence (5'-3')**[b, c, d]
Spot42-Conf-R	TTTAGCGAGATGCAGCCTG
GrxB-pRR48-F	CGCGCTGCAGGTGAAGCTATACATTTACG
GrxB-pRR48-R	CGGCGGTACCTTAAATCGCCATTGATG
Gsp-pRR48-F	CGCGCTGCAGGTGATGAGCAAAGGAACGAC
Gsp-pRR48-R	CGGCGGTACCACATGTATTACTCTTTCACC
PanC-pRR48-F	CGCGCTGCAGTTAATTATCGAAACCCTGC
PanC-Flag-pRR48-R	ATCCGGGTACC**CTATCCCTTATCGTCGTCATCCTTGTAGTCTGGTCCTCCTCCTCC**CGCCAGTTCGACCAGTTTG
YggE-pRR48-F	CGCGCTGCAGGTGAAGTTCA AAGTTATCG
YggE-pRR48-R	CGGCGGTACCTTAATGTGCAGCAGGTGTTTTAGCG
MiaA-pRR48-F	CGGCGAATTCGGCTAAAAGTTTCTGGCGAAGAAAAATCGG
MiaA-Flag-pRR48-R	CGCGGAATTC**CTATCCCTTATCGTCGTCATCCTTGTAGTCTGGTCCTCCTCCTCC**GCCTGCGATAGCACCAACAAC
Spot42-pRRK1-F	CGCGCTGCAGGTAGGGTACAGAGGT
Spot42-pRRK1-R	CGCGGGTACCTTCTTTCGCCCAATA

[a] F, forward primer; R, reverse primer; KO, knockout primer; Conf, confirmation primer.
[b] Universal Primer sequence underlined
[c] Added restriction sites underlined
[d] Flag tag and linker sequence in bold

PstI restriction enzymes and ligated into pRR48 using T4 DNA Ligase (NEB)(70). pSpot42a and pMicC1 were similarly constructed using pRRK1, a derivative of pRR48 that lacks a ribosome binding site following the p*tac* promoter. To create pMB5_MiaA-Flag, the *miaA* gene in UTI89 was amplified, along with 200 base pairs upstream of the *miaA* start site, using primers that were designed to also incorporate flanking EcoR1 restriction sites and a C-terminal FLAG tag. The PCR product was ligated into the EcoR1 site in pACYC184 (NEB). Plasmid constructs were verified by sequencing.

Growth assays

UTI89 and its derivatives were grown from frozen stocks in either Luria-Bertani (LB) broth, 100 mM morpholineethanesulfonic acid (MES)-buffered LB (LB-MES; pH 5.0), or modified M9 minimal medium (6 g/l Na_2HPO_4, 3 g/l KH_2PO_4, 1 g/l NH_4Cl, 0.5 g/l NaCl, 1 mM $MgSO_4$, 0.1 mM $CaCl_2$, 0.1% glucose, 0.0025% nicotinic acid, 0.2% casein amino acids, and 16.5 µg/ml thiamine in H_2O) (Sigma-Aldrich) at 37°C overnight in loosely capped 20-by-150-mm borosilicate glass tubes at a 30º angle with shaking at 225 rpm. Overnight cultures were diluted 1:100 into 100-well honeycomb plates and assayed for growth using a Bioscreen C instrument (Growth Curves USA) as described (34). Growth was assessed in LB-MES ± 1 mM sodium nitrite and in LB broth ± 1 mM EDTA, 0.01% sodium dodecyl sulfate, or 1 mM methyl viologen (MV, Sigma-Aldrich). Antibiotics were added to maintain plasmids as necessary for growth of overnight cultures, but not for subsequent growth assays (Sigma-Aldrich).

Superoxide dismutase (SOD) assays

A superoxide dismutase detection kit was purchased from Cell Technologies, Inc. and used according to the manufacturers specifications. Briefly, UTI899 and UTI89Δ*spf* were grown to OD_{600} of 0.1, 0.2, and 0.4 in LB broth + 1 mM MV, pelleted, and lysed in B-PER (Thermo Scientific) prior to analysis. The superoxide dismutase detection kit relies on the SOD-inhibitable conversion of a highly water-soluble tetrazolium salt (WST-1 (2-(4-Iodophenyl)-3-(4-nitrophenyl)-5-(2,4-disulfophenyl)- 2H-tetrazolium monosodium salt) to a yellow WST-1 formazan dye upon reduction with superoxide anions produced by xanthine oxidase. Reduced production of the WST-1 formazan dye, as measured by assaying absorbance at 440 nm, correlates with increased SOD activity. Measurements were normalized to the OD_{600} of each bacterial culture sample just prior to collection.

Motility assays

Bacterial swimming motility was determined by inoculating 0.2% agar plates with a toothpick dipped into an overnight culture of each strain. Care was taken to break the surface but not touch the bottom of the plate, to avoid possible initiation of twitching motility. Plates were incubated face up at 37°C and bacterial spreading was measured at 2-h intervals for 10 h. Values are from three independent experiments done in triplicate. Swarm motility assays were performed using 0.5% Eiken agar plates supplemented with 0.5% glucose. Five

μL of bacteria were spotted on the surface of the plate and allowed to swarm overnight (16 h) at 37°C.

Biofilm assays

In vitro microtiter plate-based biofilm assays were performed as previously described (34). Bacteria were diluted 1:100 from overnight shaking cultures into modified M9 medium, and quadruplicate 100-ml samples added to 96-well pinchbar flat-bottomed polystyrene microtiter plates (Nunc) were incubated with lids for 48 h without shaking at 30°C. Sample-containing wells were surrounded by wells with H_2O only to minimize evaporation. Nonadherent bacteria were removed by washing twice with H_2O prior to addition of crystal violet (150 μl of a 0.1% solution in water; Sigma-Aldrich). After a 10-min incubation at room temperature, the wells were rinsed twice with H_2O and air-dried. Dimethyl sulfoxide (200 μl; Sigma-Aldrich) was then added to each well, and the plates were shaken vigorously for 15 min on an orbital shaker to solubilize the dye. A_{562} was measured using a Synergy HT multidetection microplate reader (BioTek Instruments, Inc.).

Mouse infections

Seven- to 8-week-old female CBA/J mice (Jackson Laboratory) were anesthetized using isoflurane inhalation and slowly inoculated via transurethral catheterization with 50 μl of bacteria (~10^7 CFU from 24 h static LB broth cultures) resuspended in PBS as previously described (34). Bacterial reflux into

the kidneys using this procedure is rare, occurring in less than 1% of the test animals (unpublished data). At 6 h, 1 d, 3 d, or 9 d postinoculation, mice were sacrificed and bladders were harvested aseptically, weighed, and homogenized in 1 ml PBS containing 0.025% Triton X-100. Bacterial titers within the homogenates were determined by plating serial dilutions on LB agar plates. Eleven mice total, from two independent experiments, were used for each condition tested. Numbers of intracellular bacteria present at the 6 h time point were determined using an *ex vivo* gentamicin protection assay as described (65). Reservoir populations of UPEC within bladder tissues were enumerated as previously described (9). Briefly, at 3 d post-inoculation mice were treated for 3 consecutive days with gentamicin (200 µg in 50 ml delivered subcutaneously) in order to sterilize the urine and kill any extracellular bacteria. Control animals received subcutaneous injections of PBS. Mice were sacrificed 3 d after the final antibiotic treatment and bacterial titers within the bladder were determined as described above. Competition experiments were performed as described (1), using a final inoculating dose of 10^7 CFU with equal numbers of wild type and mutant bacteria.

IBC quantification

CBA/J mice were infected with UTI89/pGEN_GFP(LVA) or UTI89Δ*spf*/pGEN_GFP(LVA) via transurethral catheterization. Six h post-inoculation, mice were sacrificed and bladders were removed, halved, splayed, and pinned down lumenal side up on silicon disks (Sylgard 184 silicone

elastomer, Dow Corning Corp.) under Ringer solution [5 mM NaCl, 3 mM HCl, 2 mM CaCl2, 1 mM MgCl2, 3 mM NaH2PO4, 10 mM glucose, and 5 mM Hepes (pH 7.4)]. GFP positive IBCs were visualized and enumerated using a SZX10 stereomicroscope (Olympus) equipped with a Canon PowerShot A640 10.1 megapixel camera mounted via a Camadapter kit (camadapter.com).

Metabolomics

Chemicals and reagents were of the highest purity and purchased from Sigma-Aldrich, except for MSTFA (N-methyl-N-(trimethylsilyl) trifluoroacetamide), which was purchased from Thermo Scientific, and methoxyamine hydrochloride, which was purchased from MP Biomedicals (Solon, OH). Six biological replicates of each strain were used per experiment. Cultures were grown to an OD_{600} of 1.0, pelleted by centrifugation, and frozen. Pellets were resuspended in 5 ml of boiling 75% EtOH (aqueous), vortexed, and then incubated at 90°C for 5 min. Cell debris was removed by centrifugation at 5000 x g for 3 min. Supernatant were transferred to new tubes and dried *en vacuo.*

GC-MS analysis was performed using a Waters GCT Premier mass spectrometer fitted with an Agilent 6890 gas chromatograph and a Gerstel MPS2 autosampler. Dried samples were suspended in 40 µl of a pyridine solution containing 40 mg/ml O-methoxylamine hydrochloride and incubated for 1 h at 30°C. Twenty ml of each sample was transferred to an autosampler vial and incubated with MSTFA for 30 min at 37°C with shaking. One ml of sample was injected into the inlet, which was held at 250°C. The gas chromatograph was

obtained using an initial temperature of 95°C for 1 min followed by a 40°C/min ramp up to 110°C, with a hold time of 2 min. This was followed by a second 5°C/min ramp up to 250°C, and then a third ramp up to 350°C, with a final hold time of 3 min. A 30 m Restek Rxi-5 MS column with a 5 m long guard column was employed for analysis. Data were collected using MassLynx 4.1 software and analysis of known metabolites was performed using QuanLynx. To identify unknown metabolites, data from peaks that were picked using MarkerLynx and exported to SIMCA-P (ver. 12.0.1), where principal component analysis and partial least squares - differential analysis was performed.

Adhesion, invasion, and intracellular replication assays

Bacteria were grown at 37°C for 48 h in 20 ml static LB broth to induce type 1 pilus expression. Cultured 5637 bladder epithelial cells (ATCC HTB-9) were grown in RPMI 1640 supplemented with 10% fetal bovine serum (Hyclone, Logan, UT) at 37°C with 5% CO_2. Triplicate sets of confluent 5637 bladder epithelial cell monolayers in 24-well tissue culture plates were infected using a multiplicity of infection of ~15 bacteria per host cell. To facilitate and synchronize bacterial contact with the host cells, plates were centrifuged at 600 x *g* for 5 min at room temperature using a Beckman Allegra 6 Centrifuge. After a 2-h incubation at 37°C, samples were washed three times with PBS containing Ca^{2+} and Mg^{2+} (PBS^{2+}) to remove any nonadherent bacteria. For adherence assays, host cells were lysed at this point by addition of PBS containing 0.4% Triton X-100. For invasion assays, the monolayers were incubated prior to lysis for an

additional 2 h in complete RPMI medium with 100 μg/ml of gentamicin added to kill any extracellular bacteria. For intracellular growth/persistence assays, after the 2-h incubation with medium containing 100 μg/ml gentamicin, infected monolayers were washed with PBS^{2+} and fresh medium containing 10 μg/ml gentamicin was added. This submaximal concentration of gentamicin was used to prevent extracellular growth of UPEC while limiting possible leaching of the antibiotic into the host cells during longer incubations (49). After an additional 14-h incubation, monolayers were washed with PBS^{2+} and lysed. Bacteria present in the lysates recovered during these assays were enumerated by plating serial dilutions on LB agar plates.

Statistical analysis

P values were determined by Student's *t* tests or by Mann-Whitney U tests performed using Prism 5.01 software (GraphPad Software). Values of less than 0.05 were defined as significant.

Results and Discussion

Construction of sRNA deletion mutants

The sRNAs chosen for analysis in this study are well conserved among K-12 *E. coli* and UPEC isolates, and several have been implicated as important regulators of gene expression in closely related *Salmonella* strains (24, 54, 57, 74). Each of the sRNAs examined here are known to target one or more mRNAs (Table 4.3). Two of the sRNAs (DsrA and RprA) promote expression of the

Table 4.3 Tested sRNA molecules

Name	Length (UTI89)	Sequence Identity with MG1655	Known Targets*	Reference
DsrA	86	100	*H-NS,* ***rpoS****,* ***gadAX****,* ***hdeAB****,* ***gadBC****,* ***ehxCABD***	(36-38, 41, 68)
RprA	104	100	***rpoS,*** *csgD*, *ydaM*	(40, 46)
OxyS	109	100	*fhlA, rpoS, yhiV, yhiM, gadB, dps,* ***uhpT****,* ***pqqL***	(2, 3, 79)
Spot 42	108	100	*galK,* ***gsp****,* ***dppB****, fucK, fucI, ebgC, gltA, maeA, glpF, sthA, nanC, srlA, xylF, ascF, atoD, caiA, fucP, paaK, puuE*	(7, 8, 47)
RyhB	89	100	*sdhCDAB, acnA, fumA, ftnA, bfr, sodB, sodA, cysE,* ***entCEBAH****, iscRSUA, fdoG, nuoA*	(43) (20, 63, 72) (6)
MicC	108	97	*ompC, ompD*	(13, 56)
MicF	92	99	*ompF, lrp, yahO, lpxR*	(5, 17, 29)

* Genes in bold indicate targets that are activated by the indicated sRNA, all other targets are repressed.

stationary-phase sigma factor RpoS, while another (OxyS) inhibits RpoS synthesis (60). The sRNA MicC acts to repress the synthesis of OmpC and OmpD, while the sRNA MicF interferes with OmpF expression (4, 13). Recent work indicates that MicF can also repress translation of the global transcriptional regulator Lrp, the periplasmic protein YahO, and the lipid A-modifying enzyme LpxR (17, 29). The sRNA RyhB helps regulate iron homeostasis (43), and the archetypal sRNA Spot 42 (*spf*) is known to modulate basal metabolic processes in coordination with the global regulators CRP and cAMP (7, 8). Spot 42 is an abundant sRNA in both K-12 *E. coli* strains and the UPEC isolate UTI89 ((62) and manuscript in preparation), and when induced to high levels can affect the activities of other sRNA molecules by competing for Hfq binding sites (48, 62). Each of these seven conserved sRNAs was deleted individually in the UPEC reference strain UTI89 using the lambda-Red recombination system. Mutants were verified by PCR analysis and tested against the wild type strain in a series of *in vitro* experiments (Fig. 4.1).

sRNA-mediated regulation of biofilm formation by UPEC

All of the sRNA deletion mutants grew normally in standard LB broth and in modified M9 minimal medium (Fig. 4.1A and data not shown). Likewise, all mutants grew like wild type UTI89 in the presence of the divalent cation-chelating agent EDTA (1 mM) or the surfactant sodium dodecyl sulfate (0.01%) (data not shown). Each mutant also expressed wild type levels of type 1 pili, as determined by yeast agglutination assays, and each was similarly hemolytic on blood agar

Figure 4.1 sRNAs modulate biofilm formation, swim motility, and stress resistance of UTI89

(A) Growth of a wild type UTI89 and isogenic sRNA deletion mutants in LB broth. (B) Biofilm formation by UTI89 and its derivatives was measured following growth in modified M9 medium at 30°C in microtiter plates. (C) Quantitation of swim motility over the course of 10 h at 37°C. Motility of the *spf* mutant is shown separately in (D) for clarity. Graphs in (E) and (F) show growth curves of UTI89 and the sRNA mutants in MES-LB broth + 2 mM ASN and in LB broth + 1 mM MV, respectively. Data in B-D represent the mean ± SE of at least three independent experiments performed in triplicate or quadruplicate. *P* values were determined by Student's *t* test; **P*<0.05, ***P*<0.01, ****P*<0.001, versus the wild type control. Graphs in A, E, and F show the means of triplicate samples from representative experiments carried out three or more times. Error bars in these graphs were negligible.

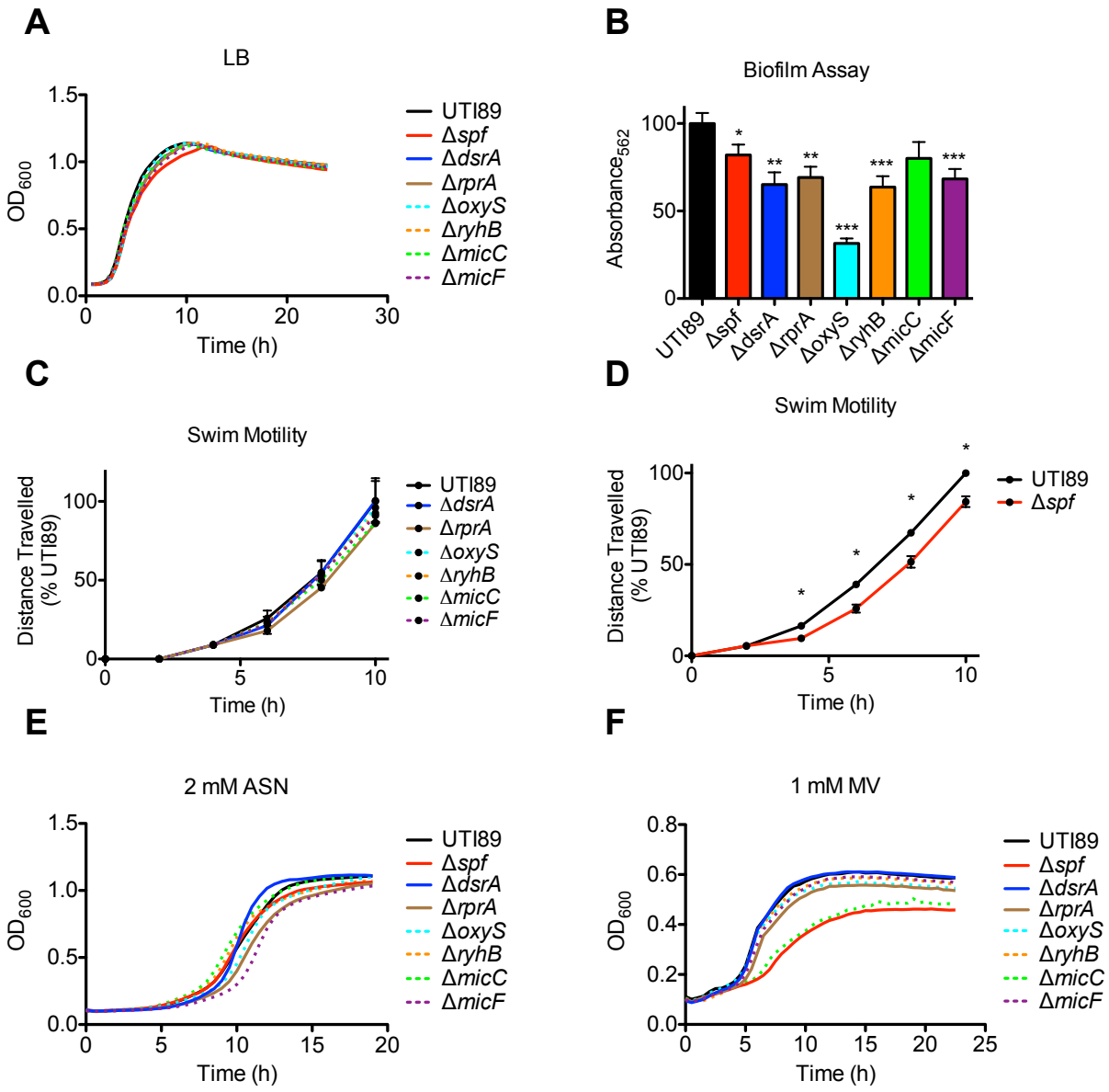
A
LB
OD600
Time (h)
UTI89
Δspf
ΔdsrA
ΔrprA
ΔoxyS
ΔryhB
ΔmicC
ΔmicF
B
Biofilm Assay
Absorbance562
C
Swim Motility
Distance Travelled (% UTI89)
D
E
2 mM ASN
F
1 mM MV

plates, indicating normal secretion of the UPEC-associated pore-forming toxin a-hemolysin (data not shown). In microtiter plate-based biofilm assays carried out at 37°C all of the sRNA knockout mutants behaved like the wild type strain, but at 30°C, where biofilm formation by UPEC is generally more robust, all of the sRNA mutants, aside from Δ*micC*, were at least modestly defective (Fig. 4.1B). In these assays, the Δ*oxyS* mutant was the most attenuated in biofilm development, a phenotype that may be in part attributable to the misregulation of OxyS targets like RpoS (80). Deletion of the sRNAs DsrA and RprA can also disrupt the balance of RpoS regulation, and could thereby compromise biofilm formation (22, 44). In addition, RprA may modulate the development of biofilms by UTI89 via effects on the stationary phase-induced biofilm regulator CsgD and the diguanylate cyclase YdaM (46).

Spot 42 promotes the motility of UPEC

Motility of the sRNA mutants was assessed using both swarm and swim assays. All strains behaved similarly on swarm motility plates, and all but the Δ*spf* mutant displayed wild type swimming phenotypes (Fig. 4.1C and D, and data not shown). In these swim motility assays, UTI89Δ*spf* consistently lagged behind the wild type strain by about 1 h. Interestingly, a recent microarray-based study implicated Spot 42 as a negative regulator of motility and chemotaxis in the salmon pathogen *Aliivibrio salmonicida* (27), indicating that Spot 42 homologues can have divergent effects on bacterial behavior across species.

Spot 42 and MicC enhance UPEC resistance to oxidative stress

Nitrosative and oxidative stresses are known to play important roles in the host response to myriad infections, including UTIs (30, 35, 39, 58). The effect of nitrosative stress on growth of the sRNA mutants was investigated using acidified sodium nitrite (ASN), which produces nitrous acid, NO and other reactive nitrogen species upon addition to LB-MES broth (pH 5.0) (78). Sensitivity to oxidative stress was tested using MV, which generates superoxide radicals in LB broth culture (28). All of the strains grew similarly in LB-MES with or without 2 mM ASN (Fig. 4.1E and data not shown). In contrast, the *micC* and *spf* mutants had clear and highly reproducible growth defects in the presence 0.5, 1, and 2 mM MV (Fig. 4.1F and data not shown). Complementation using a plasmid encoding *spf* driven by a pTac promoter rescued growth of the *spf* mutant in the presence of MV (Fig. 4.2A). The *micC* mutant could be similarly complemented, dependent upon the level of induction by IPTG (Fig. 4.2B).

A double knockout lacking both *spf* and *micC* rendered UTI89 more sensitive to MV than either single deletion alone, suggesting that these two sRNAs promote oxidative stress resistance via effects on independent pathways, potentially involving multiple targets (Fig. 4.2C). For example, by repressing the translation of OmpD and OmpC, MicC can alter the permeability of the bacterial envelope to MV and other damaging radicals (13, 53, 64). Likewise, Spot 42 might decrease the porosity of the bacterial envelope to oxygen radicals via its ability to repress translation of a number of transporters, permeases, and porin-

Figure 4.2 Spot 42 and MicC modulate oxidative stress resistance in UTI89

The strains indicated in (A-C) were grown shaking in plate format at 37°C in LB broth + 1 mM MV, and optical density (OD_{600}) measurements over time were obtained using a Bioscreen C instrument. Strains carrying the empty vector pRRK1 served as controls. In (A), Spot42 expression from the pSpot42a plasmid was induced by addition of 1 mM IPTG. To complement the *micC* mutant in (B), a range of IPTG concentrations, in 10-fold increments from 10 to 1000 mM, was used to induce MicC expression. Leaky expression of MicC was sufficient to complement growth of UTI89Δ*micC*, while increasing concentrations of IPTG negatively affected growth. Each curve (A-C) represents the means of quadruplicate samples, and are representative of experiments performed three or more times. (D) SOD activity of UTI89 and UTI89Δ*spf* following growth in LB broth + 1 mM MV. Measurements were normalized to the OD_{600} of each culture taken just before collection, and represent the means ± SE of three independent experiments performed in triplicate. *P* values were determined by the Student's *t* test; ***P<0.001, versus wild type UTI89.

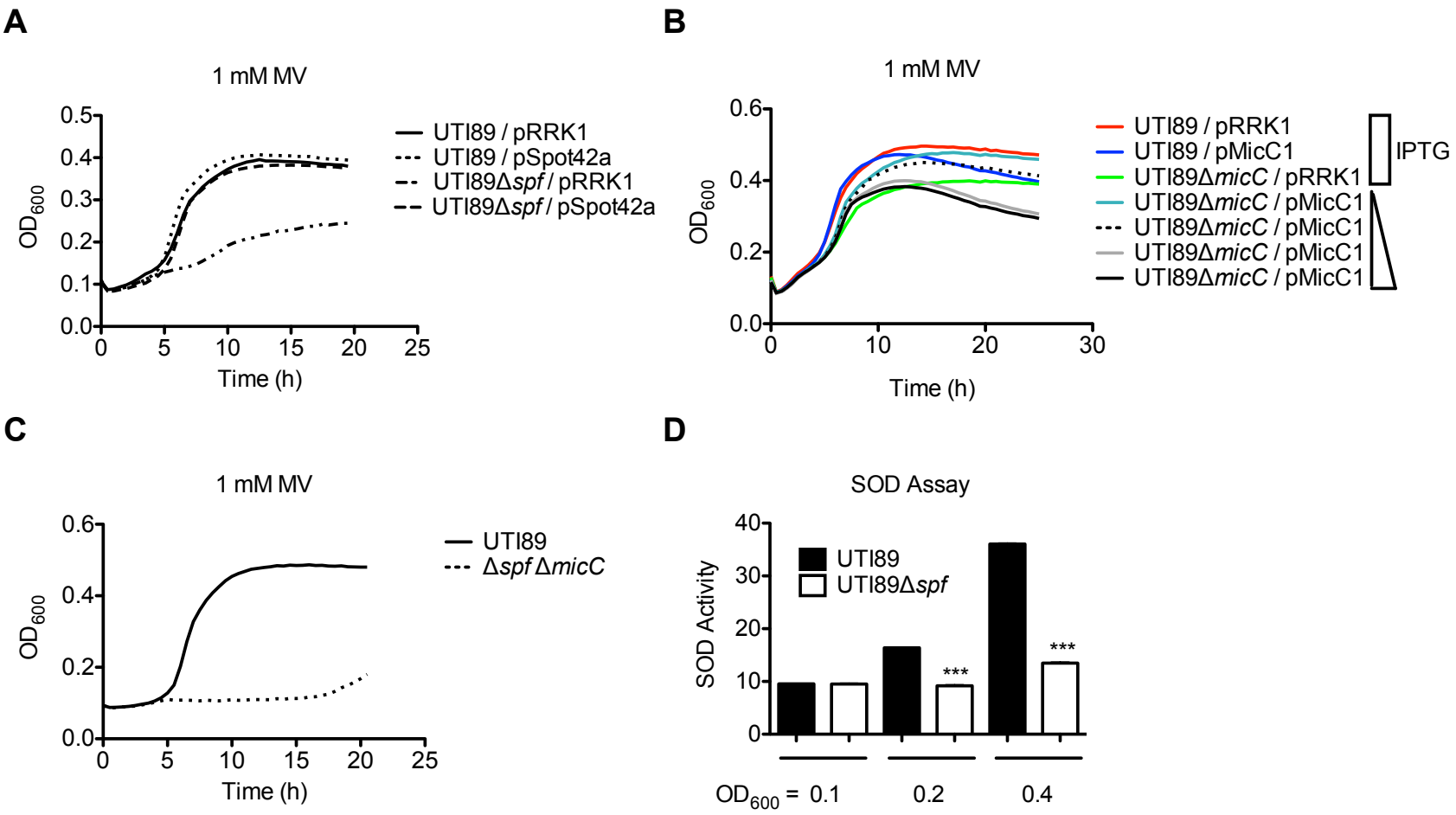
A
1 mM MV
OD600
Time (h)
UTI89 / pRRK1
UTI89 / pSpot42a
UTI89Δspf / pRRK1
UTI89Δspf / pSpot42a
B
1 mM MV
OD600
Time (h)
UTI89 / pRRK1
UTI89 / pMicC1
UTI89ΔmicC / pRRK1
UTI89ΔmicC / pMicC1
UTI89ΔmicC / pMicC1
UTI89ΔmicC / pMicC1
UTI89ΔmicC / pMicC1
IPTG
C
1 mM MV
OD600
Time (h)
UTI89
ΔspfΔmicC
D
SOD Assay
SOD Activity
UTI89
UTI89Δspf
***
***
OD600 = 0.1
0.2
0.4

like molecules, including AscF, GlpF, SlrA, NanC, FucP, and XylF (see Table 4.3) (7, 8).

Spot 42 and MicC could also influence the sensitivity of UTI89 to oxidative stress independent of effects on the bacterial envelope. For example, focusing on just Spot 42 with its broader range of known and predicted mRNA targets, we observed that, in the presence of 1 mM MV, UTI89Δ*spf* had significantly reduced SOD activity relative to the wild type strain (Fig. 4.2D). Spot 42 is not known to regulate the expression of any SOD enzymes, although the web-based tool TargetRNA predicts that Spot 42 may base pair with mRNA encoding the tRNA prenyltransferase MiaA, which we found does positively influence the resistance of UPEC to oxidative stress (unpublished observations, (71)). However, the use of reporter constructs has so far failed to establish *miaA* as a bona fide target of Spot 42. Additional *in silico* analyses indicated that Spot 42 might bind messages for the oxidative stress defense protein YggE and the atypical glutaredoxin Grx2, while a recent microarray-based study suggested that Spot 42 promotes the expression of the glutathionylspermidine synthetase/amidase fusion protein Gsp (7). Each of these gene products has the potential to enhance bacterial resistance to oxidative stress (16, 33, 73), but overexpression of recombinant YggE (pMB4_YggE), Grx2 (pMB1_GrxB) or Gsp (pMB2_Gsp) did not rescue growth of UTI89D*spf* in the presence of MV (data not shown). It is feasible that the combined effects of multiple Spot 42 targets dictate the sensitivity of UTI89 to MV. Interestingly, the *spf* mutant grew like wild type UTI89 in the presence of other oxidative stressors, including H_2O_2 (0.6 mM), menadione (40 mg/ml),

cumene hydroperoxide (25 mM), and plumbagin (0.05 mM) (data not shown), suggesting that Spot 42 does not alter UPEC resistance to all forms of oxidative stress. This sort of selective susceptibility of a mutant *E. coli* strain to different types of oxidative stress has been noted previously (e.g., glutaredoxin mutants) (73).

Altered metabolism of UTI89Δ*spf*

Spot 42 can help fine-tune the regulation of central and secondary metabolic processes in K-12 laboratory-adapted strains of *E. coli* (7, 8, 47). Taking a metabolomics approach employing gas chromatography coupled with mass spectroscopy to measure levels of 47 common metabolites in UTI89 and UTI89Δ*spf*, we found evidence that Spot 42 can also affect key metabolic processes in UPEC. Following growth in LB broth to an OD_{600} of 1.0, UTI89Δ*spf* had significantly reduced levels of lactate, 2-phosphoglycerate, and pantothenate, but higher levels of ribose, 2-hydroxyglutarate, and b-alanine (Fig. 4.3, see also Supplemental Fig. 4.1)). These changes suggest broad irregularities in carbon utilization by the *spf* mutant, potentially impacting glycolysis, fatty acid metabolism, and the pentose phosphate pathway, among others. At the root of these irregularities may be the decreased ability of UTI89Δ*spf* to efficiently convert b-alanine into pantothenate, the direct precursor of the acyl carrier Coenzyme A (CoA). Decreased levels of CoA can affect multiple metabolic processes, including the generation of reducing equivalents like NADH. Deficiencies in the production of nicotinamide adenine dinucleotide

(NADH) may contribute to the increased sensitivity of UTI89Δ*spf* to MV (see Fig. 4.1F). However, induced expression of the pantothenate synthetase PanC, which catalyzes the conversion of b-alanine and pantoate into pantothenate (18), was not sufficient to restore wild type growth of the *spf* mutant in the presence of MV (data not shown). Of note, the altered abundance of CoA precursors measured in UTI89Δ*spf* is not attributable to spurious turnover of acetyl-CoA by the chloramphenicol acetyltransferase enzyme encoded by this mutant, as another mutant (UTI89Δ*fimH*) carrying the same antibiotic resistance cassette was indistinguishable from the wild type strain with respect to its metabolomics profile.

Spot 42 regulates the intracellular persistence of UTI89

Interactions between UTI89Δ*spf* and host cells were initially assessed using the human bladder epithelial cell line known as 5637. In these cell culture-based assays, the *spf* mutant associated with the bladder cells in higher numbers than wild type UTI89, but both mutant and wild type strains invaded the host cells with similar frequencies (Fig. 4.4A - B). Over extended 14-h assays, UTI89Δ*spf* displayed a reduced ability to persist within the bladder cells (Fig. 4.4C).

These experiments were complemented using a well-established murine UTI model in which adult female CBA/J mice were infected via transurethral catheterization (9). In non-competitive assays, similar numbers of wild type UTI89 and UTI89Δ*spf* were recovered from bladders at 6 h, 1 d, and 3 d post-inoculation (Fig. 4.5A-C). Both strains were also able to colonize bladders similarly at the 3 d time point in competitive assays, in which equal numbers of

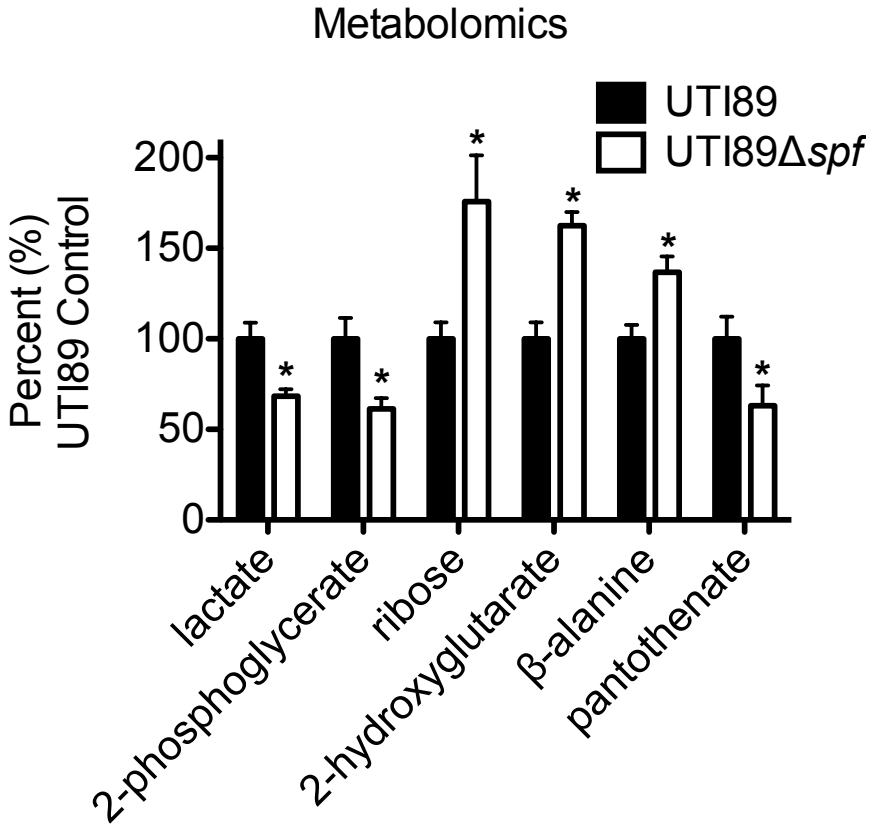

Figure 4.3 Deletion of *spf* alters key metabolic processes in UTI89

The abundance of 47 common metabolites in UTI89 and UTI89Δ*spf* was determined using gas chromatography in association with mass spectroscopy. Only metabolites that were significantly different between the wild type and mutant strain are shown. Data are presented as the means ± SD of 6 independent replicates. **P*<0.05 for all UTI89Δ*spf* samples versus wild type UTI89, as calculated by Student's *t* test.

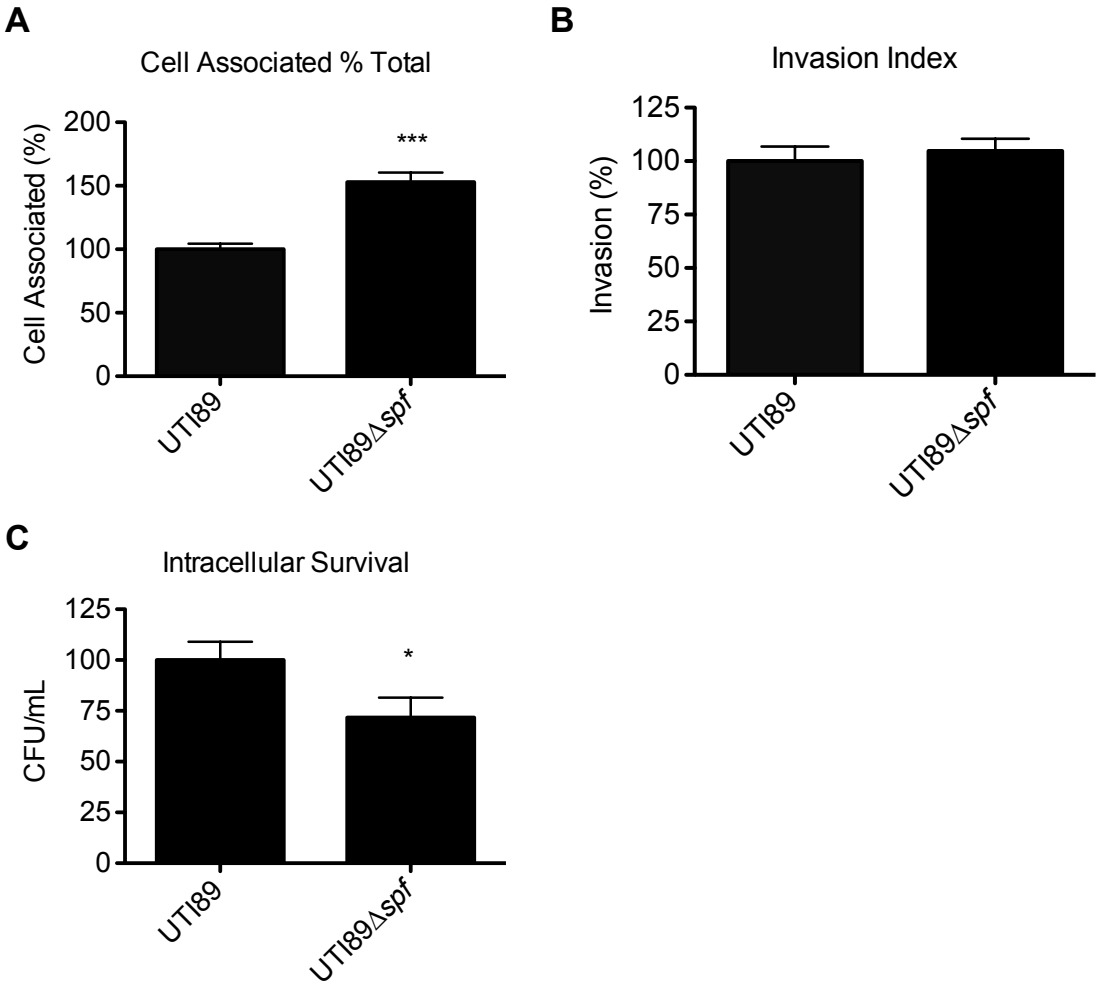

Figure 4.4 Spot 42 modulates interactions between UTI89 and host bladder cells

(A) UTI89Δ*spf* associates with cultured bladder epithelial cells at higher levels than wild type UTI89. (B) Both mutant and wild type strains invade the host cells similarly, (C) but over the course of a 14-h assay in the presence of gentamicin the *spf* mutant is less able to persist intracellularly. Data are expressed relative to wild type UTI89 as the means ± SD of three or more experiments performed in triplicate. *P<0.05 or ***P<0.001, versus the wild type control as determined by the Student's *t* test.

Figure 4.5 Spot 42 promotes the intracellular persistence of UTI89 in a murine model of UTI

Adult female CBA/J mice were inoculated via transurethral catheterization with 10^7 CFU of UTI89 or UTI89Δ*spf*. (A-C) Bacterial titers in bladders were determined at 6 h, 1 d, and 3 d postinoculation. (D) For competitive assays in which mice were infected with equal numbers of the wild type and mutant strains (10^7 CFU total), bladder titers were calculated at the 3 d time point. (E) Numbers of intracellular bacteria were determined at 6 h postinoculation using *ex vivo* gentamicin protection assays. (F) IBCs were visualized and enumerated by fluorescent microscopy of splayed bladders recovered at 6 h postinoculation with strains carrying pGEN_GFP(LVA). (G) Bladder-associated UPEC reservoirs were assessed at 8 d postinoculation, three days after a 3-d systemic treatment with gentamicin. Bars denote median values for each group. *P<0.05, as determined using the Mann-Whitney U test. Graphs depict cumulative results from two independent assays (n = 11 mice per group).

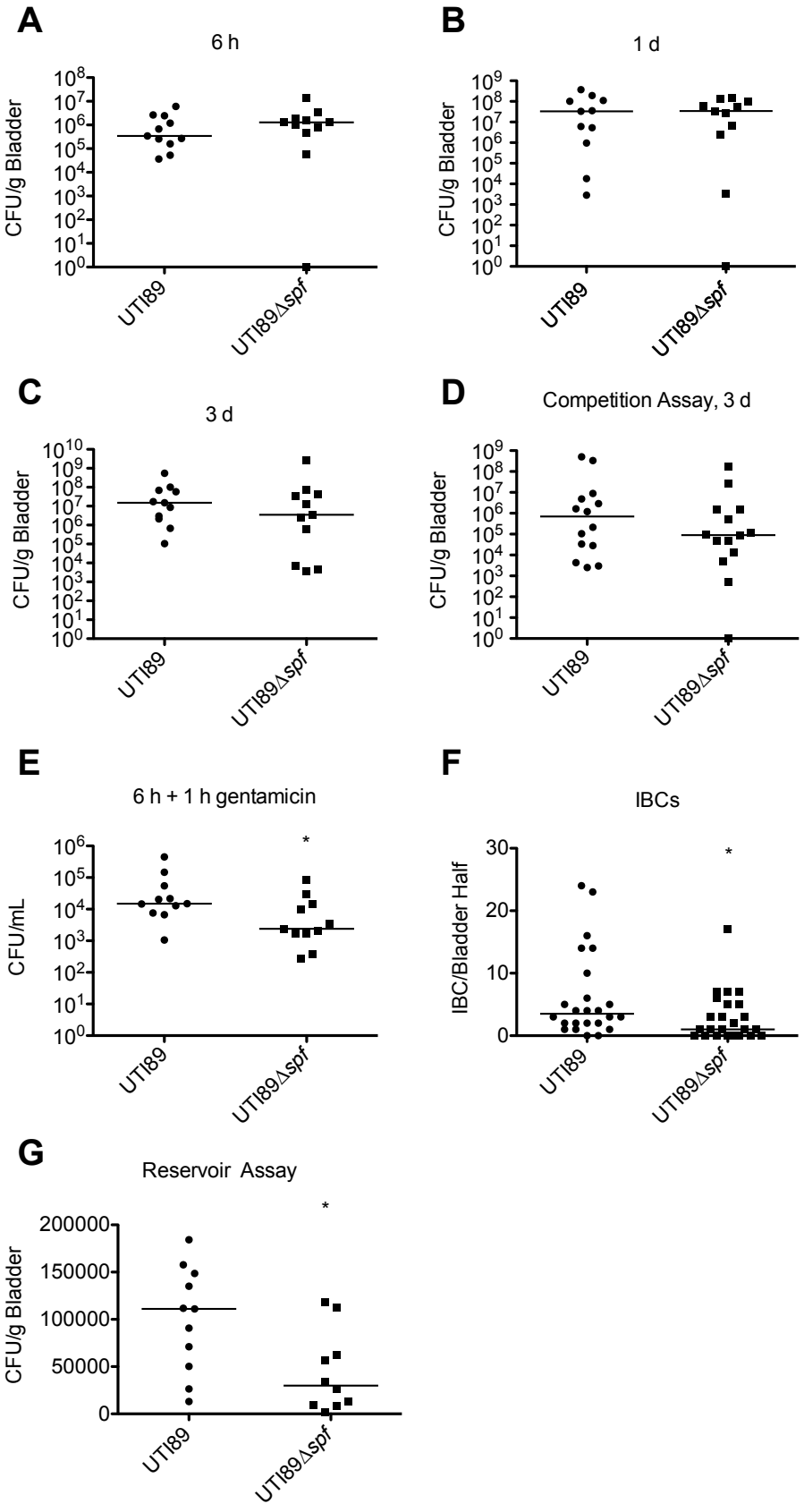
A
6 h
CFU/g Bladder
UTI89
UTI89Δspf
B
1 d
CFU/g Bladder
UTI89
UTI89Δspf
C
3 d
CFU/g Bladder
UTI89
UTI89Δspf
D
Competition Assay, 3 d
CFU/g Bladder
UTI89
UTI89Δspf
E
6 h + 1 h gentamicin
CFU/mL
*
UTI89
UTI89Δspf
F
IBCs
IBC/Bladder Half
*
UTI89
UTI89Δspf
G
Reservoir Assay
CFU/g Bladder
*
UTI89
UTI89Δspf

UTI89 and the *spf* mutant were co-inoculated into the same mice (Fig. 4.5D). When examining just the intracellular, gentamicin-protected pool of bladder-associated bacteria at the 6 h time point in noncompetitive assays, UTI89Δ*spf* had a clear defect that corresponded with reduced numbers of IBCs (Fig. 4.5E - F). The decreased levels of intracellular UTI89Δ*spf* detected during the acute phase of infection correlated with notably decreased levels of gentamicin-protected intracellular reservoirs within the bladder tissue at 9 d postinoculation (Fig. 4.1G). In total, these data indicate that the *spf* mutant is diminished in its ability to persist and replicate within intracellular niches.

Concluding remarks

Over the past several years sRNAs have received much attention as important regulators of bacterial metabolic processes and stress response pathways, but the functional relevance of sRNA molecules to wild type *E. coli* isolates, including pathogenic strains, has remained largely unexplored. Results presented here demonstrate that specific sRNAs can alter the fitness and pathogenic behavior of UPEC. Six of the seven sRNA mutants tested had significant defects in biofilm formation, in line with previous observations using K-12 *E. coli* strains and other bacterial isolates (11, 22, 32, 42, 45, 76). Biofilm formation by UPEC, both within bladder epithelial cells and on the bladder surface, likely facilitates bacterial persistence and eventual dissemination within the urinary tract (26). Interestingly, it has been noted that UPEC isolates that are prone to cause relapsing UTIs in women are often more adept than other UPEC

strains at forming biofilms in microtiter plate-based assays at 30°C (69). Our findings indicate that sRNAs can significantly affect the ability of UPEC to form biofilms, and may thereby impact the pathogenesis of UTIs. This possibility is supported by results obtained using the *spf* mutant. *In vitro*, UTI89Δ*spf* has a modest, but significant, defect in biofilm formation that corresponds with the decreased capacity of this mutant to form IBCs and to persist within bladder epithelial cells. These deficiencies may also be influenced by the increased sensitivity of this mutant to oxidative stress, which is likely encountered during the course of a UTI. Furthermore, misregulation of key metabolic processes, including the biosynthesis of the CoA precursor pantothenate, could compromise the fitness of UTI89Δ*spf* within the urinary tract via effects on multiple systems, including carbon utilization pathways and the generation of NADH and other reducing equivalents.

The specific mRNA targets of Spot 42 that regulate fitness and virulence-associated phenotypes in UTI89 were not discernable in our assays. It is feasible that each of the phenotypes observed with UTI89Δ*spf* are associated with impaired regulation of multiple Spot 42 targets, as well as with altered activity of the Hfq chaperone in absence of the potential buffering effects of Spot 42 (48). It is likely that additional sRNA molecules, including those tested here using *in vitro* assays, also modulate the fitness and virulence of UPEC within host environments. Defining these sRNAs and their relevant targets will help better delineate the regulatory networks that are critical to the ability of UPEC to colonize the host and cause disease.

Acknowledgements

We thank James Cox in the Metabolomics Facility of the University of Utah for help with the metabolomics. This study was funded by NIH grants AI095647, DK068585, AI090369, and AI088086. M.G.B. was supported by T32 AI055434 from the National Institute Of Allergy and Infectious Diseases. The content is solely the responsibility of the authors and does not necessarily represent the official views of the National Institute Of Allergy And Infectious Diseases or the National Institutes of Health.

References

1. **Alteri, C. J., S. N. Smith, and H. L. Mobley.** 2009. Fitness of *Escherichia coli* during urinary tract infection requires gluconeogenesis and the TCA cycle. PLoS Pathog. **5:**e1000448.

2. **Altuvia, S., D. Weinstein-Fischer, A. Zhang, L. Postow, and G. Storz.** 1997. A small, stable RNA induced by oxidative stress: role as a pleiotropic regulator and antimutator. Cell **90:**43-53.

3. **Altuvia, S., A. Zhang, L. Argaman, A. Tiwari, and G. Storz.** 1998. The *Escherichia coli* OxyS regulatory RNA represses fhlA translation by blocking ribosome binding. EMBO J. **17:**6069-6075.

4. **Andersen, J., and N. Delihas.** 1990. micF RNA binds to the 5' end of ompF mRNA and to a protein from *Escherichia coli*. Biochemistry **29:**9249-9256.

5. **Andersen, J., S. A. Forst, K. Zhao, M. Inouye, and N. Delihas.** 1989. The function of micF RNA. micF RNA is a major factor in the thermal regulation of OmpF protein in *Escherichia coli*. J. Biol. Chem. **264:**17961-17970.

6. **Argaman, L., M. Elgrably-Weiss, T. Hershko, J. Vogel, and S. Altuvia.** 2012. RelA protein stimulates the activity of RyhB small RNA by acting on RNA-binding protein Hfq. Proc. Natl. Acad. Sci. U. S. A.

7. **Beisel, C. L., and G. Storz.** 2011. The base-pairing RNA spot 42 participates in a multioutput feedforward loop to help enact catabolite repression in *Escherichia coli*. Molecular Cell **41:**286-297.

8. **Beisel, C. L., T. B. Updegrove, B. J. Janson, and G. Storz.** 2012. Multiple factors dictate target selection by Hfq-binding small RNAs. EMBO J.

9. **Blango, M. G., and M. A. Mulvey.** 2010. Persistence of uropathogenic Escherichia coli in the face of multiple antibiotics. Antimicrob. Agents Chemother. **54:**1855-1863.

10. **Blattner, F. R., G. Plunkett, 3rd, C. A. Bloch, N. T. Perna, V. Burland, M. Riley, J. Collado-Vides, J. D. Glasner, C. K. Rode, G. F. Mayhew, J. Gregor, N. W. Davis, H. A. Kirkpatrick, M. A. Goeden, D. J. Rose, B. Mau, and Y. Shao.** 1997. The complete genome sequence of *Escherichia coli* K-12. Science **277:**1453-1462.

11. **Boehm, A., and J. Vogel.** 2012. The csgD mRNA as a hub for signal integration via multiple small RNAs. Mol. Microbiol. **84:**1-5.

12. **Brennan, R. G., and T. M. Link.** 2007. Hfq structure, function and ligand binding. Curr. Opin. Microbiol. **10:**125-133.

13. **Chen, S., A. Zhang, L. B. Blyn, and G. Storz.** 2004. MicC, a second small-RNA regulator of Omp protein expression in *Escherichia coli*. J. Bacteriol. **186:**6689-6697.

14. **Chen, S. L., C. S. Hung, J. Xu, C. S. Reigstad, V. Magrini, A. Sabo, D. Blasiar, T. Bieri, R. R. Meyer, P. Ozersky, J. R. Armstrong, R. S. Fulton, J. P. Latreille, J. Spieth, T. M. Hooton, E. R. Mardis, S. J. Hultgren, and J. I. Gordon.** 2006. Identification of genes subject to positive selection in uropathogenic strains of *Escherichia coli*: a comparative genomics approach. Proc. Natl. Acad. Sci. U. S. A. **103:**5977-5982.

15. **Cheng, A. C., J. K. Ferguson, M. J. Richards, J. M. Robson, G. L. Gilbert, A. McGregor, S. Roberts, T. M. Korman, and T. V. Riley.** 2011. Australasian Society for Infectious Diseases guidelines for the diagnosis and treatment of *Clostridium difficile* infection. Med. J. Aust. **194:**353-358.

16. **Chiang, B. Y., T. C. Chen, C. H. Pai, C. C. Chou, H. H. Chen, T. P. Ko, W. H. Hsu, C. Y. Chang, W. F. Wu, A. H. Wang, and C. H. Lin.** 2010. Protein S-thiolation by Glutathionylspermidine (Gsp): the role of *Escherichia coli* Gsp synthetASE/amidase in redox regulation. J. Biol. Chem. **285:**25345-25353.

17. **Corcoran, C. P., D. Podkaminski, K. Papenfort, J. H. Urban, J. C. Hinton, and J. Vogel.** 2012. Superfolder GFP reporters validate diverse new mRNA targets of the classic porin regulator, MicF RNA. Mol. Microbiol. **84:**428-445.

18. **Cronan, J. E., Jr., K. J. Littel, and S. Jackowski.** 1982. Genetic and biochemical analyses of pantothenate biosynthesis in Escherichia coli and *Salmonella typhimurium*. J. Bacteriol. **149:**916-922.

19. **Datsenko, K. A., and B. L. Wanner.** 2000. One-step inactivation of chromosomal genes in *Escherichia coli* K-12 using PCR products. Proc. Natl. Acad. Sci. U. S. A. **97:**6640-6645.

20. **Desnoyers, G., A. Morissette, K. Prevost, and E. Masse.** 2009. Small RNA-induced differential degradation of the polycistronic mRNA iscRSUA. EMBO J. **28:**1551-1561.

21. **Eto, D. S., J. L. Sundsbak, and M. A. Mulvey.** 2006. Actin-gated intracellular growth and resurgence of uropathogenic *Escherichia coli*. Cell. Microbiol. **8:**704-717.

22. **Ferrieres, L., A. Thompson, and D. J. Clarke.** 2009. Elevated levels of sigma S inhibit biofilm formation in *Escherichia coli*: a role for the Rcs phosphorelay. Microbiology **155:**3544-3553.

23. **Foxman, B.** 2003. Epidemiology of urinary tract infections: incidence, morbidity, and economic costs. Dis. Mon. **49:**53-70.

24. **Gong, H., G. P. Vu, Y. Bai, E. Chan, R. Wu, E. Yang, F. Liu, and S. Lu.** 2011. A *Salmonella* small non-coding RNA facilitates bacterial invasion and intracellular replication by modulating the expression of virulence factors. PLoS Pathog. **7:**e1002120.

25. **Gorke, B., and J. Vogel.** 2008. Noncoding RNA control of the making and breaking of sugars. Genes Dev. **22:**2914-2925.

26. **Hannan, T. J., M. Totsika, K. J. Mansfield, K. H. Moore, M. A. Schembri, and S. J. Hultgren.** 2012. Host-pathogen checkpoints and population bottlenecks in persistent and intracellular uropathogenic *Escherichia coli* bladder infection. FEMS Microbiol. Rev. **36:**616-648.

27. **Hansen, G. A., R. Ahmad, E. Hjerde, C. G. Fenton, N. P. Willassen, and P. Haugen.** 2012. Expression profiling reveals Spot 42 small RNA as a key regulator in the central metabolism of *Aliivibrio salmonicida*. BMC Genomics **13:**37.

28. **Hassan, H. M., and I. Fridovich.** 1978. Superoxide radical and the oxygen enhancement of the toxicity of paraquat in *Escherichia coli*. J. Biol. Chem. **253:**8143-8148.

29. **Holmqvist, E., C. Unoson, J. Reimegard, and E. G. Wagner.** 2012. A mixed double negative feedback loop between the sRNA MicF and the global regulator Lrp. Mol. Microbiol. **84:**414-427.

30. **Johnson, J. R., C. Clabots, and H. Rosen.** 2006. Effect of inactivation of the global oxidative stress regulator oxyR on the colonization ability of *Escherichia coli* O1:K1:H7 in a mouse model of ascending urinary tract infection. Infect. Immun. **74:**461-468.

31. **Justice, S. S., C. Hung, J. A. Theriot, D. A. Fletcher, G. G. Anderson, M. J. Footer, and S. J. Hultgren.** 2004. Differentiation and developmental pathways of uropathogenic *Escherichia coli* in urinary tract pathogenesis. Proc. Natl. Acad. Sci. U. S. A. **101:**1333-1338.

32. **Kim, J., H. J. Park, J. H. Lee, J. S. Hahn, M. B. Gu, and J. Yoon.** 2009. Differential effect of chlorine on the oxidative stress generation in dormant and active cells within colony biofilm. Water Research **43:**5252-5259.

33. **Kim, S. Y., M. Nishioka, S. Hayashi, H. Honda, T. Kobayashi, and M. Taya.** 2005. The gene yggE functions in restoring physiological defects of *Escherichia coli* cultivated under oxidative stress conditions. Appl. Environ. Microbiol. **71:**2762-2765.

34. **Kulesus, R. R., K. Diaz-Perez, E. S. Slechta, D. S. Eto, and M. A. Mulvey.** 2008. Impact of the RNA chaperone Hfq on the fitness and virulence potential of uropathogenic *Escherichia coli*. Infect. Immun. **76:**3019-3026.

35. **Kurutas, E. B., P. Ciragil, M. Gul, and M. Kilinc.** 2005. The effects of oxidative stress in urinary tract infection. Mediators of Inflammation **2005:**242-244.

36. **Lease, R. A., M. E. Cusick, and M. Belfort.** 1998. Riboregulation in *Escherichia coli*: DsrA RNA acts by RNA:RNA interactions at multiple loci. Proc. Natl. Acad. Sci. U. S. A. **95:**12456-12461.

37. **Lease, R. A., D. Smith, K. McDonough, and M. Belfort.** 2004. The small noncoding DsrA RNA is an acid resistance regulator in *Escherichia coli*. J. Bacteriol. **186:**6179-6185.

38. **Li, H., A. Granat, V. Stewart, and J. R. Gillespie.** 2008. RpoS, H-NS, and DsrA influence EHEC hemolysin operon (ehxCABD) transcription in

Escherichia coli O157:H7 strain EDL933. FEMS Microbiol. Lett. **285:**257-262.

39. **Lundberg, J. O., I. Ehren, O. Jansson, J. Adolfsson, J. M. Lundberg, E. Weitzberg, K. Alving, and N. P. Wiklund.** 1996. Elevated nitric oxide in the urinary bladder in infectious and noninfectious cystitis. Urology **48:**700-702.

40. **Majdalani, N., S. Chen, J. Murrow, K. St John, and S. Gottesman.** 2001. Regulation of RpoS by a novel small RNA: the characterization of RprA. Mol. Microbiol. **39:**1382-1394.

41. **Majdalani, N., C. Cunning, D. Sledjeski, T. Elliott, and S. Gottesman.** 1998. DsrA RNA regulates translation of RpoS message by an anti-antisense mechanism, independent of its action as an antisilencer of transcription. Proc. Natl. Acad. Sci. U. S. A. **95:**12462-12467.

42. **Majdalani, N., and S. Gottesman.** 2005. The Rcs phosphorelay: a complex signal transduction system. Annual Review of Microbiology **59:**379-405.

43. **Masse, E., and S. Gottesman.** 2002. A small RNA regulates the expression of genes involved in iron metabolism in *Escherichia coli*. Proc. Natl. Acad. Sci. U. S. A. **99:**4620-4625.

44. **McCullen, C. A., J. N. Benhammou, N. Majdalani, and S. Gottesman.** 2010. Mechanism of positive regulation by DsrA and RprA small noncoding RNAs: pairing increases translation and protects rpoS mRNA from degradation. J. Bacteriol. **192:**5559-5571.

45. **Mey, A. R., S. A. Craig, and S. M. Payne.** 2005. Characterization of *Vibrio cholerae* RyhB: the RyhB regulon and role of ryhB in biofilm formation. Infect. Immun. **73:**5706-5719.

46. **Mika, F., S. Busse, A. Possling, J. Berkholz, N. Tschowri, N. Sommerfeldt, M. Pruteanu, and R. Hengge.** 2012. Targeting of csgD by the small regulatory RNA RprA links stationary phase, biofilm formation and cell envelope stress in *Escherichia coli*. Mol. Microbiol. **84:**51-65.

47. **Moller, T., T. Franch, C. Udesen, K. Gerdes, and P. Valentin-Hansen.** 2002. Spot 42 RNA mediates discoordinate expression of the *E. coli* galactose operon. Genes Dev. **16:**1696-1706.

48. **Moon, K., and S. Gottesman.** 2011. Competition among Hfq-binding small RNAs in Escherichia coli. Mol. Microbiol. **82**:1545-62

49. **Mulvey, M. A., J. D. Schilling, and S. J. Hultgren.** 2001. Establishment of a persistent *Escherichia coli* reservoir during the acute phase of a bladder infection. Infect. Immun. **69:**4572-4579.

50. **Mulvey, M. A., J. D. Schilling, J. J. Martinez, and S. J. Hultgren.** 2000. Bad bugs and beleaguered bladders: interplay between uropathogenic *Escherichia coli* and innate host defenses. Proc. Natl. Acad. Sci. U. S. A. **97:**8829-8835.

51. **Murphy, K. C., and K. G. Campellone.** 2003. Lambda Red-mediated recombinogenic engineering of enterohemorrhagic and enteropathogenic *E. coli*. BMC Mol. Biol. **4:**11.

52. **Mysorekar, I. U., and S. J. Hultgren.** 2006. Mechanisms of uropathogenic *Escherichia coli* persistence and eradication from the urinary tract. Proc. Natl. Acad. Sci. U. S. A. **103:**14170-14175.

53. **Ozkanca, R., N. Sahin, K. Isik, E. Kariptas, and K. P. Flint.** 2002. The effect of toluidine blue on the survival, dormancy and outer membrane porin proteins (OmpC and OmpF) of *Salmonella typhimurium* LT2 in seawater. J. Appl. Microbiol. **92:**1097-1104.

54. **Padalon-Brauch, G., R. Hershberg, M. Elgrably-Weiss, K. Baruch, I. Rosenshine, H. Margalit, and S. Altuvia.** 2008. Small RNAs encoded within genetic islands of *Salmonella typhimurium* show host-induced expression and role in virulence. Nucleic Acids Res. **36:**1913-1927.

55. **Papenfort, K., and J. Vogel.** 2010. Regulatory RNA in bacterial pathogens. Cell Host Microbe **8:**116-127.

56. **Pfeiffer, V., K. Papenfort, S. Lucchini, J. C. Hinton, and J. Vogel.** 2009. Coding sequence targeting by MicC RNA reveals bacterial mRNA silencing downstream of translational initiation. Nat. Struct. Mol. Biol. **16:**840-846.

57. **Pfeiffer, V., A. Sittka, R. Tomer, K. Tedin, V. Brinkmann, and J. Vogel.** 2007. A small non-coding RNA of the invasion gene island (SPI-1) represses outer membrane protein synthesis from the *Salmonella* core genome. Mol. Microbiol. **66:**1174-1191.

58. **Poljakovic, M., M. L. Svensson, C. Svanborg, K. Johansson, B. Larsson, and K. Persson.** 2001. *Escherichia coli*-induced inducible nitric oxide synthase and cyclooxygenase expression in the mouse bladder and kidney. Kidney Int. **59:**893-904.

59. **Raghavan, R., E. A. Groisman, and H. Ochman.** 2011. Genome-wide detection of novel regulatory RNAs in E. coli. Genome Res. **21:**1487-1497.

60. **Repoila, F., N. Majdalani, and S. Gottesman.** 2003. Small non-coding RNAs, co-ordinators of adaptation processes in *Escherichia coli*: the RpoS paradigm. Mol. Microbiol. **48:**855-861.

61. **Romby, P., F. Vandenesch, and E. G. Wagner.** 2006. The role of RNAs in the regulation of virulence-gene expression. Curr. Opin. Microbiol. **9:**229-236.

62. **Sahagan, B. G., and J. E. Dahlberg.** 1979. A small, unstable RNA molecule of *Escherichia coli*: spot 42 RNA. I. Nucleotide sequence analysis. J. Mol. Biol. **131:**573-592.

63. **Salvail, H., P. Lanthier-Bourbonnais, J. M. Sobota, M. Caza, J. A. Benjamin, M. E. Mendieta, F. Lepine, C. M. Dozois, J. Imlay, and E. Masse.** 2010. A small RNA promotes siderophore production through transcriptional and metabolic remodeling. Proc. Natl. Acad. Sci. U. S. A. **107:**15223-15228.

64. **Santiviago, C. A., J. A. Fuentes, S. M. Bueno, A. N. Trombert, A. A. Hildago, L. T. Socias, P. Youderian, and G. C. Mora.** 2002. The *Salmonella enterica* sv. Typhimurium smvA, yddG and ompD (porin) genes are required for the efficient efflux of methyl viologen. Mol. Microbiol. **46:**687-698.

65. **Schwartz, D. J., S. L. Chen, S. J. Hultgren, and P. C. Seed.** 2011. Population dynamics and niche distribution of uropathogenic *Escherichia coli* during acute and chronic urinary tract infection. Infect. Immun. **79:**4250-4259.

66. **Shinhara, A., M. Matsui, K. Hiraoka, W. Nomura, R. Hirano, K. Nakahigashi, M. Tomita, H. Mori, and A. Kanai.** 2011. Deep sequencing reveals as-yet-undiscovered small RNAs in *Escherichia coli*. BMC Genomics **12:**428.

67. **Skippington, E., and M. A. Ragan.** 2012. Evolutionary dynamics of small RNAs in 27 *Escherichia coli* and *Shigella* genomes. Genome Biol. Evol. **4:**330-345.

68. **Sledjeski, D. D., A. Gupta, and S. Gottesman.** 1996. The small RNA, DsrA, is essential for the low temperature expression of RpoS during exponential growth in *Escherichia coli*. EMBO J. **15:**3993-4000.

69. **Soto, S. M., A. Smithson, J. P. Horcajada, J. A. Martinez, J. P. Mensa, and J. Vila.** 2006. Implication of biofilm formation in the persistence of urinary tract infection caused by uropathogenic *Escherichia coli*. Clin. Microbiol. Infect. **12:**1034-1036.

70. **Studdert, C. A., and J. S. Parkinson.** 2005. Insights into the organization and dynamics of bacterial chemoreceptor clusters through in vivo crosslinking studies. Proc. Natl. Acad. Sci. U. S. A. **102:**15623-15628.

71. **Tjaden, B., S. S. Goodwin, J. A. Opdyke, M. Guillier, D. X. Fu, S. Gottesman, and G. Storz.** 2006. Target prediction for small, noncoding RNAs in bacteria. Nucleic Acids Res. **34:**2791-2802.

72. **Troxell, B., R. C. Fink, S. Porwollik, M. McClelland, and H. M. Hassan.** 2011. The Fur Regulon in Anaerobically Grown *Salmonella enterica* sv. Typhimurium: Identification of New Fur Targets. BMC Microbiology **11:**236.

73. **Vlamis-Gardikas, A., A. Potamitou, R. Zarivach, A. Hochman, and A. Holmgren.** 2002. Characterization of *Escherichia coli* null mutants for glutaredoxin 2. J. Biol. Chem. **277:**10861-10868.

74. **Vogel, J.** 2009. A rough guide to the non-coding RNA world of *Salmonella*. Mol. Microbiol. **71:**1-11.

75. **Vogel, J., and K. Papenfort.** 2006. Small non-coding RNAs and the bacterial outer membrane. Curr. Opin. Microbiol. **9:**605-611.

76. **White-Ziegler, C. A., S. Um, N. M. Perez, A. L. Berns, A. J. Malhowski, and S. Young.** 2008. Low temperature (23 degrees C) increases expression of biofilm-, cold-shock- and RpoS-dependent genes in *Escherichia coli* K-12. Microbiology **154:**148-166.

77. **Wiles, T. J., J. M. Bower, M. J. Redd, and M. A. Mulvey.** 2009. Use of zebrafish to probe the divergent virulence potentials and toxin requirements of extraintestinal pathogenic *Escherichia coli*. PLoS Pathog. **5:**e1000697.

78. **Woolford, G., R. J. Casselden, and C. L. Walters.** 1972. Gaseous products of the interaction of sodium nitrite with procine skeletal muscle. Biochem. J. **130:**82P-83P.

79. **Zhang, A., S. Altuvia, and G. Storz.** 1997. The novel oxyS RNA regulates expression of the sigma s subunit of *Escherichia coli* RNA polymerase. Nucleic Acids Symposium Series**:**27-28.

80. **Zhang, A., S. Altuvia, A. Tiwari, L. Argaman, R. Hengge-Aronis, and G. Storz.** 1998. The OxyS regulatory RNA represses rpoS translation and binds the Hfq (HF-I) protein. EMBO J. **17:**6061-6068.

81. **Zhou, Y., and J. Xie.** 2011. The roles of pathogen small RNAs. Journal of Cellular Physiology **226:**968-973.

Figure 4.S1 Metabolic profile of UTI89 and UTI89Δspf

The relative levels of 45 individual metabolites from stationary phase UTI89 and UTI89Δ*spf* as determined by GC/MS. *=$P<0.05$ as calculated by Student's *t*-test.

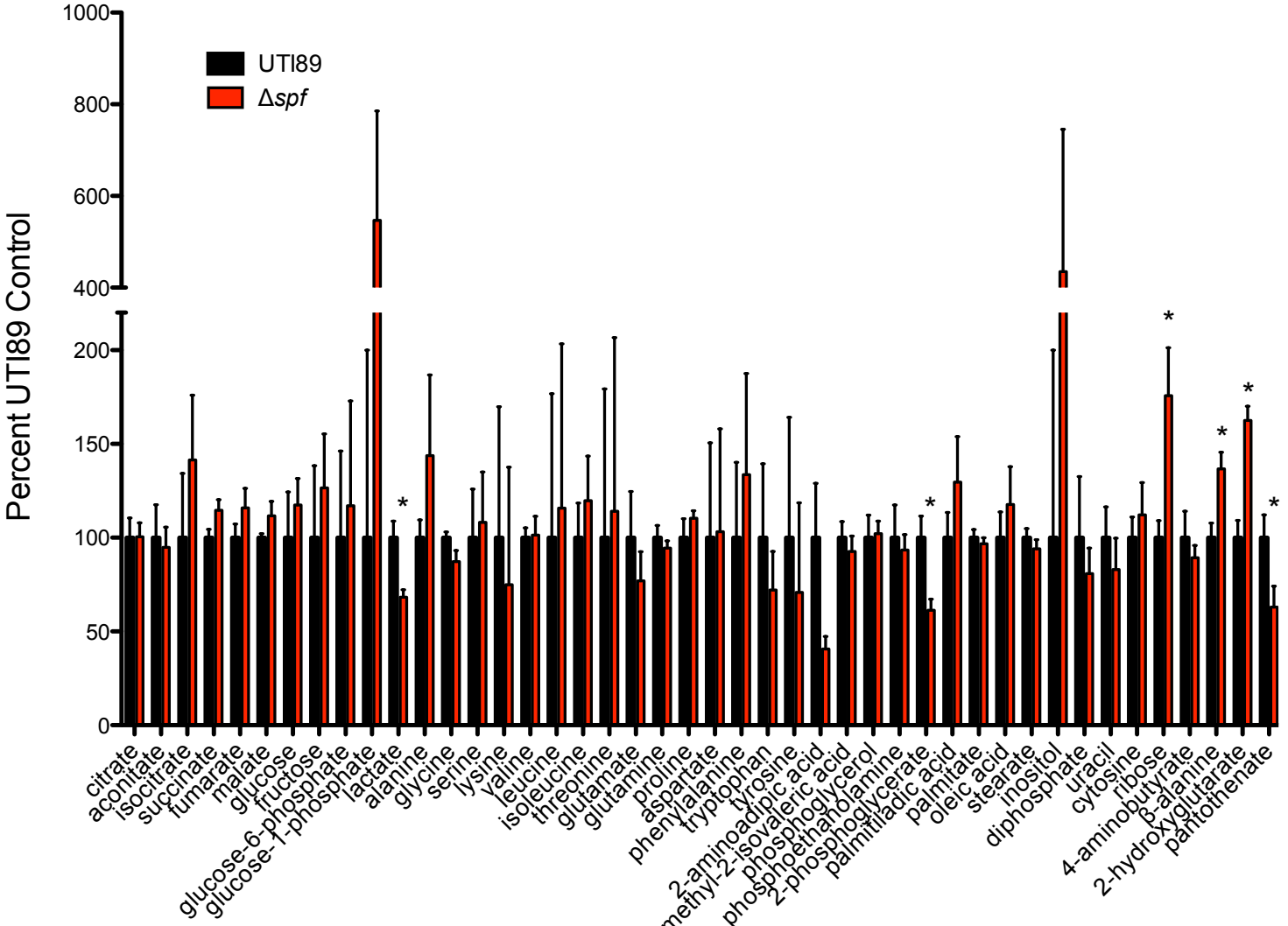
Percent UTI89 Control
1000
800
600
400
200
150
100
50
0
UTI89
Δspf
*
citrate
aconitate
isocitrate
succinate
fumarate
malate
glucose
fructose
glucose-6-phosphate
glucose-1-phosphate
lactate
alanine
glycine
serine
lysine
valine
leucine
isoleucine
threonine
glutamate
glutamine
proline
aspartate
phenylalanine
tryptophan
tyrosine
2-aminoadipic acid
4-methyl-2-isovaleric acid
phosphoglycerol
phosphoethanolamine
2-phosphoglycerate
palmitladic acid
palmitate
oleic acid
stearate
inositol
diphosphate
uracil
cytosine
ribose
4-aminobutyrate
2-hydroxyglutarate
β-alanine
pantothenate

CHAPTER 5

IDENTIFICATION OF SMALL NONCODING RNAS IN UROPATHOGENIC ESCHERICHIA COLI

Abstract

Uropathogenic *Escherichia coli* (UPEC) are the primary etiologic agents of urinary tract infections (UTIs), representing a tremendous global healthcare burden. Previous work demonstrated that the RNA chaperone Hfq and a handful of conserved, small, non-coding RNAs (sRNAs) can regulate stress responses and the virulence potential of UPEC. Despite the apparent importance of sRNAs to UPEC, the complete sRNA repertoire encoded by any UPEC isolate remains largely uncharacterized, with only conserved sRNA candidates from K-12 strains currently recognized. This manuscript describes initial efforts in identifying and characterizing the sRNA repertoire within the reference UPEC isolate UTI89 using RNA-Seq. RNA was collected from UTI89 in mid-log and stationary phase growth, following exposure to nitrosative and oxidative stresses, and after infection of mouse bladders. RNA-Seq results indicate a plethora of candidate sRNA molecules, including nearly all of the conserved sRNAs previously identified in non-pathogenic K-12 strains. Individual deletion of several novel sRNA candidates had no effect on growth of UTI89 in broth culture, but many did have modest effects on biofilm formation. One of these, a candidate sRNA designated as UsrB, appeared to negatively affect the ability of UTI89 to colonize the mouse urinary tract, although this effect was subtle. This work represents the first steps towards defining the sRNA repertoire encoded by UPEC, opening the door to their further functional characterization as regulators of bacterial pathogenesis within the urinary tract.

Introduction

Bacterial, small noncoding RNAs (sRNAs), first identified in K-12 strains of *Escherichia coli*, range in size from 50-500 nucleotide (nt) and are thought to broadly influence prokaryotic gene expression (21). Genomically, sRNAs are often located within intergenic regions and contain a specific promoter and ρ-independent terminator, which initially facilitated their identification via computational approaches (Table 5.1) (2, 9). Through imperfect base-pairing with cognate messenger RNA sequences, sRNAs typically repress translation, but in some cases promote translation, acting as posttranscriptional regulators that fine-tune gene expression (46). In order to regulate target mRNA sequences, sRNAs utilize mechanisms of repression through mRNA degradation or blocking of ribosome binding sites (21, 42). Alternatively, sRNAs can stabilize mRNA molecules and release repressive secondary structure through anti-antisense mechanisms (18). sRNAs exert influence over multiple cellular processes, ranging from basal metabolism and quorum sensing to stress responses (1, 4, 10). Historically, sRNAs were identified as abundant, low molecular weight RNA species on polyacrylamide gels; however, with the recent advent of deep sequencing technologies such as RNA-Seq, many more sRNAs are being discovered (Table 5.1) (41, 45, 47). The most recent count of validated sRNAs identified in the *E. coli* K-12 laboratory strain MG1655 is greater than 100, with >200 still to be verified (47). Although impressive, the number of sRNAs only hints at the diversity and breadth of functionality likely attributable to sRNAs.

Table 5.1 Broad scale sRNA identification studies

Organism	Putative sRNA Identified	Validated/ Tested Candidates	Method	Role in Virulence	Year	Ref.
Escherichia coli	24	14/23	Bioinformatics	NR	2001	(2)
Escherichia coli	144	7/8	Bioinformatics	NR	2002	(9)
Escherichia coli	34	7/34	cDNA Sequencing	NR	2003	(61)
Listeria Monocytogenes	3	3/3	Hfq Pull-down and Sequencing	NT	2006	(13)
Pseudomonas aeruginosa	34[1]	17/31	Bioinformatics	NT	2006	(29)
Sinorhizobium meliloti	64	14/64	Bioinformatics and Tiling Array	NR	2007	(58)
Sinorhizobium meliloti	32	8/32	Bioinformatics	NR	2007	(17)
Salmonella enterica	31	10/10	Hfq Pull-down and Deep Sequencing	NT	2008	(49)
Sinorhizobium meliloti	60	14/18	Bioinformatics	NR	2008	(59)
Pseudomonas aeruginosa	43	8/43	Bioinformatics	NT	2008	(20)
Caulobacter crescentus	27	23/27	Tiling Array	NT	2008	(26)

Table 5.1 Continued

Organism	Putative sRNA Identified	Validated/ Tested Candidates	Method	Role in Virulence	Year	Ref.
Pseudomonas aeruginosa	11	2/2	cDNA Sequencing	NT	2008	(50)
Salmonella typhimurium	28	19/28	Bioinformatics	Yes	2008	(35)
Streptomyces coelicolor	20	6/20	Bioinformatics	NT	2008	(53)
Streptomyces strains	32	20/32	Bioinformatics	NT	2008	(36)
Mycobacterium tuberculosis	9	9/9	Sequencing	NT	2009	(3)
Vibrio cholerae	2140	16/23	Deep Sequencing	NT	2009	(28)
Group A *Streptococus*	40	16/32	Tiling Array	NT	2009	(37)
Streptomyeces griseus	54	17/54	Bioinformatics	NT	2009	(54)
Staphylococcus aureus	71	16/18	Deep Sequencing	NT	2010	(6)
Streptococcus pneumoniae	50	13/14	Tiling Array	NT	2010	(25)

Table 5.1 Continued

Organism	Putative sRNA Identified	Validated/ Tested Candidates	Method	Role in Virulence	Year	Ref.
Francisella tularensis	24	2/2	Sequencing and Bioinformatics	NT	2010	(38)
Helicobacter pylori	60	60/60	Deep Sequencing	NT	2010	(45)
Streptococcus penumoniae	40	10/40	Bioinformatics	No	2010	(57)
Sinorhizobium meliloti	1125	6/6	Deep Sequencing	NR	2010	(43)
Xanthomonas campestris	7	4/4	cDNA Cloning	NT	2010	(22)
Xanthomonas oryzae	63	8/10	Tiling Array	NT	2011	(27)
Enterococcus faecalis	12	10/11	Tiling Array	NT	2011	(48)
Streptomyces coelicolor	63	14/24	Deep Sequencing	NT	2011	(60)
Clostridium strains	>200	26/72	Bioinformatics	No	2011	(12)
Listeria monocytogenes	150	4/4	Deep Sequencing	Yes	2011	(31)
Yersinia pseudotuberculosis	150	29/49	Deep Sequencing	Yes	2011	(23)

Table 5.1 Continued

Organism	Putative sRNA Identified	Validated/ Tested Candidates	Method	Role in Virulence	Year	Ref.
Escherichia coli	171	10/17	Deep Sequencing	NR	2011	(40)
Bradyrhizobium japonicum	7	7/7	Deep Sequencing	NR	2012	(30)
Agrobacterium tumefaciens	228	22/X	Deep Sequencing	NT	2012	(64)
Yersinia pestis	37	10/10	cDNA Cloning	NT	2012	(39)

[1]Identified in previous study
NT = not tested; NR = not relevant, X = unknown

In addition to regulation of stress response and metabolism, sRNAs are known to influence host-pathogen interactions by modulating virulence potential in pathogens. Specifically, sRNAs can regulate aspects of invasion and colonization, as represented by the pathogenicity island-associated sRNA, IsrM. In *Salmonella enterica*, IsrM targets *Salmonella* Pathogenicity Island-1 effectors to promote invasion of, and intracellular replication within, host cells (19). Similarly, 6 of the 84 known sRNAs in *S. enterica* were shown to be expressed during non-replicative habitation of fibroblasts, suggesting that these sRNAs influence the in intracellular survival of this pathogen (34). In *Staphylococcus aureus,* SprD, another pathogenicity island-associated sRNA, directly represses Sbi, an immune-evasion molecule involved in dampening host responses (7). Despite this interaction, SprD positively affects the outcome of infection, indicating multiple opposing effects on *S. aureus* virulence. sRNAs also directly affect virulence factor expression levels, as exhibited in the plant pathogen *Xanthomonas campestris* in regards to the expression of the master virulence regulators, HrpX and HrpG (44). Finally, many sRNA functions appear to be conserved among pathogens, as shown in *Yersinia pseudotuberculosis*, where sRNAs that promote infection in a mouse model of yersinosis also control aspects of *Yersinia pestis* infection during plague (23). Collectively, these studies provide evidence that sRNAs can regulate pathogenesis by controlling expression of virulence factors, immune evasion molecules, and global transcriptional regulators in a broad range of pathogens.

Previous work in our lab directly linked the RNA chaperone Hfq to stress resistance and virulence in uropathogenic *Escherichia coli* (UPEC), the primary etiologic agent of urinary tract infections (UTIs) (24). Hfq is required for trans-acting sRNA function in nearly all tested cases, where it promotes sRNA stability and protects against sRNA degradation by RNAses such as polynucleotide phosphorylase (16, 62). Chromosomal deletion of Hfq resulted in diminished stress resistance to redox stressors and the antimicrobial peptide, polymixin B (24). Bacteria lacking Hfq also exhibited decreased *in vitro* biofilm formation and virulence in a murine model of UTI. The observed Hfq effects on bacterial behavior were postulated to be due to dysfunctional sRNA action and were explored further in a follow up study characterizing UPEC sRNAs conserved from K-12 *E. coli* strains. The follow-up screen in UPEC illustrated a role for several sRNAs in biofilm formation, stress response and virulence. Of particular interest was a specific function for the sRNA Spot 42 in regulation of intracellular survival in a murine model of UTI (Submitted). Spot 42, and MicC, a regulator of the outer membrane porin OmpC, also contributed to oxidative stress responses upon challenge with the superoxide regenerator methyl viologen (MV), partially explaining several observed defects in an Hfq knockout strain. Collectively, these results led us to hypothesize that the UPEC sRNA repertoire likely contributes to the regulation of a wide-range of stress response and virulence signaling events during UTI.

Results

RNA-Seq experimental design

sRNAs are differentially expressed in response to environmental conditions and growth phase (3, 17). To maximize efficiency in identifying the entire UPEC sRNA repertoire using RNA-Seq, RNA was collected from the reference UPEC isolate UTI89 at different phases of growth and following exposure to different environmental stresses (Fig 5.1). Briefly, overnight cultures of UTI89 were subcultured into modified M9 minimal media and collected and immediately treated with RNAlater (Qiagen) after reaching mid-log (3 h) and stationary phase growth (5 h). Bacteria were also collected after reaching mid-log growth (3 h) and subsequent 30-min exposures to oxidative stress (1 mM methyl viologen; MV) or nitrosative stress (1 mM S-nitrosoglutathione; GSNO). Finally, RNA was isolated from UTI89 recovered from the bladders of infected mice. Adult female C57Bl/6 mice were infected with 10^7 CFU of UTI89 via transurethral catheterization and sacrificed 6 h or 9 d later. Bladders were collected and homogenized in RNAlater containing Triton X-100. Bacteria within the tissue homogenates were then harvested using magnetic beads coupled with anti-*E. coli* antibodies. RNA was isolated from the bacteria-enriched fraction and prepared for deep sequencing using an Illumina HiSeq 2000 machine. As has been described previously, prior to library creation each sample was treated with terminator exonuclease to remove unwanted tRNA and rRNA transcripts (45). However, with our UTI89 samples, the terminator exonucleause treatment failed to effectively remove rRNA and tRNA species. Even so, sufficient reads were

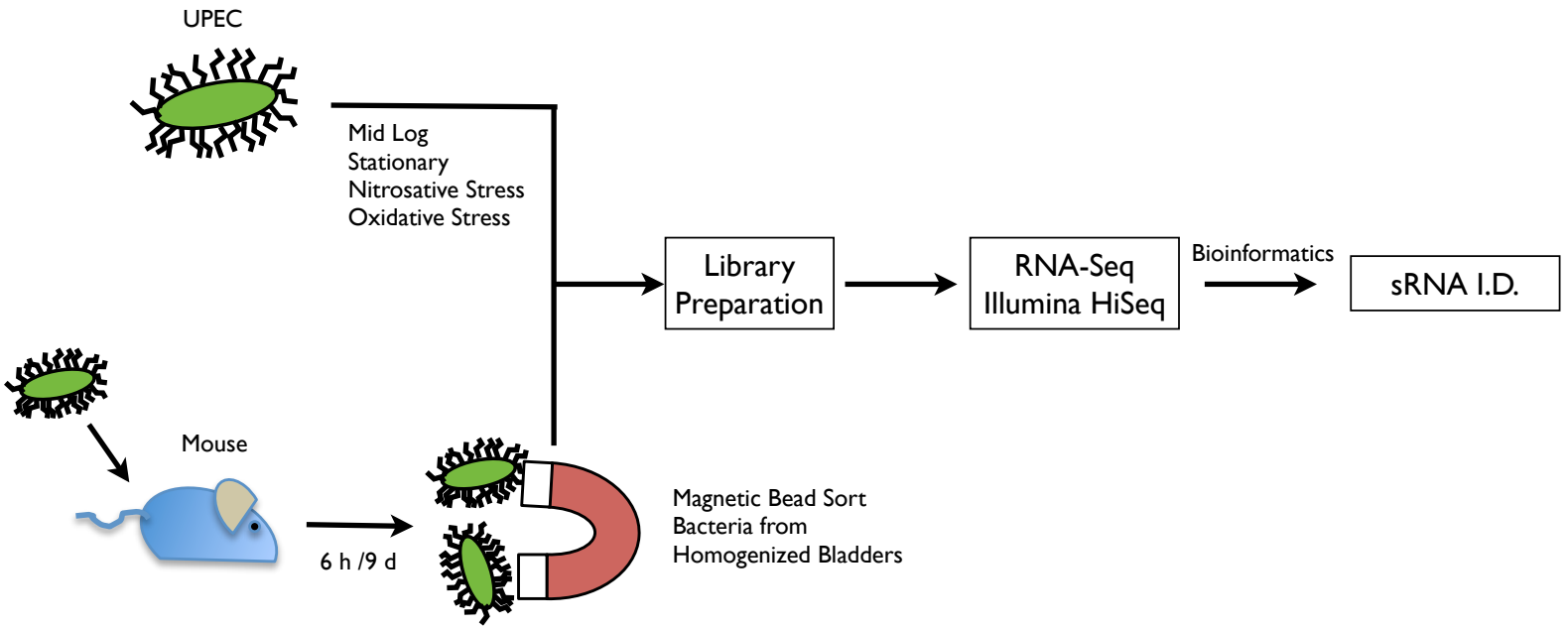

Figure 5.1 Experimental approach

After overnight growth, UTI89 was subcultured and grown for 2.5 h before addition of stressors to appropriate samples for 30 min. At 3 h postinoculation (5 h for stationary phase samples), total RNA was isolated from the bacteria. Alternatively, mice infected with 10^7 UTI89 were sacrificed at 6 h and 9 d after infection. Bladders were aseptically removed and homogenized in the presence of RNAlater before isolation of UTI89 using MACs magnetic bead separation, followed by isolation of total RNA. Sequencing then followed library preparation with a Qiagen sRNA kit on an Illumina HiSeq 2000 machine. sRNAs were identified using bioinformatics approaches as described in the methods.

obtained to analyze the UTI89 RNA profile and identify sRNAs. The RNA-Seq experiment results are summarized in Table 5.2. The *in vitro* samples provided fair coverage of the bacterial genome, whereas the majority of reads from infected mouse samples were mapped to the mouse genome. Due to the nature of these results, the infected mouse samples were not used to identify novel sRNAs; however, they were used as a guide in choosing interesting candidate sRNAs for further study.

Identification and mapping of a subset of novel UPEC sRNA molecules

Candidate sRNA loci were selected from intergenic sequences by comparing the relative mean expression of the candidates to neighboring open reading frames (ORFs), as previously described (23). The selection criteria relied on a >5 fold increase in maximal expression relative to local ORFs, to prevent unwanted identification of 5'/3' untranslated regions (UTR). Using these parameters and a minimum length of 50 nucleotides (nt), 828 unique events were identified from the four *in vitro* growth conditions. Of these 828 unique events, a large fraction mapped to known, conserved sRNA, while 125 loci appeared to be specific to UTI89, which has a notably larger genome relative to K-12 *E. coli* strains. Due to the strict parameters for candidate identification in intergenic regions, some known UPEC sRNAs were excluded from the candidate list; however, they were nonetheless still detected by RNA-Seq as shown by expression for nearly all known sRNA presented in Table 5.3.

Table 5.2. Deep sequencing statistics

Environ-ment	Time[1]	Stress[2]	Tex Treatment	Mouse			
				Total Reads	Specific Reads	Non-specific Reads	Total Alignments
M9	M		+	14,321,142	2,014	14,319,128	2,014
M9	M		-	12,049,677	1,026	12,048,651	1,026
M9	S		+	14,179,206	1,076	14,178,130	1,076
M9	S		-	12,927,971	1,090	12,926,881	1,090
M9	M	N	+	13,144,835	3,935	13,140,900	3,935
M9	M	O	+	43,893,477	6,821	43,886,659	6,821
C57BL/6	6 h		+	84,360,161	38,654,656	45,707,533	38,654,656
C57BL/6	9 d		+	55,069,845	28,097,437	26,974,861	28,097,437

[1] M = Mid-Log, S = Stationary, [2] N = Nitrosative Stress, O = Oxidative Stress

Table 5.2. Continued

Environ-ment	Time[1]	Stress[2]	Tex Treatment	UTI89			
				Total Reads	Specific Reads	Non-specific Reads	Total Alignments
M9	M		+	14,321,142	11,124,239	3,196,903	11,124,239
M9	M		-	12,049,677	8,924,796	3,124,881	8,924,796
M9	S		+	14,179,206	11,105,012	3,074,194	11,105,012
M9	S		-	12,927,971	9,948,137	2,979,834	9,948,137
M9	M	N	+	13,144,835	8,423,117	4,721,718	8,423,117
M9	M	O	+	43,893,477	30,602,556	13,290,921	30,602,556
C57BL/6	6 h		+	84,360,161	297,224	84,062,937	297,224
C57BL/6	9 d		+	55,069,845	179,764	54,890,081	179,764

[1] M = Mid-Log, S = Stationary, [2] N = Nitrosative Stress, O = Oxidative Stress

Table 5.3 Known sRNA in UTI89

sRNA	Start	Finish	Length (nt)	Identity with MG1655 (98%)	Max Intergenic Expression Over Neighbors	Max Reads per Region
6S RNA	3233628	3233810	182	100	3.920051913	33193
ArcZ (RyhA)	3570255	3570375	120	100	4.77899108	76
CO299	1303381	1303459	78	96	None	None
CO343	1526519	1526593	74	99	4.314314911	189
CO362	1618775	1618997	222	92	1.344564291	47
CO465	1997273	1997350	77	100	None	None
CO614	2801040	2800961	-79	88	6.149368843	1194
CO664	2993549	2993655	106	94	3.188661564	5
CO719	3324977	3325198	221	97	2.616038905	22
CsrB	3078979	3078611	-368	99	9.22E+18	99047
CsrC	4337194	4337438	244	99	9.22E+18	15796
CyaR	2309664	2309750	86	100	8.328235944	345
DicF (Qin)	1393159	1393107	-52	100	None	None
DsrA	2051411	2051325	-86	100	-1.096381041	23
FnrS	1526285	1526403	118	100	4.343792872	48
FlmB	74237	74137	-100	100		
GadY	3931644	3931748	104	100	1.268128131	26
GcvB	3097201	3097405	204	100	6.404945031	4370
GlmY	2833068	2832889	-179	99	9.694163397	8497
GlmZ	4246425	4246596	171	100	9.601925405	11932
IsrA	1519476	1519320	-156	89	9.22E+18	1615
IsrB	2011755	2011598	-157	99	3.889817082	49
MgrR	1685875	1685778	-97	99	11.15379267	349
MicA	2973601	2973672	71	100	0.548162738	543
MicC	1533367	1533475	108	97	1.124482031	109
MicF	2449387	2449479	92	99	-1.492496052	248
MicM	522554	522637	83	0	9.22E+18	1066
OhsC (RyfC)	2842280	2842344	64	100	1.392317423	7
OmrA	3166626	3166539	-87	99	4.96829114	36
OmrB	3166823	3166742	-81	100	6.299408475	68
OxyS	4445474	4445365	-109	100	0.231325546	169
PsrD	1191553	1191721	168	99	0.572578776	1167
PsrN	3464980	3465167	187	98	9.22E+18	1013
PsrO	3531060	3531233	173	100	-0.814712315	764
RdlA	1344644	1344706	62	98	5.027320606	44
RdlB	1344647	1344705	58	100	5.027320606	44
RdlC	1344647	1344707	60	98	5.027320606	44

Table 5.3 Continued

sRNA	Start	Finish	Length (nt)	Identity with MG1655 (98%)	Max Intergenic Expression Over Neighbors	Max Reads per Region
RdlD	3966762	3966817	55	98	None	None
RnpB	3494446	3494070	-376	99	9.22E+18	113633
RprA	1805957	1806061	104	100	1.069300912	22
RseX	2059747	2059836	89	100	None	None
RttR	1362326	1362157	-169	96	3.241084265	24041
RybA	815714	815626	-88	99	None	None
RybB	849252	849172	-80	100	-0.466880206	8
RydB	1800539	1800472	-67	97	0.527081585	38
RydC	1566408	1566345	-63	98	1.267933205	6
RyeA	1949756	1950004	248	99	6.082444766	580
RyeB	1949974	1949854	-120	99	5.925544279	580
RyfA	2801035	2801339	304	95	6.149368843	1194
RyfB	2842124	2841806	-318	95	0.914995645	73
RyfD	2878496	2878354	-142	100	6.012575607	4153
RyhB	3843047	3842958	-89	100	None	None
RyjA	4546838	4546699	-139	100	None	None
SgrS	81033	81258	225	89	3.665164243	428
SibB (RyeD)	2290698	2290833	135	96	8.804776378	508
SibC (RygC)	3234497	3234637	140	96	0.688227677	4180
SibD (RygD)	3423042	3422899	-143	90	9.240411725	5257
SibE (RygE)	3423042	3422901	-141	97	9.240411725	5257
SokA	3987929	3987957	28	100	None	None
SokB	3040121	3040173	52	81	0.322222793	155
SokC	15655	15709	54	96	-1.371226942	88
Spot 42	4336057	4336165	108	100	10.853511	15583
SraA	472902	472846	-56	100	0.697072867	107
SroA	79274	79182	-92	97	6.357552005	441
SroC	660762	660600	-162	99	3.582015217	306
SroD	1914791	1914706	-85	100	2.433178679	42
SroE	2788198	2788107	-91	100	1.571447694	36
SroG	3419460	3419312	-148	100	1.532799143	625
SsrS	3233628	3233810	182	100	3.920051913	33193
SymR	4953860	4953936	76	90	9.22E+18	1178
Tff	194778	194913	135	100	0.945405025	3360
TmRNA	2899681	2900043	362	100	9.22E+18	667119

Table 5.3 Continued

sRNA	Start	Finish	Length (nt)	Identity with MG1655 (98%)	Max Intergenic Expression Over Neighbors	Max Reads per Region
Tp2	129086	128926	-160	99	None	None
Tpke11	14131	14219	88	98	-0.760930839	11
Tpke70	2657896	2657461	-435	98	-3.064993889	4
Raghavan1	1374543	1374797	254	98	1.418789634	400
Raghavan2	1711379	1711567	188	98	2.092649288	36
Raghavan3	2020653	2020844	191	97	-0.401321506	4
Raghavan4	2418310	2418547	237	99	0.427637536	60
Raghavan5	3240457	3240602	145	93	2.789937869	41
Raghavan6	2418310	2418547	237	99	0.427637536	60
Raghavan8	4265417	4265560	143	99	3.486033767	297
Raghavan9	4344127	4344197	70	97	0.044171681	124
Raghavan 10	4721550	4721655	105	100	-0.097610797	80
ECS002	3594169	3594081	-88	98	1.312142418	582
ECS005	3924577	3924638	61	100	-0.456308723	29
ECS007	2173339	2173290	-49	100	None	None
ECS022	3909853	3909932	79	94	2.121472666	140
ECS001	3594169	3594081	-88	98	1.312142418	582

[1] Locations are UTI89 chromosome
[2] = (-) values indicate antisense strand

Characterization of sRNA candidates

Cluster analysis showed relative expression profiles for 63 candidate loci meeting several criteria: presence in at least 50% of the samples, a standard deviation of <0.5, and relative expression values as determined above compared to neighboring ORFs (Fig 5.2) (15). In Figure 5.2, red boxes indicate increased relative expression, whereas green boxes represent decreased relative expression of a given locus. 11 candidate sRNAs were chosen for further analysis as listed in Table 5.4. The candidate sRNAs were designated UPEC small RNA A-K. One candidate, UsrI, was found to share significant homology to K-12 *E. coli* SibB, and was thus omitted from further analysis. Candidates were chosen based on high relative levels of expression from multiple samples with preference given to candidates with detected expression in mouse-derived samples. Figure 5.3 shows the genomic locus and relative expression profile for each candidate sRNA molecule. Northern blot analysis is in progress to validate expression of each candidate sRNA. Possible targets of sRNA regulation were identified using the TargetRNA prediction program (55, 56). The data are compiled in Table 5.5 and indicate a large number of putative targets for each sRNA candidate.

sRNA knockouts grow normally *in vitro*

Candidate sRNA loci were chromosomally replaced with a chloramphenicol resistance cassette, shown in Table 5.6, using lambda Red recombination and the primers listed in Tables 5.7 (14). At this time, knockout

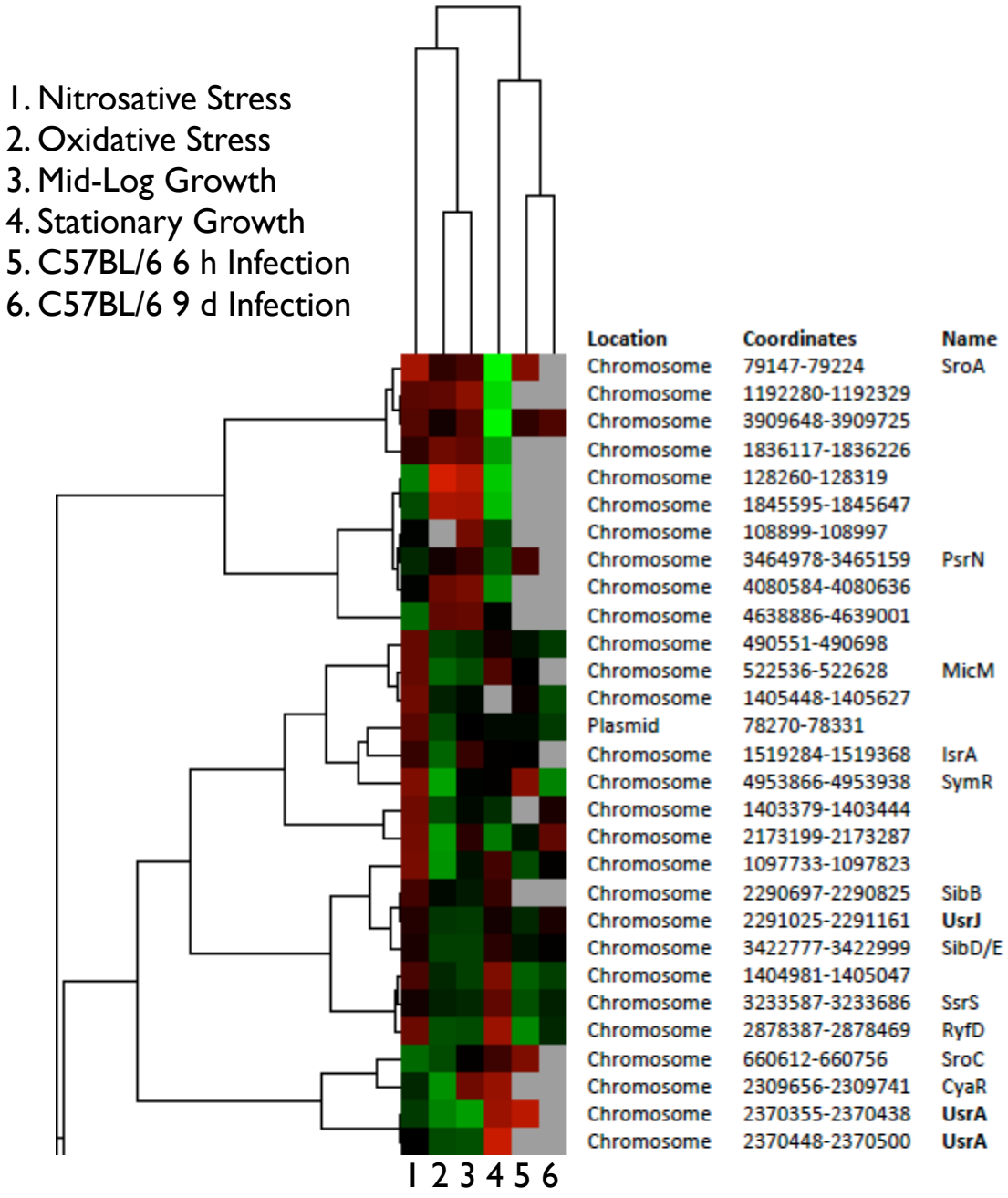

Figure 5.2 Identification of UPEC sRNAs

Cluster analysis of 828 intergenic loci resulted in 63 candidate sRNA molecules as described in the text. These candidates exhibited >5 fold higher expression compared to neighboring ORFs, were present in >50% of the samples, and showed a standard deviation below 0.5. 21 of 63 candidates in this analysis were recognized as previously annotated small RNA. Several sRNAs marked in bold were added to our queue for further characterization.

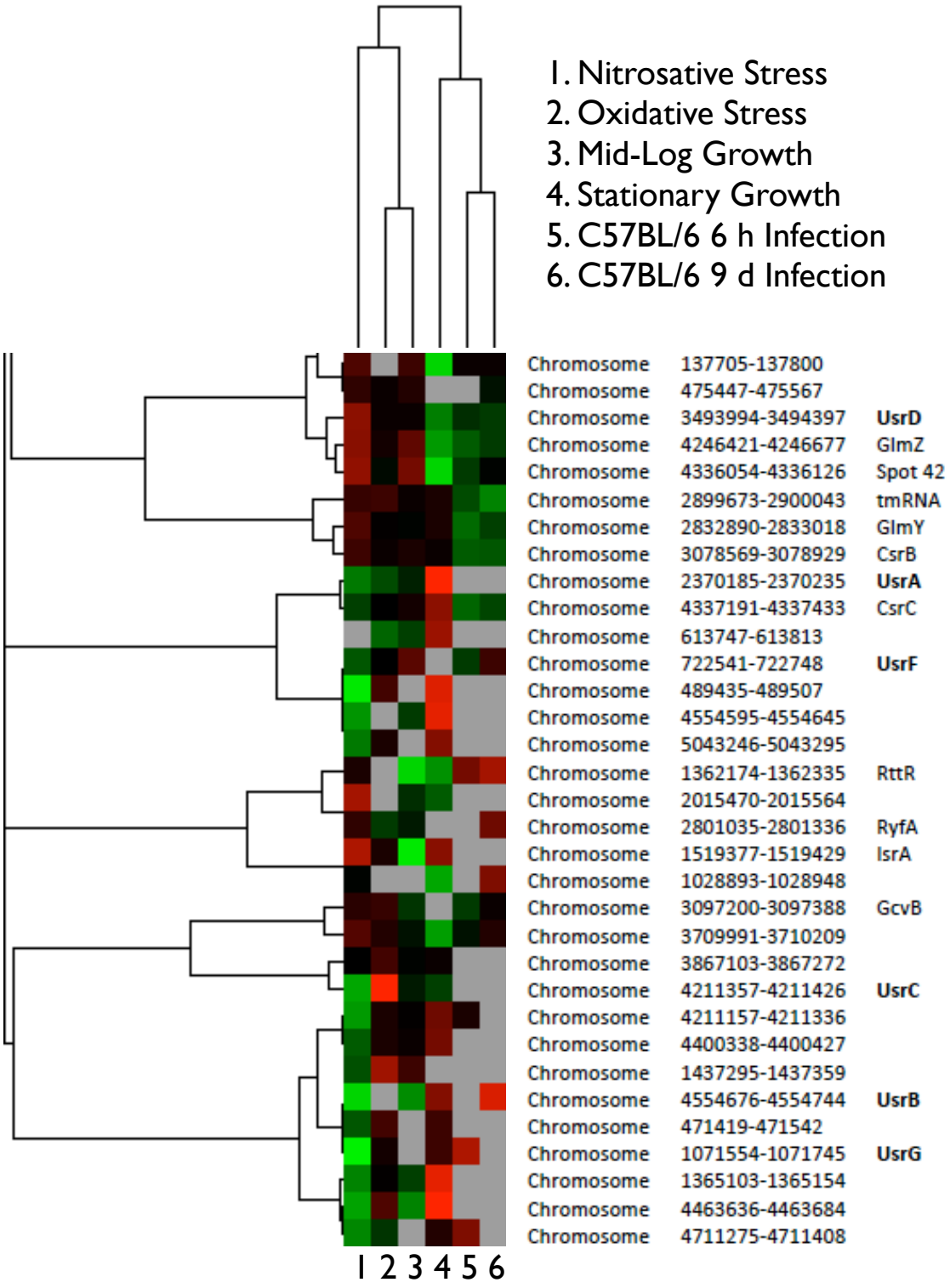

Figure 5.2 Continued

Cluster analysis of 828 intergenic loci resulted in 63 candidate sRNA molecules as described above.

Table 5.4 Candidate sRNA

Name	**Chromosomal Coordinates (from RNA-Seq)**		**Strand (prediction)**	**Flanking Genes (5'/3')**	**Confirmed Knockout**
usrA	2370149	2370532	+	*yohG*/*yohI*	Yes
usrB	4554676	4554744	+/-	*yjcH*/*acs*	Yes
usrC	4211357	4211426	-	C4323/*ilvG*	Yes
usrD	3493994	3494397	+/-	*tdcR*/*yhaD*	
usrE	2172783	2173287	+	C2233/C2234	
usrF	722460	722749	-	C0716/*sdhC*	
usrG	1071549	1071748	+	*ycdB*/*phoH*	Yes
usrH[2]	1402995	1403179	+	C1479/C1480	
usrI (sibB)	2291019	2291168	+	*yegL*/*mdtA*	
usrJ	2290694	2290838	+/-	*yegL*/*mdtA*	Yes
usrK[2]	3132555	3132694	+	C3210/C3212	

NT = not tested; (+) = sense strand; (-) = antisense strand;
[2] = Absent from MG1655

Figure 5.3 (*usrA-C*) Genomic loci for each candidate sRNA

The genetic location of each candidate is shown with neighboring genes, predicted promoters, and relative intergenic expression levels.

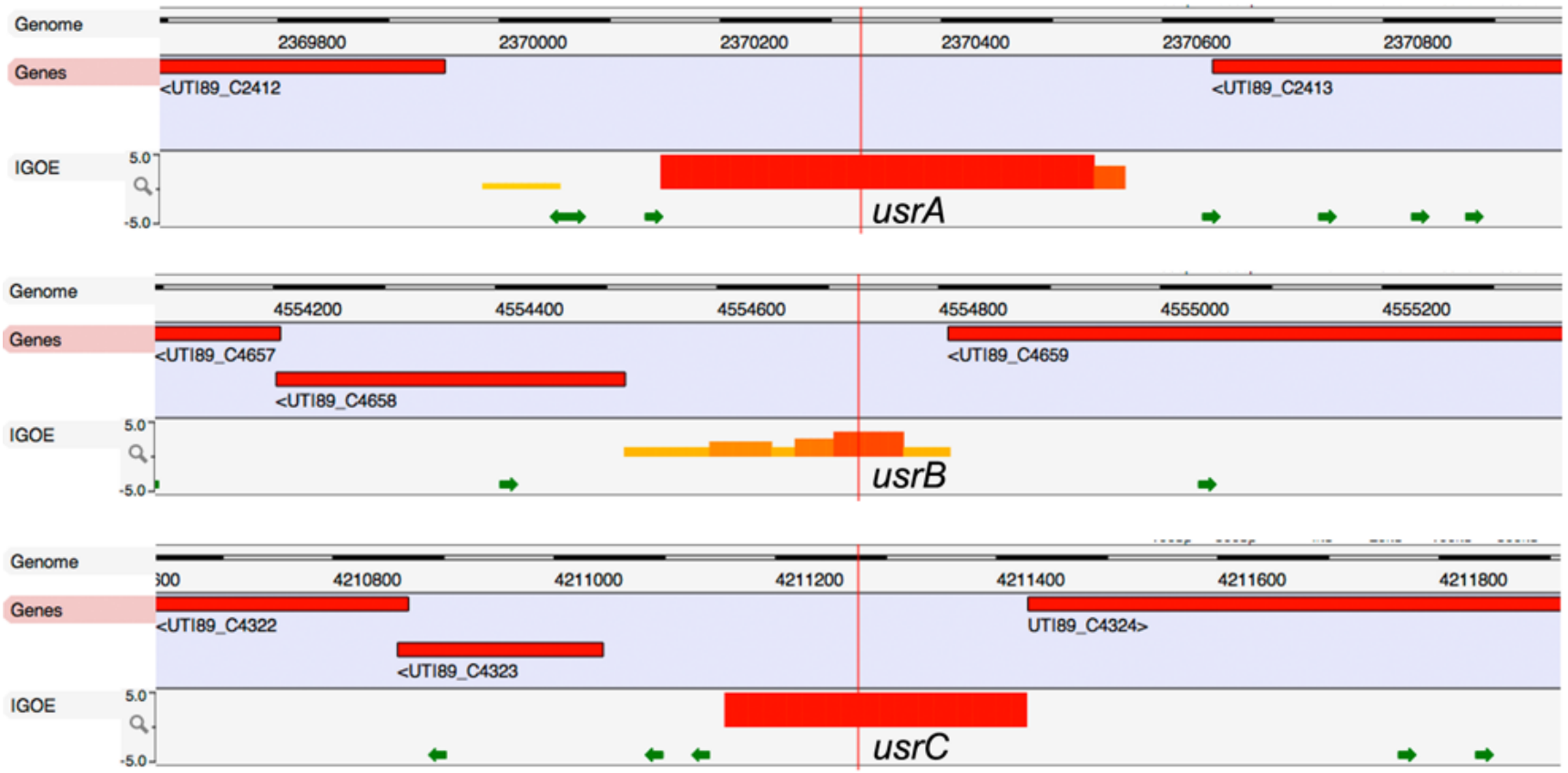
Genome
2369800
2370000
2370200
2370400
2370600
2370800
Genes
<UTI89_C2412
<UTI89_C2413
IGOE
5.0
-5.0
usrA
Genome
4554200
4554400
4554600
4554800
4555000
4555200
Genes
<UTI89_C4657
<UTI89_C4659
<UTI89_C4658
IGOE
5.0
-5.0
usrB
Genome
4210800
4211000
4211200
4211400
4211600
4211800
Genes
<UTI89_C4322
UTI89_C4324>
<UTI89_C4323
IGOE
5.0
-5.0
usrC

Figure 5.3 (*usrD-F*) Genomic loci for each candidate sRNA

The genetic location of each candidate is shown with neighboring genes, predicted promoters, and relative intergenic expression levels.

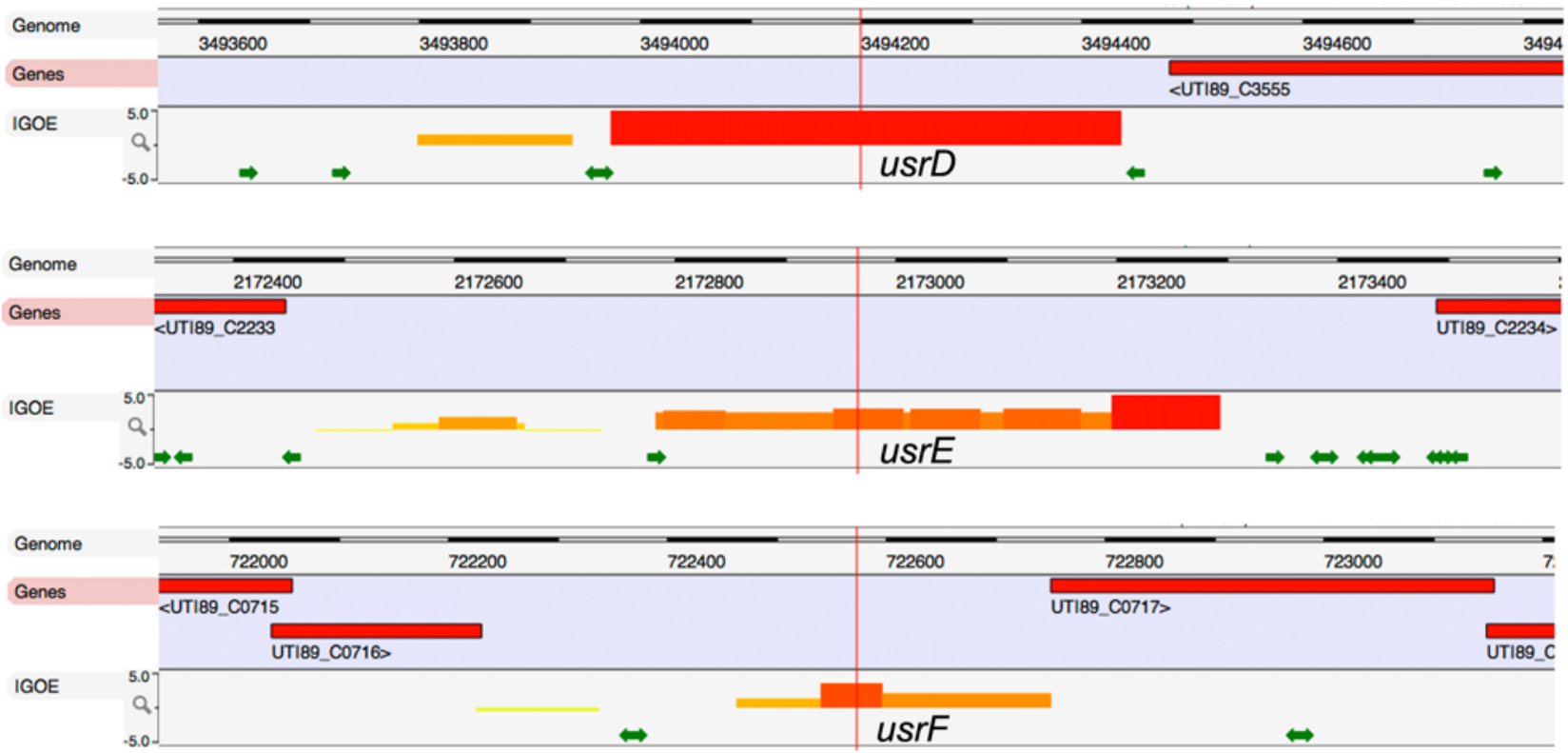
Genome
3493600
3493800
3494000
3494200
3494400
3494600
Genes
<UTI89_C3555
IGOE
5.0
-5.0
usrD
Genome
2172400
2172600
2172800
2173000
2173200
2173400
Genes
<UTI89_C2233
UTI89_C2234>
IGOE
5.0
-5.0
usrE
Genome
722000
722200
722400
722600
722800
723000
Genes
<UTI89_C0715
UTI89_C0716>
UTI89_C0717>
IGOE
5.0
-5.0
usrF

Figure 5.3 (*usrG,H)* Genomic loci for each candidate sRNA

The genetic location of each candidate is shown with neighboring genes, predicted promoters, and relative intergenic expression levels.

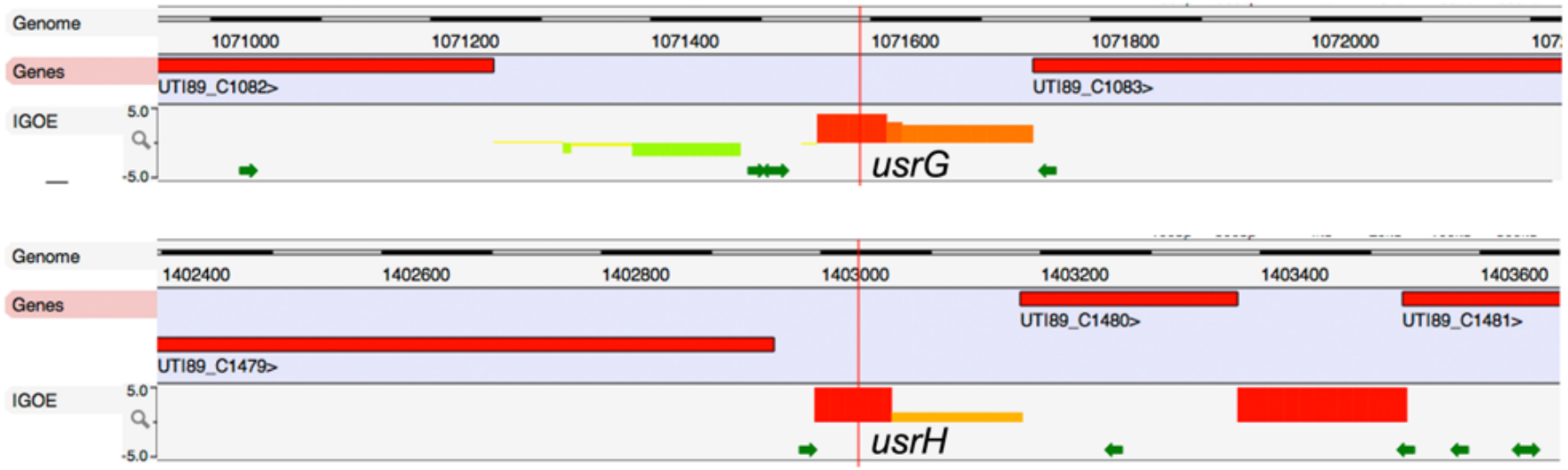
Genome
1071000
1071200
1071400
1071600
1071800
1072000
Genes
UTI89_C1082>
UTI89_C1083>
IGOE
5.0
-5.0
usrG
Genome
1402400
1402600
1402800
1403000
1403200
1403400
1403600
Genes
UTI89_C1480>
UTI89_C1481>
UTI89_C1479>
IGOE
5.0
-5.0
usrH

Figure 5.3 (*usrJ,K*) Genomic loci for each candidate sRNA

The genetic location of each candidate is shown with neighboring genes, predicted promoters, and relative intergenic expression levels.

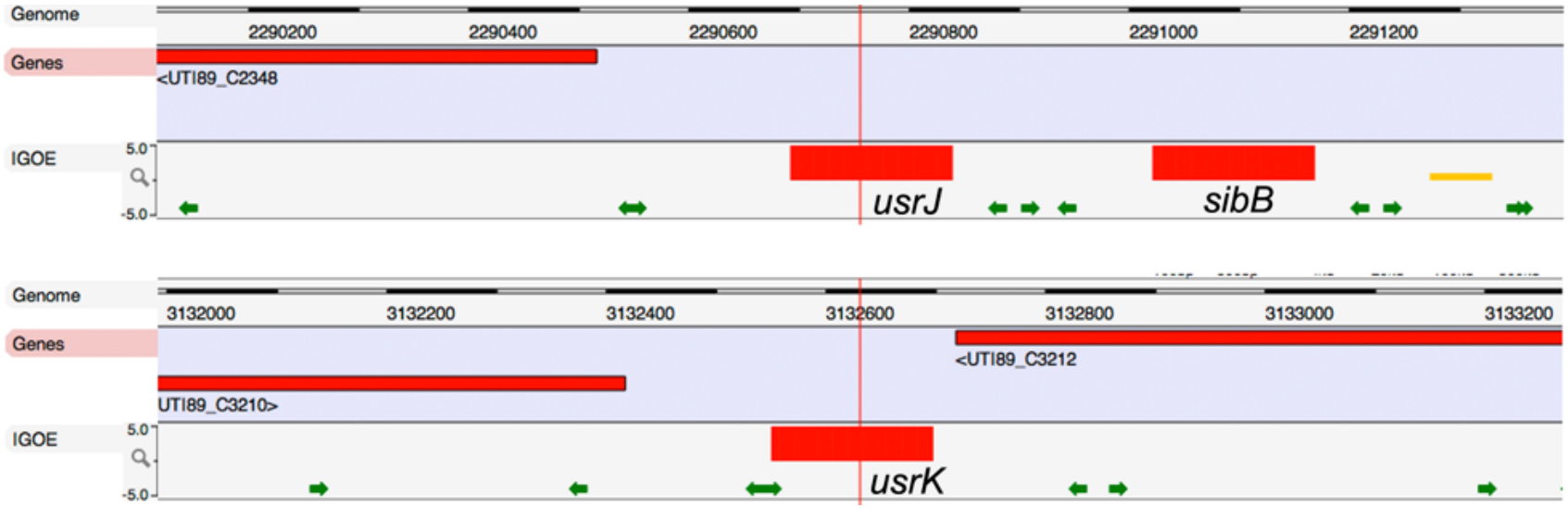
Genome
2290200
2290400
2290600
2290800
2291000
2291200
Genes
<UTI89_C2348
IGOE
5.0
-5.0
usrJ
sibB
Genome
3132000
3132200
3132400
3132600
3132800
3133000
3133200
Genes
<UTI89_C3212
UTI89_C3210>
IGOE
5.0
-5.0
usrK

Table 5.5 Target RNA predictions

sRNA	Stand for Prediction	Candid-ate	UTI89 Homo-log	P Value	Score	Annotation
usrA	+	phoH	Yes	0.0062 5011	-63	PhoB-dependent, ATP-binding pho regulon component
	-	yjfL	Yes	0.0022 482	-65	hypothetical protein
	-	blr	Yes	0.0047 5229	-61	beta-lactam resistance protein
	-	yniB	Yes	0.0057 2919	-60	hypothetical protein
usrB	+	b0725	No	1.40E-11	-168	hypothetical protein
	+	b3004	No	1.87E-10	-154	hypothetical protein
	+	phnE	Yes	6.53E-05	-85	membrane channel protein component of Pn transporter
	+	phoR	Yes	0.0031 7286	-64	positive and negative sensor protein for pho regulon
	+	tkrA	Yes	0.0079 8129	-59	2-keto-D-gluconate reductase (2-ketoaldonate reductase)
	+	yjeQ	Yes	0.0079 8129	-59	hypothetical protein
	-	b0725	No	5.60E-06	-92	hypothetical protein
	-	ybiO	Yes	2.23E-05	-85	putative transport protein
	-	yicM	Yes	7.31E-05	-79	putative tranport protein (MFS family)
	-	araD	Yes	0.0083 5072	-55	L-ribulose-5-phosphate 4-epimerase
	-	hokB	Yes	0.0083 5072	-55	small toxic membrane polypeptide

Table 5.5 Continued

sRNA	Stand for Prediction	Candid-ate	UTI89 Homo-log	P Value	Score	Annotation
usrC	+	dnaT	Yes	0.0008 90563	-71	DNA biosynthesis; primosomal protein
	+	yojI	Yes	0.0012 8814	-69	putative ATP-binding component of a transport system
	+	uppS	Yes	0.0081 3573	-59	undecaprenyl pyrophosphate synthetase (di-trans,poly-cis-decaprenylcistransferase)
	+	yjgH	No	0.0081 3573	-59	hypothetical protein
	+	sdhC	Yes	0.0097 7755	-58	succinate dehydrogenase, cytochrome b556
	-	hofB	Yes	3.21E-05	-89	putative integral membrane protein involved in biogenesis of fimbriae (type IV pilin), protein transport, DNA uptake
	-	fumC	Yes	3.21E-05	-89	fumarase C (fumarate hydratase Class II)
	-	wecG	Yes	0.0005 11881	-74	probable UDP-N-acetyl-D-mannosaminuronic acid transferase; synthesis of enterobacterial common antigen (ECA)
	-	ybcW	No	0.0007 40466	-72	DLP12 prophage
	-	glpC	Yes	0.0008 90563	-71	sn-glycerol-3-phosphate dehydrogenase (anaerobic), K-small subunit
	-	hyaE	Yes	0.0012 8814	-69	processing of HyaA and HyaB proteins
	-	yfbQ	Yes	0.0012 8814	-69	putative PLP-dependent aminotransferase
	-	ydhD	Yes	0.0015 4917	-68	hypothetical protein

Table 5.5 Continued

sRNA	Stand for Prediction	Candid-ate	UTI89 Homo-log	P Value	Score	Annotation
	-	gabP	Yes	0.0015 4917	-68	gamma-aminobutyrate transport protein, RpoS-dependent (APC family)
	-	uidB	Yes	0.0018 6305	-67	glucuronide permease
	-	rihA	Yes	0.0022 4044	-66	pyrimidine specific nucleoside hydrolase
	-	yfdI	No	0.0022 4044	-66	CPS-53 (KpLE1) prophage; putative ligase
	-	yhdP	Yes	0.0022 4044	-66	hypothetical protein
	-	yqjH	Yes	0.0026 9419	-65	hypothetical protein
	-	glcF	No	0.0026 9419	-65	glycolate oxidase iron-sulfur subunit
	-	yebE	Yes	0.0032 3968	-64	hypothetical protein
	-	yihE	Yes	0.0032 3968	-64	hypothetical protein
	-	yafP	Yes	0.0046 8352	-62	hypothetical protein
	-	yhiU	Yes	0.0046 8352	-62	multidrug resistance protein (lipoprotein)
	-	pepA	Yes	0.0056 3065	-61	aminopeptidase A, a cyteinylglycinase
	-	glnD	Yes	0.0067 6866	-60	protein PII; uridylyltransferase acts on regulator of glnA
	-	iciA	Yes	0.0067 6866	-60	inhibitor of replication initiation; transcriptional regulator of dnaA and argK (LysR family)
	-	yghW	Yes	0.0067 6866	-60	hypothetical protein
	-	mutT	Yes	0.0097 7755	-58	7,8-dihydro-8-oxoguanine-triphosphatase, prefers dGTP
	-	kdsA	Yes	0.0097 7755	-58	2-dehydro-3-deoxyphosphooctulonate aldolase
	-	goaG	No	0.0097 7755	-58	4-aminobutyrate aminotransferase

Table 5.5 Continued

sRNA	Stand for Prediction	Candid-ate	UTI89 Homo-log	P Value	Score	Annotation
usrD	+	yfdM	Yes	0.0036 8172	-77	CPS-53 (KpLE1) prophage; putative transferase
	+	ymfS	No	0.0042 84	-76	e14 prophag
	+	nagE	Yes	0.0067 4692	-73	PTS family enzyme IIC (N-terminal); enzyme IIB (center); enzyme IIC (C-terminal), N-acetylglucosamine-specific
	+	yjbL	No	0.0091 2949	-71	hypothetical protein
	-	cysG	Yes	0.0019 7729	-81	siroheme synthase, catalyses four reactions between uroporphyrinogen III and siroheme
	-	rfaC	Yes	0.0031 1789	-78	ADP-heptose; LPS heptosyl transferase I
	-	ydbH	Yes	0.0042 2324	-76	hypothetical protein
	-	ais	Yes	0.0049 1482	-75	protein induced by aluminum
	-	modB	Yes	0.0077 4335	-72	molybdate transport permease protein
	-	yghS	Yes	0.0077 4335	-72	hypothetical protein
usrE	+	galK	Yes	0.0005 15225	-92	galactokinase
	+	yafM	Yes	0.0022 7162	-82	hypothetical protein
	+	ppk	Yes	0.0026 3468	-81	polyphosphate kinase
	+	ybaS	Yes	0.0030 5569	-80	putative glutaminase
	+	yfaL	Yes	0.0074 2996	-74	hypothetical protein
	+	era	Yes	0.0074 2996	-74	GTP-binding protein
	+	wza	Yes	0.0086 139	-73	putative polysaccharide export protein

Table 5.5 Continued

sRNA	Stand for Prediction	Candid-ate	UTI89 Homo-log	P Value	Score	Annotation
	-	ygaQ	No	0.0005 86795	-91	hypothetical protein
	-	adhE	Yes	0.0046 9274	-77	CoA-linked acetaldehyde dehydrogenase and iron-dependent alcohol dehydrogenase; pyruvate-formate-lyase deactivase
	-	yggV	Yes	0.0054 428	-76	hypothetical protein
	-	agaI	Yes	0.0054 428	-76	putative galactosamine-6-phosphate isomerase
	-	wzxC	Yes	0.0098 4235	-72	probable export protein
usrF	+	ymfC	Yes	0.0063 3458	-71	hypothetical protein
	+	b1995	Yes	0.0074 0728	-70	CP4-44 prophage; putative hemine receptor
	-	sdhC	Yes	0.0029 0866	-75	succinate dehydrogenase, cytochrome b556
usrG	+	ygeA	Yes	0.0017 7428	-76	putative aspartate racemase
	+	ycbL	Yes	0.0055 5936	-69	hypothetical protein
	+	fucU	Yes	0.0065 4313	-68	conserved protein of fucose operon
	+	rihB	Yes	0.0090 612	-66	pyrimidine specific nucleoside hydrolase
	-	phoH	Yes	4.55E-15	-239	PhoB-dependent, ATP-binding pho regulon component
usrH	+	ygeY	Yes	0.0022 2102	-74	putative deacetylase
	+	yciA	Yes	0.0059 5914	-68	hypothetical protein
	+	yibO	Yes	0.0059 5914	-68	phosphoglycerate mutase III, cofactor-independent

Table 5.5 Continued

sRNA	Stand for Prediction	Candid-ate	UTI89 Homo-log	P Value	Score	Annotation
	+	cysU	Yes	0.0070 2305	-67	sulfate, thiosulfate transport system permease T protein
	+	ydaV	No	0.0082 7611	-66	Rac prophage; putative DNA replication protein
	-	yfcE	Yes	0.0010 4863	-77	hypothetical protein
	-	hlyE	Yes (trun)	0.0014 6748	-75	hemolysin E
	-	yebW	Yes	0.0017 3595	-74	hypothetical protein
	-	ynjC	Yes	0.0040 1929	-69	putative transport protein (ABC superfamily, membrane)
	-	ygaV	Yes	0.0040 1929	-69	hypothetical protein
	-	endA	Yes	0.0040 1929	-69	DNA-specific endonuclease I
	-	yghS	Yes	0.0078 5957	-65	hypothetical protein
	-	yjjI	Yes	0.0092 9196	-64	hypothetical protein
usrJ	+	chpR	Yes	0.0005 66207	-78	part of proteic killer gene system, suppressor of inhibitory function of ChpA
	+	erfK	Yes	0.0011 3482	-74	hypothetical protein
	+	yehI	Yes	0.0013 502	-73	putative regulator
	+	ygfM	Yes	0.0013 502	-73	hypothetical protein
	+	tolB	Yes	0.0032 1797	-68	periplasmic protein involved in the tonb-independent uptake of group A colicins
	+	ymgD	Yes	0.0032 1797	-68	hypothetical protein
	+	yecG	Yes	0.0038 2796	-67	hypothetical protein
	+	cydA	Yes	0.0045 5332	-66	cytochrome d terminal oxidase, polypeptide subunit I

Table 5.5 Continued

sRNA	Stand for Prediction	Candid-ate	UTI89 Homo-log	P Value	Score	Annotation
	+	lpdA	Yes	0.0054 1575	-65	dihydrolipoamide dehydrogenase, FAD/NAD(P)-binding, component of the 2-oxoglutarate dehydrogenase and the pyruvate dehydrogenase complexes
	+	yfbP	No	0.0054 1575	-65	hypothetical protein
	+	ybjP	Yes	0.0076 5959	-63	hypothetical protein
	+	yieH	No	0.0076 5959	-63	putative enzyme with a phophatase-like domain
	+	argH	Yes	0.0076 5959	-63	argininosuccinate lyase
	+	hflC	Yes	0.0076 5959	-63	protease specific for phage lambda cII repressor
	+	ybeQ	Yes	0.0091 0767	-62	hypothetical protein
	-	fdnI	Yes	0.0003 36101	-81	formate dehydrogenase-N, cytochrome B556(Fdn) gamma subunit, nitrate-inducible
	-	tonB	Yes	0.0038 2796	-67	energy transducer; uptake of iron, cyanocobalimin; sensitivity to phages, colicins
	-	deoA	Yes	0.0045 5332	-66	thymidine phosphorylase
	-	pspF	Yes	0.0054 1575	-65	psp operon transcriptional activator
	-	cyoE	Yes	0.0064 41	-64	protohaeme IX farnesyltransferase (haeme O biosynthesis)
	-	rhtB	Yes	0.0064 41	-64	amino acid exporter (homoserine, HSL)
	-	kefA	Yes	0.0076 5959	-63	component of the MscS mechano-sensitive channel

Table 5.5 Continued

sRNA	Stand for Prediction	Candid-ate	UTI89 Homo-log	P Value	Score	Annotation
	-	recT	No	0.0076 5959	-63	Rac prophage; recombinase, DNA renaturation
	-	ygiA	Yes	0.0076 5959	-63	hypothetical protein
	-	yhjT	Yes	0.0076 5959	-63	hypothetical protein
usrK	+	glxR	Yes	0.0014 0146	-73	tartronic semialdehyde reductase
	+	dacD	No	0.0028 0197	-69	DD-carboxypeptidase, penicillin-binding protein 6b
	+	fldA	Yes	0.0039 6099	-67	flavodoxin 1
	+	srlR	Yes	0.0039 6099	-67	regulator for gut (srl), glucitol operon
	+	hflB	Yes	0.0055 9809	-65	ATP-dependent zinc-metallo protease
	+	elaC	Yes	0.0066 5435	-64	hypothetical protein
	+	yfdN	Yes	0.0066 5435	-64	CPS-53 (KpLE1) prophage; putative transcriptional regulator
	-	fldA	Yes	0.0007 55175	-78	flavodoxin 1
	-	celB	Yes	0.0029 4365	-70	PEP-dependent phosphotransferase enzyme II for cellobiose, arbutin, and salicin
	-	eutB	Yes	0.0029 4365	-70	ethanolamine ammonia-lyase, heavy chain
	-	hslO	Yes	0.0034 8885	-69	Hsp33; redox regulated chaperone
	-	yncG	Yes (trun)	0.0049 0008	-67	hypothetical GST-like protein
	-	ycbW	Yes	0.0096 5654	-63	hypothetical protein
	-	serA	Yes	0.0096 5654	-63	D-3-phosphoglycerate dehydrogenase

Table 5.6 Strains and plasmids used in this study

Strains	**Description**	**Reference**
E. coli		
UTI89	UPEC reference strain and cystitis isolate	(5, 11, 32)
DH5α	Cloning strain	
Recombinant Strains		
UTI89Δ*usrA*	UTI89 *usrA::cat*	This work
UTI89Δ*usrB*	UTI89 *usrB::cat*	This work
UTI89Δ*usrC*	UTI89 *usrC::cat*	This work
UTI89Δ*usrG*	UTI89 *usrG::cat*	This work
UTI89Δ*usrJ*	UTI89 *usrJ::cat*	This work
Plasmids		
pKM208	Encodes lambda Red recombinase for creation of knockout strains	(33)
pKD3	Plasmid containing chloramphenicol resistance cassette for use in lambda-Red recombination	(14)
pRR48	IPTG inducible overexpression of protein coding sequence Ap^r	(52)
pRRK1	Modified pRR48 lacking Shine-Delgarno sequence for overexpression of sRNA Ap^r	R. Kulesus

Table 5.7 Oligonucleotides employed during the study

Primer Name[a]	Sequence (5'-3')[b, c]
usrA-KO-F	GATAACGGCAAAGGGCTTCGTTTTTTCCTATACTTATTCA GTGTGTAGGCTGGAGCTGCTTCG
usrA-KO-R	GAGCTAAGCCACATATTGCCACTGGCGCAAGGAGCGCG CCATATGAATATCCTCCTTAG
usrA-Conf-F	GCGTGGCAATACATCAGTAG
usrA-Conf-R	GCCATTGATATCGATAAGCTGC
usrB-KO-F	GGCAATCAATGCCTGATGCGACGCTGTCGCGTCTTATCT GTGTAGGCTGGAGCTGCTTCG
usrB-KO-R	GGTAACGGTTTGTAGGCCTGATAAGACGCGACAGCGGC ATATGAATATCCTCCTTAG
usrB-Conf-F	GTAGGGATTGTTTTAATTC
usrB-Conf-R	CCTCGACGCTTGCCGATC
usrC-KO-F	CACCGAAAGGTCCGGGGGTTTTTTTTGACCTTAAAAACT GTGTAGGCTGGAGCTGCTTCG
usrC-KO-R	TGCCCGCAACGCATGTACCACCCACTGTGCGCCATTCA CATATGAATATCCTCCTTAG
usrC-Conf-F	CTGGTCGTGATTAGCGTG
usrC-Conf-R	CGTGTCGGCACAGCAAGT
usrG-KO-F	GTGAATATATTGTTGCAATGAATGCGAGATCTGTTGTTGT GTAGGCTGGAGCTGCTTCG
usrG-KO-R	CACCGTTTGCGGCGTCGGTAACACGAGTAAAGAGAGGA CATATGAATATCCTCCTTAG
usrG-Conf-F	CCTGCTGAAAGCACACAG
usrG-Conf-R	CCCATGGAGAGCACCTTG
usrJ-KO-F	GCCGTCGATTGACACTAAGGGCGGAGTGACATAATTTCT GTGTAGGCTGGAGCTGCTTCG
usrJ-KO-R	GGGCGAAAGGAGGTAAGCCGAAGATTTCAGCGGGACG CCATATGAATATCCTCCTTAG
usrJ-Conf-F	CATACCGATTGCAATAATG
usrJ-Conf-R	TGCAGTCTGCGATCCTG

[a] F, forward Primer; R, reverse Primer; KO, knockout primer; Conf, confirmation primer

[b] Universal Primer sequence underlined

[c] Added restriction sites underlined

Figure 5.4 Growth and biofilm formation of candidate knockouts

Growth of UTI89Δ*usrA/B/C/G/J* in (A) LB, (B), modified M9 minimal media, (C) M9 containing 0.3 mM MV, and (D) M9 containing 1.0 mM GSNO. Each experiment (A-D) is representative data from one of three experiments performed in quadruplicate. Error bars were negligible and thus omitted. *In vitro* biofilm formation assays in modified M9 minimal media at (E) 30°C and (F) 37°C. Data represents the mean ±SE of at least three independent experiments performed in quadruplicate. *P* values were determined by Student's *t* test; **P*<0.05, ***P*<0.01, ****P*<0.001, versus the wild type control.

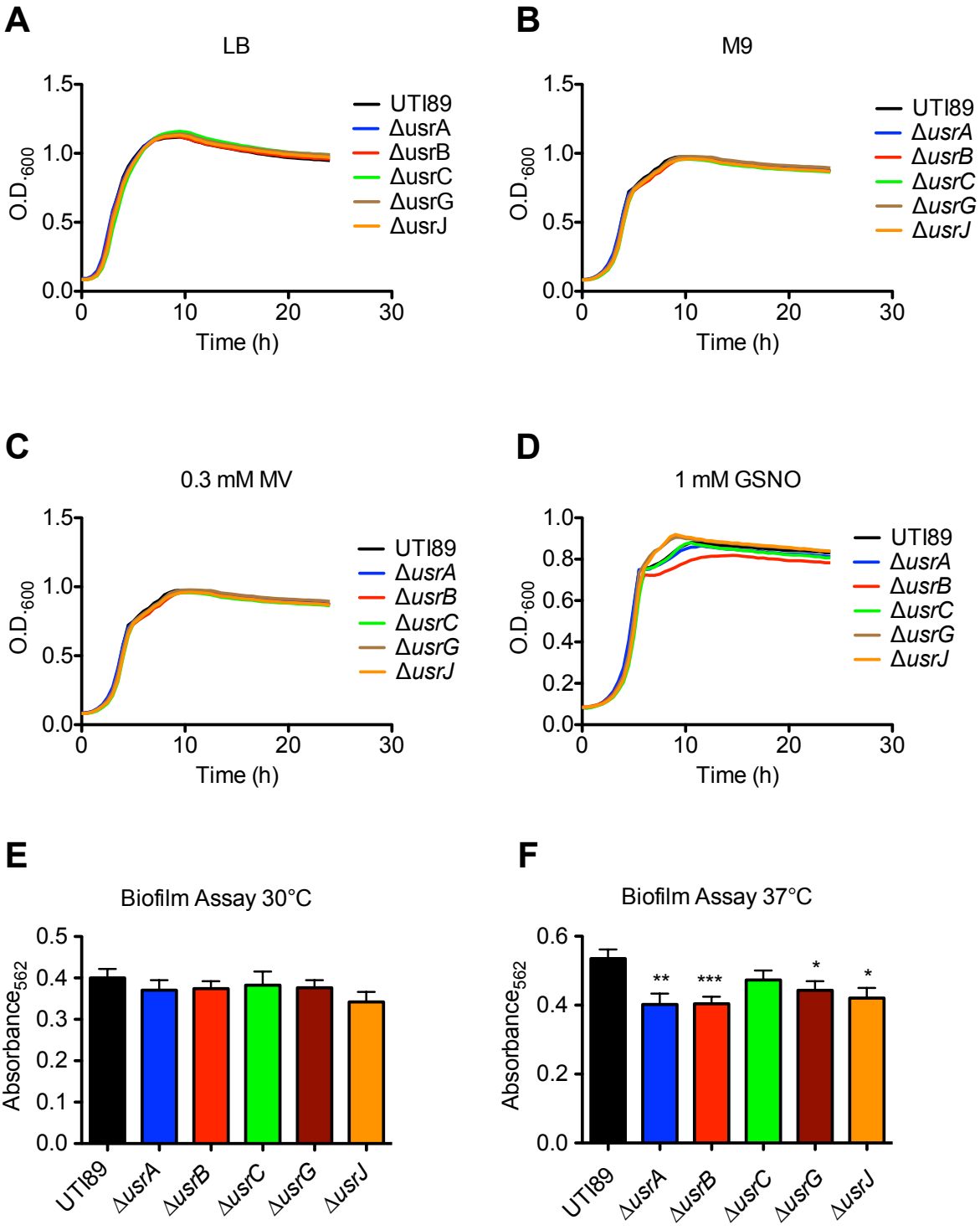
A
LB
O.D.600
Time (h)
UTI89
ΔusrA
ΔusrB
ΔusrC
ΔusrG
ΔusrJ
B
M9
C
0.3 mM MV
D
1 mM GSNO
E
Biofilm Assay 30°C
Absorbance562
F
Biofilm Assay 37°C
**
***
*
*

strains of the *usrA, B, C, G, and J* regions have been successfully generated. The sRNA knockouts exhibited no deviations from wild type in Luria Bertani (LB) broth or modified M9 minimal media (Fig 5.4A-B). Knockouts challenged with 1 mM MV or 1 mM GSNO also exhibited no alterations in growth (Fig 5.4C-D).

sRNA knockouts contribute to biofilm formation

Despite normal growth under stress conditions, UTI89Δ*usrA, B, G, and J* exhibited mild defects when challenged to form biofilms *in vitro* in plastic microtiter plates. All of the defects were observed at 37°C, with no changes observed at 30°C in modified M9 minimal media (Fig 5.4E-F). Defects in biofilm formation in these assays is not attributable to the presence of the chloramphenicol resistance cassette used to construct the mutants, as many strains carrying the same cassette in this and other assays behave like the wild type strain with respect to biofilm formation. Examination of UTI89Δ*usrA* and UTI89Δ*usrB* indicated normal levels of yeast agglutination, indicating normal formation of type I pili.

UsrB contributes to virulence in a mouse model of UTI

RNA-Seq analysis from infected mouse samples was utilized as a tool for selection of candidate sRNA molecules, and thus each knockout strain was assessed for virulence potential using a murine model of UTI. Mice were infected with 10^7 CFU of wild type or mutant UTI89 via transurethral catheterization and

bacterial titers within the bladder were determined at 6 h and 9 d postinoculation. Interestingly, at 6 h postinfection, UTI89Δ*usrB* consistently showed ~4.5 fold greater titers than wild type (Fig 5.5A). UTI89 lacking *usrA, C, or G* behaved like the wild type strain 6 h post infection. By 9 d postinfection, titers UTI89Δ*usrA* and UTI89Δ*usrB* were not significantly altered from wild type UTI89 (Fig 5.5B). In competitive infection assays, in which UTI89Δ*usrA* or UTI89Δ*usrB* are infected with an equal number of wild type UTI89, no differences between the wild type and mutant strains were observed at a 3 d time point (Fig 5.5C). In total, these data indicate that these sRNAs so far examined have at best only minimal impact on the fitness and pathogenic behavior of UTI89.

Discussion

An explosion of deep sequencing studies has flooded the field of bacterial RNA in recent years, with many focused on the identification of previously elusive sRNA molecules. The data in Table 5.1 clearly demonstrate the recent accretion of sRNA sequencing efforts, which have brought many novel sRNAs to the forefront. Since pathogenic strains often exhibit more robust stress response, iron scavenging, and antibiotic resistance characteristics than traditional laboratory strains of *E. coli*, we concentrated on sRNA molecules which could be identified during these processes, namely during growth in redox stressors and during murine UTI. Hence we utilized UPEC as a model organism to study the infection of the sterile niche of the bladder.

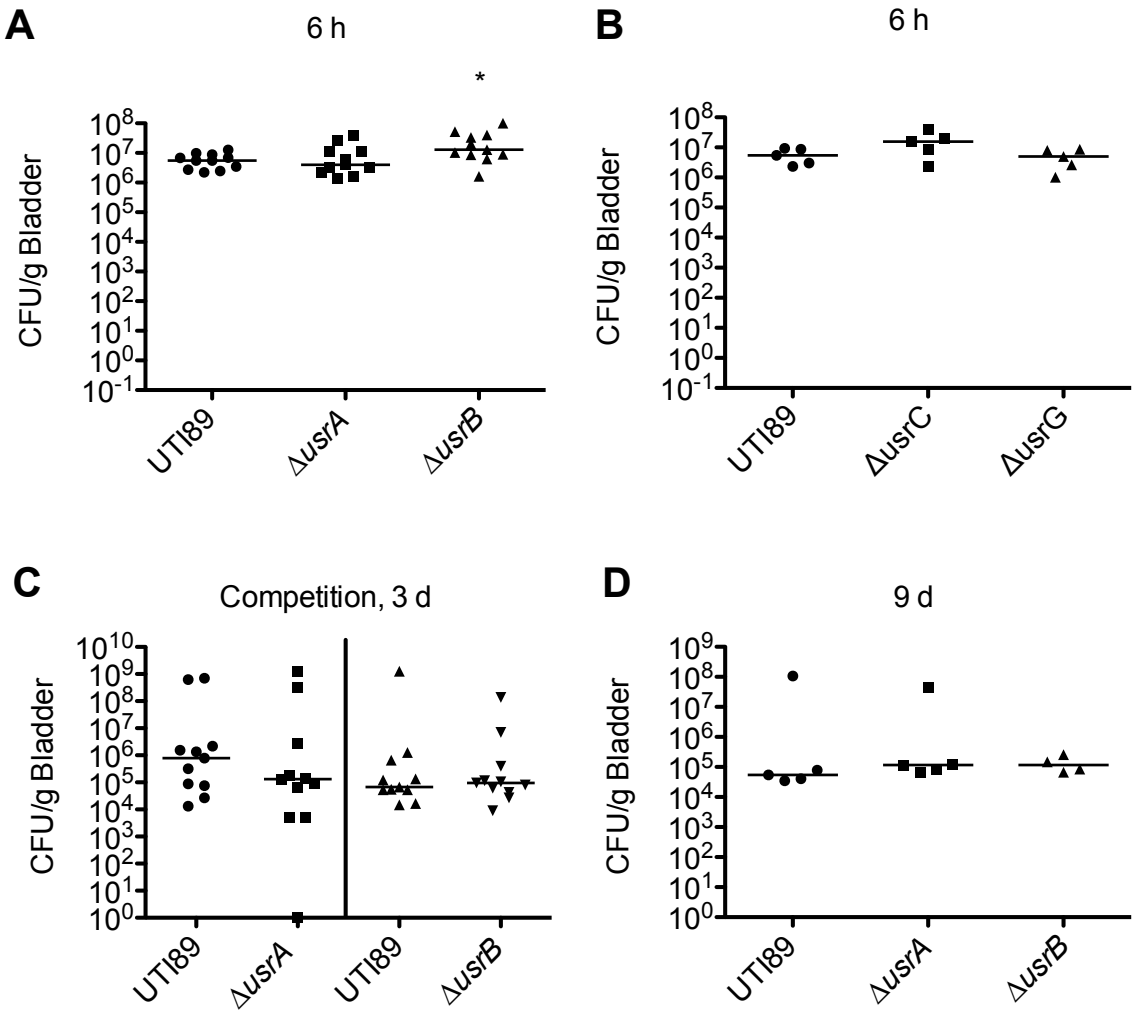

Figure 5.5 UsrB represses bladder colonization

Adult female CBA/J mice were inoculated via transurethral catheterization with 10^7 CFU of UTI89, UTI89Δ*usrA*, UTI89Δ*usrB*, UTI89Δ*usrC*, or UTI89Δ*usrG*. (A-C) Bacterial titers were determined from infected bladders 6 h and 9 d post-inoculation, in agreement with time points from RNA-Seq. (C) For competitive assays, mice were infected with equal numbers of the wild type and mutant strains (10^7 CFU total) and bladder titers were calculated 3 d postinfection. Bars denote median values for each group. Graph A + C depict cumulative results from two independent assays (n = 11 mice per group). Panels B + D are in progress and indicate data from one experiment. **P*<0.05, as determined using the Mann-Whitney U test.

RNA-Seq and subsequent bioinformatics analysis provided us with a putative list of sRNA loci. Interestingly, these results suggested a slightly enriched sRNA population in UTI89 specific genomic sequences (135%) compared to the K-12 strain, MG1655. A higher frequency of sRNAs in UPEC-specific sequences suggests that pathogens may acquire or even evolve more sRNAs to refine stress response and virulence regulatory cascades. UPEC strains also exhibit increased resistance to stress challenge as compared to K-12 strains, which would likely require more intricate regulatory capacity (unpublished data). RNA-Seq experiments provide a wealth of sequence information, but still likely fail to identify all possible sRNA species due to overwhelming quantities of certain prevalent species. Deeper sequencing would thus be required to unequivocally prove that pathogens have an inflated sRNA repertoire compared to nonpathogenic strains.

828 candidate sRNA loci were revealed in intergenic regions of UTI89 through RNA-Seq. Of these candidate loci, 11 were chosen for further study due to their relative levels of expression compared to neighboring ORFs and across multiple samples. Six candidates were initially knocked out using lambda Red recombination. Chromosomal knockouts of candidate loci exhibited no change in growth *in vitro* in rich media, minimal media, or after challenge with redox stressors. Biofilm formation was, however attenuated in UTI89Δ*usrA, B, G, and J*, as quantified by *in vitro* biofilm formation assays in plastic microtiter plates. Biofilm formation *in vitro* has been shown to correlate with pathogen virulence *in vivo* (51), and thus acts as a proxy for identification of factors that may affect the

virulence potential of a given UPEC strain. Intriguingly, deletion of the sRNA UsrB was found to promote colonization of the murine bladder at 6 h postinfection, suggesting that this sRNA is a negative regulator of bacterial fitness and/or virulence within the acute phase of a UTI.

In order to glean more information of putative downstream targets of sRNAs, candidate regions were run through the sRNA target prediction program, TargetRNA, against the genome of a MG1655 K-12 *E. coli* (Table 6) (55, 56). TargetRNA predicts mRNA targets of sRNAs by searching for homology over a defined region of the mRNA. The standard search narrows this window to the 50 nt surrounding the ribosome binding site. The caveat to using TargetRNA to predict mRNA targets in UTI89 is the reliance on the K-12 genome as the query, since the UTI89 genome sequence is currently not available with this analysis. As it stands, all identified putative sRNA targets are present in MG1655, which has a reduced genome compared to the pathogens and fails to express many of the known UTI89 virulence factors. Nonetheless, the list of putative targets provides insight into the possible cellular focus of each sRNA. One possible explanation for UsrB effects on virulence could be through direct repression of the PhoR expression. PhoR has been implicated in virulence factor expression in *Edwardsiella tarda* in response to changes in inorganic phosphate levels, which are typically depleted in host niches in response to infection (8). It is possible that UsrB may repress PhoR in UTI89, resulting in accelerated virulence factor production by this pathogen early on during UTI, while later during the infection

process this effect may be countered by host-mediated depletion of inorganic phosphate.

In conclusion, this study presents the putative sRNA repertoire of a reference UPEC isolate, and begins to probe the potential roles of several novel UPEC sRNAs in UTI pathogenesis. These early results indicate that UPEC isolates likely encode an expanded set of sRNAs in comparison with non-pathogenic K-12 strains, and suggest roles for both conserved, and possibly UPEC-specific, sRNA molecules as regulators of bacterial virulence and fitness within the urinary tract. The example of UTI89Δ*usrB* demonstrates that sRNA molecules may also be utilized to reign in overzealous virulence effectors during the course of infection, a previously underappreciated function of sRNAs. Additional work is required to validate the expression and functionality of the putative sRNAs identified here, but the data already in hand open up exciting new avenues by which we can better understand and manipulate the virulence potential of UPEC and related pathogens.

Materials and Methods

RNA isolation

RNA isolation was performed using the Norgen Total RNA Isolation Kit (Norgen Biotek) according to the manufacturers protocol with minor alterations. Briefly, 500 µl of cultured bacteria are mixed with 1 ml of RNA Later (Ambion) and incubated for 10 min at RT. Bacterial cells are then pelleted at 10000 X g for 10 min in a table top centrifuge followed by addition of RNase-free Tris-EDTA

Buffer (Fluka Analytical) containing 15 mg/ml lysozyme (Sigma-Aldrich) and 15 mg/ml proteinase K (Sigma-Aldrich) for 30 min at RT to prepare bacteria for lysis. 300 µl of Norgen lysis solution is then added to samples and vortexed for 15 s, followed by addition of 200 µl of 4°C ethanol and 15 s of vortexing. Samples are then added to the Norgen RNA isolation column and centrifuged at max speed in a tabletop centrifuge for 1 min at RT. After three washes in 400 µl of Norgen Wash Buffer, two additional minutes of centrifugation ensured removal of ethanol before elution with 50 µl of H_2O (2 min 200 x g followed by 1 min max speed at RT).

Total RNA isolated from UPEC strains was then treated with Turbo DNase (Ambion) extensively to remove DNA contamination. Samples were treated with 10-14 U Turbo DNase in a reaction volume of 200 µl for 1 h at 37°C. In certain cases a second DNase reaction was performed after using a Norgen RNA Clean-Up and Concentrate Kit (Norgen Biotek). Following DNase treatment, RNA was mixed with 200 µl acid-phenol-chloroform pH 6.7 and centrifuged for 5 min at max speed. Aqueous phase was transferred to a new 1.5 ml tube and 180-200 µl of chloroform was added, followed by centrifugation for 5 in at max speed at RT. Aqueous phase was again transferred to a new tube and precipitated with ethanol using 0.1 volume 5 M NH_4Ac, linear acrylamide as a carrier, and 2.5 volumes ice-cold ethanol at -80°C overnight. RNA was then recovered by centrifugation for 30 min at 4°C before drying for 5 min, and resuspension in ~25 µl of H_2O. The Turbo DNase treatment was then repeated followed by acid

phenol chloroform and ethanol precipitation. Sample concentrations were determined by Nanodrop analysis (Thermo Scientific).

RNA-Seq

Total RNA depleted of DNA from all samples was treated with Terminator 5'-Phosphate-Dependent Exonuclease (EpiCentre Biotechnologies) in 1X Terminator Reaction Buffer, RiboGuard RNase Inhibitor, and 1 U enzyme per 2.5 µg total RNA, for 30 min at 37°C to remove rRNA and tRNA as previously described (45). Samples were then acid-phenol-chloroform- and ethanol-precipitated as described above. All samples were then provided to the Huntsman Cancer Institute Sequencing Core for library creation and sequencing on an Illumina HiSeq 2000 via directional mRNA sequencing with single end reads.

Bioinformatics

The sequencing reads were processed as follows: homopolymeric and low quality (Illumina pipeline quality scores less than 15 in 15 or more positions) sequences were removed; exact duplicate reads were compressed in to single fasta records, noting the number of occurrences of the duplicate sequences. Sequences from *in vitro* and *in vivo* samples were aligned to the UTI89 chromosome and plasmid, GenBank IDs 91209055 and 91206245 respectively. Additionally the *in vivo* samples were aligned to the *Mus musculus* genome (UCSC build: mm9). All alignments were performed using the bowtie aligner

(PMC2690996). RNA expression of a region (e.g. ORF, sRNA, etc.) was calculated as the number of reads which overlap one or more positions in the region per thousand reads obtained per sample and normalized to the length of the region: (region reads)/(kiloreads * kilobase). Intergenic expression was also considered relative to the adjacent 3' and 5' OFRs and expressed as the log2 ratio of the intergenic region vs. the expression of the 3' of 5' ORF, whichever is greater. Putative rho independent terminator sites were identified using TransTermHP (PMC1852404), and σ70 binding sites were calculated using an *E. coli* specific position weight matrix and custom software written in python (KF Fischer pers. comm.). These data were exposed to the internet using Distributed Annotation System and displayed using a custom genome browser, developed using Dalliance (http://www.biodalliance.org).

Growth conditions

The prototypic UPEC isolate UTI89 and its derivatives were cultured from freezer stocks in LB broth or modified M9 minimal media (6 g/l Na_2HPO_4, 3 g/l KH_2PO_4, 1 g/l NH_4Cl, 0.5 g/l NaCl, 1 mM $MgSO_4$, 0.1 mM $CaCl_2$, 0.1% glucose, 0.0025% nicotinic acid, 0.2% casein amino acids, and 16.5 μg/ml thiamine in H_2O) (Sigma-Aldrich) as previously described (63). Bacteria were grown at 37°C overnight in loosely capped 20-by-150-mm borosilicate glass tubes at a 30° angle with shaking at 225 rpm. Overnight cultures were diluted 1:100 into 100-well honeycomb plates and assayed for growth using a Bioscreen C instrument (Growth Curves USA). Growth was assessed in LB broth, M9 media, M9 media ±

1 mM GSNO (Sigma-Aldrich), or M9 media ± 1 mM methyl viologen (MV; Sigma-Aldrich). As previously described, antibiotics were added only for maintenance of plasmids in overnight cultures and were not included during growth assays (Sigma-Aldrich). Strains utilized in this study are listed in Table 7.

Biofilm assays

Microtiter plate-based biofilm assays were performed as described previously (24). Briefly, overnight cultures of UTI89 were grown shaking at 225 rpm at 37°C in LB broth before subculture 1:100 into M9 minimal media. 100 µl of sample was then plated in quadruplicate on 96-well pinchbar flat-bottomed polystyrene microtiter plates (NUNC). Samples were surrounded by a row of H_2O to minimize evaporation. After 48 h at 30 or 37°C, planktonic bacteria were removed by washing with tap water two times. 150 µl of 0.1% crystal violet solution was added for 10 min. The wells were then rinsed twice with H_20 and air-dried. To solubilize the dye, 200 µl of dimethyl sulfoxide (Sigma-Aldrich) was then added to each well and vigorously shaken for 15 min on an orbital shaker. The absorbance of each well was then read by measuring A_{562} using a Synergy HT multi-detection microplate reader (BioTek Instruments, Inc.).

Mouse infections

Seven- to 8-week-old female C57BL/6 mice (Jackson Laboratory) were anesthetized by isoflurane inhalation. Mice were then slowly inoculated by transurethral catheterization with 50 µl of bacteria (~10^7 CFU from 24 h static M9

minimal media cultures) resuspended in PBS as described previously (24). Mice were infected for use in multiple downstream applications, including RNA isolation for RNA-Seq and knockout characterization. Infected mice for RNA-Seq were sacrificed at 6 h or 9 d post infection. The bladders were aseptically removed and pooled in RNA Later (Ambion) containing 0.025% Triton X-100 and homogenized to lyse host cells. Pooled samples were centrifuged at 10,000 X g for 3 min in a tabletop centrifuge at RT. After resuspension in RNA Later, samples were filtered through 100 micron nylon mesh (Sefar) to remove large particulates from the bladder. Samples were then incubated with rabbit anti-*E. coli* antibody (Meridian Life Science, Inc) for 5-10 min at 4°C at a dilution of 1:50. Cells were washed with 1 mL RNA Later and centrifuged for 3 min at 10000 X g. Samples were resuspended in 80 µl of RNA Later and added to 20 µl of α-Rb IgG antbody-coated MACs Beads (Miltenyi Biotec) for 15 min at 4°C. The cells were then washed by adding 1 ml RNA Later followed by centrifugation at 600 X g for 10 min at RT followed by complete removal of supernatant. Samples were resuspended in RNA Later and passed through a MACs beads magnetic column according to manufacturers instructions. All washes were done using RNA Later to minimize changes to RNA profile. Bacteria were eluted from the column in 1 ml of RNA Later and RNA was immediately isolated using the Norgen Total RNA Isolation kit (Norgen Biotek).

Candidate sRNA knockouts were characterized in the murine model of UTI for contributions to pathogenesis. Seven- to 8-week- old female C57BL/6 mice were infected with 10^7 UTI89 or knockout strain for 6 h or 9 d as described

above. For competition experiments, equal titers of wild type and a single knockout strain were co-infected as described into mouse bladders for 3 d before sacrifice. For both experimental approaches mice were sacrificed and bladders aseptically removed, weighed, and homogenized in 0.025% Triton X-100 as previously described (24). Samples were serially diluted and plated to determine bacterial titers per gram of bladder tissue. Eleven mice total, from two independent experiments, were used for each group.

Statistical analysis

P values were determined by Student's *t* test or Mann-Whitney U tests performed using Prism 5.01 software (GraphPad Software). Values of less than 0.05 were deemed significant.

Acknowledgements

We would like to thank Brian Dalley and Nicole Moss in the Huntsman Cancer Institute sequencing core. This study was funded by NIH grants AI095647, DK068585, AI090369, and AI088086. M.G.B. was supported by T32 AI055434 from the National Institute Of Allergy and Infectious Diseases. The content is solely the responsibility of the authors and does not necessarily represent the official views of the National Institute Of Allergy And Infectious Diseases or the National Institutes of Health.

References

1. **Altuvia, S., D. Weinstein-Fischer, A. Zhang, L. Postow, and G. Storz.** 1997. A small, stable RNA induced by oxidative stress: role as a pleiotropic regulator and antimutator. Cell **90:**43-53.

2. **Argaman, L., R. Hershberg, J. Vogel, G. Bejerano, E. G. Wagner, H. Margalit, and S. Altuvia.** 2001. Novel small RNA-encoding genes in the intergenic regions of *Escherichia coli*. Curr. Biol. **11:**941-950.

3. **Arnvig, K. B., and D. B. Young.** 2009. Identification of small RNAs in *Mycobacterium tuberculosis*. Mol. Microbiol. **73:**397-408.

4. **Beisel, C. L., and G. Storz.** 2011. The base-pairing RNA spot 42 participates in a multioutput feedforward loop to help enact catabolite repression in *Escherichia coli*. Mol. Cell **41:**286-297.

5. **Blattner, F. R., G. Plunkett, 3rd, C. A. Bloch, N. T. Perna, V. Burland, M. Riley, J. Collado-Vides, J. D. Glasner, C. K. Rode, G. F. Mayhew, J. Gregor, N. W. Davis, H. A. Kirkpatrick, M. A. Goeden, D. J. Rose, B. Mau, and Y. Shao.** 1997. The complete genome sequence of *Escherichia coli* K-12. Science **277:**1453-1462.

6. **Bohn, C., C. Rigoulay, S. Chabelskaya, C. M. Sharma, A. Marchais, P. Skorski, E. Borezee-Durant, R. Barbet, E. Jacquet, A. Jacq, D. Gautheret, B. Felden, J. Vogel, and P. Bouloc.** 2010. Experimental discovery of small RNAs in *Staphylococcus aureus* reveals a riboregulator of central metabolism. Nucleic Acids Res. **38:**6620-6636.

7. **Chabelskaya, S., O. Gaillot, and B. Felden.** 2010. A *Staphylococcus aureus* small RNA is required for bacterial virulence and regulates the expression of an immune-evasion molecule. PLoS Pathog. **6:**e1000927.

8. **Chakraborty, S., J. Sivaraman, K. Y. Leung, and Y. K. Mok.** 2011. Two-component PhoB-PhoR regulatory system and ferric uptake regulator sense phosphate and iron to control virulence genes in type III and VI secretion systems of *Edwardsiella tarda*. J. Biol. Chem. **286:**39417-39430.

9. **Chen, S., E. A. Lesnik, T. A. Hall, R. Sampath, R. H. Griffey, D. J. Ecker, and L. B. Blyn.** 2002. A bioinformatics based approach to discover small RNA genes in the *Escherichia coli* genome. Biosystems **65:**157-177.

10. **Chen, S., A. Zhang, L. B. Blyn, and G. Storz.** 2004. MicC, a second small-RNA regulator of Omp protein expression in *Escherichia coli*. J. Bacteriol. **186:**6689-6697.

11. **Chen, S. L., C. S. Hung, J. Xu, C. S. Reigstad, V. Magrini, A. Sabo, D. Blasiar, T. Bieri, R. R. Meyer, P. Ozersky, J. R. Armstrong, R. S. Fulton, J. P. Latreille, J. Spieth, T. M. Hooton, E. R. Mardis, S. J. Hultgren, and J. I. Gordon.** 2006. Identification of genes subject to positive selection in uropathogenic strains of *Escherichia coli*: a comparative genomics approach. Proc. Natl. Acad. Sci. U. S. A. **103:**5977-5982.

12. **Chen, Y., D. C. Indurthi, S. W. Jones, and E. T. Papoutsakis.** 2011. Small RNAs in the genus *Clostridium*. MBio **2:**e00340-00310.

13. **Christiansen, J. K., J. S. Nielsen, T. Ebersbach, P. Valentin-Hansen, L. Sogaard-Andersen, and B. H. Kallipolitis.** 2006. Identification of small Hfq-binding RNAs in *Listeria monocytogenes*. RNA **12:**1383-1396.

14. **Datsenko, K. A., and B. L. Wanner.** 2000. One-step inactivation of chromosomal genes in *Escherichia coli* K-12 using PCR products. Proc. Natl. Acad. Sci. U. S. A. **97:**6640-6645.

15. **de Hoon, M. J., S. Imoto, J. Nolan, and S. Miyano.** 2004. Open source clustering software. Bioinformatics **20:**1453-1454.

16. **De Lay, N., and S. Gottesman.** 2011. Role of polynucleotide phosphorylase in sRNA function in *Escherichia coli*. RNA **17:**1172-1189.

17. **del Val, C., E. Rivas, O. Torres-Quesada, N. Toro, and J. I. Jimenez-Zurdo.** 2007. Identification of differentially expressed small non-coding RNAs in the legume endosymbiont *Sinorhizobium meliloti* by comparative genomics. Mol. Microbiol. **66:**1080-1091.

18. **Frohlich, K. S., and J. Vogel.** 2009. Activation of gene expression by small RNA. Curr. Opin. Microbiol. **12:**674-682.

19. **Gong, H., G. P. Vu, Y. Bai, E. Chan, R. Wu, E. Yang, F. Liu, and S. Lu.** 2011. A *Salmonella* small non-coding RNA facilitates bacterial invasion and intracellular replication by modulating the expression of virulence factors. PLoS Pathog. **7:**e1002120.

20. **Gonzalez, N., S. Heeb, C. Valverde, E. Kay, C. Reimmann, T. Junier, and D. Haas.** 2008. Genome-wide search reveals a novel GacA-regulated small RNA in *Pseudomonas* species. BMC Genomics **9:**167.

21. **Gottesman, S., and G. Storz.** 2011. Bacterial small RNA regulators: versatile roles and rapidly evolving variations. Cold Spring Harb Perspect. Biol. **3**.

22. **Jiang, R. P., D. J. Tang, X. L. Chen, Y. Q. He, J. X. Feng, B. L. Jiang, G. T. Lu, M. Lin, and J. L. Tang.** 2010. Identification of four novel small non-coding RNAs from *Xanthomonas campestris* pathovar campestris. BMC Genomics **11:**316.

23. **Koo, J. T., T. M. Alleyne, C. A. Schiano, N. Jafari, and W. W. Lathem.** 2011. Global discovery of small RNAs in *Yersinia pseudotuberculosis* identifies Yersinia-specific small, noncoding RNAs required for virulence. Proc. Natl. Acad. Sci. U. S. A. **108:**E709-717.

24. **Kulesus, R. R., K. Diaz-Perez, E. S. Slechta, D. S. Eto, and M. A. Mulvey.** 2008. Impact of the RNA chaperone Hfq on the fitness and virulence potential of uropathogenic *Escherichia coli*. Infect. Immun. **76:**3019-3026.

25. **Kumar, R., P. Shah, E. Swiatlo, S. C. Burgess, M. L. Lawrence, and B. Nanduri.** 2010. Identification of novel non-coding small RNAs from *Streptococcus pneumoniae* TIGR4 using high-resolution genome tiling arrays. BMC Genomics **11:**350.

26. **Landt, S. G., E. Abeliuk, P. T. McGrath, J. A. Lesley, H. H. McAdams, and L. Shapiro.** 2008. Small non-coding RNAs in *Caulobacter crescentus*. Mol. Microbiol. **68:**600-614.

27. **Liang, H., Y. T. Zhao, J. Q. Zhang, X. J. Wang, R. X. Fang, and Y. T. Jia.** 2011. Identification and functional characterization of small non-coding RNAs in *Xanthomonas oryzae* pathovar oryzae. BMC Genomics **12:**87.

28. **Liu, J. M., J. Livny, M. S. Lawrence, M. D. Kimball, M. K. Waldor, and A. Camilli.** 2009. Experimental discovery of sRNAs in *Vibrio cholerae* by direct cloning, 5S/tRNA depletion and parallel sequencing. Nucleic Acids Res. **37:**e46.

29. **Livny, J., A. Brencic, S. Lory, and M. K. Waldor.** 2006. Identification of 17 *Pseudomonas aeruginosa* sRNAs and prediction of sRNA-encoding genes in 10 diverse pathogens using the bioinformatic tool sRNAPredict2. Nucleic Acids Res. **34:**3484-3493.

30. **Madhugiri, R., G. Pessi, B. Voss, J. Hahn, C. M. Sharma, R. Reinhardt, J. Vogel, W. R. Hess, H. M. Fischer, and E. Evguenieva-Hackenberg.** 2012. Small RNAs of the *Bradyrhizobium/Rhodopseudomonas* lineage and their analysis. RNA Biol. **9**.

31. **Mraheil, M. A., A. Billion, W. Mohamed, K. Mukherjee, C. Kuenne, J. Pischimarov, C. Krawitz, J. Retey, T. Hartsch, T. Chakraborty, and T.**

Hain. 2011. The intracellular sRNA transcriptome of *Listeria monocytogenes* during growth in macrophages. Nucleic Acids Res. **39:**4235-4248.

32. **Mulvey, M. A., J. D. Schilling, and S. J. Hultgren.** 2001. Establishment of a persistent *Escherichia coli* reservoir during the acute phase of a bladder infection. Infect. Immun. **69:**4572-4579.

33. **Murphy, K. C., and K. G. Campellone.** 2003. Lambda Red-mediated recombinogenic engineering of enterohemorrhagic and enteropathogenic *E. coli*. BMC Mol. Biol. **4:**11.

34. **Ortega, A., J. Gonzalo-Asensio, and F. Garcia-Del Portillo.** 2012. Dynamics of Salmonella small RNA expression in non-growing bacteria located inside eukaryotic cells. RNA Biol. **9**.

35. **Padalon-Brauch, G., R. Hershberg, M. Elgrably-Weiss, K. Baruch, I. Rosenshine, H. Margalit, and S. Altuvia.** 2008. Small RNAs encoded within genetic islands of *Salmonella typhimurium* show host-induced expression and role in virulence. Nucleic Acids Res. **36:**1913-1927.

36. **Panek, J., J. Bobek, K. Mikulik, M. Basler, and J. Vohradsky.** 2008. Biocomputational prediction of small non-coding RNAs in *Streptomyces*. BMC Genomics **9:**217.

37. **Perez, N., J. Trevino, Z. Liu, S. C. Ho, P. Babitzke, and P. Sumby.** 2009. A genome-wide analysis of small regulatory RNAs in the human pathogen group A *Streptococcus*. PLoS One **4:**e7668.

38. **Postic, G., E. Frapy, M. Dupuis, I. Dubail, J. Livny, A. Charbit, and K. L. Meibom.** 2010. Identification of small RNAs in *Francisella tularensis*. BMC Genomics **11:**625.

39. **Qu, Y., L. Bi, X. Ji, Z. Deng, H. Zhang, Y. Yan, M. Wang, A. Li, X. Huang, R. Yang, and Y. Han.** 2012. Identification by cDNA cloning of abundant sRNAs in a human-avirulent *Yersinia pestis* strain grown under five different growth conditions. Future Microbiol. **7:**535-547.

40. **Raghavan, R., E. A. Groisman, and H. Ochman.** 2011. Genome-wide detection of novel regulatory RNAs in *E. coli*. Genome Res. **21:**1487-1497.

41. **Rice, P. W., and J. E. Dahlberg.** 1982. A gene between polA and glnA retards growth of *Escherichia coli* when present in multiple copies: physiological effects of the gene for spot 42 RNA. J. Bacteriol. **152:**1196-1210.

42. **Richards, J., and J. G. Belasco.** 2008. A new window onto translational repression by bacterial sRNAs. Mol. Cell **32:**751-753.

43. **Schluter, J. P., J. Reinkensmeier, S. Daschkey, E. Evguenieva-Hackenberg, S. Janssen, S. Janicke, J. D. Becker, R. Giegerich, and A. Becker.** 2010. A genome-wide survey of sRNAs in the symbiotic nitrogen-fixing alpha-proteobacterium *Sinorhizobium meliloti*. BMC Genomics **11:**245.

44. **Schmidtke, C., S. Findeiss, C. M. Sharma, J. Kuhfuss, S. Hoffmann, J. Vogel, P. F. Stadler, and U. Bonas.** 2012. Genome-wide transcriptome analysis of the plant pathogen *Xanthomonas* identifies sRNAs with putative virulence functions. Nucleic Acids Res. **40:**2020-2031.

45. **Sharma, C. M., S. Hoffmann, F. Darfeuille, J. Reignier, S. Findeiss, A. Sittka, S. Chabas, K. Reiche, J. Hackermuller, R. Reinhardt, P. F. Stadler, and J. Vogel.** 2010. The primary transcriptome of the major human pathogen *Helicobacter pylori*. Nature **464:**250-255.

46. **Shimoni, Y., G. Friedlander, G. Hetzroni, G. Niv, S. Altuvia, O. Biham, and H. Margalit.** 2007. Regulation of gene expression by small non-coding RNAs: a quantitative view. Mol. Syst. Biol. **3:**138.

47. **Shinhara, A., M. Matsui, K. Hiraoka, W. Nomura, R. Hirano, K. Nakahigashi, M. Tomita, H. Mori, and A. Kanai.** 2011. Deep sequencing reveals as-yet-undiscovered small RNAs in *Escherichia coli*. BMC Genomics **12:**428.

48. **Shioya, K., C. Michaux, C. Kuenne, T. Hain, N. Verneuil, A. Budin-Verneuil, T. Hartsch, A. Hartke, and J. C. Giard.** 2011. Genome-wide identification of small RNAs in the opportunistic pathogen *Enterococcus faecalis* V583. PLoS One **6:**e23948.

49. **Sittka, A., S. Lucchini, K. Papenfort, C. M. Sharma, K. Rolle, T. T. Binnewies, J. C. Hinton, and J. Vogel.** 2008. Deep sequencing analysis of small noncoding RNA and mRNA targets of the global post-transcriptional regulator, Hfq. PLoS Genet. **4:**e1000163.

50. **Sonnleitner, E., T. Sorger-Domenigg, M. J. Madej, S. Findeiss, J. Hackermuller, A. Huttenhofer, P. F. Stadler, U. Blasi, and I. Moll.** 2008. Detection of small RNAs in *Pseudomonas aeruginosa* by RNomics and structure-based bioinformatic tools. Microbiology **154:**3175-3187.

51. **Soto, S. M., A. Smithson, J. P. Horcajada, J. A. Martinez, J. P. Mensa, and J. Vila.** 2006. Implication of biofilm formation in the persistence of

urinary tract infection caused by uropathogenic *Escherichia coli*. Clin. Microbiol. Infect. **12:**1034-1036.

52. **Studdert, C. A., and J. S. Parkinson.** 2005. Insights into the organization and dynamics of bacterial chemoreceptor clusters through in vivo crosslinking studies. Proc. Natl. Acad. Sci. U. S. A. **102:**15623-15628.

53. **Swiercz, J. P., Hindra, J. Bobek, H. J. Haiser, C. Di Berardo, B. Tjaden, and M. A. Elliot.** 2008. Small non-coding RNAs in *Streptomyces coelicolor*. Nucleic Acids Res. **36:**7240-7251.

54. **Tezuka, T., H. Hara, Y. Ohnishi, and S. Horinouchi.** 2009. Identification and gene disruption of small noncoding RNAs in Streptomyces griseus. J. Bacteriol. **191:**4896-4904.

55. **Tjaden, B.** 2008. TargetRNA: a tool for predicting targets of small RNA action in bacteria. Nucleic Acids Res. **36:**W109-113.

56. **Tjaden, B., S. S. Goodwin, J. A. Opdyke, M. Guillier, D. X. Fu, S. Gottesman, and G. Storz.** 2006. Target prediction for small, noncoding RNAs in bacteria. Nucleic Acids Res. **34:**2791-2802.

57. **Tsui, H. C., D. Mukherjee, V. A. Ray, L. T. Sham, A. L. Feig, and M. E. Winkler.** 2010. Identification and characterization of noncoding small RNAs in *Streptococcus pneumoniae* serotype 2 strain D39. J. Bacteriol. **192:**264-279.

58. **Ulve, V. M., A. Cheron, A. Trautwetter, C. Fontenelle, and F. Barloy-Hubler.** 2007. Characterization and expression patterns of *Sinorhizobium meliloti* tmRNA (ssrA). FEMS Microbiol. Lett. **269:**117-123.

59. **Valverde, C., J. Livny, J. P. Schluter, J. Reinkensmeier, A. Becker, and G. Parisi.** 2008. Prediction of *Sinorhizobium meliloti* sRNA genes and experimental detection in strain 2011. BMC Genomics **9:**416.

60. **Vockenhuber, M. P., C. M. Sharma, M. G. Statt, D. Schmidt, Z. Xu, S. Dietrich, H. Liesegang, D. H. Mathews, and B. Suess.** 2011. Deep sequencing-based identification of small non-coding RNAs in *Streptomyces coelicolor*. RNA Biol. **8:**468-477.

61. **Vogel, J., V. Bartels, T. H. Tang, G. Churakov, J. G. Slagter-Jager, A. Huttenhofer, and E. G. Wagner.** 2003. RNomics in *Escherichia coli* detects new sRNA species and indicates parallel transcriptional output in bacteria. Nucleic Acids Res. **31:**6435-6443.

62. **Vogel, J., and B. F. Luisi.** 2011. Hfq and its constellation of RNA. Nat. Rev. Microbiol. **9:**578-589.

63. **Wiles, T. J., B. K. Dhakal, D. S. Eto, and M. A. Mulvey.** 2008. Inactivation of host Akt/protein kinase B signaling by bacterial pore-forming toxins. Mol. Biol. Cell **19:**1427-1438.

64. **Wilms, I., A. Overloper, M. Nowrousian, C. M. Sharma, and F. Narberhaus.** 2012. Deep sequencing uncovers numerous small RNAs on all four replicons of the plant pathogen *Agrobacterium tumefaciens*. RNA Biol. **9**.

CHAPTER 6

BALANCED INPUT FROM THE TRNASFER RNA PRENYLTRANSFERASE MIAA CONTROLS THE STRESS RESISTANCE AND VIRULENCE POTENTIAL OF UROPATHOGENIC *ESCHERICHIA COLI*

Abstract

In *Escherichia coli* the enzymes MiaA and MiaB modify adenosine-37 of UNN-recognizing tRNAs. The first enzyme in this pathway, MiaA, has been extensively linked to translational efficiency and reading frame maintenance, while the function of the second enzyme, MiaB, remains elusive. In this study, we directly compare MiaA and MiaB for their contribution to stress resistance, behavior in the form of motility and biofilm assays, and virulence in uropathogenic *E. coli*. Interestingly, MiaA and MiaB did not contribute equally to stress response. MiaA was shown to contribute to growth in osmotic, oxidative, and nitrosative stress in the pathogen, whereas MiaB did not affect growth. We observed a dosage effect with MiaA, where both limiting and excess expression of MiaA resulted in decreased growth in response to stressors. We observed a corresponding decrease in MiaA protein expression after stress treatment. In regards to behavior, both MiaA and MiaB were shown to differentially regulate biofilm formation, however only MiaA regulates motility. A murine model of urinary tract infection indicated that MiaA contributes to virulence, whereas MiaB had no effect on pathogenesis. Infection of mouse urinary tracts with a *miaA* knockout resulted in attenuated infection at 1, 3, and 9 days, and a decreased reservoir population at day 9 of infection. Of note, the pore-forming toxin α-hemolysin was not expressed in a *miaA* knockout, despite increased levels of transcript. Therefore, differential regulation of A-37 specifically by MiaA results in drastic deviations to uropathogenic *E. coli* stress response, behavior, and virulence.

Author Summary

The bacterial ribosome translates a messenger RNA into a functional protein with the help of another form of RNA, known as transfer RNA. To accurately achieve high fidelity protein translation, transfer RNA molecules are often modified with additional chemical groups to increase specificity within the ribosome. Previous studies have elicited roles for tRNA molecules in a wide range of bacterial behaviors, including translation efficiency, stress response, and virulence, among others. The MiaA enzyme imparts a modification that is linked to translational fidelity and, subsequently, stress response and virulence. It is hypothesized that decreased levels of MiaA allows for alternate protein folding motifs and possibly functions by incorporation of errors in the protein sequence. In our study, we find that uropathogenic *E. coli* down-regulates MiaA in response to stressors, consistent with the above model. Additionally, MiaA activity is implicated in bacterial behavior, toxin formation, and virulence in a mouse model of infection. Our study shows further evidence that transfer RNA modification is important as a global switch to modulation bacterial behaviors and stress response in an ever-changing environment.

Introduction

The ribosome is among the most important, indispensible molecular machines in the cell. The charge of the ribosome is to turn stored genetic information into a physical output in the form of functional proteins. Ribosomal proteins and catalytic RNA molecules coalesce into an elegant structure, which

binds to and translates messenger RNA (mRNA) (for review see (15, 34, 36, 45)). Along with ribonucleoproteins and ribosomal RNA, a molecular translator, or transfer RNA (tRNA), is required to bridge the gap between mRNA and protein. A unique portion of the tRNA known as the anticodon sequence recognizes a codon in frame on the mRNA presented in the A-site of the ribosome. Once a tRNA molecule correctly identifies the anticodon in the A-site of the ribosome, the appropriate amino acid is added to the growing peptide chain in the P-site. The tRNA then exits the ribosomal E-site to complete its reaction. Multiple levels of regulation further complicate this simplified model of translation. In particular, extensive modification of both rRNA and tRNA molecules alters and often improves the efficiency of translation by the ribosome. tRNA molecules, in particular, may be modified with more than 75 moieties, including methyl, hydroxyl, and prenyl groups (38). The fully modified, or mature, tRNA properly fits into the ribosome and interacts correctly with the mRNA, contributing to maintenance of both reading frame and translational fidelity (5).

tRNA modification is now known to affect the regulation of cellular physiology and myriad other processes in bacteria through mammals. Although classically thought to primarily affect translational fidelity and efficiency, recent studies have implicated tRNA modification as more of a global regulator of cellular processes. In addition to functioning in translational fidelity, Chan et al. recently observed dynamic control of tRNA modification marks in response to cellular stresses, including oxidative stress (9). Similarly, studies in *Streptomyeces pyogenes* have implicated tRNA modification by GidA/MnmE as

necessary for virulence in a murine subcutaneous ulcer model (11). Another example of stress response and virulence regulation by tRNA modification can be observed with the pseudouridine synthesis gene TruA, which is required for type III secretory genes in *Pseudomonas aeruginosa* (1). Finally, deletion of enzymes required for addition of specific tRNA modifications have been utilized as attenuated vaccines in bacterial pathogens such as *Streptomyeces pyogenes*, further necessitating the need for more study in alternate organisms (11). Consequently, tRNA modifications play diverse roles in regulation of stress response and virulence in a wide range of bacterial pathogens.

One of the most commonly modified tRNA residues in bacteria is adenosine-37 (A-37), which lies adjacent to the anticodon loop (27). A-37 of UNN (U=uridine, N=any nucleotide)-recognizing tRNA, in its final form, is both prenylated and methylthiolated (38). The *miaA* gene of *Escherichia coli* encodes a tRNA prenyltransferase responsible for catalyzing the addition of a prenyl group onto the N^6-nitrogen of A-37 to create i^6A-37 tRNA (8) (Fig. 6.1A). The modified i^6A-37 residue is then further methylthiolated by the radical-S-adenosylmethionine enzyme MiaB to create ms^2i^6A-37 (39-41). The ms^2i^6A-37 modification is then required to correctly identify target codons (UNN) in the ribosomal A-site and, ultimately, functions in reading frame maintenance and translational fidelity (46). The ms^2i^6A-37 modification is highly conserved in prokaryotes through eukaryotes, yet the enzymes that mediate this modification have diverged through evolutionary time. However, in prokaryotes MiaA and

Figure 6.1 UTI89Δ*miaA* exhibits wild type growth despite severely altered metabolism

(A) Model of MiaA and MiaB action modified from Leung et al. (32). (B- D) Growth of *miaA* and *miaB* knockouts in LB broth, M9 minimal media, and LB-MES (pH 5.0) broth. Graphs in B-D show representative data of the mean of 4 replicates from at least 3 independent experiments. Error bars were negligible and omitted for clarity. (E) Metabolomics of common bacterial metabolites as determined by GC/MS. Bar graph shows list of significantly altered metabolites in UTI89Δ*miaA* compared to UTI89 with a list of unchanged metabolites to the right of the figure. Data are presented as the mean of six independent replicates ±SD, with $P < 0.05$ as calculated by Student's *t* test.

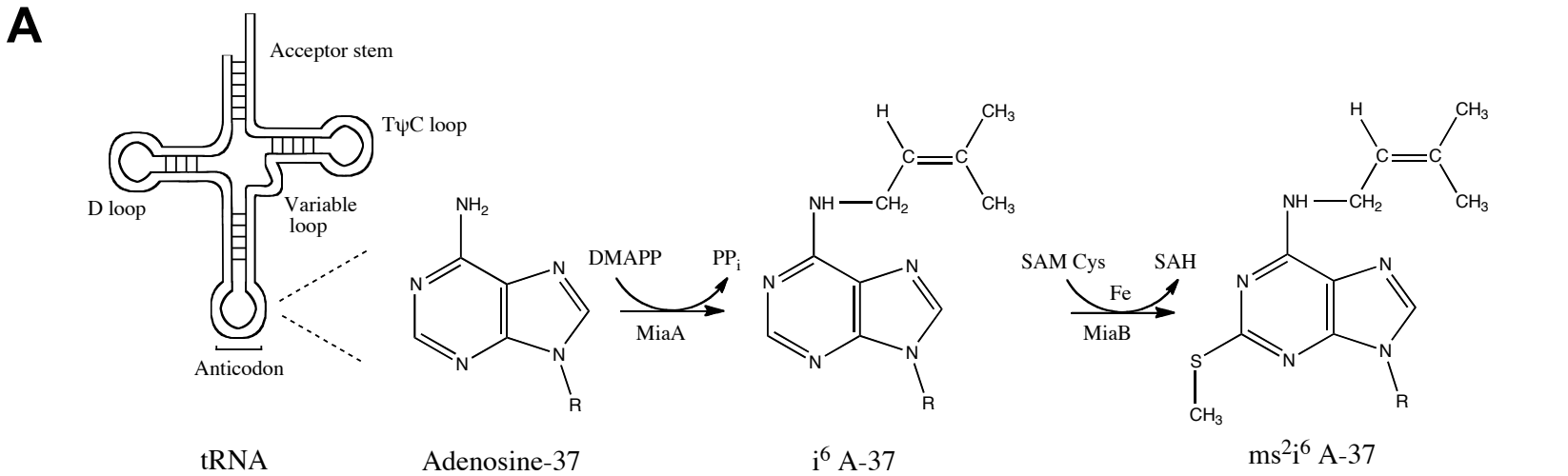
A
Acceptor stem
TψC loop
D loop
Variable loop
Anticodon
DMAPP
PPi
MiaA
SAM Cys
SAH
Fe
MiaB
tRNA
Adenosine-37
i6 A-37
ms2i6 A-37

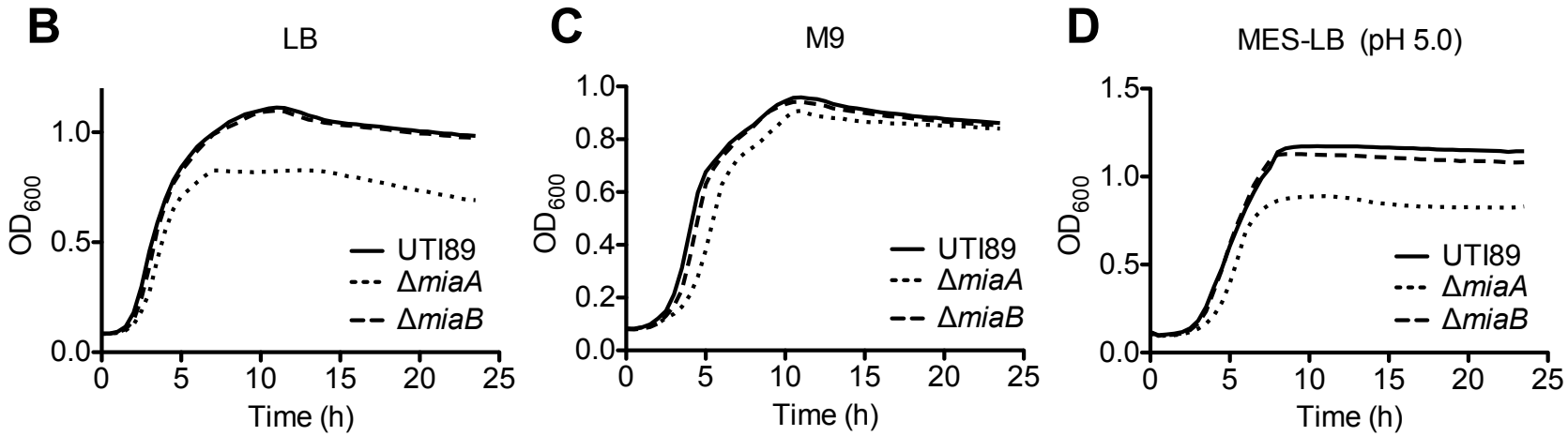
B
LB
C
M9
D
MES-LB (pH 5.0)
OD600
Time (h)
UTI89
ΔmiaA
ΔmiaB

Figure 6.1 Continued

(A) Model of MiaA and MiaB action modified from Leung et al. (32). (B- D) Growth of *miaA* and *miaB* knockouts in LB broth, M9 minimal media, and LB-MES (pH 5.0) broth. Graphs in B-D show representative data of the mean of 4 replicates from at least 3 independent experiments. Error bars were negligible and omitted for clarity. (E) Metabolomics of common bacterial metabolites as determined by GC/MS. Bar graph shows list of significantly altered metabolites in UTI89Δ*miaA* compared to UTI89 with a list of unchanged metabolites to the right of the figure. Data are presented as the mean of six independent replicates ±SD, with $P < 0.05$ as calculated by Student's *t* test.

E

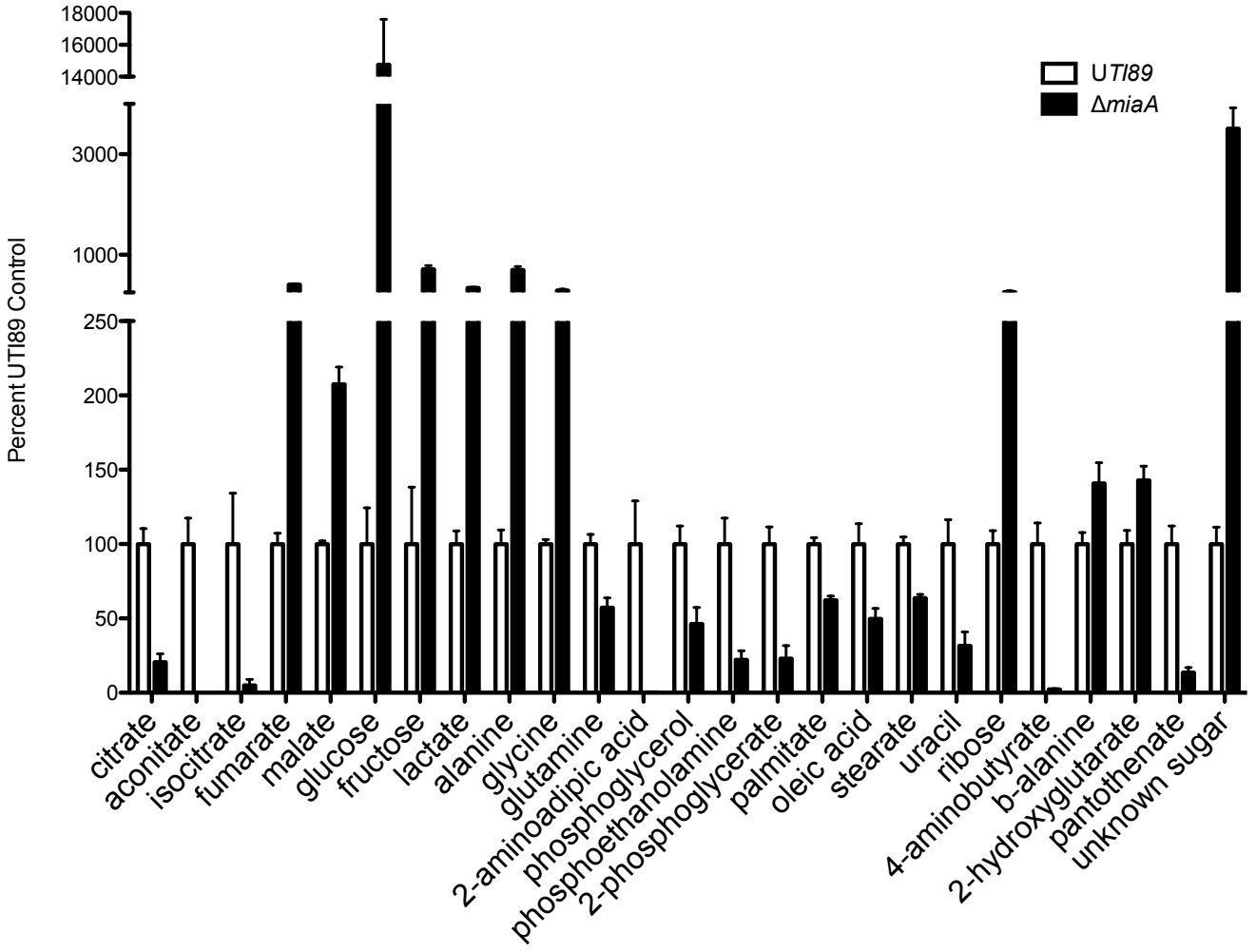

Unchanged
- aspartate
- cytosine
- diphosphate
- glucose-6-phosphate
- glucose-1-phosphate
- glutamate
- inositol
- isoleucine
- lysine
- leucine
- palmitiladic acid
- phenylalanine
- proline
- tryptophan
- tyrosine
- serine
- succinate
- threonine
- valine
- 4-methyl-2-isovaleric acid

MiaB have relatively high conservation levels across species, and the enzymes appear to function similarly in all tested microorganisms (32).

MiaA consists of two domains, a large core domain and a small helix insertion domain, separated by a large basic fissure (43). The anticodon of the tRNA binds to the basic rift of MiaA, causing a rearrangement in the tRNA anticodon loop structure, juxtapositioning the A-37 residue for modification (31). Mutations in the *miaA* locus result in inefficient modification of the A-37 residue, leading to hypomodified tRNAs having altered A-site ribosomal interactions and increased peptidyl-tRNA slippage (47). In K-12 *E. coli* strains, disruption of MiaA-dependent translational regulation appears to influence tryptophan operon attenuation, aerobiosis, phenylalanine utilization, and spectinomycin resistance (37). Furthermore, *miaA* mutants show increased spontaneous mutagenesis, a process, which is mimicked by iron limitation (13). In addition, expression of *miaA* is increased in response to the mismatch mutagen 2-aminopurine, consistent with a role for MiaA in preventing DNA mutagenesis and contributing to stress response (12). It has thus been hypothesized that regulation of *miaA* expression may be modulated in response to environmental stress to increase spontaneous mutation frequency, allowing for adaptation to hostile environments through increased protein diversity and flexibility (12).

Iron limitation results in tRNA undermodification by interfering with the conversion of i^6A-37 to ms^2i^6A-37 (13). This process, the methylthiolation of A-37, is catalyzed by MiaB, which has received little attention relative to MiaA. MiaB acts as a monomer containing a [4Fe-4S] cluster under reducing conditions, with

[2Fe-2S] and [3Fe-4S] clusters present in anaerobic conditions (39, 40). The [4Fe-4S] cluster is bound by a cysteine from a CxxxCxxC motif contained in a radical S-adenosylmethionine (SAM) fold (39). A reducing equivalent from the [4Fe-4S]+ is then used to cleave SAM for the catalytic step of the methylthiolation of A-37. MiaB-like enzymes are widespread across phyla, and include bacterial proteins like Rim-O that function in the methylthiolation of the ribosomal S12 protein, CDKAL1 proteins found in eukaryotes and some archaebacteria, and mammalian CDK5 subunits (27, 41). The breadth of mechanistic data on MiaA/B indicates conserved function across species of bacteria; however, there are potentially altered consequences downstream of the A-37 modification, which remain unexplored.

MiaA is known to govern expression of virulence determinants and stress response cascades in a variety of pathogens. In *Salmonella enterica* serotype Typhimurium, *miaA* mutants are defective at growth under oxidative stress and high temperature (42ºC)(7). In the plant pathogen *Agrobacterium tumefaciens*, mutants lacking *miaA* express decreased levels of the *vir* regulon, resulting in decreased virulence upon infection of red potato plants (22). MiaA also regulates virulence in *Shigella flexneri* by altering the translational efficiency of multiple genes, including the VirF transcriptional regulator (18, 19). Altered VirF expression leads to dysfunctional virulence in the form of decreased contact-dependent hemolytic activity and delayed responses in focus plaque assays (18). The regulation of virulence-associated genes in multiple bacterial species suggests a conserved role for MiaA in the control of bacterial pathogenesis.

In this study, we test the role of MiaA and MiaB in the modulation of virulence and stress responses in uropathogenic *Escherichia coli* (UPEC). UPEC are the primary causative agents of urinary tract infections (UTIs), including both cystitis (bladder infection) and pyelonephritis (kidney infection) (21). During the course of infection, UPEC face many challenges, including colonization and survival in multiple host niches and stress conditions. Initially, UPEC traverse the urethra to gain access to the bladder lumen, where they can replicate in the urine. A fraction of the population then takes up residence within host bladder epithelial cells (35). Invasion of the host epithelium occurs via a zipper-like endocytic mechanism, resulting in delivery of UPEC into host late endosome-like compartments (20). Once internalized, UPEC may form quiescent intracellular reservoir populations thought to contribute to long-term bacterial persistence within the host (6, 20, 35). Alternatively, UPEC can exit the vacuole and replicate freely in the cytosol in association with host cytokeratin, forming intracellular bacterial communities (IBCs)(20). IBCs are large inclusions of bacteria that appear to act as dispersal sites for UPEC to re-infect the bladder lumen. UPEC face multiple stresses during this lifecycle. Some commonly encountered stresses include nutrient deprivation, redox stress in the form of oxygen and nitrogen radicals generated by cells, extreme pH, membrane stresses such as high salt concentrations, as well as many host immune effector cells and antimicrobial compounds (2, 3, 24, 26). Additionally, UPEC must be able to transition from sessile to motile forms, and vice versa, during the infectious process. Proper regulation of stress response pathways and sessile-to-motile

transitions is required for maximal virulence. Our knowledge of the UPEC life cycle offers a novel dimension in which to probe tRNA modification as it pertains to unique aspects of host-pathogen interactions during UTI. In this study, we show that varying levels of expression of MiaA, but not MiaB, can greatly impact multiple stress response pathways and virulence-related phenotypes in UPEC.

Results

Growth and metabolomics of UTI89Δ*miaA* and UTI89Δ*miaB*

Knockouts of the *miaA* and *miaB* genes were generated in the reference UPEC cystitis isolate UTI89 using the lambda Red-recombination system (14). The knockout strains were tested for growth defects in modified M9 minimal media, Luria Bertani (LB) broth, and low pH morpholineethanesulfonic acid (MES)-buffered LB broth (LB-MES; pH 5.0) (Fig 6.1B-D). UTI89Δ*miaA* grew similar to wild type in modified M9 minimal media but showed slight defects in LB-MES and LB broth, as previously noted with a K-12 *E. coli* strain (51), In contrast, the *miaB* mutant showed no overt growth defects in these media. It is known that *miaA* deletion can result in altered amino acid biosynthesis (4). Thus, we used gas chromatography/ mass spectroscopy to determine the levels of 47 common bacterial metabolites in UTI89Δ*miaA* during late exponential/stationary phase growth in M9 minimal media. This experiment uncovered broad scale metabolic changes, with significant differences in 27 of 47 metabolites despite normal growth of the mutant in this medium (Fig 6.1E). In this analysis, the changes in the mutant could not be attributed to one pathway, but rather

suggested vastly different metabolism in the knockout, consistent with known manipulation of metabolic pathways by MiaA (5).

UTI89Δ*miaA* exhibits growth defects in response to stressors

The knockout strains were tested with exogenous stressors in growth assays. Challenge of UTI89Δ*miaA* and UTI89Δ*miaB* with the divalent cation chelator EDTA (1 mM) or the iron chelator desferal (10 mM) both caused no change in growth compared to wild type (Fig. 6.2A-B). This result is consistent with known up-regulation of MiaA by the addition of exogenous iron (12). The UTI89Δ*miaA* strain grew poorly in a high salt medium (exogenous addition of 5% NaCl to standard LB broth) indicative of increased membrane stress (Fig. 6.2C). Challenge with the nitrosative stressor, acidified sodium nitrite (ASN), at 1 and 2 mM resulted in significant growth defects for UTI89Δ*miaA,* but not UTI89Δ*miaB* (Fig. 6.2D-E). Further, growth in the presence of an oxidative stressor methyl viologen (MV), in both LB broth and modified M9 media, inhibited growth of UTI89Δ*miaA,* but not the *miaB* mutant (Fig. 6.2D-I). Complementation of UTI89Δ*miaA* with a plasmid containing *miaA* driven by its native promoter restored wild type level growth of the mutant in 1 mM MV (Fig. 6.2J). Interestingly, high-level expression of MiaA from an IPTG-inducible P*tac* promoter hindered growth of UTI89Δ*miaA* in the presence of MV, while leaky or low-level expression of MiaA rescued growth of the *miaA* mutant (Fig. 6.2K). These results indicate that too much MiaA can be even more detrimental to bacterial fitness than the complete absence of the enzyme. MiaB was not

Figure 6.2 UTI89Δ*miaA* grows poorly under stress conditions in a dose-dependent manner

(A) Growth of UTI89Δ*miaA* and UTI89Δ*miaB* in LB with 1 mM EDTA, (B) 10 mM desferal, or (C) 5% NaCl. (D-E) Growth curve analysis of UTI89Δ*miaA* in LB with 1 and 2 mM acidified sodium nitrite. (F) Growth analysis of knockouts in LB with 1 mM MV stress. Graphs in A-K show representative data consisting of four replicates from one of at least three independent experiments. Error bars were negligible and thus omitted.

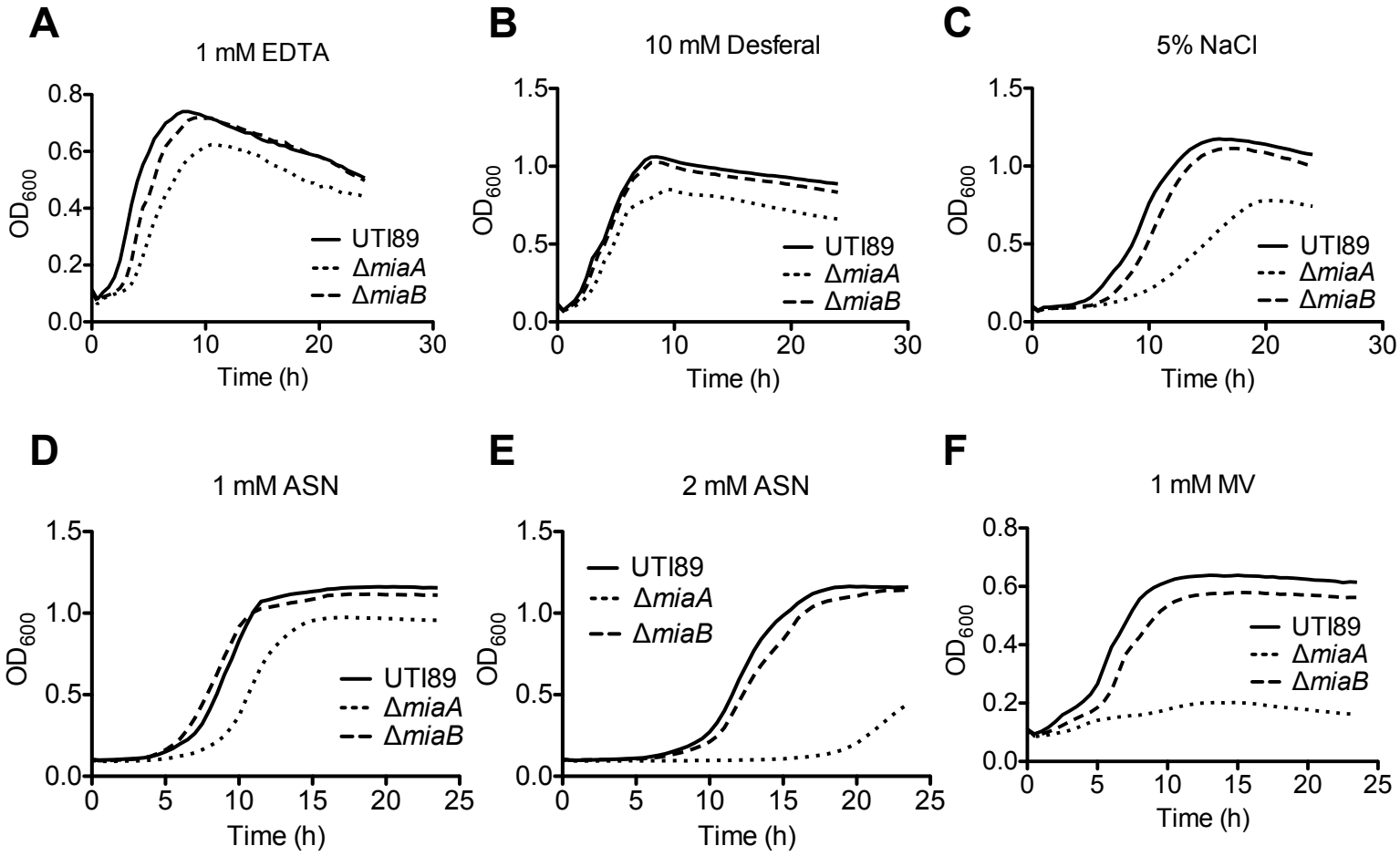
A
1 mM EDTA
B
10 mM Desferal
C
5% NaCl
D
1 mM ASN
E
2 mM ASN
F
1 mM MV
OD600
Time (h)
UTI89
ΔmiaA
ΔmiaB

Figure 6.2 Continued

(G-I) Growth curve analysis of UTI89Δ*miaA* and UTI89Δ*miaB* in modified M9 minimal media with 0.1, 0.2, and 0.3 mM MV. (J) Complementation of UTI89Δ*miaA* growth defects in 1 mM MV using a plasmid (pMiaA2) containing MiaA driven by its native promoter (nMiaA). (K) Growth curve analysis of UTI89 and UTI89Δ*miaA* with an empty vector (pRR48) or plasmid containing *miaA* driven by an IPTG inducible promoter. IPTG was added at 10-fold dilutions from 0 to 1000 μM. Graphs in A-K show representative data consisting of four replicates from one of at least three independent experiments. Error bars were negligible and thus omitted.

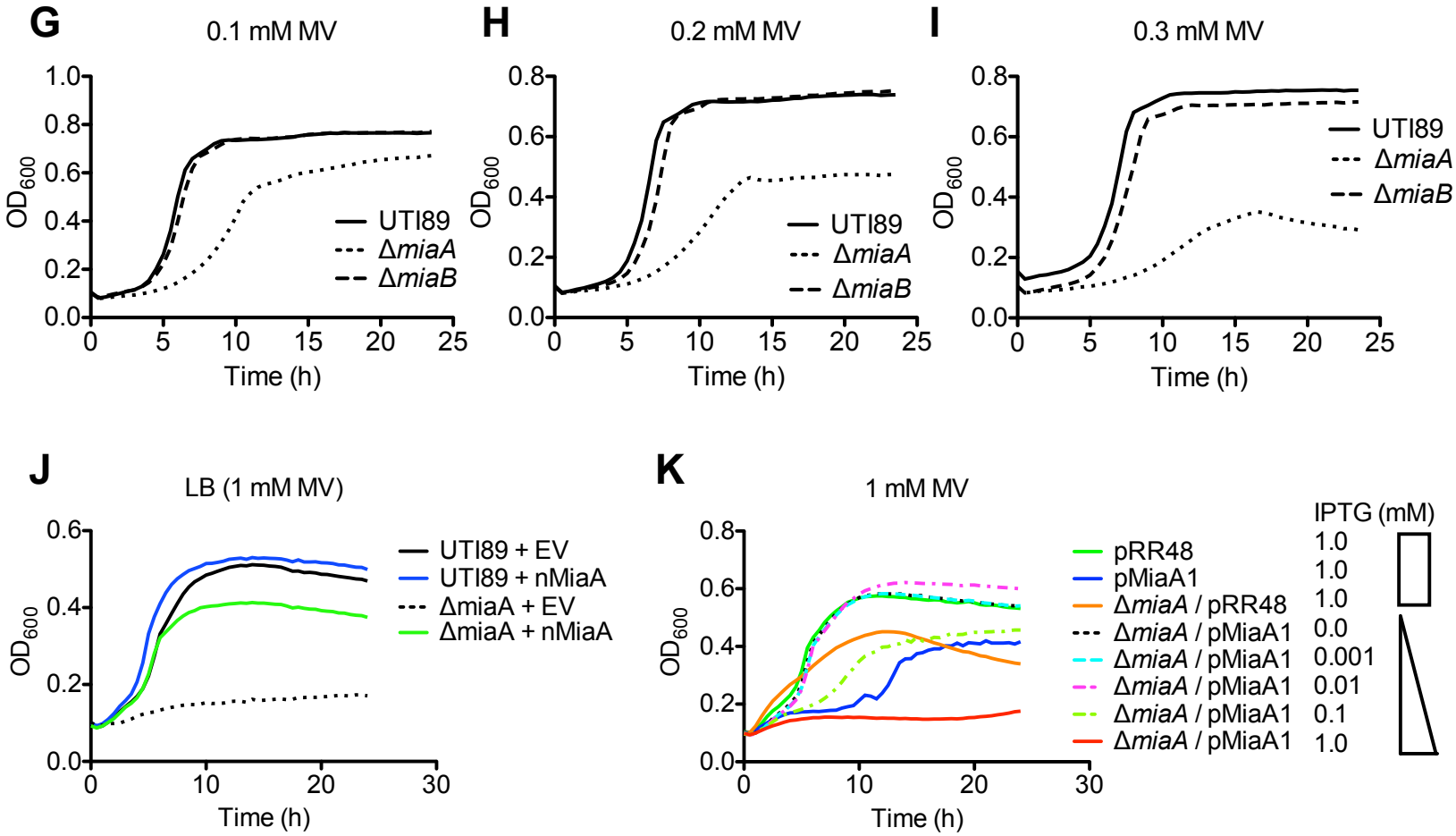
G
0.1 mM MV
H
0.2 mM MV
I
0.3 mM MV
OD600
Time (h)
UTI89
ΔmiaA
ΔmiaB
J
LB (1 mM MV)
UTI89 + EV
UTI89 + nMiaA
ΔmiaA + EV
ΔmiaA + nMiaA
K
1 mM MV
pRR48
pMiaA1
ΔmiaA / pRR48
ΔmiaA / pMiaA1
IPTG (mM)
1.0
1.0
1.0
0.0
0.001
0.01
0.1
1.0

required for growth under oxidative stress and does not appear to be required for stress response in these assays.

MiaA expression is altered in response to stress

Growth assays indicated a role for MiaA in stress response to multiple stressors, leading us to question if MiaA levels are altered in response to stressful stimuli. UTI89Δ*miaA* carrying a plasmid containing a C-terminal flag-tagged MiaA (pMB5_MiaA-Flag; Table 6.1) under control of the native *miaA* promoter was assayed for MiaA expression following the addition of 1 mM MV to

Table 6.1 Bacterial strains and plasmid

Strain or Plasmid	**Description**	**Source or Reference**
Strains		
E. coli		
UTI89	UPEC reference strain and cystitis isolate	(10, 35)
Recombinant Strains		
UTI89Δ*miaA*	UTI89 containing a chromosomal deletion of *miaA*	This work
UTI89Δ*miaB*	UTI89 containing a chromosomal deletion of *miaB*	This work
pKD3/4	Plasmids containing chloramphenicol (3) or kanamycin (4) resistance cassettes for use in lambda-Red recombination	(14)
Plasmids		
pRR48	IPTG inducible overexpression of protein coding sequence Ap^r	(30)
pMiaA1	IPTG inducible overexpression of MiaA Ap^r	This work
pMiaB1	IPTG inducible overexpression of MiaB Ap^r	This work
pACYC184	Low copy cloning vector Tet^r Clm^r	NEB
pMiaA2	pACYC184 containing MiaA and surrounding 200 nt	This work
pMB5_MiaA-Flag	pACYC184 containing C-Terminal Flag-tagged MiaA Tet^r	Submitted

bacterial cultures after reaching mid-log growth (OD600 = ~0.5). Within 60 min after addition of LB broth alone (100 µl into 5 ml cultures), levels of MiaA were notably elevated in the control samples as determined by Western blot analysis using anti-Flag (M2) antibody (Fig. 6.3A). This spike in MiaA expression was not observed following addition of MV, and MiaA levels remained depressed relative to the negative control up to the 90 min time point. MiaA levels varied less noticeably in UTI89 stationary phase cultures following challenge with MV (Data not shown). Desferal had no effect on MiaA levels, while the addition of high salt (5% NaCl) to mid-log cultures repressed expression of MiaA, similar to MV (Fig. 6.3B). In contrast, EDTA elicited a substantial boost in MiaA levels. Interestingly, growth of UTI89 in MES-LB broth (pH 5.0) led to the appearance of slightly larger MiaA species that may represent modified forms of MiaA or products of read-through errors beyond the artificial stop codon following the Flag-epitope tag sequence.

Regulation of biofilm development and motility by MiaA

The effects of MiaA expression on bacterial behavior were tested using several assays, including *in vitro* biofilm formation and motility assays. Microtiter plate-based biofilm assays performed in modified M9 minimal media at 30°C indicated significant defects for both UTI89Δ*miaA* and Δ*miaB* compared to the wild type strain (Fig. 6.4A). UTI89Δ*miaA* was also defective at biofilm formation at 37°C (Data not shown). As seen with growth assays in the presence of MV (Fig. 6.2K), low-level expression of recombinant MiaA rescued the ability of

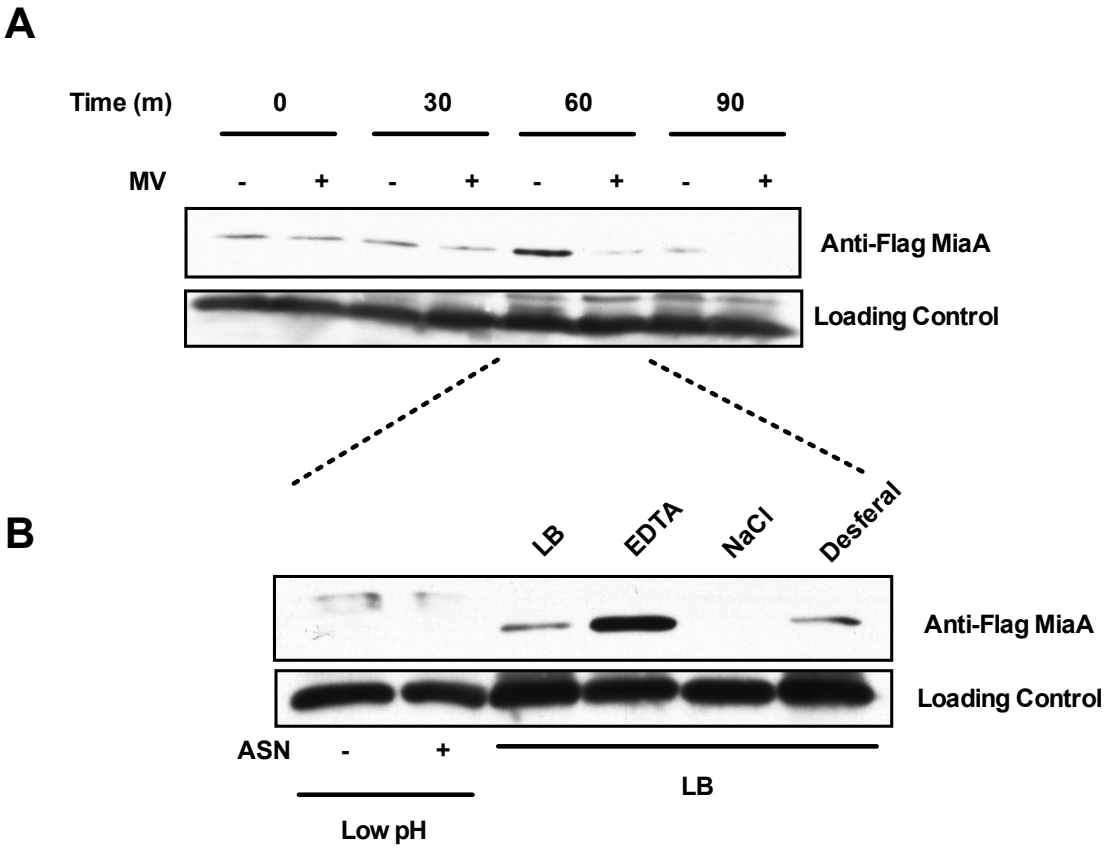

Figure 6.3 MiaA protein level responds to stressors

(A) Overnight grown bacteria were subcultured into fresh media and incubated for 2.5 h before addition of 1 mM MV resuspended in LB broth. LB broth alone (volume??) was used as a negative (-) control. Western blot analysis was performed using anti-Flag M2 antibody to MiaA-Flag at time points after stress addition. (B) Western blot analysis of 60 m time point as described above, after stressor addition with 1 mM ASN, 1 mM EDTA, 5% NaCl, and 10 mM desferal or control media. Loading controls for A-B are non-specific bands using a bacterial alkaline phosphatase antibody. Data are representative data from at least 3 independent experiments. It is important to note that growth of these strains was not affected by the stressors in these assays.

Figure 6.4 MiaA/B differentially regulate UPEC motility and biofilm formation

(A-C) *In vitro* biofilm formation assays in plastic dishes were measured using crystal violet as described in the methods. (A) Biofilm growth of mutants without complementation. (B-C) The strains utilized contain empty vector or IPTG-inducible overexpression of MiaA/B. Data is the combination of at least 3 separate experiments in quadruplicate (D-E) A time course of movement on swim motility plates (0.2% agar). Graph is from three independent experiments done in triplicate. Error bars are standard error of the mean with *= $P < 0.05$ (F-G) Swarm motility of UTI89Δ*miaA* with complementation or overexpression. In F UTI89 and UTI89Δ*miaA* contain an empty vector (pACYC184) or a plasmid containing MiaA driven by its native promoter (pMiaA2) for complementation. Panel G shows UTI89 and UTI89Δ*miaA* with an empty vector (pRR48) or a plasmid containing IPTG inducible MiaA (pMiaA1) for overexpression. F-G photos are of representative data from one of three independent experiments.

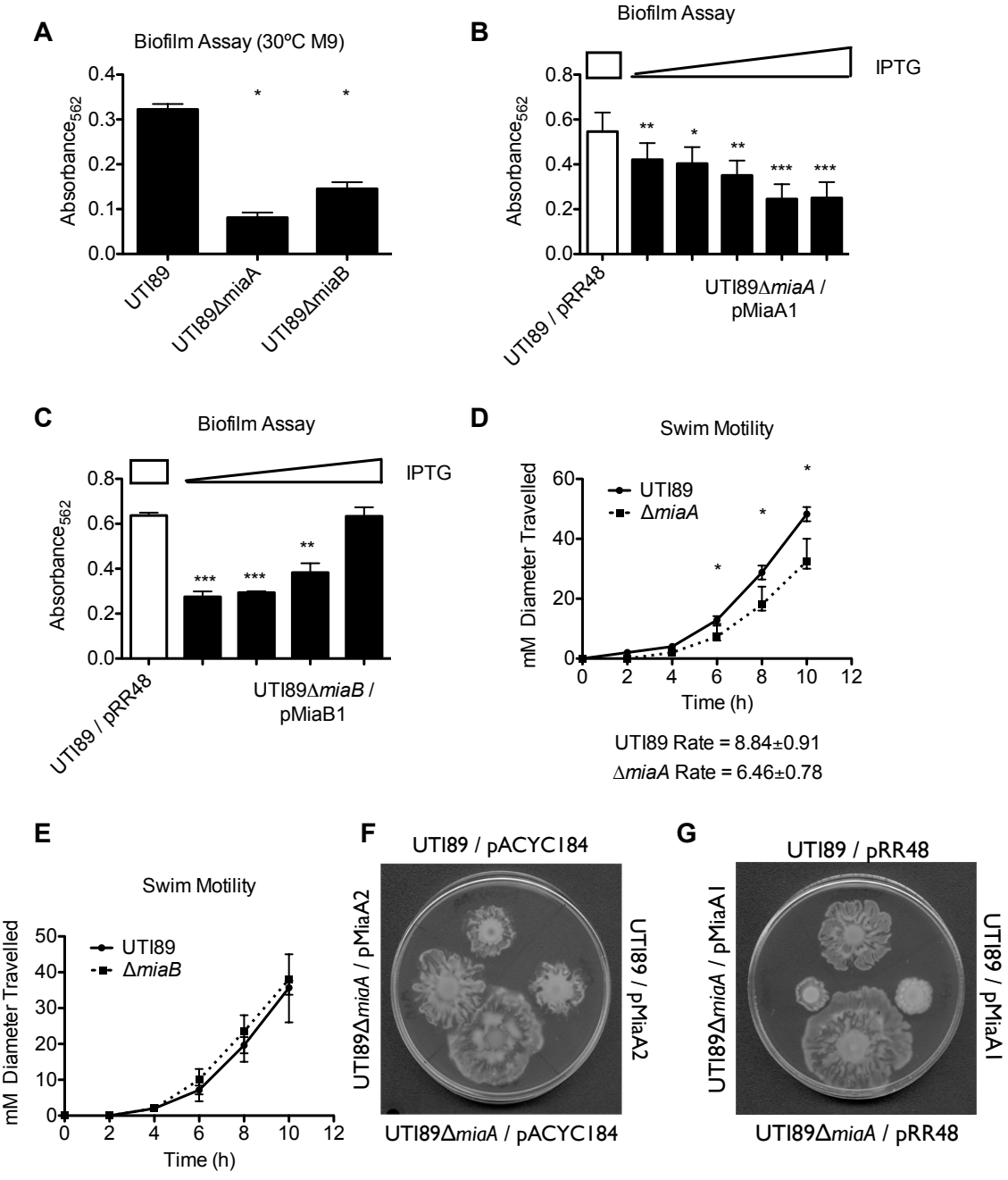
A
Biofilm Assay (30ºC M9)
Absorbance562
UTI89
UTI89ΔmiaA
UTI89ΔmiaB
B
Biofilm Assay
IPTG
Absorbance562
UTI89 / pRR48
UTI89ΔmiaA / pMiaA1
C
Biofilm Assay
IPTG
Absorbance562
UTI89 / pRR48
UTI89ΔmiaB / pMiaB1
D
Swim Motility
UTI89
ΔmiaA
mM Diameter Travelled
Time (h)
UTI89 Rate = 8.84±0.91
ΔmiaA Rate = 6.46±0.78
E
Swim Motility
UTI89
ΔmiaB
mM Diameter Travelled
Time (h)
F
UTI89 / pACYC184
UTI89ΔmiaA / pMiaA2
UTI89 / pMiaA2
UTI89ΔmiaA / pACYC184
G
UTI89 / pRR48
UTI89ΔmiaA / pMiaA1
UTI89 / pMiaA1
UTI89ΔmiaA / pRR48

UTI89ΔmiaA to form biofilms, whereas high-level induction of MiaA was inhibitory (Fig. 6.4B). Importantly, the biofilm defect observed with a UTI89Δ*miaA* was not rescued by complementation with Hfq, an RNA chaperone that is encoded downstream of *miaA* on the UTI89 chromosome, further confirming that the observed phenotypes are specifically attributable to disruption of the *miaA* gene (Data not shown). The biofilm defect associated with the miaB mutant was rescued by complementation using a plasmid encoding IPTG-inducible *miaB*, but unlike MiaA, higher levels of MiaB expression correlated with improved biofilm formation (Fig. 6.4C).

The ability of bacteria to move within their environment is key to their survival within the host. Motility assays were performed *in vitro* to explore the regulation of bacterial movement by MiaA expression. Swim motility plates are used to determine the ability of bacteria to move through agar, whereas swarm motility plates test the ability of the bacteria to undergo a differentiation process before moving in a social manner on the surface of a slightly higher concentration agar. In swim plates, the motility of UTI89Δ*miaA* was significantly delayed relative to the wild type strain, whereas no defect was observed with UTI89Δ*miaB* (Fig. 6.4D and E). On swarm plates, UTI89Δ*miaA* displayed drastically increased motility compared with wild type UTI89 (Fig. 6.4F and G). Expression of MiaA off its native promoter from a low-copy number plasmid (pMiaA2 constructed using pACYC184) reduced the swarming of UTI89Δ*miaA* to near-wild type levels (Fig. 6.4F). In contrast, high-level expression of MiaA from

an IPTG-inducible promoter almost completely inhibited swarming by both the wild type and *miaA* mutant strains (Fig. 6.4G).

MiaA promotes bacterial colonization of the bladder

In cell culture-based assays UTI89Δ*miaA* and UTI89Δ*miaB* were able to bind, invade, and survive within host cells normally (Fig 6.S1). The ability of these mutants to colonize bladder cells *in vivo* was assessed using a well-established mouse UTI model system (6, 30). Mutant and wild type strains were inoculated via transurethral catheterization into adult female CBA/J mice, and bacterial titers present in the bladders were determined 3 d later. In these non-competitive assays, the *miaB* mutant showed no obvious defect relative to wild type UTI89 (Fig.6.5A), while the *miaA* mutant was significantly attenuated (Fig. 6.5B). Defects in bladder colonization by UTI89Δ*miaA* where apparent by 6 h postinoculation (Fig. 6.5C), although this mutant was still able to form similar numbers of IBCs as the wild type strain (data not shown). At 9 d post-inoculation, UTI89Δ*miaA* still had significantly decreased titers compared to wild type (Fig. 6.5D), suggesting that UTI89 required *miaA* to effectively establish and/or maintain longer-lived intracellular reservoirs. To address this further, infected mice were treated with the cell-impermeable antibiotic gentamicin on days 4, 5, and 6 postinoculation in order to eliminate any extracellular bacteria residing in the lumen of the bladder. After a 3 d recovery period (day 9 post-inoculation), mice were sacrificed and the number of bacteria present within the bladder tissue enumerated. This experimental setup enables quantification of

Figure 6.5 MiaA promotes UPEC infection of a murine host

(A-E) Mice were infected with 10^7 CFU of UTI89Δ*miaA* or Δ*miaB*. Mice were sacrificed at 6 h, 3 d, or 9 d postinfection as indicated and bladders titers were enumerated. (E) Reservoir assays were performed as described in the materials and methods with mice sacrificed at 9 d. Each panel in A-E is 11 mice from two separate independent experiments. *P* values were determined by Mann Whitney U test with *= $P < 0.05$. (F) Antibiotic persistence assays were performed by subculturing overnight bacterial cultures into fresh media containing antibiotic for 6 hours followed by titering of bacterial levels. Each antibiotic challenge compares UTI89Δ*miaA* and UTI89Δ*miaB* to the wild type UTI89 strain. Data are the combination of 3 separate experiments with SEM. *= $P < 0.05$.

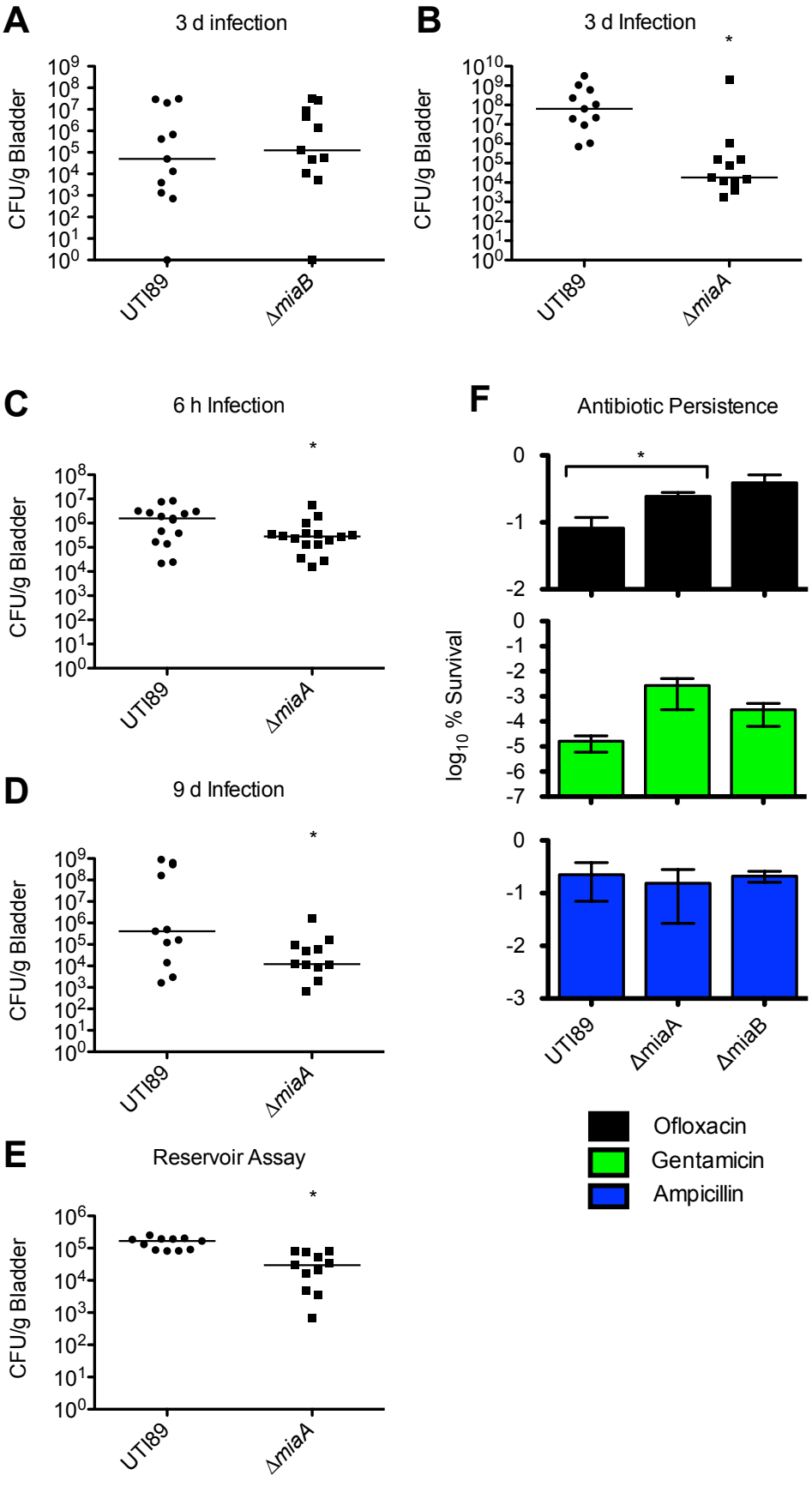
A
3 d infection
CFU/g Bladder
UTI89
ΔmiaB
B
3 d Infection
CFU/g Bladder
UTI89
ΔmiaA
C
6 h Infection
CFU/g Bladder
UTI89
ΔmiaA
D
9 d Infection
CFU/g Bladder
UTI89
ΔmiaA
E
Reservoir Assay
CFU/g Bladder
UTI89
ΔmiaA
F
Antibiotic Persistence
log10 % Survival
UTI89
ΔmiaA
ΔmiaB
Ofloxacin
Gentamicin
Ampicillin

bacterial populations (or reservoirs) that are, or were, contained within intracellular niches within the bladder urothelium during the gentamicin treatments (6). In these assays, UTI89Δ*miaA* was recovered significantly less frequently than the wild type strain (Fig. 6.5E), reflecting the overall decreased abundance of the *miaA* mutant at the 9 d time point (Fig. 6.5D).

miaA promotes persistence during antibiotic challenge

E. coli and other bacteria are often able to develop dormant, stress- and antibiotic-resistant cells known as persisters, which may facilitate bacterial survival within hostile host environments such as the bladder (29). One way to assess persister cell development is to challenge bacteria with the effects of *miaA* and *miaB* on persister cell development by UTI89 were assessed using standard assays (28). Wild type and mutant bacteria were grown to stationary phase, diluted 1:10 into fresh media ± ampicillin (20 μg/mL), ofloxacin (10 μg/mL), or gentamicin (10 μg/ml), and incubated at 37°C for 6 h prior to plating. In these assays a ~7 fold increase in survival of UTI89Δ*miaA* after treatment with the DNA gyrase inhibitor ofloxacin was observed (Fig 6.5F), but no significant effects were seen with the other two antibiotics tested. UTI89Δ*miaB* was not significantly different from wild type UTI89 in any case. The aminoglycoside gentamicin killed most of the bacteria, regardless of *miaA* presence, making it unlikely that antibiotic-resistant persisters account for the bacterial populations that remain in the bladder following *in vivo* gentamicin treatments (see Fig. 6.5E).

The α-hemolysin toxin is not expressed in a *miaA* knockout

During growth on blood agar plates, we noticed that UTI89Δ*miaA* fails to lyse red blood cells like the wild type strain. Complementation of UTI89Δ*miaA* with a plasmid encoding *miaA* driven by its native promoter restored hemolytic activity to wild type levels (Fig. 6.6A, top panels and data not shown). These observations are consistent with literature showing that *Shigella flexneri* contact-dependent hemolytic activity is decreased when *miaA* is deleted, a phenomenon that was linked to decreased expression of the master virulence regulator VirF in this pathogen (18). The hemolytic activity of UTI89 is attributable to an unrelated exotoxin, α-hemoylsin (HlyA). This toxin is not necessary for UTI89 to colonize and persist within the murine urinary tract, but it does enhance the ability of UPEC strains to damage host tissues and immune effector cells ((16, 33, 48, 49) and data not shown). By western blot, we found that UTI89Δ*miaA* does not express HlyA (Fig. 6.6A, bottom panels). However, qRT-PCR indicated that deletion of *miaA* results in significantly increased levels of *hlyA* transcript (Fig 6.6B). This correlated with enhanced transcript levels of *hlyD*, a gene within the *hly* operon that encodes a translocator for the HlyA toxin (42). MiaA therefore promotes the expression of HlyA via a posttranscriptional mechanism. A possible reason for the lack of HlyA expression is that frameshift errors accumulated during the translation in the absence of *miaA* may preclude efficient production of large proteins like HlyA (1025 amino acids). However, this is unlikely, as another protein of identical length (β-galactosidase, encoded by *lacZ*) is expressed at wild type levels by UTI89Δ*miaA*, as determined by growth on MacConkey agar plates

Figure 6.6 MiaA contributes to α-hemolysin formation, possibly through manipulation of host chaperone production

(A) Hemolytic activity of UTI89 and UTI89Δ*miaA* on blood agar plates and visualized by Western blot using an anti-α-hemolysin antibody courtesy of Rod Welch. Representative image from one of at least three independent experiments. (B) qRT-PCR analysis of levels of HlyA and HlyD, (C) bacterial chaperones, (D) proteases, and (E) sigma factors. Expression was normalized to the housekeeping sigma factor RpoD. Experiments are combinations of data from three independent RNA preparations, each with two technical repeats in duplicate. (F) Expression of periplasmic chaperone activity using a CpxP-GFP reporter for the CpxP periplasmic stress response protein. Experimen F is data collected from three independent experiments in triplicate. Graphs B-E show SEM with *= $P < 0.05$.

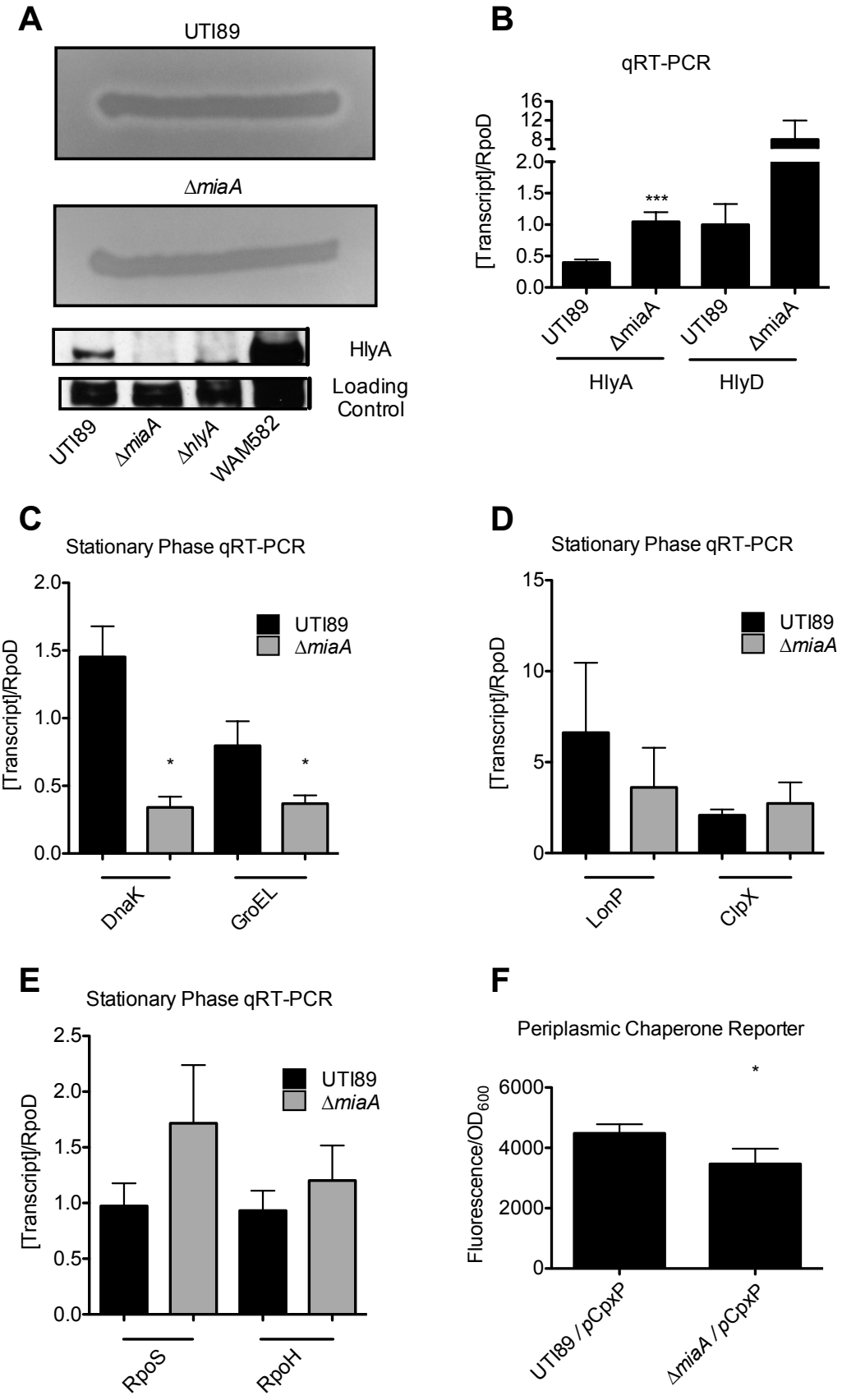
A
UTI89
ΔmiaA
HlyA
Loading Control
UTI89
ΔmiaA
ΔhlyA
WAM582
B
qRT-PCR
[Transcript]/RpoD
16
12
8
2.0
1.5
1.0
0.5
0.0
***
UTI89
ΔmiaA
UTI89
ΔmiaA
HlyA
HlyD
C
Stationary Phase qRT-PCR
[Transcript]/RpoD
2.0
1.5
1.0
0.5
0.0
UTI89
ΔmiaA
*
*
DnaK
GroEL
D
Stationary Phase qRT-PCR
[Transcript]/RpoD
15
10
5
0
UTI89
ΔmiaA
LonP
ClpX
E
Stationary Phase qRT-PCR
[Transcript]/RpoD
2.5
2.0
1.5
1.0
0.5
0.0
UTI89
ΔmiaA
RpoS
RpoH
F
Periplasmic Chaperone Reporter
Fluorescence/OD600
6000
4000
2000
0
*
UTI89 / pCpxP
ΔmiaA / pCpxP

(data not shown). Of note, the *lacZ* and *hlyA* protein coding sequences contain similar fractions of both rare codons and codons recognized by tRNAs that are modified by MiaA. UTI89Δ*miaB* showed no defects in hemolytic activity or lactose fermentation, suggesting that loss of HlyA expression in the miaA mutant is due to decreased prenylation of A-37 and not downstream modifications.

MiaA mutants show altered chaperone and protease levels

The ablation of HlyA expression and the overall decreased fitness of UTI89Δ*miaA* suggested that this mutant might have multiple defects in basic housekeeping processes, including perhaps general protein chaperone and protease activities. In support of this possibility, we found by qRT-PCR that expression of the cytosolic chaperone GroEL and DnaK were substantially downregulated in the miaA mutant (Fig. 6.6C). No significant changes were observed with expression of genes encoding the proteases Lon or ClpX (Fig. 6.6D). Likewise, expression of the stress response sigma factors RpoS and RpoH were similar in wild type and miaA mutant bacteria (Fig. 6.6E). However, activation of the Cpx envelope stress response system, as determined by use of a CpxP-GFP promoter fusion, was modestly, though significantly reduced in the *miaA* mutant (Fig. 6.6F). CpxP acts as a periplasmic chaperone as well as a negative regulator of the Cpx two-component system, regulating the expression of additional periplasmic chaperones and nearly 100 other proteins (50). MiaA therefore affects the expression of at least three key chaperones within UTI89, meaning that it has a much greater role as a posttranscriptional regulator of

protein expression and functionality beyond its direct effects on tRNA modification.

Discussion

Classically, the modification of tRNA residues was thought to be required strictly for correct incorporation of amino acids into growing polypeptide chains. Recent studies suggest that in addition to optimization of translation, tRNA modification is a dynamic process that can be used to modulate cellular physiology, stress responses, and virulence (9). MiaA and MiaB both add modifications to A-37, adjacent to the anticodon within UNN-encoding tRNA molecules found in *E. coli* and many other bacteria (27, 38). The MiaA tRNA prenyltransferase adds a prenyl group onto the UNN subset of tRNA, which promotes reading frame maintenance and translational fidelity. MiaB then methylthiolates A-37 to its final form, completing the modification of A-37. Regulation of tRNA modification reactions has been posited as a means to quickly adjust large-scale bacterial responses to stimuli. In particular, previous literature has suggested a role for m*iaA* expression in fine-tuning cellular adaptation under stressful conditions through regulation of protein diversity (12). In this model, increased expression of MiaA would promote translational fidelity while limiting protein diversity (stringent regulation of correct amino acid incorporation). In contrast, decreased expression of *miaA* would reduce translational fidelity and frameshifting, allowing for more error-prone translation and subsequent diversification of expressed proteins in stressful environments.

We sought to define the functional relevance of MiaA to the stress resistance and virulence capacity of UPEC, making comparisons with MiaB when appropriate.

In vitro growth assays indicated that both MiaA and MiaB were dispensable to the ability of UPEC to replicate within modified M9 minimal media and LB broth. However, deletion of *miaA*, but not *miaB*, greatly reduced bacterial fitness when challenged with oxidative, nitrosative, and high salt stresses. These data demonstrate distinct functions for the two different modifications of A-37 mediated by MiaA and MiaB, with MiaA being much more critical to bacterial survival under stress. Interestingly, while low-level expression of MiaA restored the stress resistance of the *miaA* mutant, overexpression of MiaA was detrimental. The benefit of MiaA expression in stressful situations is therefore sensitive to dosage effects. This finding is consistent with the idea that tRNA modifications are not all-or-nothing events. Rather, shifts in the prevalence of specific modifications, such as A-37 prenylation mediated by MiaA, can help optimize bacterial responses to stress by affecting the fidelity of translation and ultimately the spectrum of available wild type and mutant proteins.

Dosage effects of MiaA expression seen in growth assays with UPEC under stress were also observed in biofilm and swarm motility assays. In contrast, the *miaB* mutant was found to be defective only in biofilm formation, and overexpression of MiaB was not detrimental. These results suggest that MiaA is required for optimal bacterial fitness under diverse conditions, while conditions that require MiaB are more limited. Combined, these data indicate that MiaA acts as a global stress response regulator that can significantly alter UPEC

behavior and stress resistance. Consistent with these results, expression of MiaA was shown to be differentially responsive to diverse stresses, including MV and high salt.

In line with its apparent role as a global stress response regulator, MiaA was found to also control expression of the pore-forming toxin HlyA. Deletion of *miaA* ablates translation of HlyA, even though *hlyA* transcripts are significantly elevated. Previous work has highlighted HlyA regulation by *leuX*-encoded $tRNA_5^{Leu}$ (17). This tRNA can be modified by MiaA, suggesting that the observed phenotypic defects associated with UTI89Δ*miaA* may be due to a lack of modified $tRNA_5^{leuX}$. However, it has been reported that deletion of *leuX* does not affect HlyA transcript levels, even though HlyA protein expression is reduced (17). Furthermore, a UPEC mutant lacking *leuX* is defective in its ability to bind and invade BECs and subsequently forms IBCs (23), whereas *miaA* is dispensable for all of these activities. These data suggest that *leuX* is not the only factor regulated by MiaA that can contribute to the phenotypic defects we observed with UTI89Δ*miaA.* For example, we found that deletion of miaA results in decreased expression of at least three key chaperone proteins and regulatory proteins - DnaK, GroEL, and CpxP. Modulation of these factors by MiaA can conceivably have global effects on the stress resistance and virulence potential of UPEC. Results from a small metabolomics screen lead to a similar conclusion, showing that MiaA expression can have profound effects on the spectrum of metabolites available to UPEC, which may in turn affect bacterial resistance to oxygen radicals and other stresses.

In a murine UTI model, UTI89Δ*miaA*, but not the *miaB* mutant, was significantly attenuated in its ability to colonize and persist within the bladder. These *in vivo* defects appear to include the reduced ability of UTI89Δ*miaA* to establish and maintain intracellular reservoirs within the bladder mucosa. During the course of a UTI, UPEC will encounter multiple stresses within the urinary tract (2, 24, 26). Motility and the ability to form biofilms are thought to aid bacterial survival within this harsh host environment (44). The effects of MiaA on these processes, as well as many others, likely explain why MiaA is necessary to the optimal survival of UPEC within the urinary tract. It is likely that rapidly changing conditions within the host necessitate altered levels of MiaA expression and subsequent tRNA modifications, as appears to be the case upon exposure of UPEC to stresses *in vitro*. How changes in MiaA levels influence the protein landscape and pathogen adaptability is not yet entirely clear and will require additional approaches like ribosomal profiling to discern in detail (25). In total, this work offers a compelling case study of how pathogens can integrate rudimentary metabolic genes to modulate and refine stress resistance and virulence-associated phenotypes.

Materials and Methods

Bacterial strains and plasmids

Strains used in this manuscript are described in Table 6.1. Mutant strains were constructed in the human cystitis isolate *Escherichia coli* strain UTI89 using the lambda Red recombination system and primers list in Table 6.2 as previously

Table 6.2 Oligonucleotides employed during the study

Primer Name[a]	Sequence (5'-3')[b, c, d]
MiaA-pRR48-F	CGCGCTGCAGATGAGTGATATCAGTAAGGCG
MiaA-pRR48-R	CGGCGGTACCTCAGCCTGCGATAGCACCAAC
MiaB-pRR48-F	CGCGCTGCAGATGACCAAAA AACTCCATAT TAAAACC
MiaB-pRR48-R	CGGCGGTACCGAATTACGGCTGATAATAAC
MiaA-Flag-pACYC184-F	CGGCGAATTCGGCTAAAAGTTTCTGGCGAAGAAAAATCGG
MiaA-Flag-pACYC184-R	CGCGGAATTC**CTATCCCTTATCGTCGTCATCCTTGTAGTCT GGTCCTCCTCCTCC** GCCTGCGATAGCACCAACAAC
MiaA-pACYC184-F	CGCGGAATTCGCCCCTTAGCCATTCTCTCTTTTCCTTATATG
MiaA-pACYC184-R	CGGCGAATTCCCAGTCCGATGCGCAGCATGTGACCATC
MiaA-KO-F	CGATAAAAGCCCTGAAAGATGAGTGATATCAGTAAGGCTGTGTAGGCTGGAGCTGCTTCG
MiaA-KO-R	CGTCTCCTGACGTTTGCGTCAGTTCCGTTAAAGTTTTACCCATATGAATATCCTCCTTAG
MiaA-KO-Conf-F	GCCGCCGGGTGGTCTGTTAC
MiaA-KO-Conf-R	CAGCCTGCGATAGCACCAAC
MiaB-KO-F	CCTGCATTCCTGGCTACTATTTCGCAAGAGCAAGTCGTGTGTAGGCTGGAGCTGCTTCG
MiaB-KO-R	CGGCGGGCCTGAGAATTACGGCTGATAATAACCCACGCCATATGAATATCCTCCTTAG
MiaB-KO-Conf-F	GCCGACCATTCCTCCGCCGAC
MiaB-KO-Conf-R	CATTGTCTGCTGGCTCCAGG
ClpX-F	GTTATGTGGGCGAAGACGTTG
ClpX-R	GAAACGTCTCGGGTAATGGA
DnaK-F	CGTACTGCTGCTGGACGTTA
DnaK-R	GATGGTTACCGCAGACTGGT
GroEL-F	GAAGATGTTGAAGGCGAAGC
GroEL-R	ATTACGGTACCGCCAGTCAG
HlyA-F	ACGTTGCCTTTAAGCGAGAA
HlyA-R	GTGTGATTACCCTGCCGTCT
HlyD-F	GCTGGAGGTTACTGCTCTGG
HlyD-R	GCTTATTCCCGGTTGACAAA
LonP-F	CTCTCTGACAATGGCGAACA
LonP-R	CGAACTGGCTGATTGCAGTA
RpoD-F	TTCGTACGCAAGAACGTCTG
RpoD-R	AGGTATCCTGGTTTCGTTG
RpoH-F	ACGCTGATCCTGTCTCACCT
RpoH-R	CATCAGGCCGATGTTACCTT
RpoS-F	CTATTCGTTTGCCGATTCAC
RpoS-R	GGCTTATCCAGTTGCTCTGC

[a] F, forward Primer; R, reverse Primer; KO, knockout primer; Conf, confirmation primer, [b] Universal Primer sequence underlined, [c] Added restriction sites underlined, [d] Flag tag and linker sequence in bold

described (14). The chloramphenicol cassette flanked by LoxP sites was amplified from plasmid pKD3. Primers for amplification of chloramphenicol were designed with overhanging ends with 39 bp of homology to the 5' and 3' ends of target knockout sites. PCR products were then introduced by electroporation into UTI89 pkm208, a strain containing a plasmid encoding the IPTG-inducible recombinase. Knockouts were verified by PCR by using flanking primers specific for target genes.

Growth assays

UTI89 and its derivatives were grown from frozen stocks in either Luria-Bertani (LB) broth or M9 minimal medium (6 g/liter Na_2HPO_4, 3 g/liter KH_2PO_4, 1 g/liter NH_4Cl, 0.5 g/liter NaCl, 1 mM $MgSO_4$, 0.1 mM $CaCl_2$, 0.1% glucose, 0.0025% nicotinic acid, 0.2% casein amino acids, and 16.5 μg/ml thiamine in H_2O) at 37°C overnight in loosely capped 20-by-150-mm borosilicate glass tubes with shaking at 225 rpm at a 30º angle. Overnight cultures were diluted 1:100 into 100-well honeycomb plates and assayed for growth using a Bioscreen C instrument (Growth Curves USA). Stressors were added to subcultured bacteria to reach the appropriate final concentration (0.1, 0.2, 0.3, or 1.0 mM MV; 1.0 or 2.0 mM ASN; 10 mM desferal; 1 mM EDTA; 5% additional NaCl). LB-MES (pH 5.0) media was used for low pH and ASN treated samples. Antibiotics were added when applicable for the overnight growth but not for subsequent growth assays.

Metabolomics sample preparation

Chemicals and reagents were of the highest purity and purchased from Sigma-Aldrich except for MSTFA was purchased from Pierce and 2-methylcitrate was purchased from CDN isotopes. Six biological replicates of each strain were used per experiment. The cultures were grown to an OD_{600} of 1 and harvested by centrifugation and the pellet frozen. To each frozen pellet was added 5 ml of boiling 75% EtOH (aqueous), vortexed then incubated at 90°C for 5 min. Cell debris was removed by centrifugation at 5000 x g for 3 m. The supernatant was removed to new tubes and dried *en vacuo.*

GC-MS analysis

All GC-MS analysis was performed with a Waters GCT Premier mass spectrometer fitted with an Agilent 6890 gas chromatograph and a Gerstel MPS2 autosampler. Dried samples were suspended in 40 µl of a 40 mg/ml O-methoxylamine hydrochloride in pyridine and incubated for one hour at 30°C. To autosampler vials was added 20 ul of this solution with MSTFA added using the autosampler and incubation for 30 min at 37°C with shaking. One ul of sample was injected to the inlet which was held at 250°C. The gas chromatograph an initial temperature of 95°C for 1 min followed by a 40°C/min ramp to 110°C and a hold time of 2 min. This was followed by a second 5°C/min ramp to 250°C then a third ramp to 350°C and a final hold time of 3 min. A 30 m Restek Rxi-5 MS column with a 5 m long guard column was employed for analysis. Data were collected by MassLynx 4.1. Data analysis for known metabolites was performed

using QuanLynx. To find possible unknown metabolites MarkerLynx was used for peak picking and these data were exported to SIMCA-P ver. 12.0.1 where PCA and PLS-DA analysis was performed.

Western blot analysis

Bacterial cultures were grown to desired O.D. (~1.0-1.2) and mixed directly with 2x sample buffer (without β-mercaptoethanol for non-reducing gels). Samples were then vortexed for 30 s and boiled for 5 m (heated to 60ºC for non-reducing gels). Samples were resolved in 12.5% acrylamide using sodium dodecyl sulfate polyacrylamide gel electrophoresis (SDS-PAGE) and subsequently transferred to PVDF membranes (Millipore) for Western blot analysis. All antibody incubations were performed in 2.5% powdered milk, 0.1% Tween-20 in Tris-Buffered Saline (pH 7.4). Blots were incubated with Mouse anti-Flag M2 (1:3000; Sigma) or Rabbit anti-Hemolysin A (1:800: Rod Welch) overnight at 4ºC, followed by a 30 m incubation with secondary anti-mouse/rabbit HRP-conjugated IgG antibody (1:3,000; Amersham Biosciences). Blots were then washed, developed using the SuperSignal West 1 Pico (Pierce), and exposed to CL-XPosure Film (Pierce). To ensure that equivalent amounts of protein from each sample were loaded, duplicate gels were stained using GelCode Blue (Pierce) and/or blots were re-probed using Rabbit anti-*E.coli* antisera (1:2,000; Iowa Hybridoma Bank?).

Biofilm assay

In vitro microtiter plate-based biofilm assays were performed as previously described. Briefly, UTI89 was diluted 1:100 from overnight shaking cultures into M9 medium, and triplicate 100 µl samples in 96-well pinchbar flat-bottomed polystyrene microtiter plates with lids (Nunc) were incubated for 48 h without shaking at 30°C. Nonadherent bacteria were then removed by washing twice with H2O prior to addition of crystal violet (150 µl of a 0.1% solution in water; Sigma-Aldrich). After a 10 min incubation at room temperature, the wells were rinsed twice with H_2O and air dried. Dimethyl sulfoxide (200 µl; Sigma-Aldrich) was then added to each well, and the plates were shaken vigorously for 15 min on an orbital shaker to solubilize the dye. A 150 µl aliquot from each well was transferred to a fresh microtiter plate, and A_{562} was measured using a Synergy HT multidetection microplate reader (BioTek Instruments, Inc.).

Motility assays

Bacterial swarm motility was determined by inoculating 0.2% agar plates with a toothpick dipped into an overnight culture of each strain. Care was taken to break the surface but not touch the bottom of the plate, to avoid initiating twitch motility. Plates were incubated face up at 37ºC for ~12 hours and the diameter of spreading was measured every 2 h. Values are from three separate experiments done in quadruplicate. Swarm motility assays were performed using 0.5% Eiken agar plates supplemented with 0.5% glucose. Five µL of bacteria were spotted on the surface of the plate and allowed to swarm overnight (16 h) at 37°C.

Invasion, association, and replication assays

UTI89 was grown at 37°C for 48 h in static LB broth to induce type 1 pilus expression. Triplicate sets of confluent 5637 bladder epithelial cell monolayers grown in 24-well tissue culture plates were infected with UTI89 using a multiplicity of infection of ~15 bacteria per host cell. To facilitate and synchronize bacterial contact with the host cells, plates were centrifuged at 600 x *g* for 5 min at room temperature at the start of infection (Beckman Allegra 6 Centrifuge). After a 2 h incubation at 37°C, samples were washed three times with PBS containing Ca^{2+} and Mg^{2+} (PBS^{2+}) to remove any nonadherent bacteria. Wells for adherence and total growth assays were collected at this time point and lysed in PBS plus 0.4% Triton X-100, and bacteria present within the lysates were enumerated by plating serial dilutions on LB agar plates. Monolayers for invasion and intracellular replication assays were then incubated for another 2 h with complete RPMI medium plus 100 μg/ml of gentamicin to kill extracellular bacteria. Monolayers for invasion assays were collected at this time point of 4 h and processed as described above. For intracellular replication assays, additional washes with PBS^{2+} were performed, followed by addition of fresh medium containing a lower concentration of gentamicin (10 μg/ml). Incubations were continued for another 14 h. This submaximal concentration of gentamicin was used to prevent extracellular growth of UPEC while limiting possible leaching of the antibiotic into the host cells during longer incubations (13). After final washes in PBS^{2+}, host cells were again lysed as described above in PBS plus

0.4% Triton X-100, with bacteria enumerated by plating serial dilutions on LB agar plates.

Mouse infection experiments

Seven- to 8-week-old female CBA/J mice (Jackson Laboratory) were anesthetized with isoflurane by inhalation and slowly inoculated via transurethral catheterization with 50 µL of the bacterial suspension (~10^7 CFU from 24 h static LB broth cultures of UTI89) in PBS as previously described. Bacterial reflux into the kidneys using this procedure is rare, occurring in less than 1% of the test animals. At 1, 3, or 9 days postinoculation, mice were sacrificed and bladders were harvested aseptically, weighed, and homogenized in 1 mL PBS containing 0.025% Triton X-100. Bacterial titers within the homogenates were determined by plating serial dilutions on LB agar plates. Eleven mice total, from two independent experiments, were used for each condition tested. Previous published results indicate no need for mock-infected mice to be housed in cages with the infected. Reservoir populations were determined by infecting mice as described above. At 3 days post infection, mice were treated for 3 consecutive days with one dose of Gentamicin (200 µg) subcutaneously. Control animals received subcutaneous injections of PBS. All antibiotics were delivered in 50 µl volumes. Mice were sacrificed 3 d after the final antibiotic treatment and treated as described above.

Persister assays

Persister cell assays were performed as previously described. Briefly, an overnight bacterial culture was subcultured 1:10 into fresh media containing appropriate antibiotic (ampicillin (20μg/mL), ofloxacin (10μg/mL), and gentamicin (10μg/ml)). An aliquot of the input was titered for reference. Cultures with antibiotics incubated shaking at 37ºC for 6 h before bacteria were titered.

Hemolytic activity phenotypic assays

Hemolytic activity was determined by streaking bacteria onto 5% sheep's blood agar plates and incubated for 18 h at 37˚C (Sigma-Aldrich). Plates were visually observed for presence of a halo of red blood cell lysis around the bacterial growth. β-galactosidase activity was qualified by pink growth on MacConkey agar plates overnight at 37˚C (Sigma-Aldrich). pH of bacterial growth media was determined by applying culture bacteria to pH strips (Sigma-Aldrich).

Quantitative reverse transcriptase polymerase chain reaction

Total RNA was collected from bacterial cultures (grown to O.D. ~1.0-1.2) using the Norgen Total RNA Isolation Kit (Norgen Biotek) and treated twice with Turbo DNase (Life Technologies). Superscript III using random hexamers was used to reverse transcribe RNA into cDNA (Life Technologies). qRT-PCR was performed using Syber Green Mix and primers listed in Table 6.2 and run on a Lightcycler 480 machine (Roche). Reactions were set up with and without RT as a control. All primer sets were optimized for use, and run on a 1.5% agarose gel,

stained with ethidium bromide, and imaged on a GelDoc (Bio-Rad Technologies), to verify the presence of only one band. qRT-PCR results were normalized to the housekeeping sigma factor, RpoD, transcript level.

Statistical analysis

P values were determined by Student's *t* Test and Mann-Whitney U tests performed using Prism 5.01 software (GraphPad Software). Values of less than 0.05 were defined as significant.

Acknowledgements

We thank James Cox in the Metabolomics Facility of the University of Utah for help with the GC/MS metabolite analysis. This study was funded by NIH grants AI095647, DK068585, AI090369, and AI088086. M.G.B. was supported by T32 AI055434 from the National Institute Of Allergy And Infectious Diseases. The content is solely the responsibility of the authors and does not necessarily represent the official views of the National Institute Of Allergy And Infectious Diseases or the National Institutes of Health.

References

1. **Ahn, K. S., U. Ha, J. Jia, D. Wu, and S. Jin.** 2004. The truA gene of *Pseudomonas aeruginosa* is required for the expression of type III secretory genes. Microbiology **150:**539-547.

2. **Billips, B. K., S. G. Forrestal, M. T. Rycyk, J. R. Johnson, D. J. Klumpp, and A. J. Schaeffer.** 2007. Modulation of host innate immune response in the bladder by uropathogenic *Escherichia coli*. Infect. Immun. **75:**5353-5360.

3. **Billips, B. K., A. J. Schaeffer, and D. J. Klumpp.** 2008. Molecular basis of uropathogenic *Escherichia coli* evasion of the innate immune response in the bladder. Infect. Immun. **76:**3891-3900.

4. **Bjork, G. R.** 1980. A novel link between the biosynthesis of aromatic amino acids and transfer RNA modification in *Escherichia coli*. J. Mol. Biol. **140:**391-410.

5. **Bjork, G. R., J. M. Durand, T. G. Hagervall, R. Leipuviene, H. K. Lundgren, K. Nilsson, P. Chen, Q. Qian, and J. Urbonavicius.** 1999. Transfer RNA modification: influence on translational frameshifting and metabolism. FEBS Lett. **452:**47-51.

6. **Blango, M. G., and M. A. Mulvey.** 2010. Persistence of uropathogenic *Escherichia coli* in the face of multiple antibiotics. Antimicrob. Agents Chemother. **54:**1855-1863.

7. **Blum, P. H.** 1988. Reduced leu operon expression in a *miaA* mutant of *Salmonella typhimurium*. J. Bacteriol. **170:**5125-5133.

8. **Caillet, J., and L. Droogmans.** 1988. Molecular cloning of the Escherichia coli *miaA* gene involved in the formation of delta 2-isopentenyl adenosine in tRNA. J. Bacteriol. **170:**4147-4152.

9. **Chan, C. T., M. Dyavaiah, M. S. DeMott, K. Taghizadeh, P. C. Dedon, and T. J. Begley.** 2010. A quantitative systems approach reveals dynamic control of tRNA modifications during cellular stress. PLoS Genet. **6:**e1001247.

10. **Chen, S. L., C. S. Hung, J. Xu, C. S. Reigstad, V. Magrini, A. Sabo, D. Blasiar, T. Bieri, R. R. Meyer, P. Ozersky, J. R. Armstrong, R. S. Fulton, J. P. Latreille, J. Spieth, T. M. Hooton, E. R. Mardis, S. J. Hultgren, and J. I. Gordon.** 2006. Identification of genes subject to positive selection in uropathogenic strains of *Escherichia coli*: a comparative genomics approach. Proc. Natl. Acad. Sci. U. S. A. **103:**5977-5982.

11. **Cho, K. H., and M. G. Caparon.** 2008. tRNA modification by GidA/MnmE is necessary for *Streptococcus pyogenes* virulence: a new strategy to make live attenuated strains. Infect. Immun. **76:**3176-3186.

12. **Connolly, D. M., and M. E. Winkler.** 1989. Genetic and physiological relationships among the *miaA* gene, 2-methylthio-N6-(delta 2-isopentenyl)-adenosine tRNA modification, and spontaneous mutagenesis in *Escherichia coli* K-12. J. Bacteriol. **171:**3233-3246.

13. **Connolly, D. M., and M. E. Winkler.** 1991. Structure of *Escherichia coli* K-12 miaA and characterization of the mutator phenotype caused by miaA insertion mutations. J. Bacteriol. **173:**1711-1721.

14. **Datsenko, K. A., and B. L. Wanner.** 2000. One-step inactivation of chromosomal genes in *Escherichia coli* K-12 using PCR products. Proc. Natl. Acad. Sci. U. S. A. **97:**6640-6645.

15. **Decatur, W. A., and M. J. Fournier.** 2002. rRNA modifications and ribosome function. Trends Biochem. Sci. **27:**344-351.

16. **Dhakal, B. K., and M. A. Mulvey.** 2012. The UPEC pore-forming toxin alpha-hemolysin triggers proteolysis of host proteins to disrupt cell adhesion, inflammatory, and survival pathways. Cell Host Microbe **11:**58-69.

17. **Dobrindt, U., L. Emody, I. Gentschev, W. Goebel, and J. Hacker.** 2002. Efficient expression of the alpha-haemolysin determinant in the uropathogenic *Escherichia coli* strain 536 requires the leuX-encoded tRNA(5)(Leu). Mol. Genet. Genomics **267:**370-379.

18. **Durand, J. M., G. R. Bjork, A. Kuwae, M. Yoshikawa, and C. Sasakawa.** 1997. The modified nucleoside 2-methylthio-N6-isopentenyladenosine in tRNA of *Shigella flexneri* is required for expression of virulence genes. J. Bacteriol. **179:**5777-5782.

19. **Durand, J. M., B. Dagberg, B. E. Uhlin, and G. R. Bjork.** 2000. Transfer RNA modification, temperature and DNA superhelicity have a common target in the regulatory network of the virulence of *Shigella flexneri*: the expression of the virF gene. Mol. Microbiol. **35:**924-935.

20. **Eto, D. S., J. L. Sundsbak, and M. A. Mulvey.** 2006. Actin-gated intracellular growth and resurgence of uropathogenic *Escherichia coli*. Cell. Microbiol. **8:**704-717.

21. **Foxman, B.** 1990. Recurring urinary tract infection: incidence and risk factors. Am. J. Public Health **80:**331-333.

22. **Gray, J., J. Wang, and S. B. Gelvin.** 1992. Mutation of the *miaA* gene of *Agrobacterium tumefaciens* results in reduced vir gene expression. J. Bacteriol. **174:**1086-1098.

23. **Hannan, T. J., I. U. Mysorekar, S. L. Chen, J. N. Walker, J. M. Jones, J. S. Pinkner, S. J. Hultgren, and P. C. Seed.** 2008. LeuX tRNA-dependent and -independent mechanisms of *Escherichia coli* pathogenesis in acute cystitis. Mol. Microbiol. **67:**116-128.

24. **Hjelm, E. M.** 1984. Local cellular immune response in ascending urinary tract infection: occurrence of T-cells, immunoglobulin-producing cells, and Ia-expressing cells in rat urinary tract tissue. Infect. Immun. **44:**627-632.

25. **Ingolia, N. T., S. Ghaemmaghami, J. R. Newman, and J. S. Weissman.** 2009. Genome-wide analysis in vivo of translation with nucleotide resolution using ribosome profiling. Science **324:**218-223.

26. **Johnson, J. R., C. Clabots, and H. Rosen.** 2006. Effect of inactivation of the global oxidative stress regulator oxyR on the colonization ability of *Escherichia coli* O1:K1:H7 in a mouse model of ascending urinary tract infection. Infect. Immun. **74:**461-468.

27. **Kaminska, K. H., U. Baraniak, M. Boniecki, K. Nowaczyk, A. Czerwoniec, and J. M. Bujnicki.** 2008. Structural bioinformatics analysis of enzymes involved in the biosynthesis pathway of the hypermodified nucleoside ms(2)io(6)A37 in tRNA. Proteins **70:**1-18.

28. **Kawano, H., Y. Hirokawa, and H. Mori.** 2009. Long-term survival of *Escherichia coli* lacking the HipBA toxin-antitoxin system during prolonged cultivation. Biosci. Biotechnol. Biochem. **73:**117-123.

29. **Keren, I., N. Kaldalu, A. Spoering, Y. Wang, and K. Lewis.** 2004. Persister cells and tolerance to antimicrobials. FEMS Microbiol. Lett. **230:**13-18.

30. **Kulesus, R. R., K. Diaz-Perez, E. S. Slechta, D. S. Eto, and M. A. Mulvey.** 2008. Impact of the RNA chaperone Hfq on the fitness and virulence potential of uropathogenic *Escherichia coli*. Infect. Immun. **76:**3019-3026.

31. **Lamichhane, T. N., N. H. Blewett, and R. J. Maraia.** 2011. Plasticity and diversity of tRNA anticodon determinants of substrate recognition by eukaryotic A37 isopentenyltransferases. RNA **17:**1846-1857.

32. **Leung, H. C., Y. Chen, and M. E. Winkler.** 1997. Regulation of substrate recognition by the MiaA tRNA prenyltransferase modification enzyme of *Escherichia coli* K-12. J. Biol. Chem. **272:**13073-13083.

33. **May, A. K., T. G. Gleason, R. G. Sawyer, and T. L. Pruett.** 2000. Contribution of *Escherichia coli* alpha-hemolysin to bacterial virulence and to intraperitoneal alterations in peritonitis. Infect. Immun. **68:**176-183.

34. **Moore, P. B., and T. A. Steitz.** 2002. The involvement of RNA in ribosome function. Nature **418:**229-235.

35. **Mulvey, M. A., J. D. Schilling, and S. J. Hultgren.** 2001. Establishment of a persistent *Escherichia coli* reservoir during the acute phase of a bladder infection. Infect. Immun. **69:**4572-4579.

36. **Nomura, M.** 1987. The role of RNA and protein in ribosome function: a review of early reconstitution studies and prospects for future studies. Cold Spring Harbor symposia on quantitative biology **52:**653-663.

37. **Olekhnovich, I., and G. N. Gussin.** 2001. Effects of mutations in the *Pseudomonas putida miaA* gene: regulation of the *trpE* and *trpGDC* operons in *P. putida* by attenuation. J. Bacteriol. **183:**3256-3260.

38. **Persson, B. C.** 1993. Modification of tRNA as a regulatory device. Mol. Microbiol. **8:**1011-1016.

39. **Pierrel, F., G. R. Bjork, M. Fontecave, and M. Atta.** 2002. Enzymatic modification of tRNAs: MiaB is an iron-sulfur protein. J. Biol. Chem. **277:**13367-13370.

40. **Pierrel, F., T. Douki, M. Fontecave, and M. Atta.** 2004. MiaB protein is a bifunctional radical-S-adenosylmethionine enzyme involved in thiolation and methylation of tRNA. J. Biol. Chem. **279:**47555-47563.

41. **Pierrel, F., H. L. Hernandez, M. K. Johnson, M. Fontecave, and M. Atta.** 2003. MiaB protein from *Thermotoga maritima*. Characterization of an extremely thermophilic tRNA-methylthiotransferase. J. Biol. Chem .**278:**29515-29524.

42. **Pimenta, A. L., K. Racher, L. Jamieson, M. A. Blight, and I. B. Holland.** 2005. Mutations in HlyD, part of the type 1 translocator for hemolysin secretion, affect the folding of the secreted toxin. J. Bacteriol. **187:**7471-7480.

43. **Seif, E., and B. M. Hallberg.** 2009. RNA-protein mutually induced fit: structure of *Escherichia coli* isopentenyl-tRNA transferase in complex with tRNA(Phe). J. Biol. Chem. **284:**6600-6604.

44. **Soto, S. M., A. Smithson, J. P. Horcajada, J. A. Martinez, J. P. Mensa, and J. Vila.** 2006. Implication of biofilm formation in the persistence of urinary tract infection caused by uropathogenic *Escherichia coli*. Clin. Microbiol. Infect. **12:**1034-1036.

45. **Spirin, A. S.** 2002. Ribosome as a molecular machine. FEBS Lett. **514:**2-10.

46. **Sprinzl, M., T. Hartmann, F. Meissner, J. Moll, and T. Vorderwulbecke.** 1987. Compilation of tRNA sequences and sequences of tRNA genes. Nucleic Acids Res. **15 Suppl:**r53-188.

47. **Urbonavicius, J., Q. Qian, J. M. Durand, T. G. Hagervall, and G. R. Bjork.** 2001. Improvement of reading frame maintenance is a common function for several tRNA modifications. EMBO J. **20:**4863-4873.

48. **Wiles, T. J., B. K. Dhakal, D. S. Eto, and M. A. Mulvey.** 2008. Inactivation of host Akt/protein kinase B signaling by bacterial pore-forming toxins. Mol. Biol. Cell. **19:**1427-1438.

49. **Wiles, T. J., R. R. Kulesus, and M. A. Mulvey.** 2008. Origins and virulence mechanisms of uropathogenic *Escherichia coli*. Exp. Mol. Pathol. **85:**11-19.

50. **Wolfe, A. J., N. Parikh, B. P. Lima, and B. Zemaitaitis.** 2008. Signal integration by the two-component signal transduction response regulator CpxR. J Bacteriol **190:**2314-2322.

51. **Yanofsky, C.** 1977. Mutations affecting tRNATrp and its charging and their effect on regulation of transcription termination at the attenuator of the tryptophan operon. J. Mol. Biol. **113:**663-677.

Supplemental Material

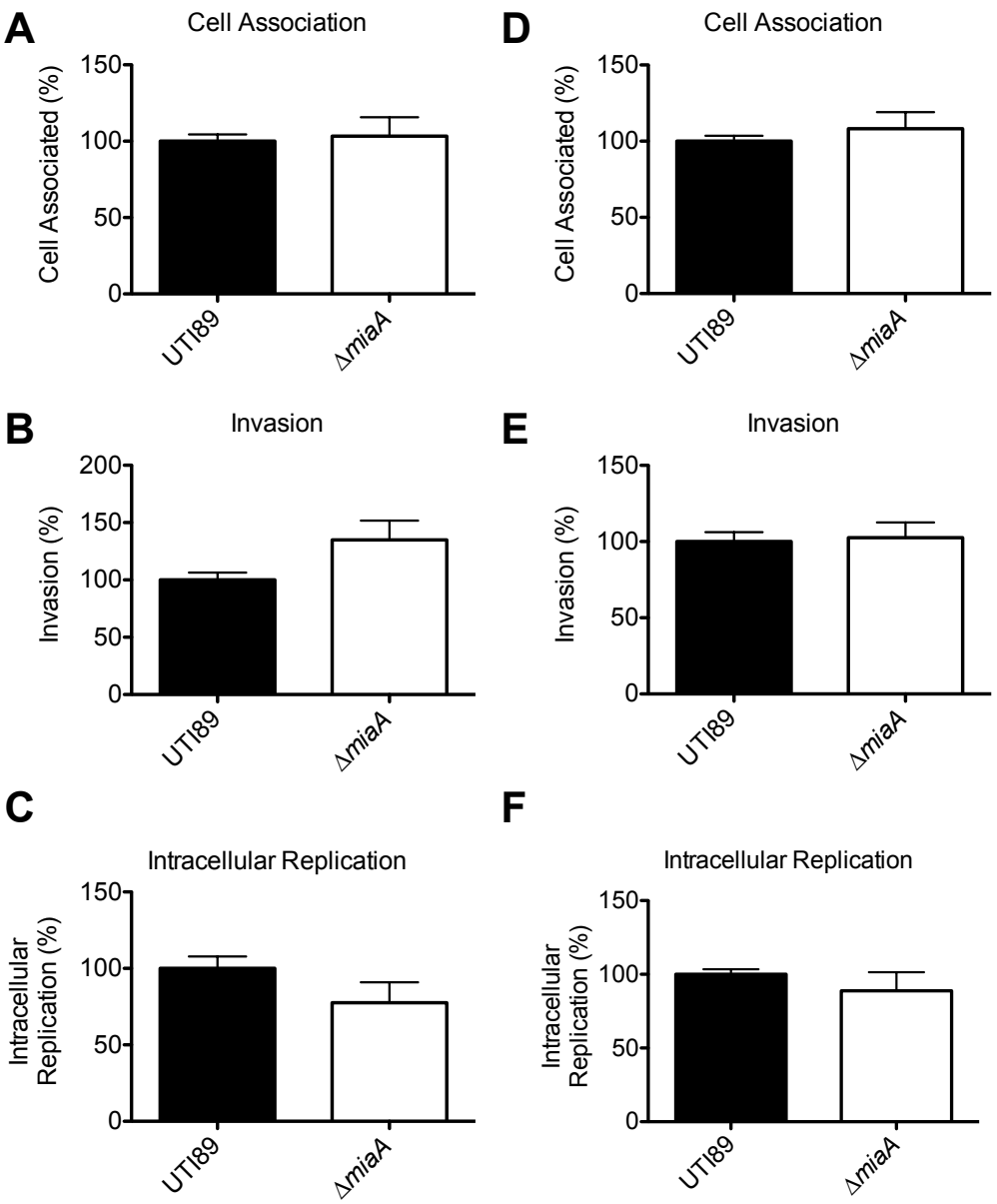

Figure 6.S1 *miaA/B* mutants exhibit no effects on host cell invasion, association, or intracellular replication

(A-C) Cell culture assays were performed using 5637 bladder epithelial carcinoma cells to test for bacterial association, invasion, and replication within host cells using the *miaA* knockout and (D-F) *miaB* knockout. Bar graphs in A-F are from three independent experiments performed in triplicate with error bars representative of SEM.

CHAPTER 7

DISCUSSION

The research presented in these chapters provides insight into UPEC pathogenesis during a UTI, specifically in regards to the establishment and maintenance of the reservoir population responsible for chronic and recurrent infections.

In Chapter 2, the susceptibility of UPEC strain UTI89 to antibiotic challenges was tested *in vitro* and during a murine UTI. While most of the tested antibiotics killed UPEC in broth cultures, many were ineffective against intracellular UPEC in a bladder cell culture model. Similarly, a large percentage of antibiotics were unable to affect UPEC growing in biofilms on plastic dishes. A few host cell-permeable antibiotics did prove promising in these assays and were tested in a mouse model of UTI. Of the antibiotics tested *in vivo* (gentamicin, ciprofloxacin sparfloxacin, and fosfomycin), all were able to effectively sterilize the urine, but none completely eliminated the reservoir populations associated with the bladder tissue. Previous studies suggested that the reservoir population consists of an intracellular subset of UPEC (13, 24, 30). However, in this study IBCs were sensitive to treatment with the cell-permeable antibiotic sparfloxacin *ex vivo*, suggesting that IBCs are not the primary reservoir. Rather, the reservoirs likely consist of small bacterial clusters, or single bacteria, distributed throughout the urothelium (13, 24, 30). The robust barrier function of the urothelium, coupled with the quiescent nature of the UPEC reservoirs, limits the effectiveness of antibiotics (3). The research described in Chapter 2 laid the framework for the rest of this thesis by further defining the confounding issues surrounding

treatment of recurrent UTIs, namely resistance to antibiotic treatment through bacterial internalization and bacterial quiescence in the host epithelium.

The existence of UPEC reservoirs provides a roadblock to efficacious treatment options (20, 30). Several hypothetical approaches could solve the issue of UPEC persistence in the bladder. An effective UPEC vaccine could promote clearance of bacterial infections by UPEC; however, ongoing research in this field has so far not yielded vaccines that are effective in human patients (28, 34). A second strategy would be to treat infected bladders with a combination of antibiotics and an epithelial cell exfoliant to disrupt the barrier function of the urothelium and permit penetration of antibiotics to underlying tissues: a technique explored in Chapter 3. A third possible approach, as outlined in Chapters 4 through 6, is to target the mechanisms used by UPEC to persist in the urinary tract, specifically in regards to regulation of stress response and virulence.

Chapter 3 unveils a therapeutic strategy to dislodge UPEC reservoirs from the bladder epithelium through the use of chitosan, a chitin-based bladder exfoliant. Hultgren and colleagues recently took a similar approach using protamine sulfate to induce exfoliation of bladder cells (25, 26). Unfortunately, significant inflammation, tissue destruction, and pain associated with use of protamine sulfate made this approach an impractical treatment option for clearance of UPEC reservoir populations in human patients. In contrast, chitosan disrupts epithelial cell tight junctions to trigger exfoliation of primarily the superficial cell layer in the mammalian bladder with little inflammation (19, 21,

33). Chitosan is also approved for clinical use in humans as a drug-carrier molecule (4). In this study infected mice were treated with a combination of chitosan and the host cell-permeable antibiotics, sparfloxacin or ciprofloxacin, for seven days. This combination therapy almost completely eliminated the reservoir population from the bladder, yet many mice still exhibited recurrent or relapsing infections as measured by urine titers over the course of two weeks following treatment. A chitosan and sparfloxacin combination treatment was, however, significantly more effective at inhibiting recurrence compared to control untreated mice. Although promising as a therapeutic, administration of chitosan to the bladder has a damaging effect on the epithelium and potentially offers pathogens increased opportunity to invade underlying tissues. Furthermore, the efficacy of chitosan use should be tested in additional mammalian model systems, as well as against alternative pathogens. For example, chitosan has been shown to trigger exfoliation of superficial bladder epithelial cells in pig bladders, but no human studies have confirmed the effectiveness of chitosan as an exfoliant (19, 21). Secondly, therapies effective against one UPEC strain may fail to eradicate strains of *Klebsiella* or other common causes of UTI, which would render this treatment less effective. Incubation of UPEC in chitosan also resulted in increased inter-bacterial connections and extracellular matrix-like material as observed by SEM and immunofluorescence, likely contributing to increased biofilm formation and host-cell association. The increased association of UPEC with host cells is concerning, since increased adhesion likely promotes invasion, propagating the infection. Invasion assays did, however, suggest a decrease in

the rate of epithelial cell invasion in these assays. Taken together, chitosan-based therapies appear promising; but much work remains to elucidate their full potential for treatment of UTI.

The second major aim of Chapter 2 was to use chitosan as a tool to probe the contribution of underlying tissues in reservoir formation and recurrence. It was shown that UPEC invade underlying tissues as efficiently as the superficial epithelium, and both superficial epithelia and underlying tissues contribute to formation of the reservoir population. Imaging and mouse infection experiments also suggested a resurgence of UPEC titers in the urine after chitosan treatment. Figure 7.1 depicts a model of UPEC pathogenesis, synthesizing the data presented here with decades of UTI study. According to the model, UPEC invade superficial epithelial cells triggering exfoliation of large swaths of the urothelium (11, 23). Rarely, UPEC are able to invade underlying epithelial tissues to establish additional quiescent intracellular reservoir populations, where the bacteria reside metabolically inactive encased in host actin (12, 13). Upon turnover or damage to superficial bladder epithelial cells, quiescent intracellular UPEC reservoirs move towards the apical surface, by traveling as passengers within differentiating underlying and intermediate cells. UPEC then recognize the differentiation of superficial bladder epithelial cells as an environmental cue to replicate intracellularly and form an IBC; a possible signal being the loss of high actin expression in differentiated superficial epithelial cells (13). The IBC then releases a bolus of UPEC into the bladder lumen to initiate a new round of infection (2, 18, 23). This model posits the periodic resurgence of UTI in

Figure 7.1 Model of UPEC Pathogenesis

(1.) UPEC gain entry to the bladder lumen where they replicate rapidly to high numbers in the urine. (2.) The infrequent event of cellular invasion occurs to create an intracellular UPEC niche. (3.) Shear forces from urine flow remove the majority of the non-adherent bacteria from the bladder, while UPEC begins to replicate intracellularly to form an IBC before exit to the cytosol. (4.) IBC formation triggers exfoliation of host cells to remove infected cells, allowing for infection of underlying tissues. (5.) The host epithelium is repaired to regain barrier integrity, effectively establishing persistent, quiescent, intracellular UPEC reservoirs in the underlying epithelium encased in host actin. (6) UPEC act as passengers in host epithelial cells and are trafficked to the surface during superficial cell differentiation. Upon arrival at the surface, UPEC break out of the host cell through IBC formation to reinoculate the bladder lumen, triggering subsequent rounds of infection.

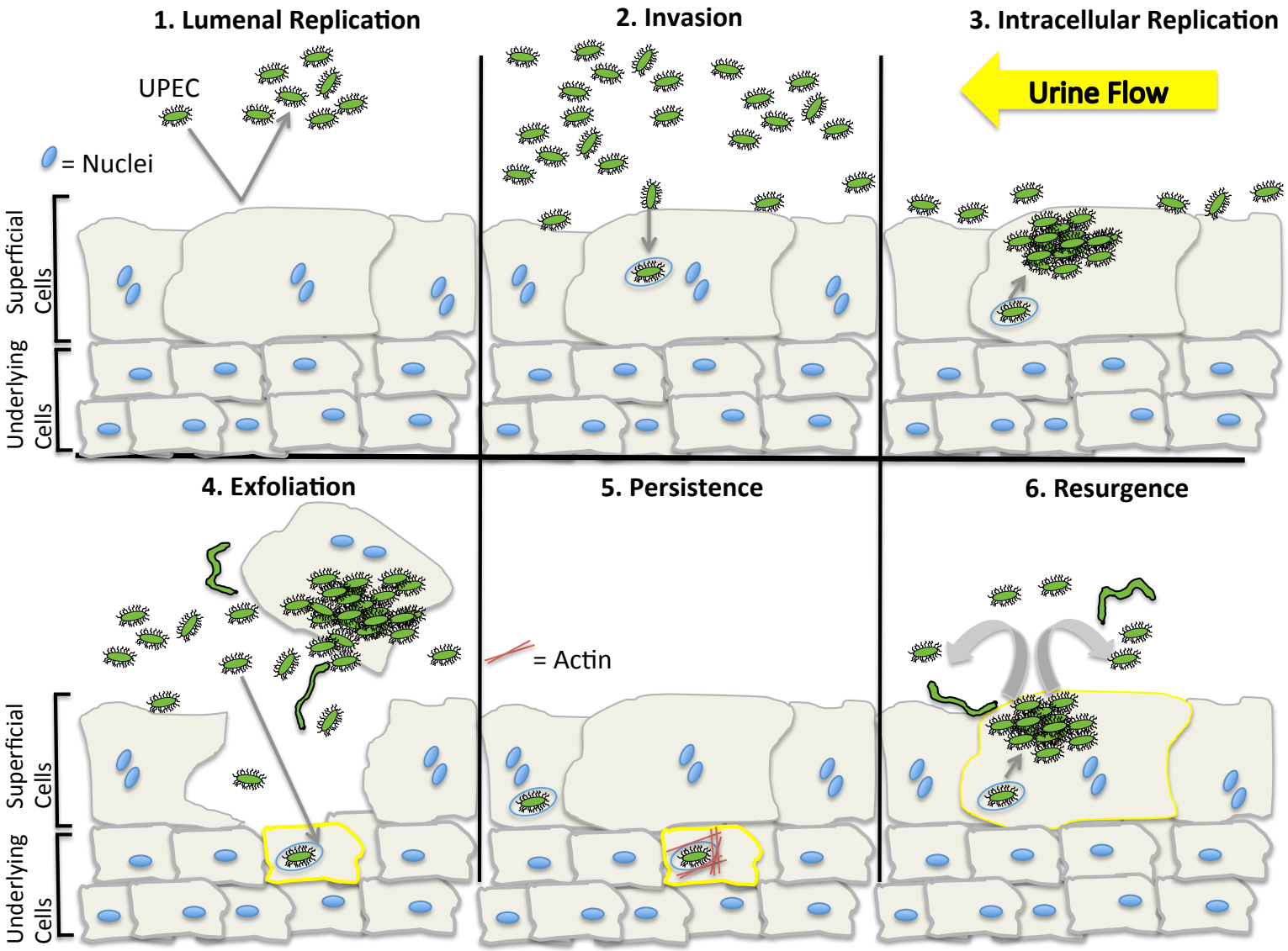
1. Lumenal Replication
2. Invasion
3. Intracellular Replication
UPEC
= Nuclei
Urine Flow
Superficial Cells
Underlying Cells
4. Exfoliation
5. Persistence
6. Resurgence
= Actin
Superficial Cells
Underlying Cells

mammalian hosts as being caused primarily by the slow turnover of host superficial cells (17). It also reaffirms data suggesting that IBCs are a facilitator of productive infection through inoculation of the bladder with an acute burst of bacteria (2, 18, 24). Chapters 4 through 6 aimed to elucidate mechanisms underlying the establishment and maintenance of the UPEC reservoir populations. In order to establish an infection in the urinary tract, pathogens must survive challenge from a wide range of stressors, including low pH challenge, nitrosative and oxidative stressors, immune challenge, and nutrient deprivation (1, 5, 32). To more fully understand the mechanisms in place in UPEC to cope with these challenges, two underappreciated regulatory mechanisms were tested for their roles in bacterial stress response and pathogenesis: the regulation of gene expression by sRNAs and regulation of translation by tRNA modification.

sRNAs modulate many aspects of bacterial gene expression, often in association with the RNA chaperone Hfq (35). Previous work has indicated a role for Hfq, and likely sRNAs, in UPEC virulence and stress response (22). To further define the contribution of sRNAs to UPEC pathogenesis and the observed effects of an Hfq deletion, a panel of conserved sRNAs was screened for alterations to stress response *in vitro* as described in Chapter 4. Nearly all tested sRNAs exhibited defects in biofilm formation; however, only two knockouts exhibited defects in stress resistance, Spot 42 and MicC. A double knockout of the two sRNAs showed a synthetic defect, suggesting alternate pathways of action. Focus on Spot 42, an sRNA known to affect multiple metabolic pathways, revealed altered levels of several metabolic intermediates and a contribution to

oxidative stress responses *in vitro*. Spot 42 also positively affected intracellular survival of UPEC in both cell culture and a murine model of infection. Extrapolation of these data suggests that UPEC persistence requires fully functional metabolic and/or stress response pathways for intracellular survival during UTI.

Much of the mechanistic data surrounding bacterial sRNAs comes from analysis of laboratory strains of *E. coli*, such as MG1655, which, compared to wild type strains, fare poorly under stressful challenges and are severely attenuated outside of laboratory conditions (6, 36). The study of sRNAs in UPEC provides the opportunity to test their roles in host-pathogen interactions and robust stress resistance pathways and supplement work in *Salmonella* and enteropathogenic strains of *E. coli*. In addition to comparing non-pathogens to pathogens, the large number of sequenced, annotated *E. coli* isolates enables study of evolutionary aspects of sRNA acquisition and function across strains and species. Future analyses highlighting the contributions of sRNA molecules to stress response cascades in multiple isolates will likely help to explain the process of co-opting genomic features such as sRNAs for use in new genetic backgrounds, as has occurred in UPEC.

Chapter 5 extended the breadth of UPEC sRNAs by using RNA-Seq to identify novel sRNA molecules in UTI89. Putative UPEC sRNA molecules were identified both *in vitro* and *in vivo* directly from the bladders of infected mice by sequencing using an Illumina HiSeq 2000 machine. Novel sRNA molecules were

identified from *in vitro* isolated samples as containing >5 fold increased expression compared to neighboring open reading frames (ORFs) as previously described (29). The data gained from infected mouse bladders was used to guide our selection of candidate sRNAs for further study. Several hundred, candidate sRNAs were identified using this approach. Eleven promising candidates, exhibiting high relative levels of expression compared to neighboring ORFs, low standard deviations, and expression in multiple samples, were chromosomally deleted using lambda Red recombination and shown to be modestly defective in biofilm formation (10). One particular sRNA, UsrB*,* appears to slightly repress virulence (~4.5 fold) in the mouse UTI model. The mechanism of repression by UsrB is unknown at this time, but it is hypothesized that UsrB may regulate virulence factor expression in some capacity to prevent overzealous activation of virulence cascades, possibly through negative regulation of the PhoR-PhoP two component system controlling inorganic phosphate levels, as discussed in Chapter 5 (8, 16). In addition to testing regulation of PhoR, much work remains surrounding the candidate sRNA molecules. Several additional putative sRNAs, including UPEC-specific sRNAs, still remain to be chromosomally deleted. All of the candidate sRNAs require validation by complementation, Northern blot analysis, and 5’ and 3’ end mapping by RACE to determine the exact size and sequence of the sRNAs. Further characterization of their effects on stress response and virulence are also forthcoming. Overall, RNA-Seq provided us with more support for UPEC as a valid system in which to elucidate and further characterize sRNA function, and has opened many avenues of future research.

In Chapter 6, the global role of tRNA modifications in UPEC stress response and virulence was tested. Chromosomal knockouts were generated in two enzymes, MiaA and MiaB that modify adenosine-37 in a subset of tRNA molecules (7, 27). Knockouts indicated differential control of virulence and stress responses by MiaA and MiaB. MiaB appeared to influence only biofilm formation, whereas MiaA exhibited defects in nearly all tested aspects of stress response, metabolism, and virulence, including production of the α-hemolysin toxin. In particular, a knockout of MiaA was defective in survival and colonization of the bladder: at 3 days postinoculation, UPEC lacking MiaA showed a 10,000-fold decrease in titers relative to the wild type strain. Interestingly, despite a severe defect in bladder colonization, MiaA knockouts still formed reservoir populations albeit significantly decreased in size. The relative defect in reservoir formation was quite small compared to the defect in bladder colonization observed at 3 days postinfection, suggesting that the intracellular niche provides UPEC with a more hospitable habitat for long-term persistence in the urinary tract as compared to the bladder lumen.

In addition to learning more of UPEC biology in the urinary tract through studies of tRNA modifications, several interesting mechanisms of regulation by tRNA modifications were elucidated in these studies. Specifically, changes in MiaA expression through the use of either a gene knockout or overexpression constructs resulted in defective stress resistance, suggesting a requirement for proper MiaA gene dosage in responding to stressful conditions. MiaA protein levels were shown to decrease in response to environmental oxidative stress in

the form of methyl viologen. Altered gene dosage of MiaA also influenced various aspects of motility, with overexpression completely preventing swarm motility, while a MiaA knockout exhibited more robust swarming than wild type. It has previously been hypothesized that tRNA modifying enzymes may act as global regulators of stress response due to their pleiotropic affects on translation (9). In this model, levels of tRNA modification serve to alter the translational landscape by providing altered flexibility to protein structures, through changes in translational fidelity. The results presented here support this idea, as MiaA was shown to regulate multiple stress response pathways, behavioral transitions, and virulence, dependent upon levels of MiaA expression. Manipulation of MiaA expression levels resulted in pleiotropic effects, suggesting that MiaA acts as a global regulator of UPEC stress response, virulence, and behavior.

The study of two separate enzymes, MiaA and MiaB, required to modify the same tRNA residue, provides a noteworthy comparison of the functional diversity arising from different tRNA modifications. MiaA affects growth and survival of UPEC under nearly all conditions and stresses tested, whereas MiaB only contributed to biofilm formation in our assays. It will be interesting to assess the contribution of other A-37 modifications on stress resistance and virulence in UPEC - e.g., the YfiC enzyme that modifies valine-recognizing tRNAs and contributes to K-12 stress resistance (15). In addition to YfiC, many other tRNA modification enzymes present in the UPEC genome could be assessed for virulence and stress response regulation. Previously published and ongoing gene expression profiling and mutant screens may highlight tRNA modifying enzymes

that are likely important for infection. Overall, a direct comparison of MiaA and MiaB functions in UPEC has revealed that MiaB, but not MiaA, is dispensable for many aspects of UPEC stress response, behavior, and virulence. These conclusions would be difficult to make using only K-12 *E. coli* strains that are less amenable to use with phenotypic assays that gauge stress resistance and virulence beyond what K-12 strains can handle. Thus UPEC serves as a valuable system in which to study conserved mechanisms of regulation, such as sRNAs and tRNA modifying enzymes, which may be difficult to discern using standard attenuated K-12 strains.

The contents of this thesis cover a wide-range of topics relevant to host-pathogen interactions. The common theme throughout, however, is the maintenance and persistence of UPEC reservoir populations in the urinary tract. Initially, attempts were made to eradicate the UPEC reservoirs through use of highly cell-permeable antibiotics. On their own, these antibiotics had little effect on the reservoirs, but when coupled with a potent exfoliant (chitosan), the reservoirs were more readily targeted. In order to understand the maintenance of the reservoir, studies were performed on the mechanisms utilized by UPEC to regulate virulence traits and to cope with environmental stresses. Results presented indicate that both the sRNA repertoire and tRNA modification pathways promote UPEC resistance persistence.

Ultimately, this dissertation asserts that the UPEC reservoir population is an impervious, staunch foe. Despite advanced therapies, bacteria persist in the urinary tract, in part due to a reservoir population that reinoculates the bladder

lumen to trigger subsequent rounds of infection. In the future, novel, more cell-permeable therapeutics may be developed that can more effectively transit the urothelial barrier to eradicate bacteria, or perhaps more potent antibiotics might be identified that better eliminate metabolically inactive, quiescent bacteria. A new series of drugs targeting metabolically inactive *M. tuberculosis* promises hope that such novel therapeutics could be developed to target UPEC reservoirs in the future (14, 31). The adaptation and application of similar treatments towards quiescent UPEC populations within the urinary tract will necessitate further basic research into UPEC pathogenesis, similar to data presented in chapters 4 through 6. In addition to providing a model for treatment of chronic UTIs, this thesis established UPEC as a robust system in which to study bacterial sRNA molecules and tRNA modifying enzymes. Future studies aimed at defining the contributions of additional conserved sRNAs to virulence and stress response will help to elucidate both the regulation and evolution of these RNA molecules. Likewise, tRNA molecules are a fundamental building block of biology: and continued work in UPEC will help further the understanding of these essential modifications as global regulators of bacterial behavior. Together, these regulatory mechanisms provide UPEC with the tools needed to respond to environmental challenges and persist in the urinary tract through formation and maintenance of reservoir populations.

References

1. **Alteri, C. J., S. N. Smith, and H. L. Mobley.** 2009. Fitness of *Escherichia coli* during urinary tract infection requires gluconeogenesis and the TCA cycle. PLoS Pathog. **5:**e1000448.

2. **Anderson, G. G., K. W. Dodson, T. M. Hooton, and S. J. Hultgren.** 2004. Intracellular bacterial communities of uropathogenic *Escherichia coli* in urinary tract pathogenesis. Trends Microbiol. **12:**424-430.

3. **Apodaca, G.** 2004. The uroepithelium: not just a passive barrier. Traffic **5:**117-128.

4. **Aspden, T. J., J. D. Mason, N. S. Jones, J. Lowe, O. Skaugrud, and L. Illum.** 1997. Chitosan as a nasal delivery system: the effect of chitosan solutions on in vitro and in vivo mucociliary transport rates in human turbinates and volunteers. J. Pharm. Sci. **86:**509-513.

5. **Billips, B. K., S. G. Forrestal, M. T. Rycyk, J. R. Johnson, D. J. Klumpp, and A. J. Schaeffer.** 2007. Modulation of host innate immune response in the bladder by uropathogenic *Escherichia coli*. Infect. Immun. **75:**5353-5360.

6. **Brzuszkiewicz, E., H. Bruggemann, H. Liesegang, M. Emmerth, T. Olschlager, G. Nagy, K. Albermann, C. Wagner, C. Buchrieser, L. Emody, G. Gottschalk, J. Hacker, and U. Dobrindt.** 2006. How to become a uropathogen: comparative genomic analysis of extraintestinal pathogenic *Escherichia coli* strains. Proc. Natl. Acad. Sci. U. S. A. **103:**12879-12884.

7. **Caillet, J., and L. Droogmans.** 1988. Molecular cloning of the *Escherichia coli* miaA gene involved in the formation of delta 2-isopentenyl adenosine in tRNA. J. Bacteriol. **170:**4147-4152.

8. **Chakraborty, S., J. Sivaraman, K. Y. Leung, and Y. K. Mok.** 2011. Two-component PhoB-PhoR regulatory system and ferric uptake regulator sense phosphate and iron to control virulence genes in type III and VI secretion systems of *Edwardsiella tarda*. J. Biol. Chem. **286:**39417-39430.

9. **Connolly, D. M., and M. E. Winkler.** 1989. Genetic and physiological relationships among the miaA gene, 2-methylthio-N6-(delta 2-isopentenyl)-adenosine tRNA modification, and spontaneous mutagenesis in *Escherichia coli* K-12. J. Bacteriol. **171:**3233-3246.

10. **Datsenko, K. A., and B. L. Wanner.** 2000. One-step inactivation of chromosomal genes in *Escherichia coli* K-12 using PCR products. Proc. Natl. Acad. Sci. U. S. A. **97:**6640-6645.

11. **Dhakal, B. K., and M. A. Mulvey.** 2012. The UPEC pore-forming toxin alpha-hemolysin triggers proteolysis of host proteins to disrupt cell adhesion, inflammatory, and survival pathways. Cell Host Microbe **11:**58-69.

12. **Eto, D. S., T. A. Jones, J. L. Sundsbak, and M. A. Mulvey.** 2007. Integrin-mediated host cell invasion by type 1-piliated uropathogenic *Escherichia coli*. PLoS Pathog. **3:**e100.

13. **Eto, D. S., J. L. Sundsbak, and M. A. Mulvey.** 2006. Actin-gated intracellular growth and resurgence of uropathogenic *Escherichia coli*. Cell Microbiol. **8:**704-717.

14. **Fukuwatari, T., E. Sugimoto, and K. Shibata.** 2002. Growth-promoting activity of pyrazinoic acid, a putative active compound of antituberculosis drug pyrazinamide, in niacin-deficient rats through the inhibition of ACMSD activity. Biosci. Biotechnol. Biochem. **66:**1435-1441.

15. **Golovina, A. Y., P. V. Sergiev, A. V. Golovin, M. V. Serebryakova, I. Demina, V. M. Govorun, and O. A. Dontsova.** 2009. The *yfiC* gene of *E. coli* encodes an adenine-N6 methyltransferase that specifically modifies A37 of tRNA1Val(cmo5UAC). RNA **15:**1134-1141.

16. **Gonzalo Asensio, J., C. Maia, N. L. Ferrer, N. Barilone, F. Laval, C. Y. Soto, N. Winter, M. Daffe, B. Gicquel, C. Martin, and M. Jackson.** 2006. The virulence-associated two-component PhoP-PhoR system controls the biosynthesis of polyketide-derived lipids in *Mycobacterium tuberculosis*. J. Biol. Chem. **281:**1313-1316.

17. **Hicks, R. M.** 1975. The mammalian urinary bladder: an accommodating organ. Biol. Rev. Camb. Philos. Soc. **50:**215-246.

18. **Justice, S. S., C. Hung, J. A. Theriot, D. A. Fletcher, G. G. Anderson, M. J. Footer, and S. J. Hultgren.** 2004. Differentiation and developmental pathways of uropathogenic *Escherichia coli* in urinary tract pathogenesis. Proc. Natl. Acad. Sci. U. S. A. **101:**1333-1338.

19. **Kerec, M., M. Bogataj, P. Veranic, and A. Mrhar.** 2005. Permeability of pig urinary bladder wall: the effect of chitosan and the role of calcium. Eur. J. Pharm. Sci. **25:**113-121.

20. **Kerrn, M. B., C. Struve, J. Blom, N. Frimodt-Moller, and K. A. Krogfelt.** 2005. Intracellular persistence of *Escherichia coli* in urinary bladders from mecillinam-treated mice. J. Antimicrob. Chemother. **55:**383-386.

21. **Kos, M. K., M. Bogataj, P. Veranic, and A. Mrhar.** 2006. Permeability of pig urinary bladder wall: time and concentration dependent effect of chitosan. Biol. Pharm. Bull. **29:**1685-1691.

22. **Kulesus, R. R., K. Diaz-Perez, E. S. Slechta, D. S. Eto, and M. A. Mulvey.** 2008. Impact of the RNA chaperone Hfq on the fitness and virulence potential of uropathogenic *Escherichia coli*. Infect. Immun. **76:**3019-3026.

23. **Mulvey, M. A., Y. S. Lopez-Boado, C. L. Wilson, R. Roth, W. C. Parks, J. Heuser, and S. J. Hultgren.** 1998. Induction and evasion of host defenses by type 1-piliated uropathogenic *Escherichia coli*. Science **282:**1494-1497.

24. **Mulvey, M. A., J. D. Schilling, and S. J. Hultgren.** 2001. Establishment of a persistent *Escherichia coli* reservoir during the acute phase of a bladder infection. Infect. Immun. **69:**4572-4579.

25. **Mysorekar, I. U., and S. J. Hultgren.** 2006. Mechanisms of uropathogenic *Escherichia coli* persistence and eradication from the urinary tract. Proc. Natl. Acad. Sci. U. S. A. **103:**14170-14175.

26. **Parsons, C. L., C. W. Stauffer, and J. D. Schmidt.** 1988. Reversible inactivation of bladder surface glycosaminoglycan antibacterial activity by protamine sulfate. Infect. Immun. **56:**1341-1343.

27. **Pierrel, F., G. R. Bjork, M. Fontecave, and M. Atta.** 2002. Enzymatic modification of tRNAs: MiaB is an iron-sulfur protein. J. Biol. Chem. **277:**13367-13370.

28. **Prat, V., K. Matousovic, M. Horcickova, M. Hatala, and Z. Milotova.** 1989. [Prevention of recurrent urinary infections using Solco Urovac, a polymicrobial vaccine]. Cas. Lek. Cesk. **128:**1106-1109.

29. **Raghavan, R., E. A. Groisman, and H. Ochman.** 2011. Genome-wide detection of novel regulatory RNAs in E. coli. Genome Res. **21:**1487-1497.

30. **Schilling, J. D., R. G. Lorenz, and S. J. Hultgren.** 2002. Effect of trimethoprim-sulfamethoxazole on recurrent bacteriuria and bacterial persistence in mice infected with uropathogenic *Escherichia coli*. Infect. Immun. **70:**7042-7049.

31. **Shi, W., X. Zhang, X. Jiang, H. Yuan, J. S. Lee, C. E. Barry, 3rd, H. Wang, W. Zhang, and Y. Zhang.** 2011. Pyrazinamide inhibits trans-translation in *Mycobacterium tuberculosis*. Science **333:**1630-1632.

32. **Tree, J. J., G. C. Ulett, C. L. Ong, D. J. Trott, A. G. McEwan, and M. A. Schembri.** 2008. Trade-off between iron uptake and protection against oxidative stress: deletion of cueO promotes uropathogenic *Escherichia coli* virulence in a mouse model of urinary tract infection. J. Bacteriol. **190:**6909-6912.

33. **Veranic, P., A. Erman, M. Kerec-Kos, M. Bogataj, A. Mrhar, and K. Jezernik.** 2009. Rapid differentiation of superficial urothelial cells after chitosan-induced desquamation. Histochem. Cell Biol. **131:**129-139.

34. **Vigil, P. D., C. J. Alteri, and H. L. Mobley.** 2011. Identification of in vivo-induced antigens including an RTX family exoprotein required for uropathogenic *Escherichia coli* virulence. Infect. Immun. **79:**2335-2344.

35. **Vogel, J., and B. F. Luisi.** 2011. Hfq and its constellation of RNA. Nat. Rev. Microbiol. **9:**578-589.

36. **Wiles, T. J., R. R. Kulesus, and M. A. Mulvey.** 2008. Origins and virulence mechanisms of uropathogenic *Escherichia coli*. Exp. Mol. Pathol. **85:**11-19.

APPENDIX A

BACTERIAL LANDLINES: CONTACT-DEPENDENT SIGNALING IN BACTERIAL POPULATIONS

Reprint of: Blango, M.G. and Mulvey, M.A. (2009). Bacterial landlines: contact-dependent signaling in bacterial populations. Current Opinion in Microbiology 12, 1-5. Reprinted with permission of Elsevier Limited.

Available online at www.sciencedirect.com
ScienceDirect
Current Opinion in Microbiology

Bacterial landlines: contact-dependent signaling in bacterial populations

Matthew G Blango and Matthew A Mulvey

Bacterial populations utilize a variety of signaling strategies to exchange information, including the secretion of quorum-sensing molecules and contact-dependent signaling cascades. Although quorum sensing has received the bulk of attention for many years, contact-dependent signaling is forging a niche in the research world with the identification of novel systems and the emergence of more mechanistic data. Contact-dependent signaling is probably a common strategy by which bacteria in close contact, such as within biofilms, can modulate the growth and behavior of both siblings and competitors. Ongoing work with diverse bacterial systems, including *Myxococcus xanthus*, pathogenic *Escherichia coli* strains, *Bacillus subtilis*, and dissimilatory metal-reducing soil bacteria, is providing increasingly detailed insight into the dynamic mechanisms and potential of contact-dependent signaling processes.

Address
Division of Cell Biology and Immunology, Pathology Department, University of Utah, Room 2520, JMRB, 15 North Medical Drive East #2100, Salt Lake City, UT 84112-0565, United States

Corresponding author: Mulvey, Matthew A (mulvey@path.utah.edu)

Current Opinion in Microbiology 2009, **12**:177–181

This review comes from a themed issue on
Cell regulation
Edited by Charles Dorman and Urs Jenal

Available online 24th February 2009

1369-5274/$ – see front matter

DOI 10.1016/j.mib.2009.01.011

Introduction

We live in an information rich, highly interconnected world, much of which lies beyond our unaided senses in the domain of microbes. As a means of coordinating responses to changing environmental settings and surrounding microbes, bacteria have evolved a number of often-complex communication systems [1]. These can be broadly described as contact-independent and contact-dependent signaling mechanisms. The former is known classically as quorum sensing and involves the transfer of secreted molecules called autoinducers. As autoinducer levels increase throughout a growing bacterial population, changes in gene transcription are triggered resulting in altered growth rates and group dynamics [2]. Under some conditions, the secretion of autoinducers may become too taxing on available resources or may even stimulate unwanted attention from neighbors or host cells. Contact-dependent signaling cascades offer a means for more direct, and possibly less costly, communication between bacteria [1]. Like quorum sensing, contact-dependent signaling is also prone to modulation by cell density, with high cell numbers increasing the likelihood of interbacterial contact and subsequent signaling. The capacity of contact-dependent signaling cascades to modulate the behavior of both pathogenic and non-pathogenic bacteria remains incompletely understood, although emerging data indicate that this mode of direct cell-to-cell signaling can have profound impact on bacterial populations [1,3•,4•]. Here we review several of the known types of contact-dependent signaling, including C-signaling in myxobacteria and contact dependent inhibition in strains of *Escherichia coli*, emphasizing recent findings from the past two years.

C-signaling by *Myxococcus xanthus*

Myxobacteria are social, predatory, Gram-negative microbes that roam through soil in large packs stalking and consuming bacterial prey [3•]. When faced with starvation, myxobacteria undergo a remarkable multicellular developmental process resulting in the formation of macroscopic fruiting bodies containing thousands of spores [3•,5]. Complex intercellular signaling cascades drive sporulation, which promotes bacterial resistance to harsh environmental conditions and thereby enhances colony survival. Myxobacteria move by gliding motility to create foci where fruiting body formation is initiated, a process that relies on two types of bacterial motors [6–8]. The S (social) motor consists of type IV pili that extend and retract at the leading poles of migrating myxobacteria, pulling the microbes forward. At the trailing poles, nozzle-like structures comprising the A (adventurous) motor extrude slime that push the bacteria ahead. Pole-to-pole oscillations of motor components and regulators like FrzS appear to modulate activities of the S and A motors and consequently alter the reversal frequency of gliding motility. Changes in reversal frequencies cause mycobacteria to move as a traveling wave (rippling) or to aggregate, forming nascent fruiting bodies. Work with *Myxococcus xanthus* has demonstrated that rippling, aggregation, and subsequent sporulation require direct cell-to-cell contact. In some cases, this may involve transient fusion of membranes between adjacent bacteria, allowing the transfer and equilibration of A and S motor components among siblings [9]. These brief fusion events may help fine-tune fruiting body development, which is

also heavily reliant upon another contact-dependent process known as C-signaling.

C-signaling is mediated by a non-diffusable 17 kDa surface protein (p17) encoded by the *csgA* gene [3•]. Contact between neighboring myxobacteria initiates a bifurcated p17-dependent signaling cascade resulting in expression of genes required for either (1) rippling and aggregation or for (2) sporulation and further *csgA* expression [3•,10]. Low levels of p17-mediated C-signaling elevate the reversal frequencies of the A and S motors and thereby induce rippling, while high levels of C-signal reduce reversal frequencies and promote aggregation [6]. It is currently unclear how p17 promotes contact-dependent C-signaling and orchestrates the opposing processes of rippling and aggregation. However, recent work has delineated an intriguing mechanism by which C-signaling is initially activated [11••]. The p17 C-signal protein is derived from proteolytic cleavage of an inactive precursor, p25, which accumulates at the surface of both vegetative and starving cells. During starvation, Rolbetzki *et al.* found that a subtilisin-like protease referred to as the *protease required for processing of C-signal precursor* (PopC) cleaves p25–p17. PopC is retained within the cytoplasm of vegetative cells and is slowly secreted from myxobacteria only during starvation. Once secreted, PopC is rapidly degraded and is unable to act *in trans* on neighboring microbes. This system ensures the gradual build-up of C-signaling as nutrient levels are depleted and represents the first example of regulated proteolysis by secretion of a protease to the extracellular environment. PopC has no recognizable signal peptide and the pathway by which it is secreted is not yet known. It will be interesting to learn what specifically triggers PopC secretion and its subsequent rapid degradation outside of the cell.

Crosstalk in *Bacillus subtilis*

Like *M. xanthus*, the Gram-positive soil bacteria *Bacillus subtilis* also undergoes a contact-dependent differentiation process as a means to produce dormant spores when faced with starvation [12]. Under nutrient poor conditions, a vegetative *B. subtilis* cell will divide asymmetrically, forming a large mother cell and a smaller daughter cell called a forespore [12,13]. Internalization of the forespore by the mother cell creates a two-chamber sporangium in which the forespore matures into an endospore. Despite their intimate association within the sporangium, mother cell and forespore remain separated by two membrane bilayers and maintain distinct gene expression profiles [12,14,15]. Endospore formation is an energy intensive process that is coordinated by multiple signaling pathways involving several different sigma factors in both the forespore and mother cell. Consideration of one of these sigma factors, σ^G, highlights the degree of crosstalk between forespore and mother cell during sporulation.

Activation of σ^G stimulates late gene expression within the forespore and is dependent upon two other genes, *spoIIIAH* and *spoIIQ*, expressed by the mother cell [16••,17,18•]. SpoIIIAH is homologous to the YscJ/FliF family of proteins that form ring-shaped multimeric complexes as part of type III secretion and flagella systems. Recent work indicates that SpoIIQ anchors SpoIIIAH in punctate foci within the membranes (septum) surrounding the forespore [17]. These complexes made up of SpoIIIAH and SpoIIQ may then act as scaffolding for the assembly of export channels leading from mother cell to forespore [16••,18•]. Presumably, the delivery of one or more substrates into the forespore via SpoIIIAH-dependent channels is required for σ^G activation and completion of endospore formation. Whether the required substrate is a protein, nutrients, or some other small molecule remains to be determined. The formation of channels within the septum of sporangium does not appear to be restricted to SpoIIIAH/SpoIIQ, as evidence by recent results indicating that an ATPase known as SpoIIIE can assemble into linked membrane spanning channels involved in the translocation of DNA from mother cell to forespore [19].

Contact-dependent inhibition in *E. coli*

In 2005, Low and co-workers discovered a novel contact-dependent inhibition (CDI) system while working with the wild-type *E. coli* isolate EC93 [20]. While in logarithmic growth phase, a single *E. coli* cell expressing the CDI system can inhibit the growth of hundreds of susceptible target cells in mixed cultures, forcing them to enter a viable but non-replicating state. CDI requires direct contact between effector and target cells and is mediated by expression of two contiguous genes, *cdiB* and *cdiA*, that encode members of the two-partner secretion (TPS) family. On the basis of the similarities with other TPS members, it is likely that CdiB forms a β-barrel channel within the outer membrane of *E. coli* through which CdiA is exported. CdiA is an exceptionally large protein by bacterial standards, having an initial mass of about 303 kDa. However, during maturation CdiA is proteolytically cleaved at two sites within its C-terminus, causing the release of soluble CdiA fragments and leaving two thirds of the protein bound to the outer membrane. Recent results indicate that inter-bacterial interactions between membrane-bound CdiA and the outer membrane protein BamA (β-barrel assembly machine protein A) probably initiate CDI in susceptible target cells [21••]. BamA is a conserved member of the YaeT/Omp85 family of proteins required for the biogenesis of β-barrel outer membrane proteins (OMPs) in bacteria, mitochondria, and chloroplasts [22–24]. Anti-BamA antibodies, as well as reduced BamA expression, decrease the susceptibility of target *E. coli* cells to CDI [21••]. Interestingly, mutation of BamA so that it no longer functions in the assembly of β-barrel OMPs does not protect against CDI. The same genetic screen that identified BamA as a

Figure 1

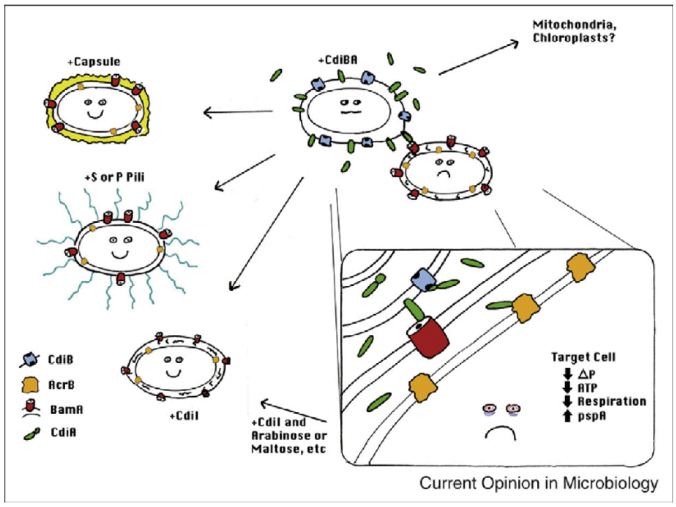

Model of the contact-dependent inhibition system. Contact with CdiBA-positive *E. coli* cells triggers decreased membrane potential (Δ*p*), ATP levels, and respiration in susceptible target cells (sad face). This metabolic downregulation coincides with activation of the phage shock response (pspA). BamA acts as the receptor for CDI, with AcrB as a downstream target (close-up inset). Other targets may potentially include BamA homologs expressed by mitochondria and chloroplasts. Expression of capsule, P or S pili, or CdiI renders bacterial cells (happy faces) resistant to CDI. Growth arrest by CDI is reversible by induced expression of CdiI in the presence of suitable carbon sources.

putative receptor for CdiA also indicated a role for *acrB* in CDI susceptibility. The AcrB gene product is an inner membrane protein that associates with AcrA in the periplasm and TolC within the outer membrane to form an envelope-spanning multi-drug efflux pump [25]. Mutation of *acrB* renders *E. coli* cells resistant to CDI, while *tolC* and *acrA* mutants are still susceptible [21••].

Natural resistance to CDI is afforded by expression of a small immunity gene, *cdiI*, which is physically linked with *cdiBA* in some *E. coli* isolates [20]. In the absence of CdiI, the expression of capsule and certain types of filamentous adhesive organelles known as S and P pili can also provide immunity [4•,20]. The mechanisms by which these factors mediate immunity to CDI are not yet clear. One potential argument that S and P pili block CDI by sterically hindering contact between CDI^+ effector cells and target bacteria is countered by observations that expression of related type 1 pilus structures does not provide immunity [20]. By using an inducible *cdiI* construct, Low and co-workers recently generated an inducible CDI autoinhibition system, allowing them to monitor a single population of *E. coli* undergoing CDI [4•]. Use of this system revealed that the onset of CDI correlates with substantial drops in proton motive force (Δ*p*), ATP levels, and aerobic respiration, although it is not yet clear if these metabolic effects are the cause or consequence of CDI. The CDI-induced decrease in Δ*p* was also found to induce a phage shock response, but this did not appear to be necessary for CDI [4•]. Induction of CdiI expression in the presence of a suitable carbon source (maltose, ribose, lactose, or glycerol) prompted CDI-arrested cells to resume growth, demonstrating that the effects of CDI are reversible.

A summary of our current understanding of CDI and CDI resistance is presented in Figure 1. One intriguing scenario for induction of CDI put forth by Aoki *et al.* involves delivery of a proteolytic fragment of CdiA into target cells via a BamA-dependent process [21••]. Once internalized, this peptide may alter the antiporter activity of AcrB, resulting in ion leakage and subsequent breakdown of Δ*p*. Alternately, AcrB may act to transport the CdiA fragment further into the cell where it modulates the activities of other factors. Determination of whether CdiA acts in such a direct fashion or functions more indirectly by triggering specific signaling cascades at the bacterial cell surface awaits further study. Similarly mysterious is the role of CDI within wild bacterial populations. Comparative bioinformatics studies have revealed that homologous CDI systems are encoded by many strains of uropathogenic *E. coli* as well as pathogens like *Yersinia pestis* and *Burkholderia pseudomallei* [20]. CDI may enable these pathogens to inhibit competing bacteria or may enhance their own resistance to oxidative stress and antibacterial peptides, most of which are ineffective when Δ*p* is low [4•]. Many of the

bacteria that possess CDI systems can act as opportunistic intracellular pathogens, raising the possibility that CdiA may also target host components. Specifically, by interacting with the BamA homologs Sam50 and Toc75 expressed by mitochondria and chloroplasts, respectively, CdiA may allow some intracellular pathogens to manipulate vital host organelles during the course of an infection.

Nanowires

One of the first recognized instances of contact-dependent communication between bacteria is, arguably, conjugation mediated by sex (F) pili [26]. Bacteria encode a large variety of other pilus types and adhesive molecules, many of which have been studied primarily with respect to their abilities to modulate bacteria–host cell interactions. However, it is feasible that some of these organelles also function in inter-bacterial communication. For example, recent studies indicate that several types of soil bacteria known as dissimilatory metal reducing bacteria can express complex networks of electrically conductive pili known as nanowires [27•,28,29]. It is proposed that nanowires function in the transfer of electrons from the environment to and between bacteria within a localized population, presumably as a means to augment more standard energy exchange mechanisms. It is conceivable that such a system may also be adopted to transmit signals between bacteria as a possible means to coordinate group bacterial behavior. Nanowires, like other pilus types, can also apparently promote biofilm formation independent of their ability to transfer electrons [30]. Emerging data suggest that nanowire expression is widespread among metabolically and taxonomically diverse groups [28,29], raising the possibility that these structures can impact many bacterial processes, including pathogenesis.

Conclusions

Since the 2005 discovery of CdiA and CdiB, two other CDI systems have been identified in *E. coli* [31,32]. In contrast to the original CDI system defined by Aoki *et al.* [20], these other systems are active only with stationary phase cultures and currently have no clear mechanism of action. These findings indicate that contact-dependent mechanisms like CDI may be more wide spread among *E. coli* and other bacteria than previously suspected. Defining the functional relevance of these and related systems within environmental and host settings is emerging as a major challenge. A greater understanding of contact-dependent bacterial communication promises to highlight novel anti-bacterial therapeutic targets in pathogens and may also help advance fields such as fuel cell biology, where increased inter-bacterial connectivity via nanowires or other structures can potentially enhance productivity [33•]. Furthermore, continued analysis of diverse contact-dependent bacterial communication systems may shed light on the development of true multicellularity during evolution.

Conflicts of interest

The authors have no conflicts of interest with respect to this manuscript.

Acknowledgement

Work in the authors' laboratory is supported by Grant DK068585 from the National Institutes of Health.

References and recommended reading

Papers of particular interest, published within the annual period of review, have been highlighted as:

- • of special interest
- •• of outstanding interest

1. Bassler BL, Losick R: **Bacterially speaking**. *Cell* 2006, **125**:237-246.

2. Miller MB, Bassler BL: **Quorum sensing in bacteria**. *Annu Rev Microbiol* 2001, **55**:165-199.

3. • Kaiser D: **Myxococcus-from single-cell polarity to complex multicellular patterns**. *Annu Rev Genet* 2008, **42**:109-130.
This is a well-written, comprehensive review of myxococal C-signaling and fruiting body formation.

4. • Aoki SK, Webb JS, Braaten BA, Low DA: **Contact-dependent growth inhibition causes reversible metabolic downregulation in *Escherichia coli***. *J Bacteriol* 2009.
The authors demonstrate that CDI is reversible and correlates with decreases in ATP levels, proton motive force, and respiration in target cells.

5. Curtis PD, Taylor RG, Welch RD, Shimkets LJ: **Spatial organization of *Myxococcus xanthus* during fruiting body formation**. *J Bacteriol* 2007, **189**:9126-9130.

6. Stevens A, Sogaard-Andersen L: **Making waves: pattern formation by a cell-surface-associated signal**. *Trends Microbiol* 2005, **13**:249-252.

7. Kaiser D: **Social gliding is correlated with the presence of pili in *Myxococcus xanthus***. *Proc Natl Acad Sci USA* 1979, **76**:5952-5956.

8. Wolgemuth C, Hoiczyk E, Kaiser D, Oster G: **How myxobacteria glide**. *Curr Biol* 2002, **12**:369-377.

9. Nudleman E, Wall D, Kaiser D: **Cell-to-cell transfer of bacterial outer membrane lipoproteins**. *Science* 2005, **309**:125-127.

10. Sogaard-Andersen L, Slack FJ, Kimsey H, Kaiser D: **Intercellular C-signaling in *Myxococcus xanthus* involves a branched signal transduction pathway**. *Genes Dev* 1996, **10**:740-754.

11. •• Rolbetzki A, Ammon M, Jakovljevic V, Konovalova A, Sogaard-Andersen L: **Regulated secretion of a protease activates intercellular signaling during fruiting body formation in *M. xanthus***. *Dev Cell* 2008, **15**:627-634.
The authors demonstrate that starvation triggers the secretion of a short-lived subtilisin-like protease PopC, which cleaves and activates the C-signal. These results represent the example in bacteria of regulated proteolysis via compartmentalization.

12. Errington J: **Regulation of endospore formation in *Bacillus subtilis***. *Nat Rev Microbiol* 2003, **1**:117-126.

13. Ben-Yehuda S, Losick R: **Asymmetric cell division in *B. subtilis* involves a spiral-like intermediate of the cytokinetic protein FtsZ**. *Cell* 2002, **109**:257-266.

14. Doan T, Marquis KA, Rudner DZ: **Subcellular localization of a sporulation membrane protein is achieved through a network of interactions along and across the septum**. *Mol Microbiol* 2005, **55**:1767-1781.

15. Serrano M, Vieira F, Moran CP Jr, Henriques AO: **Processing of a membrane protein required for cell-to-cell signaling during endospore formation in *Bacillus subtilis***. *J Bacteriol* 2008, **190**:7786-7796.

16. •• Meisner J, Wang X, Serrano M, Henriques AO, Moran CP Jr: **A channel connecting the mother cell and forespore during bacterial endospore formation**. *Proc Natl Acad Sci USA* 2008, **105**:15100-15105.
Using compartmentalized biotinylation assays, the authors show that SpoIIIAH forms part of a multimeric channel between the forespore and mother cell during sporulation of *B. subtilis*. These results suggest a mechanism by which substrate is transferred between mother cell and forespore, leading to activation of σ^G.

17. Campo N, Marquis KA, Rudner DZ: **SpoIIQ anchors membrane proteins on both sides of the sporulation septum in *Bacillus subtilis***. *J Biol Chem* 2008, **283**:4975-4982.

18. • Camp AH, Losick R: **A novel pathway of intercellular signalling in *Bacillus subtilis* involves a protein with similarity to a component of type III secretion channels**. *Mol Microbiol* 2008, **69**:402-417.
Using genetic analysis and bioinformatics, the authors conclude that SpoIIIAH forms a channel between mother cell and forespore that is crucial for σ^G activation. See reference [16••].

19. Burton BM, Marquis KA, Sullivan NL, Rapoport TA, Rudner DZ: **The ATPase SpoIIIE transports DNA across fused septal membranes during sporulation in *Bacillus subtilis***. *Cell* 2007, **131**:1301-1312.

20. Aoki SK, Pamma R, Hernday AD, Bickham JE, Braaten BA, Low DA: **Contact-dependent inhibition of growth in *Escherichia coli***. *Science* 2005, **309**:1245-1248.

21. •• Aoki SK, Malinverni JC, Jacoby K, Thomas B, Pamma R, Trinh BN, Remers S, Webb J, Braaten BA, Silhavy TJ *et al.*: **Contact-dependent growth inhibition requires the essential outer membrane protein BamA (YaeT) as the receptor and the inner membrane transport protein AcrB**. *Mol Microbiol* 2008, **70**:323-340.
Using transposon mutagenesis, this study defines BamA as the target cell receptor for the CDI system while AcrB was identified as a potential downstream target of the CdiA signaling. This study represents a major step toward understanding the mechanism of CDI.

22. Bredemeier R, Schlegel T, Ertel F, Vojta A, Borissenko L, Bohnsack MT, Groll M, von Haeseler A, Schleiff E: **Functional and phylogenetic properties of the pore-forming beta-barrel transporters of the Omp85 family**. *J Biol Chem* 2007, **282**:1882-1890.

23. Chan NC, Lithgow T: **The peripheral membrane subunits of the SAM complex function codependently in mitochondrial outer membrane biogenesis**. *Mol Biol Cell* 2008, **19**:126-136.

24. Kim S, Malinverni JC, Sliz P, Silhavy TJ, Harrison SC, Kahne D: **Structure and function of an essential component of the outer membrane protein assembly machine**. *Science* 2007, **317**:961-964.

25. Murakami S: **Multidrug efflux transporter, AcrB—the pumping mechanism**. *Curr Opin Struct Biol* 2008, **18**:459-465.

26. Brinton CC Jr: **The structure, function, synthesis and genetic control of bacterial pili and a molecular model for DNA and RNA transport in Gram-negative bacteria**. *Trans NY Acad Sci* 1965, **27**:1003-1054.

27. • Ntarlagiannis D, Atekwana EA, Hill EA, Gorby YA: **Microbial nanowires: Is the subsurface 'hardwired'?** *Geophys Res Lett* 2007:34.
This study describes the ability of nanowires produced by the dissimilatory metal-reducing soil bacteria *Shewanella oneidensis* to conduct electrical current through a column of sand. Mutants lacking conductive pili were unable to transfer.

28. Reguera G, McCarthy KD, Mehta T, Nicoll JS, Tuominen MT, Lovley DR: **Extracellular electron transfer via microbial nanowires**. *Nature* 2005, **435**:1098-1101.

29. Gorby YA, Yanina S, McLean JS, Rosso KM, Moyles D, Dohnalkova A, Beveridge TJ, Chang IS, Kim BH, Kim KS *et al.*: **Electrically conductive bacterial nanowires produced by *Shewanella oneidensis* strain MR-1 and other microorganisms**. *Proc Natl Acad Sci USA* 2006, **103**:11358-11363.

30. Reguera G, Pollina RB, Nicoll JS, Lovley DR: **Possible nonconductive role of *Geobacter sulfurreducens* pilus nanowires in biofilm formation**. *J Bacteriol* 2007, **189**:2125-2127.

31. Lemonnier M, Levin BR, Romeo T, Garner K, Baquero MR, Mercante J, Lemichez E, Baquero F, Blazquez J: **The evolution of contact-dependent inhibition in non-growing populations of *Escherichia coli***. *Proc Biol Sci* 2008, **275**:3-10.

32. Murat D, Goncalves L, Dassa E: **Deletion of the *Escherichia coli* uup gene encoding a protein of the ATP binding cassette superfamily affects bacterial competitiveness**. *Res Microbiol* 2008, **159**:671-677.

33. • Lovley DR: **The microbe electric: conversion of organic matter to electricity**. *Curr Opin Biotechnol* 2008, **19**:564-571.
This clear and recent review describes the broad applications of bacterial nanowires in microbial fuel cell production.

APPENDIX B

UROPATHOGENIC *ESCHERICHIA COLI* INDUCES SERUM AMYLOID A IN MICE FOLLOWING URINARY TRACT AND SYSTEMIC INOCULATION

Reprint of: Erman A, Lakota K, Mrak-Poljsak K, Blango MG, Krizan-Hergouth V, et al. (2012) Uropathogenic *Escherichia coli* Induces Serum Amyloid A in Mice following Urinary Tract and Systemic Inoculation. PLoS ONE 7(3): e32933. doi:10.1371/journal.pone.0032933

OPEN ACCESS Freely available online

PLoS one

Uropathogenic *Escherichia coli* Induces Serum Amyloid A in Mice following Urinary Tract and Systemic Inoculation

Andreja Erman[1], Katja Lakota[2], Katjusa Mrak-Poljsak[2], Matthew G. Blango[3], Veronika Krizan-Hergouth[4], Matthew A. Mulvey[3], Snezna Sodin-Semrl[2]*, Peter Veranic[1]

1 Faculty of Medicine, Institute of Cell Biology, University of Ljubljana, Ljubljana, Slovenia, **2** Department of Rheumatology, University Medical Centre-Ljubljana, Ljubljana, Slovenia, **3** Division of Microbiology and Immunology, Department of Pathology, University of Utah, Salt Lake City, Utah, United States of America, **4** Faculty of Medicine, Institute of Microbiology and Immunology, University of Ljubljana, Ljubljana, Slovenia

Abstract

Serum amyloid A (SAA) is an acute phase protein involved in the homeostasis of inflammatory responses and appears to be a vital host defense component with protective anti-infective properties. SAA expression remains poorly defined in many tissues, including the urinary tract which often faces bacterial challenge. Urinary tract infections (UTIs) are usually caused by strains of uropathogenic *Escherichia coli* (UPEC) and frequently occur among otherwise healthy individuals, many of whom experience bouts of recurrent and relapsing infections despite the use of antibiotics. To date, whether SAA is present in the infected urothelium and whether or not the induction of SAA can protect the host against UPEC is unclear. Here we show, using mouse models coupled with immunofluorescence microscopy and quantitative RT-PCR, that delivery of UPEC either directly into the urinary tract via catheterization or systemically via intraperitoneal injection triggers the expression of SAA. As measured by ELISA, serum levels of SAA1/2 were also transiently elevated in response to UTI, but circulating SAA3 levels were only up-regulated substantially following intraperitoneal inoculation of UPEC. In *in vitro* assays, physiological relevant levels of SAA1/2 did not affect the growth or viability of UPEC, but were able to block biofilm formation by the uropathogens. We suggest that SAA functions as a critical host defense against UTIs, preventing the formation of biofilms both upon and within the urothelium and possibly providing clinicians with a sensitive serological marker for UTI.

Citation: Erman A, Lakota K, Mrak-Poljsak K, Blango MG, Krizan-Hergouth V, et al. (2012) Uropathogenic *Escherichia coli* Induces Serum Amyloid A in Mice following Urinary Tract and Systemic Inoculation. PLoS ONE 7(3): e32933. doi:10.1371/journal.pone.0032933

Editor: Adam J. Ratner, Columbia University, United States of America

Received July 22, 2011; **Accepted** February 3, 2012; **Published** March 12, 2012

Funding: This work was supported by the Ministry of High Education, Science and Technology of Slovenia and National Institutes of Health (NIH) Public Health Service grants DK068585 and AI095647 (USA). M.G.B. was supported by NIH Microbial Pathogenesis Training Grant T32 AI055434. The funders had no role in study design, data collection and analysis, decision to publish, or preparation of the manuscript.

Competing Interests: The authors have declared that no competing interests exist.

* E-mail: ssodin1@yahoo.com

Introduction

Upon entering the urinary tract, strains of uropathogenic *Escherichia coli* (UPEC) face a barage of both constitutive and inducible host defenses. Despite this hostile environment, which often includes the presence of antibiotics, UPEC is frequently able to establish itself within the host, multiply, and persist for many days to months. Persistence of UPEC within the bladder is in part attributable to the ability of these pathogens to invade urothelial cells where they can either multiply, forming large biofilm-like communities, or alternatively establish latent resevoirs which may ultimately lead to episodes of recurrent or relapsing urinary tract infections (UTIs) [1,2]. Persistent and recurring UTIs due to UPEC represent a major clinical and financial burden worldwide [1]. The development of better approaches for the prevention and treatment of UTIs is dependent upon improved understanding of UPEC virulence strategies as well as the make-up and limitations of the host defenses employed against UPEC.

Serum amyloid A (SAA) is an acute phase protein thought to be involved in inflammation and homeostasis. SAA is a seemingly critical host defense component and has been reported to have beneficial properties in the protection against fungal, viral, and bacterial infections [3,4,5,6,7,8,9], and may help reduce the incidence of recurrent infections [4]. In planar lipid bilayers, SAA can assemble into hexameric structures, each containing a central channel of about 2.5 nm in diameter, and having the potential to damage bacterial membranes [10,11]. Overexpression of SAA by intestinal epithelial cells in culture can reduce *E. coli* viability [12], and in *in vitro* assays SAA can act as an opsonin for various Gram-negative bacteria by binding to the highly expressed outer membrane protein OmpA [9]. Of note, the ability of some *E. coli* strains to invade host cells and form biofilms is critically dependent upon OmpA [13,14,15,16]. Preferential binding of SAA to OmpA over endogenous host ligands, including high density lipoprotein (HDL) [4], may significantly impact both the host environment and pathogen fitness during the course of an infection.

During acute phase responses to infection, SAA secretion by hepatocytes can be greatly increased, leading to highly elevated concentrations of SAA in the circulation. This phenomenon is common among vertebrate species. For example, LPS treatment stimulates SAA expression by salmon hepatocytes [17] and in zebrafish infection models, SAA is often among the most highly upregulated gene products [18,19,20,21]. In reindeer, as well as mice and humans, SAA can be used as a sensitive marker of the acute phase response to bacterial infection [22]. Similarities in SAA as an acute-phase marker in both mice and humans make mice an accessible model for investigating the regulatory and

functional roles of SAA. This has not been the case with the classical human inflammatory marker C-reactive protein (CRP), which is not expressed in mice. It was recently reported, based on measurements from 219 blood donors, that SAA concentrations in sera have a median value of 20 μg/ml as determined by ELISA [23]. SAA is induced in murine models of both *E. coli*-associated mastitis [24] and colitis [12,25], but there is currently no data regarding changes in localized or systemic levels of SAA during a UTI.

Four functional isoforms of SAA are present in mice [26]. SAA1 and SAA2 are highly homologous isotypes produced primarily in the liver. SAA3 is evolutionarily distinct from SAA1/2 and can be synthesized extrahepatically, with abundant expression found in adipose tissue and the mouse colon [12,25]. SAA3 has also been identified as the most up-regulated message following *E. coli* infection of primary mammary epithelial cells [27]. In addition, *in vitro* experiments showed that a 10-mer peptide derived from human mammary-associated serum amyloid A3 (M-SAA3) can interfere with the adherence of enteropathogenic *E. coli* (EPEC) to intestinal epithelial cells [28]. Results presented here demonstrate that SAA1/2, and to a lesser extent SAA3, are induced both locally within the bladder and systemically in response to infection with UPEC. Furthermore, we show that UPEC is resistant to any bactericidal or bacteriostatic effects associated with SAA, although this acute phase protein can effectively inhibit biofilm formation by the uropathogens.

Materials and Methods

Ethics Statement

Mice were used for this study in accordance with European guidelines and the Slovenian legislation. The study was approved by the Veterinary Board of Slovenia Ethics Committee with the permit number 34401-8/2009/6.

Animals and bacterial strains

Adult 8-week-old female C57BL/6JOLaHsd mice were housed at room temperature (22–24°C) with 45–65% humidity and a 12-hr light/12-hr dark cycle and received food and water *ad libitum*. Animals were euthanized by CO_2 inhalation. The K-12 strain MG1655 and the UPEC isolates UTI89 and F11 have been described previously [29,30,31].

SAA

Lyophilized human recombinant serum amyloid A (SAA, endotoxin-tested) (Peprotech, London, UK) was spun down, reconstituted according to manufacturer's instructions in cell culture grade sterile water to a stock concentration of 1 μg/μl, and stored at −20°C until used. This recombinant SAA is a hybrid between SAA1 and SAA2, being identical to human SAA1α except for the presence of an N-terminal methionine and SAA2β-like substitutions of asparagine to aspartic acid and arginine to histidine at positions 60 and 71, respectively.

Mouse UTI model

Mice were anesthetized with ketamine HCl (100 mg/kg i.p.) and xylazine (10 mg/kg i.p.) prior to inoculation with a 100 μl suspension of UTI89 (10^8 CFU) in phosphate-buffered saline (PBS) via transurethral catheterization using a sterile polyethylene catheter with 0.28 mm inside diameter (Intramedic, Becton Dickinson, Sparks, MD, USA). Before catheterization, the bladder of each animal was emptied by gentle pressure on the abdomen. Infusions were performed gradually and at a slow rate to avoid injury or vesicoureteral reflux. The catheter, sheathed over a 30 G needle connected to a 1 ml syringe, was retained in the urinary bladder for 30 min. After removal of the catheter, mice were allowed to void normally. To check if this infection protocol resulted in pyelonephritis, we tested the kidneys of infected mice. Paraffin sections of kidneys, which were recovered 24 h, 4 days

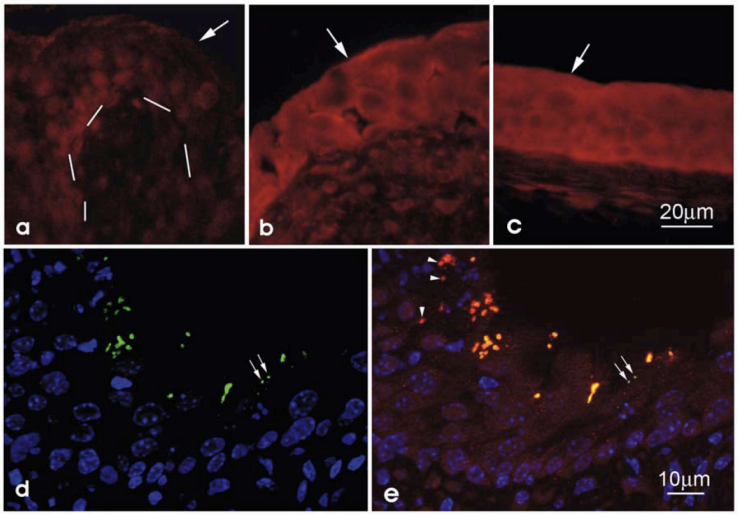

Figure 1. Induction and localization of SAA1/2 following inoculation of the bladder with UPEC. Immunofluorescence miscroscopy of bladder sections showing SAA1/2 (red) levels and distribution in sham-infected (PBS-treated) mice (A) and mice that were infected for either one (B) or four days (C) via intravesical instillation of the UPEC isolate UTI89. (D and E) Localization of UPEC (green) with host cell nuclei (blue) and SAA1/2 at 4 d post - inoculation of the bladder with UTI89. Large arrows point to the apical membrane of urothelium and bars mark the border between urothelium and lamina propria. Small arrows indicate a few bacteria that do not co-localize with SAA1/2.
doi:10.1371/journal.pone.0032933.g001

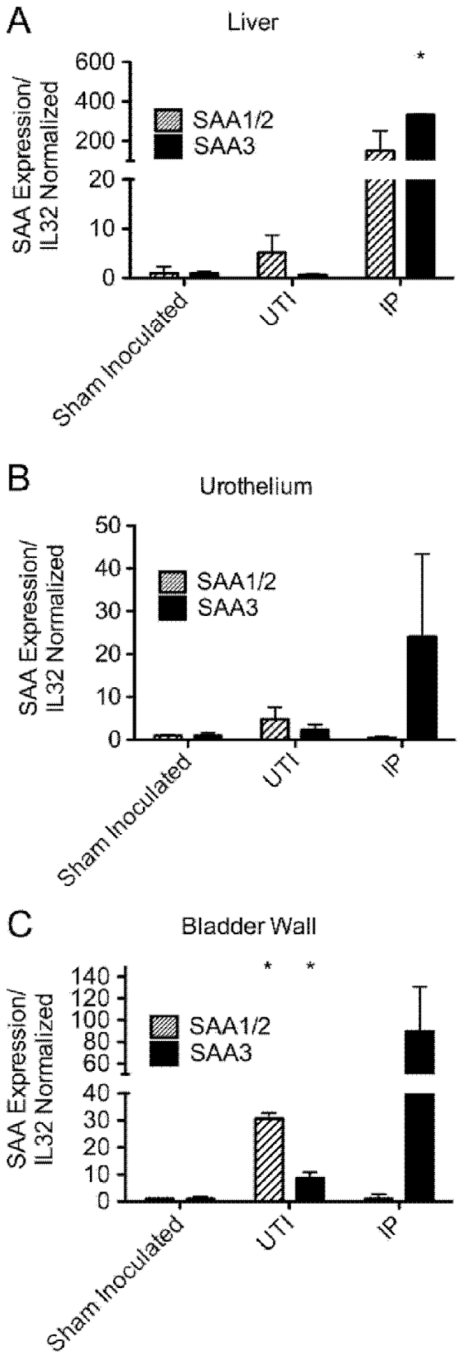

Figure 2. Quantification of SAA mRNA expression in response to UPEC. Four mice were either sham inoculated with PBS alone or infected with UTI89 via catheterization to initiate UTI. Alternatively, mice were infected systemically via IP injections of UTI89, with control animals recieving only PBS. After 1 d, levels of SAA1/2 and SAA3 in the (A) bladder wall, (B) isolated urothelium, and (C) liver were quantified relative to ribosomal L32 transcript levels. *, $p<0.05$ relative to sham inoculated animals as determined by Student's *t* test. The mean +/− SD of triplicate experiments are shown.
doi:10.1371/journal.pone.0032933.g002

and 14 days after instillation of UPEC were analyzed by a pathologist, provided no evidence of bacterial infection or inflammation. Urinary bladders, liver and blood were taken immediately after sacrifice.

Intraperitoneal infections

Four mice were inoculated via intraperitoneal injection with 200 µl of a suspension containing 10^8 CFU of UTI89 in PBS. The same amount of sterile PBS was received by four sham inoculated animals. After 1 day, mice were sacrificed and bladders, liver and blood were taken immediately.

Immunofluorescence labeling

Bladders were fixed for 2 h using 3% paraformaldehyde in PBS, rinsed overnight in 30% saharose, frozen, and cut into 7-µm-thick sections. After washing in PBS, sections were permeabilized in cold acetone for 5 min, quick-dried, blocked in 3% BSA in PBS and incubated overnight at 4°C with primary antibodies against SAA (rabbit polyclonal antibodies developed against synthetically produced peptides of SAA1/2; a gift of Prof. Malle, Medical University of Graz) diluted 1:100 in 1% BSA in PBS. After washing in PBS, samples were incubated in the dark at 37°C for 1 h with Alexa Fluor® 555 labelled goat anti-rabbit secondary antibodies (Invitrogen, Molecular Probes, Leiden, Netherlands) diluted 1:300 in 1% BSA in PBS. After prolonged washing in PBS, sections were incubated at 37°C for 1 h with fluorescein isothiocyanate (FITC)-labelled rabbit polyclonal antibodies against *E. coli* (1:10; Abcam, Cambridge, UK). After additional washing in PBS, sections were mounted in antibleaching mounting medium Vectashield containing 4′, 6-diamidino-2-phenylindole (DAPI) (Vector Laboratories, Burlingame, CA, USA) to stain DNA. Proper negative controls, in which both primary antibodies were replaced with serum from non-immunized animals, were performed. The samples were analysed using a Nikon Eclipse TE 300 fluorescence microscope (Amstelveen, Netherlands).

ELISA

Mouse serum was centrifuged from whole blood collected using a syringe in the heart, aliquoted, and stored at −20°C until used. The concentrations of SAA1 (Invitrogen, CA, USA) and SAA3 (Millipore, MA, USA) were measured in duplicate assays following the manufacturer's instructions. Samples were thawed, allowed to reach room temperature and, if necessary, diluted with standard diluent buffer (1:40 for SAA1, undiluted for SAA3, except in samples from IP injected mice, where an 1:2000 was used) provided in the ELISA kits. After obtaining absorbance readings, SAA concentrations were calculated from standard curves. Statistical analysis was performed using mean ± SD and Student's t-tests.

RNA isolation and quantitative PCR analysis

Total RNA from various mouse tissues, including the liver, urothelium (mechanically peeled away from the bladder), and urinary bladder wall without the urothelium, was isolated using PureLink RNA Mini Kit (Invitrogen, CA, USA) following the manufacturer's instructions. The purity and amount of RNA was determined by measuring the OD at a ratio of 260 to 280 nm. cDNA was generated from 1 µg of total RNA using the Reverse Transcription System (Promega, WI, USA) with oligo(dT) primers, and qPCR was performed with StepOne (Applied Biosystems, CA,

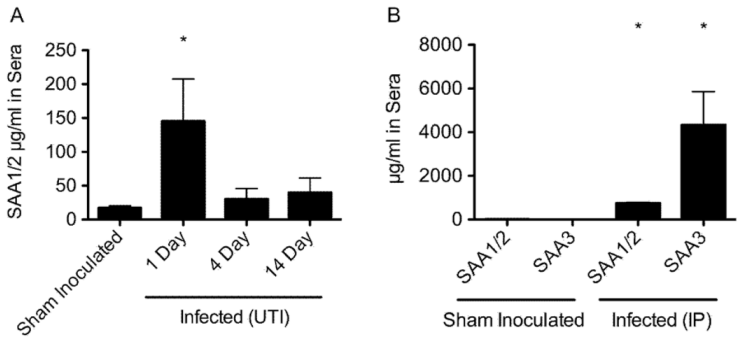

Figure 3. ELISA of mouse sera at different time points after infection. Four mice were inoculated with UTI89 via either (A) transurethral catheterization or (B) IP injection. (A) Serum levels of SAA1/2 and SAA3 in mice were quantified by ELISA in sham inoculated animals and at 1, 4, and 14 d after UTI89 instillation into the bladder (UTI). SAA3 was not detected in these samples. (B) Substantially higher serum levels of SAA1/2 and SAA3 were detected 1 d after infection with UTI89 via IP injection. *, $p<0.05$ relative to sham inoculated animals as determined by Student's *t* test. The mean +/− SD of triplicate experiments are shown.
doi:10.1371/journal.pone.0032933.g003

USA) and Power SYBR Green PCR Master Mix (Applied Biosystems, Warrington, UK) using SAA-specific primers and ribosomal protein L32 primers serving as endogenous control for normalization as described in [25]. Dissociation curves of products showed only one peak in each PCR reaction. 900 nM of forward and reverse primers were used to amplify SAA1/2 and SAA3, while 300 nM of primers were used for L32. Data analysis was done using 2ΔΔCt method with normalization to the level of L32.

Biofilm and Bacterial Growth Assays

Microtiter plate-based biofilm assays were carried out as previously described [2]. In brief, bacterial strains from overnight shaking cultures were diluted 1:100 in M9 minimal medium, and quadruplicate 100-µl samples were incubated ±0, 0.5, 1 and 5 µg/ml SAA in 96-well pinchbar flat-bottomed polystyrene microtiter plates with lids for two days at 30°C without shaking. Nonadherent bacterial cells were then removed by gentle washings with distilled H_2O and the remaining biofilm-associated bacteria were stained for 10 min at room temperature with 150 µl of a 0.1% solution of crystal violet in water, (Sigma-Aldrich, MO, USA). Wells were then washed with H_2O, air dried for 30 min, and incubated for 15 min with 200 µl dimethyl sulfoxide (DMSO) to release the incorporated dye. After transferring a 150-µl aliquot from each well to a new microtiter plate, A_{562} was measured using a Synergy HT multidetection plate reader (BioTek Instruments, Inc., VT, USA).

Bacterial growth curves were acquired using quadruplicate 200-µl cultures of MG1655, UTI89, and F11 shaking in M9 minimal medium ±0, 5, or 20 µg/ml SAA at 37°C in 100-well honeycomb plates using a Bioscreen C instrument (Growth Curves, USA), as previosuly described [32].

Results

To investigate the ability of UPEC to affect SAA expression in the host, we employed a well-established mouse UTI model system. At 1 and 4 d following catheterization of adult female C57BL/6JOLaHsd mice with the UPEC isolate UTI89, levels of SAA1/2 in the urothelium were observed to be notably elevated relative to uninfected controls (**Fig. 1A–C**). Within the urothelial cells, SAA1/2 was primarily situated within the cytosol, where it co-localized strongly with internalized UPEC (**Fig. 1D and E**). Upregulation of SAA at day 1 post-inoculation of the bladder with UTI89 was confirmed by qRT-PCR of the bladder wall as well as the isolated urothelium and the liver (**Fig. 2**). SAA1/2 expression levels were elevated more than 4.8-fold in the liver and urothelium, and more than 30-fold in the bladder wall, while the relative induction of SAA3 expression in these tissues in response to UTI was less robust. However, in control experiments in which mice were infected systemically with UTI89 delivered via intraperitoneal (IP) injection, SAA3 expression was markedly increased in the liver (more than 300-fold) as well as in the urothelium (~20-fold) and bladder wall (~90-fold).

Within 1 d following instillation of mouse bladders with UTI89, we observed by ELISA a substantial 8-fold increase in SAA1 serum levels, which decreased by day 4 and remained subdued up to day 14 (**Fig. 3A**). In contrast, serum levels of SAA3 were not altered in response to UTI (data not shown). However, following IP injection of UTI89 we did detect significant and notably large increases in circulating SAA3 levels along with corresponding, although smaller, increases in SAA1/2 levels (**Fig. 3B**). This is the first time, to our knowledge, that serum SAA3 protein levels have been shown to increase substantially in response to UPEC delivered intraperitoneally.

Previous work indicated that recombinant SAA1/2 expressed by cultured host cell lines can inhibit the growth and viability of laboratory *E. coli* K-12 strains [12], raising the possibility that SAA may act similarly against UPEC isolates during the course of a UTI. However, in *in vitro* assays, we found that growth of the UPEC isolates UTI89 and F11 in M9 medium was unfazed by SAA concentrations up to 100 µg/ml (data not shown and **Fig. 4**), indicating that SAA does not have direct bactericidal or bacteriostatic effects on UPEC. Interestingly, SAA also had no effect on growth of the reference K-12 isolate MG1655 in our assays. In considering alternate means by which SAA could potentially affect the pathogenesis of UTIs, we noted previous reports indicating that SAA can opsonize Gram-negative bacteria by binding the abundant outer membrane protein OmpA [4,9]. OmpA is an important facilitator of biofilm formation by UPEC and other *E. coli* isolates (unpublished observations and [15]), and biofilm formation both on and within the urothelium is thought to promote the establishment and persistence of UPEC within the urinary tract [1,30]. To test possible effects of SAA on biofilm formation by UPEC, we employed standard *in vitro* microtiter plate

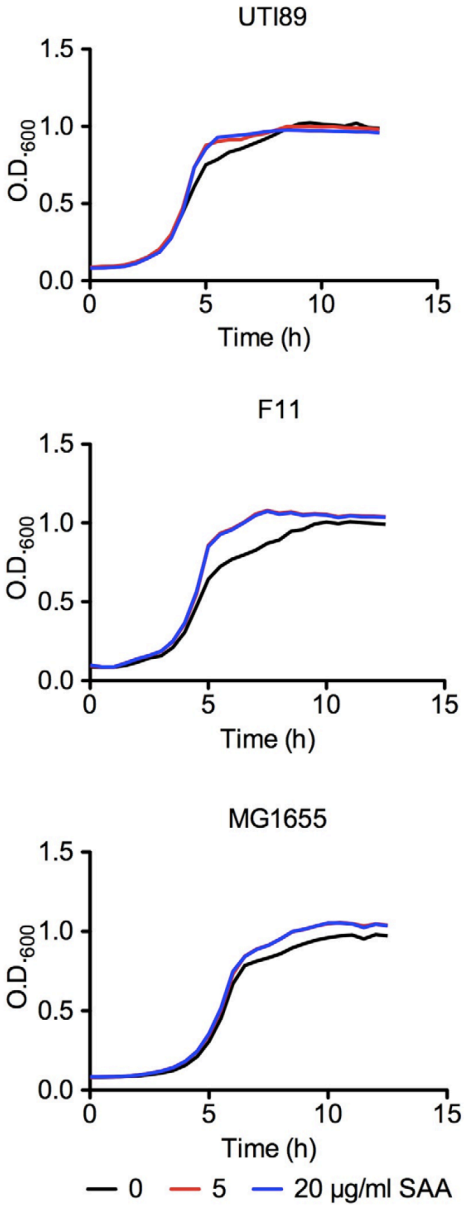

Figure 4. Growth of UTI89, F11, and MG1655 ± SAA. Bacterial growth in M9 medium with 0, 5, or 20 µg/ml SAA was determined by measuring OD_{600} over time. Each curve represents the means of results from quadruplicate samples.
doi:10.1371/journal.pone.0032933.g004

biofilm assays. In these assays, the addition of a physiological concentration of SAA (5 ug/ml) significantly inhibited biofilm formation by UTI89 as well as F11 (**Fig. 5**).

Discussion

A few decades ago the first publication emerged indicating that SAA and CRP act as the most reliable markers for monitoring

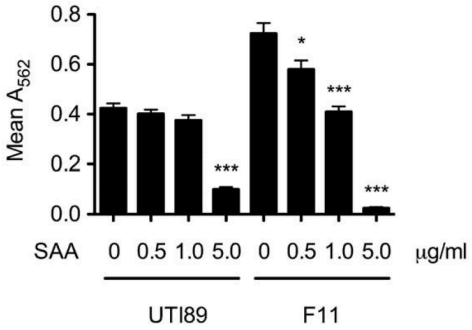

Figure 5. Biofilm formation by the UPEC isolates UTI89 and F11 ± SAA. Biofilm levels were quantified by measuring A_{562} after 48 h static growth in M9 medium ±0, 0.5, 1 and 5 µg/ml SAA. *, $p<0.001$, as determined by Student's *t* test. Results show the mean values ± SEM of three independent experiments performed in quadruplicate.
doi:10.1371/journal.pone.0032933.g005

antimicrobial therapy in patients with UTIs [33]. SAA and CRP levels were also found to be higher in bacterial infections than in viral infections, although SAA appeared to be more clinically relevant as a marker of inflammation in acute viral infections [34]. Initial reports on the anti-microbial activities of SAA were published about a decade ago with work showing that recombinant SAA can enhance the anti-fungal activities of polymorphonuclear cells (PMNs) [35]. Within 30 min of stimulation, SAA was found to promote the upregulation of cytosolic Ca^{++} concentrations, cell-surface expression of CD11c and CD16 (antigens involved in adhesion and microbial recognition), and elevation of lactoferrin secretion. Lactoferrin itself is an anti-microbial agent, which enchances PMN phagocytic activity against heat-killed yeast *Candida albicans*.

More recently, SAA was shown to interact with hepatitis C (HCV) virions, thereby blocking viral entry [6]. Although no clinical correlation in this study could be found between sera levels of SAA and HCV viral loads, a tight relationship between SAA and HDL levels in modulating HCV infectivity has been proposed [3,5]. SAA has also been shown to inhibit HIV-1 infection of host cells via CCR5 receptors [5,7]. SAA appears to be one of the earliest systemic anti-viral responses to HIV-1, being induced as early as 5–7 days prior to the first detection of plasma viral RNA and considerably earlier than other systemic cytokines. Such observations indicate that SAA can act as a front line anti-viral defense prior to systemic activation of other immune responses [5].

SAA also appears to play a major role as host defense against bacterial pathogens, acting as an opsonin able to rapidly bind with high affinity to many Gram-negative bacteria, including *E. coli*, *Pseudomonas aeruginosa*, *Salmonella typhimurium*, *Shigella flexneri*, *Klebsiella pneumoniae*, and *Vibrio cholerae* [4]. Binding of SAA to *E. coli* was found to be mediated primarily through interactions with OmpA, as OmpA deficient *E. coli* did not to bind SAA [9]. Importantly, the concentration of SAA required for half-maximal binding to *E. coli* is within physiologically relevant levels and does not require other acute phase responses [4]. *In vitro*, neutrophils phagocytose K-12 *E. coli* more readily and in higher numbers following opsonization of the bacteria with physiologically normal levels of SAA [9]. More recently, overexpression of SAA1/2 by epithelial cells has been shown to reduce the viability of a co-cultured K-12 *E. coli* strain via an as-yet undefined mechanism [12]. In contrast to these antimicrobial effects, SAA may in some cases be detrimental to the host. For example, SAA has been shown to

inhibit local inflammatory responses to *Actinetobacter baumannii Pneumonia* (a Gram-negative pathogen that is often resistant to many antibiotics), and may thereby actually facilitate, rather than inhibit, bacterial survival and outgrowth [8].

Here we report for the first time that SAA (specifically SAA1/2 and to a smaller extent SAA3) is greatly induced in the bladder wall and, to a lesser extent, the urothelium in response to UPEC instilled into the urinary tract via catheterization. As seen by immunofluorescence microscopy, infection with UPEC resulted in high levels of cytoplasmic SAA in comparison to the more subdued, primarily nuclear expression pattern of SAA in uninfected urothelial cells (see Fig. 1). Heightened levels of SAA expression within the bladder wall versus the urothelium suggest that infiltrating immune effector cells and resident host cells within this compartment are primary contributors to SAA production during a UTI. Enhanced levels of SAA1 expression in response to UPEC within the urinary tract were also observed systemically, being detected in the liver and transiently within the serum of infected mice. Direct inoculation of UPEC into the peritoneum also increased levels of SAA1 and SAA3 within both the liver and general circulation, with only SAA3 increased in the bladder wall and urothelium.

Although the physiological role of SAA during a UTI remains to be tested *in vivo*, the robust localized and systemic amplification of SAA in response to infection with UPEC suggests a critical role for this acute phase protein as a host defense against UTIs. UPEC isolates are often more resistant to environmental stresses and host defense mechanisms [36], and this phenomenon appears to also be true in the case of SAA. While SAA expressed by cultured host cells can interfere with the viability of laboratory *E. coli* K-12 strains [12], we found that growth of UPEC as well as the K-12 strain MG1655 proceeds unhindered even in the presence of high levels of SAA. It may be that the previously reported bacteridal effects of SAA require additional co-factors not present in our *in vitro* assays. However, we did find that SAA can potently inhibit the ability of UPEC isolates to form biofilms, possibly by binding to and occluding OmpA. The formation of both extra- and intracellular biofilm communities by UPEC can impact the establishment and persistence of these microbes within the urinary tract [13,32,37]. By interfering with biofilm development, SAA may increase the susceptibility of UPEC to other host defense mechanisms while also depriving the pathogens of a strong foothold within the urothelium in which to expand their numbers.

Author Contributions

Conceived and designed the experiments: PV MAM AE KL MGB SS-S. Performed the experiments: AE KL KM-P MGB VK-H. Analyzed the data: AE KL PV MGB MAM SS-S. Contributed reagents/materials/analysis tools: PV MAM SS-S VK-H. Wrote the paper: KL AE SS-S MAM PV. Read and approved the final version of the manuscript: AE KL KM-P MGB VK-H MAM SS-S PV.

References

1. Blango MG, Mulvey MA (2010) Persistence of uropathogenic Escherichia coli in the face of multiple antibiotics. Antimicrob Agents Chemother 54: 1855–1863.
2. Eto DS, Sundsbak JL, Mulvey MA (2006) Actin-gated intracellular growth and resurgence of uropathogenic Escherichia coli. Cell Microbiol 8: 704–717.
3. Cai Z, Cai L, Jiang J, Chang KS, van der Westhuyzen DR, et al. (2007) Human serum amyloid A protein inhibits hepatitis C virus entry into cells. J Virol 81: 6128–6133.
4. Hari-Dass R, Shah C, Meyer DJ, Raynes JG (2005) Serum amyloid A protein binds to outer membrane protein A of gram-negative bacteria. J Biol Chem 280: 18562–18567.
5. Kramer HB, Lavender KJ, Qin L, Stacey AR, Liu MK, et al. (2010) Elevation of intact and proteolytic fragments of acute phase proteins constitutes the earliest systemic antiviral response in HIV-1 infection. PLoS Pathog 6: e1000893.
6. Lavie M, Voisset C, Vu-Dac N, Zurawski V, Duverlie G, et al. (2006) Serum amyloid A has antiviral activity against hepatitis C virus by inhibiting virus entry in a cell culture system. Hepatology 44: 1626–1634.
7. Misse D, Yssel H, Trabattoni D, Oblet C, Lo Caputo S, et al. (2007) IL-22 participates in an innate anti-HIV-1 host-resistance network through acute-phase protein induction. J Immunol 178: 407–415.
8. Renckens R, Roelofs JJ, Knapp S, de Vos AF, Florquin S, et al. (2006) The acute-phase response and serum amyloid A inhibit the inflammatory response to Acinetobacter baumannii Pneumonia. J Infect Dis 193: 187–195.
9. Shah C, Hari-Dass R, Raynes JG (2006) Serum amyloid A is an innate immune opsonin for Gram-negative bacteria. Blood 108: 1751–1757.
10. Hirakura Y, Carreras I, Sipe JD, Kagan BL (2002) Channel formation by serum amyloid A: a potential mechanism for amyloid pathogenesis and host defense. Amyloid 9: 13–23.
11. Wang L, Lashuel HA, Walz T, Colon W (2002) Murine apolipoprotein serum amyloid A in solution forms a hexamer containing a central channel. Proc Natl Acad Sci U S A 99: 15947–15952.
12. Eckhardt ER, Witta J, Zhong J, Arsenescu R, Arsenescu V, et al. (2010) Intestinal epithelial serum amyloid A modulates bacterial growth in vitro and pro-inflammatory responses in mouse experimental colitis. BMC Gastroenterol 10: 133.
13. Nicholson TF, Watts KM, Hunstad DA (2009) OmpA of uropathogenic Escherichia coli promotes postinvasion pathogenesis of cystitis. Infect Immun 77: 5245–5251.
14. Prasadarao NV, Wass CA, Weiser JN, Stins MF, Huang SH, et al. (1996) Outer membrane protein A of Escherichia coli contributes to invasion of brain microvascular endothelial cells. Infect Immun 64: 146–153.
15. Smith SG, Mahon V, Lambert MA, Fagan RP (2007) A molecular Swiss army knife: OmpA structure, function and expression. FEMS Microbiol Lett 273: 1–11.
16. Wu HH, Yang YY, Hsieh WS, Lee CH, Leu SJ, et al. (2009) OmpA is the critical component for Escherichia coli invasion-induced astrocyte activation. J Neuropathol Exp Neurol 68: 677–690.
17. Jorgensen JB, Lunde H, Jensen L, Whitehead AS, Robertsen B (2000) Serum amyloid A transcription in Atlantic salmon (Salmo salar L.) hepatocytes is enhanced by stimulation with macrophage factors, recombinant human IL-1 beta, IL-6 and TNF alpha or bacterial lipopolysaccharide. Dev Comp Immunol 24: 553–563.
18. Lin B, Chen S, Cao Z, Lin Y, Mo D, et al. (2007) Acute phase response in zebrafish upon Aeromonas salmonicida and Staphylococcus aureus infection: striking similarities and obvious differences with mammals. Mol Immunol 44: 295–301.
19. Meijer AH, Verbeek FJ, Salas-Vidal E, Corredor-Adamez M, Bussman J, et al. (2005) Transcriptome profiling of adult zebrafish at the late stage of chronic tuberculosis due to Mycobacterium marinum infection. Mol Immunol 42: 1185–1203.
20. Ordas A, Hegedus Z, Henkel CV, Stockhammer OW, Butler D, et al. (2011) Deep sequencing of the innate immune transcriptomic response of zebrafish embryos to Salmonella infection. Fish Shellfish Immunol 31: 716–724.
21. Wu Z, Zhang W, Lu Y, Lu C (2010) Transcriptome profiling of zebrafish infected with Streptococcus suis. Microb Pathog 48: 178–187.
22. Orro T, Sankari S, Pudas T, Oksanen A, Soveri T (2004) Acute phase response in reindeer after challenge with Escherichia coli endotoxin. Comp Immunol Microbiol Infect Dis 27: 413–422.
23. Lakota K, Thallinger GG, Cucnik S, Bozic B, Mrak-Poljsak K, et al. (2011) Could antibodies against serum amyloid A function as physiological regulators in humans? Autoimmunity 44: 149–158.
24. Notebaert S, Demon D, Vanden Berghe T, Vandenabeele P, Meyer E (2008) Inflammatory mediators in Escherichia coli-induced mastitis in mice. Comp Immunol Microbiol Infect Dis 31: 551–565.
25. Reigstad CS, Lunden GO, Felin J, Backhed F (2009) Regulation of serum amyloid A3 (SAA3) in mouse colonic epithelium and adipose tissue by the intestinal microbiota. PLoS One 4: e5842.
26. Uhlar CM, Whitehead AS (1999) Serum amyloid A, the major vertebrate acute-phase reactant. Eur J Biochem 265: 501–523.
27. Gunther J, Koczan D, Yang W, Nurnberg G, Repsilber D, et al. (2009) Assessment of the immune capacity of mammary epithelial cells: comparison with mammary tissue after challenge with Escherichia coli. Vet Res 40: 31.
28. Gardiner GE, O'Flaherty S, Casey PG, Weber A, McDonald TL, et al. (2009) Evaluation of colostrum-derived human mammary-associated serum amyloid A3 (M-SAA3) protein and peptide derivatives for the prevention of enteric infection: in vitro and in murine models of intestinal disease. FEMS Immunol Med Microbiol 55: 404–413.
29. Lloyd AL, Rasko DA, Mobley HL (2007) Defining genomic islands and uropathogen-specific genes in uropathogenic Escherichia coli. J Bacteriol 189: 3532–3546.
30. Mulvey MA, Schilling JD, Hultgren SJ (2001) Establishment of a persistent Escherichia coli reservoir during the acute phase of a bladder infection. Infect Immun 69: 4572–4579.

31. Blattner FR, Plunkett G, 3rd, Bloch CA, Perna NT, Burland V, et al. (1997) The complete genome sequence of Escherichia coli K-12. Science 277: 1453–1462.
32. Kulesus RR, Diaz-Perez K, Slechta ES, Eto DS, Mulvey MA (2008) Impact of the RNA chaperone Hfq on the fitness and virulence potential of uropathogenic Escherichia coli. Infect Immun 76: 3019–3026.
33. Casl MT, Sabljar-Matovinovic M, Kovacevic S, Pocanic D, Preden-Kerekovic V, et al. (1993) Clinical relevance of serum amyloid A protein monitoring in urinary tract infections. Ann Clin Biochem 30(Pt 3): 272–277.
34. Nakayama T, Sonoda S, Urano T, Yamada T, Okada M (1993) Monitoring both serum amyloid protein A and C-reactive protein as inflammatory markers in infectious diseases. Clin Chem 39: 293–297.
35. Badolato R, Wang JM, Stornello SL, Ponzi AN, Duse M, et al. (2000) Serum amyloid A is an activator of PMN antimicrobial functions: induction of degranulation, phagocytosis, and enhancement of anti-Candida activity. J Leukoc Biol 67: 381–386.
36. Bower JM, Gordon-Raagas HB, Mulvey MA (2009) Conditioning of uropathogenic Escherichia coli for enhanced colonization of host. Infect Immun 77: 2104–2112.
37. Soto SM, Smithson A, Horcajada JP, Martinez JA, Mensa JP, et al. (2006) Implication of biofilm formation in the persistence of urinary tract infection caused by uropathogenic Escherichia coli. Clin Microbiol Infect 12: 1034–1036.